Spring 2010

From the valleys to the mountains: The biographic history of antelope squirrels, bats, and chipmunks in Western North America

Stacy James Mantooth
University of Nevada Las Vegas

FROM THE VALLEYS TO THE MOUNTAINS: THE BIOGEOGRAPHIC HISTORY OF ANTELOPE SQUIRRELS, BATS, AND CHIPMUNKS IN WESTERN NORTH AMERICA

by

Stacy James Mantooth

Bachelor of Science
Angelo State University, San Angelo, TX
1997

Master of Science
Texas Tech University, Lubbock, TX
1999

A dissertation submitted in partial fulfillment
of the requirements for the

Doctor of Philosophy in Biological Sciences
School of Life Sciences
College of Sciences

Graduate College
University of Nevada, Las Vegas
May 2010

UNLV
UNIVERSITY OF NEVADA LAS VEGAS

THE GRADUATE COLLEGE

We recommend the dissertation prepared under our supervision by

Stacy James Mantooth

entitled

From the Valleys to the Mountains: The Biogeographic History of Antelope Squirrels, Bats, and Chipmunks in Western North America

be accepted in partial fulfillment of the requirements for the degree of

Doctor of Philosophy In Biological Sciences
School of Life Sciences

Brett R. Riddle, Committee Chair

John Klicka, Committee Member

Javier A. Rodríguez, Committee Member

Gary Voelker, Committee Member

Andrew Kirk, Graduate Faculty Representative

Ronald Smith, Ph. D., Vice President for Research and Graduate Studies
and Dean of the Graduate College

May 2010

ABSTRACT

From the Valleys to the Mountains: the Biogeographic History of Antelope Squirrels, Bats, and Chipmunks in Western North America

by

Stacy James Mantooth

Dr. Brett R. Riddle, Examination Committee Chair
Professor of Biological Sciences
University of Nevada, Las Vegas

Genetic differentiation within and between species often coincides with significant geological or climatic changes that have shaped the sizes and locations of their geographic ranges and altered the connectivity between populations over time. Across western North America, many endemic taxa experienced high levels of initial divergence associated with geological transformations of the Neogene (insert timeframe), with subsequent diversification and geographic structuring of populations associated with climatic changes during the Quaternary (insert timeframe). As such, we can use a combination of molecular markers and genetic analyses to effectively examine the evolutionary and biogeographic histories of populations, species, and regional biotas whose signatures of differentiation are driven by the older geological events as well as more recent episodes of climatic change. Much of western North America is composed of a mosaic of regional deserts and associated aridlands separated from one another by a number of isolated mountain ranges. I employ a suite of phylogenetic, phylogoegraphic, and population genetic analyses, in combination with ecological niche modeling, to examine the biogeographic history of antelope squirrels (*Ammospermophilus*), western pipistrelle bats (*Pipistrellus hesperus*), and Uinta chipmunks (*Neotamias umbrinus*) in

western North America. Antelope squirrels (*Ammospermophilus*) include five species collectively widespread throughout the North American deserts. Data presented herein support the hypothesis that early divergences of the three major extant lineages within this genus were driven by the initial formation of the deserts and the uplift of mountain ranges (e.g., the Sierra Nevada Occidental and Central Mexican Plateau) in the mid to late Neogene, and recent divergences were driven by ongoing geologic events in the late Pliocene (e.g., uplift of the Transverse Range). Genetic patterns reveal that populations were affected by habitat shifts associated with repeated glacial cycles throughout the Pleistocene, including the late glacial maximum (LGM). The western pipistrelle (*Pipistrellus hesperus*) is the smallest bat in North America and is distributed across many of the same habitats as *Ammospermophilus*. Within this species, there are three major geographically defined lineages with divergences dated to the early Pleistocene. These divergences were likely driven by the earliest glacial cycles in this region and genetic patterns indicate that populations of this species were confined to multiple glacial refugia during the LGM, reinforcing the already existing genetic patterns. The Uinta chipmunk (*Neotamias umbrinus*) is confined to montane habitats on mountain ranges throughout the intermountain west. Genetic analyses of populations within the Great Basin indicate that lineages in this region coalesce within the earliest Pleistocene, suggesting that most populations were restricted to the isolated mountain ranges at this time with little to no gene subsequent gene flow between them. While many mammals distributed across western North America have experienced a common set of abiotic factors, they have responded in unique ways leading to specific evolutionary and biogeographic patterns that are detectable in contemporary species and populations.

ACKNOWLEDGMENTS

This dissertation represents many years of hard work…in the classroom, in the field, and in the laboratory. While my name is listed as the author, no dissertation of this size is the result of the efforts of only one person. I owe a tremendous debt of gratitude to people and organizations that have enabled me to complete this project. I would like to thank my advisor, Dr. Brett Riddle, for allowing a student from Texas to move to the desert and work in his laboratory. He has taught me the true meaning and importance of biogeography as a science and as a method for understanding the world. I would also like to thank Dr. Gary Voelker for making me feel welcome and for treating me not only as a student but also as a friend in the early stages of my degree. Dr. John Klicka has always been a strong voice of support and he has taught me how to objectively look at my data with an open mind to reveal the patterns in the genes. Dr. Javier Rodríguez has shown me that being a scientist is more than just about generating data but also about contributing to the scientific community in meaningful ways. Dr. Andrew Kirk, an environmental historian, has always shown me a warm welcome and provided a fresh perspective with a genuine interest in my research. These individuals have collectively contributed to my professional development as my advisory committee, but each has uniquely influenced me as a scientist and as a person and I thank them for their support and guidance.

My graduate student colleagues and friends have made this journey truly memorable. I would like to thank Garth Spellman, Markus Mika, Derek Houston, Christine Serway, Connie Herr, and Jeff DaCosta for sharing the experiences that will shape the rest of my life. You have each enriched my life and my science.

This research was funded in part by the National Science Foundation, the American Museum of Natural History Theodore Roosevelt Memorial Fund, the American Society of Mammalogists, the Nevada Department of Wildlife, the UNLV Graduate & Professional Student Association, and the UNLV School of Life Sciences. A long list of individuals provided invaluable help in the laboratory and in the field. I would like to especially thank Marcin Chmiel, Michael Krainock, Lois Alexander, Dianne Bangle, Jennifer Berger, Chris Lowrey, Jason Williams, and Zane Marshall. Additional support in the final stages of this project was provided by Rob Bryson, Jr., Sean Neiswenter, Adam Leland, and other members of the UNLV systematics research group.

Several organizations provided samples used in this project. These include the Angelo State Natural History Collection (Angelo State University), Arizona Game and Fish Department (Linden Piest), Field Museum of Natural History, Humboldt State University (Tim Lawlor), Museum of Southwestern Biology (University of New Mexico), Museum of Vertebrate Zoology (Harvard), Natural Science Research Laboratory (Texas Tech University), Nevada Department of Wildlife, the Nevada State Museum (George Baumgardner), Texas Cooperative Wildlife Collection (Texas A&M), and Universidad Nacional Autonóma de México (Mexico City).

And finally I would like to thank my parents, Karen and James Mantooth. It is because of your strength, encouragement, and generosity of spirit that I have been able to accomplish everything in my life. I dedicate this milestone to you, Mom and Dad…your love and support have carried me through life and it is because of you I have made it here.

TABLE OF CONTENTS

LIST OF TABLES

LIST OF FIGURES

CHAPTER 1

MOLECULAR BIOGEOGRAPHY: THE INTERSECTION BETWEEN GEOGRAPHIC AND MOLECULAR VARIATION

Abstract

The rapid growth of techniques employed in the generation and analysis of DNA variation has led to significant advances throughout the life sciences. Herein, we explore the impacts of this molecular revolution on the science of biogeography and how it has enhanced or altered long-standing biogeographic hypotheses in this revitalized discipline. We examine the recent development of molecular biogeography and address issues dealing with data generation and interpretation, and review newer analytical techniques that have been developed to handle the explosion of available data. We explore several important issues, including analyses of molecular time estimates, and phylogenetic, phylogeographic, and population genetic approaches to reconstructing the evolutionary histories of taxa and whole biotas. Specialized topics of growing importance include advances in the use of ancient DNA, and the importance of incorporating biogeographic theory with DNA barcodes, used to catalog the diversity of life. Finally, we investigate some of the newest and most exciting techniques for generating, analyzing, and visualizing genetic data that will shape the future of molecular biogeography.

> *The definition of biogeography may be simple – the study of the geographical distributions of organisms – but this simplicity hides the great complexity of the subject...No one who studies biogeography can fail to be impressed, or perplexed, by the diversity of approaches to the subject.* – Crisci (2001)

What is Molecular Biogeography?

With the exponential increase in the amount of molecular sequence data being generated from a diverse array of taxa, the use of these data to reconstruct evolutionary events is becoming increasingly commonplace (Crandall and Templeton 1996; Rokas and Carroll 2006). Molecular data can be used to resolve evolutionary relationships among species or higher taxa within a *phylogeny* (see Glossary), under the assumption that genetic similarity decreases as time since divergence increases. Within a species or collection of closely-related species, we can assess phylogenetic and population genetic signatures across the geographic distribution of genetic lineages, a practice referred to as *phylogeography* (Avise 2000; 2009). Alone, a phylogeny examines only the branching order of taxa, but calibrating the phylogeny by time adds another layer of information, and allows for estimation of time since divergence of lineages. A time-calibrated phylogeny allows us to examine the geographic context of evolution as never before possible, by associating the timing of divergences with past geologic and climatic events or other aspects of Earth's history. Built on a strong foundation of basic biogeographic theory, the synergy between these modern techniques with many others has led to the development of *molecular biogeography*.

We refer to molecular biogeography as that set of approaches that use genetic data to address the biogeographic structure of lineages and biotas, and the evolutionary and Earth history processes that have shaped current population genetic, phylogenetic, and distributional patterns (Riddle et al. 2008). Molecular biogeography is applicable to recently diverged populations or species as well as more distantly related taxa (Avise

2004; Lomolino et al. 2006), and therefore provides a foundation for examining the complete biogeographic and evolutionary history of any group of organisms across both restricted and broad geographic spaces through time (Figure 1.1).

Here, we first provide a brief overview of the relevance of molecular biogeography, both as it has served to reinvigorate long-standing arenas in biogeography and as it positions biogeography to become a key component of emerging areas of research. We then explore several controversial issues in molecular biogeography, including the calibration of time in biogeographic reconstructions (using molecular clock techniques), approaches to measuring genetic diversity, and choosing from the increasingly extensive variety of molecular data. We end with a few thoughts on current and future trends and the role of molecular biogeography in shaping our understanding of the diversity and history of life.

Molecular Biogeography in a Hypothetico-Deductive World

In the early development of analytical biogeographic thought, *vicariance* (Figure 1.2a) was viewed as the only rigorously testable pattern within a *cladistic* framework. Vicariant events create congruent phylogenetic patterns across multiple taxa, detectable in comparative biogeographic analyses. *Dispersalism*, the movement of individuals across a geographic barrier, (Figure 1.2a; Lieberman 2004) was considered an *ad hoc* biogeographic explanation not testable within a comparative context because it was considered an idiosyncratic, lineage-specific process, failing to produce congruent patterns across multiple taxa – as such, any number of *dispersal* scenarios could be construed as consistent with a particular pattern of divergence. Regardless of vicariant or

dispersal histories (Figure 1.2), biogeographic reconstructions that contain only geographic and topological congruence can be positively misleading in the absence of temporal information. Concordance across multiple taxa can result from *pseudo-congruence* (Figure 1.3; Cunningham and Collins 1994), in which lineage specific processes lead to the false conclusion that congruent patterns result from the same or similar biogeographic histories (Donoghue and Moore 2003). *Pseudo-incongruence* can present similarly confounding effects when lineage-specific processes result in common yet undetectable patterns (Figure 1.3). Incorporating a temporal component into analyses can reveal the true biogeographic nature within a comparative framework across multiple taxa (Donoghue and Moore 2003).

The confounding effects of congruence and incongruence are common in geographic areas that experience repetitive cycles of historical processes. Within relatively shallow timeframes, Pleistocene glacial cycles have continually altered distributions and dispersal routes for multiple taxa within an array of biotas. *Comparative phylogeographic* approaches with well constrained time estimates aim to unravel the complex biogeographic histories of these taxa and biotas (Arbogast and Kenagy 2001). Such studies include comparative phylogeographic analysis of the mesic forest ecosystem in the American Pacific (Carstens et al. 2005), and plant-insect interactions in the Rocky Mountains of North America (DeChaine and Martin 2006). These and other studies have shown that molecular biogeographic analyses can provide convincing evidence as to the direction, timing, and extent of dispersal out of Pleistocene glacial refugia—moreover, rejection of traditional hypotheses in favor of more plausible alternatives is possible.

In deeper timeframes, inferences of biogeographic histories from phylogenetic trees alone can be misleading without incorporating additional data. McGlone (2005) summarizes evidence for dispersal scenarios including the origination of several Australian groups in the Northern Hemisphere, and post-Gondwana groups (i.e., formed since the breakup of Gondwana) found on isolated continental fragments such as those distributed across the Tasman Sea separating New Zealand and Australia. These and other examples indicate that the evolutionary history, fossil record, and current distributions of these groups do not support vicariance scenarios.

Recent work combining molecular systematics and paleontology has shown that even in evolutionarily deep time, patterns of range expansion can produce congruent patterns across multiple lineages, further suggesting that dispersal is not entirely the lineage-specific and therefore untestable process it was considered to be within the vicariance biogeographic paradigm. These paleomolecular analyses explore congruent patterns of *geo-dispersal* across multiple lineages (Lieberman 2003). Geo-dispersal (Figure 1.2c) can produce biogeographic congruence, though it differs from traditional dispersal hypotheses (Lieberman and Eldredge 1996; Lieberman 2003) by invoking the removal of a geographic barrier followed by coincident dispersal events in multiple species. Subsequently, a new barrier is formed in the same or similar position as the original barrier, isolating populations that then diverge in *allopatry* (Lieberman 2004). Because this process affects multiple, co-distributed lineages in a similar manner and at a comparable point in time, the resulting patterns can be detected in subsequent phylogenetic analyses. Within these biotas, the taxa exhibit not only phylogenetic, but

also temporal congruence, and molecular data are critical to rejecting an alternative hypothesis of pseudo-congruence.

The information component of molecular biogeography is not limited to simply creating patterns in the form of phylogenies. At shallower evolutionary depths, analytical techniques can unravel details about the histories of populations within species. Through these data, we can address the differential roles of various processes, including allopatric fragmentation (i.e., vicariance) and range expansion histories (i.e., dispersal; Templeton et al. 1995; Crandall and Templeton 1996) in producing current phylogeographic architectures. For example, the statistical framework of *Nested Clade Phylogeographic Analysis* (NCPA – Templeton 1998; 2004) uses *haplotype networks* (Figure 1.3A) of molecular data to test the null hypothesis of no geographic correlation with genetic diversity against alternative hypotheses including past range fragmentation or expansion (Templeton 1998). The validity of NCPA has been questioned (reviewed in Beaumont and Panchal 2008), and alternative *statistical phylogeographic* methods have been advocated that incorporate *coalescent* models of population dynamics into the evolutionary processes that underlie recently diverged or diverging populations (Knowles and Maddison 2002; Knowles 2004; Carstens and Richards 2007).

The inclusion of molecular data into rigorous biogeographic analyses allows biogeographers to create statistically testable hypotheses of dispersal and range expansion within the hypothetico-deductive framework long championed by strict vicariance biogeographers. The explanatory power of these analyses has grown as the analytical techniques have increased in complexity. We now have powerful tools with which to examine evolutionary dynamics of taxa within a comparative framework of complex

biogeographic histories regardless of the depth of divergence or the size of the geographic area under investigation. The use of molecular data has become a vital tool for incorporating explicitly the temporal aspect of evolutionary histories in the process of unraveling complex biogeographic histories.

Molecular Calibrations – the Importance of Time

A great advantage conferred by molecular biogeography is that, once the basic phylogenetic structure between taxonomic groups is established, we can often add a temporal component through a procedure called *molecular dating*. The estimation of divergence time is possible when evolutionary rates of molecular change (i.e., mutation rate) across lineages have been calibrated. Molecular dating has been applied broadly across a wide diversity of organisms and depths of divergence (reviewed by Wray 2001; Kumar 2005), creating time calibrated phylogenies, or *time trees* (Figure 1.3B). In different groups of organisms–including mammals (Douady et al. 2003b), birds (Barker et al. 2004), insects (Moreau et al. 2006), and plants (Good-Avila et al. 2006) – time trees have had a profound impact on depictions of evolutionary histories. The calibrations used to construct time trees are based on a combination of paleogeographic and paleoclimatic events, or the ages of fossils within a group, or more specifically the ages of the geologic strata from which the fossils were collected. Because the fossil record is incomplete and fossils underestimate (sometimes considerably) the true divergence time of lineages (Hedges and Kumar 2004), evolutionary rate analysis can benefit from well-constrained fossil calibrations in combination with well-dated biogeographic events (e.g., mobile terrains or glacial advance). The most common calibrations rely on fossil specimens that

can be reliably traced onto a phylogeny, predating a specific divergence event (Hedges and Kumar 2004). Using such calibrations, the minimum time of divergence or lower bound is defined by the geologic formation containing the fossil and the time of divergence cannot be younger than the age of a well-dated fossil. The maximum age of divergence is different because the calibration fossil is unlikely to be the true ancestral fossil leading to a particular divergence, but rather is a member of the ancestral lineage. An unrealistically high upper bound may be needed, so the time estimate does not eliminate the possibility of an ancient age for a particular clade (Yang and Rannala 2005). The actual time of divergence is therefore estimated within a range of possible times, creating a range of evolutionary rates within these limits. These calibrations represent a "hard bound" on the dates of divergence, and place considerable confidence in the reliability of the fossil record (Figure 1.4).

Molecular time estimates (MTEs) have become increasingly common as a powerful tool in the investigation of the timing of past divergences, especially for groups that have a poor fossil record. Both fossil and molecular time estimates can be reciprocally informative, either corroborating or refuting estimated divergence dates. Early clock approaches used simple linear regression and a single global clock to create *ultrametric trees* (i.e., each tip is the same distance from the root) in which the depth of nodes correlated with divergence times (Nei 1987; Sanderson 1998). Early advances in rate estimation optimized the application of the clocks while still maintaining a global clock across all lineages, and while the earliest molecular studies used single protein sequences (Zuckerkandl and Pauling 1965), modern studies use large numbers of genes (sometimes

hundreds), which can improve the precision and reduce bias in the MTEs (Hedges and Kumar 2003; Yang and Yoder 2003; Kumar et al. 2005).

The fundamental premise of MTEs and their role in biogeographic reconstructions has been challenged (Graur and Martin 2004; Heads 2005), suggesting that application of a molecular clock to biogeographic and systematic hypotheses is a futile exercise. While a strictly enforced molecular clock can be misleading, the errors associated with application of a global clock can be compensated for by using analytical techniques that relax the strict assumptions of a global clock approach. As phylogenetic analyses have grown in complexity, representing more lineages and a broader range of organismal diversity and divergence depths, it has become evident that rate heterogeneity can pervade a phylogeny, occurring along a single lineage as well as between different lineages (Gillespie 1986). Analyses have been developed to detect rate differences (Felsenstein 1981) and take rate heterogeneity into account, attempting to either correct for the rate differences within a phylogeny, or incorporate the rates into the analyses by applying local clocks to specific lineages, effectively relaxing the rate of the molecular clock (methods compared in Lepage et al. 2007). Recent work has suggested the utility of calibration points that incorporate "soft bounds" on the dates of divergence so that multiple calibrations can be adjusted simultaneously, relaxing the assumptions of hard bounds. Relaxed clock (Figure 1.5) methods also have been developed that estimate phylogenies and divergence times simultaneously when there is considerable uncertainty in evolutionary rates and calibration times (Drummond et al. 2006). These methods can accommodate poor calibrations when multiple fossils conflict with each other or with molecular data, and increase the reliability of estimating calibration errors (Yang and

Rannala 2005). A number of computer programs have been developed to address these varied molecular clock approaches, including r8s (Sanderson 2003) and BEAST (Drummond and Rambaut 2007).

For more recent divergences, such as those during the Pleistocene, it is increasingly difficult to accurately estimate divergence times because of basic demographic properties of recently diverged taxa. Factors such as incomplete lineage sorting and mutational stochasticity increase the difficulty of estimating divergence times under traditional models of divergent evolution. *Coalescent* models have been developed to assess both the accuracy and precision of divergences while estimating ancestral genetic diversity and incorporating a migration parameter that accounts for the possibility of gene flow since initial divergence (Hey and Nielsen 2004). *Coalescent theory* is a population genetic model whereby a genealogy of alleles within a particular population is reconstructed to determine when these alleles coalesce to a single ancestral copy (Figure 1.6; see Wakeley 2008 for an overview of coalescent theory) for an overview on coalescent theory). A coalescent approach can be used to assess the adequacy of empirical data to estimate divergence times simulated under an array of plausible coalescent models (Knowles 2004). These techniques have been used to test the recent biogeographic history of some North American songbirds, in which patterns of divergence were driven by Quaternary climate changes (Spellman and Klicka 2006; Spellman et al. 2007). Expanding upon this basic approach by analyzing multiple unlinked genetic loci, a coalescent analysis can account for patterns where the genetic divergence predates the species divergences as well as estimating divergence times while incorporating the possibility of speciation with gene flow (Carstens and Knowles 2007).

It is essential to use accurate phylogenies, calibrated by well-constrained time estimates, to reconstruct the very complex biogeographic history of organisms. However, the accurate calibration of a time tree is not always a simple task for reasons including incomplete taxon sampling, an incomplete or uninformative fossil record, conflicting phylogenetic signals due to rate differences among loci/taxa, stochastic sorting and mutational properties of different loci, and differential selection on loci. The harshest criticisms of these techniques point out the imprecision of molecular clocks, but for the purposes of distinguishing between alternative biogeographic hypotheses that differ by several million years, the estimated dates of divergence may not need to be particularly precise (Lomolino et al. 2006). Well calibrated phylogenies add an important temporal element to analyses, enabling researches to more thoroughly examine the processes that underlie the patterns of evolution.

Measuring Genetic Diversity

The growing list of molecular markers available to evolutionary biologists is making even the most complicated biogeographic questions tractable at the molecular level. Mitochondrial DNA (mtDNA) has long been the tool of choice for phylogenetic and biogeographic inference and it has been widely used in phylogeographic and population genetic analysis (Avise 2000). The basic characteristics of mtDNA and the tremendous number of published studies that rely on these data reflect its utility. Mitochondrial DNA is generally a neutral, maternally-inherited marker that is transferred between generations without recombination, has a reduced effective population size, and a simple genetic structure with both protein-coding genes and non-coding regions (Brown et al. 1979;

Harrison 1989; Avise 2000; Shevchuk and Allard 2001). Molecular markers within this genome are among the most widely used measures of organismal genetic diversity (Avise et al. 1987; Ballard and Whitlock 2004). The various rates of evolutionary change of mtDNA (compared with nuclear DNA) allow researchers to use it to explore population dynamics as well as phylogenetic relationships among closely related taxa (Funk and Omland 2003). Mitochondrial DNA has been used for detecting gene flow, identifying hybrid zones, assessing levels of reproductive isolation, detecting historical patterns of population structure and cryptic speciation, and examining conservation concerns across countless taxa (Rubinoff and Holland 2005).

The supremacy of mtDNA for evolutionary questions has been challenged on the grounds that this marker may produce misleading patterns of variation that are inconsistent with nuclear DNA (nDNA; Zhang and Hewitt 2003; Rubinoff and Holland 2005). The qualities that make mtDNA a useful marker are the same characteristics that may limit its utility. However, it is no surprise that patterns resulting from nDNA may yield patterns that are inconsistent with mtDNA (Avise 2000) because of the difference in time that it theoretically takes each marker to achieve reciprocal monophyly within lineages (e.g., the expected time to coalesce to a single point or most recent common ancestor is four times longer for nDNA than for mtDNA). Typically considered a neutral marker, some recent analyses suggest that mtDNA may be under both direct and indirect selection (via gene linkage), show low levels of recombination in some species, and may be particularly susceptible to selective sweeps because of the low effective population size, decreasing genetic diversity (Ballard and Whitlock 2004).

These criticisms suggest that mtDNA may not be the most appropriate marker to address phylogeographic and population genetic questions. Population genetics theory for mtDNA indicates that genetic diversity is proportional to population size but mitochondrial diversity may not accurately reflect population size in animals, further challenging the genetic neutrality of this marker especially if the genome frequently experiences adaptive evolution (Bazin et al. 2006). This may be especially true for species with very large populations, suggesting that mitochondrial diversity may only coalesce to the most recent selective genetic sweep within the species, not to the most recent common ancestor with the sister taxon. Additional evidence from eutherian mammals indicates that for species with small but stable populations, mitochondrial diversity is correlated with population size (Mulligan et al. 2006). Nevertheless, mitochondrial DNA is still considered to be a useful marker with which to explore recent biogeographic histories (Zink and Barrowclough 2008). Ultimately, the most informative solution may be to use an integrated genetic approach that incorporates both mitochondrial and nuclear DNA in order to account for the shortcomings of each (Rubinoff and Holland 2005).

For very recent events affecting population genetic and phylogeographic patterns, techniques have been developed that survey the nuclear genome for genetic changes, allowing a nuclear approximation of population histories to compare with mitochondrial patterns. These population level techniques include analyses of *microsatellites*, *intersimple sequence repeats* (ISSR), *amplified fragment length polymorphisms* (AFLP), and *single nucleotide polymorphisms* (SNP). Microsatellites consist of a repeated sequence of DNA that follow the patterns of Mendelian inheritance. Developed for use in

studying the population genetics of cultivated plants, ISSR markers are population and species-specific, derived from di- and trinucleotide microsatellite repeats (Wolfe et al. 1998). AFLP analysis involves restriction digests of genomic DNA followed by selective amplification of the fragmented pieces of DNA. The resulting variation in fragment length after AFLP analysis can be tracked between populations. SNPs are sequence variations that occur when a single nucleotide in the genome is altered. Unlike idiosyncratic variations within the genome, a SNP is a mutation that occurs within at least 1% of the population (Wang et al. 1998). Analyses have revealed that these markers are evolutionarily stable and show little change across generations, making them tractable at the population level.

Ancient DNA and Measurably Evolving Taxa

The use of DNA sequences extracted from the remains of naturally and artificially preserved organisms, the emerging field of ancient DNA (aDNA), is becoming a standard approach used in molecular biogeographic studies (Figure 1.6). The earliest deposition of aDNA sequences in GenBank (an online resource for molecular biology information) occurred in 1984-1985 (Higuchi et al. 1984; Pääbo 1985; NCBI 1999). Ancient DNA techniques have been used to address questions ranging from demographic factors in extant populations to genetic characteristics of extinct taxa, represented by partially fossilized remains from the late Pleistocene. The problems associated with using aDNA (*e.g.*, inconsistent results, short sequences, and contamination–Pääbo 1989; 1993) have been rapidly overcome (Pruvost et al. 2007), leading to important advances in molecular biogeography (Karanth et al. 2005).

Biogeographic studies that incorporate aDNA from extinct taxa allow the development of more precise analyses of evolutionary patterns. There is an increasing amount of sequence data from extinct organisms stored in GenBank, including 57 mammals, 40 birds, one lizard, one amphibian, four insects, one gastropod, and five green plants (NCBI 2009). Ancient DNA has been used to address biogeographic questions relating to the origin and population histories of various species (Figure 1.6).With a series of sub-fossil remains taken over time, we can examine the *phylochronology* of populations and investigate how specific populations within a given area responded to climate changes (Hadly et al. 2004; Ramakrishnan and Hadly 2009). Human evolution has benefited from aDNA molecular biogeographic analyses, shedding considerable light on the biogeographic history of our own genus *Homo* (Guitierrez et al. 2002; Lalueza-Fox et al. 2005). The report of genomic DNA (Noonan et al. 2006) and the first complete mitochondrial genome (Green et al. 2008) from 38,000 year old Neanderthal (*H. neanderthalensis*) specimens and the recent announcement of the first near-complete draft version of a Neanderthal genome (Pääbo 2009, unpublished data widely publicized in the media) will inevitably yield more clues to the biogeographic history of humans.

Ancient DNA techniques are not just having a profound impact on our understanding of the evolutionary histories of extinct taxa, but the effects can be found in contemporary population genetics (Pääbo et al. 2004). Natural history museums have long been the repositories of voucher specimens that are suddenly gaining new life as sources of aDNA for studies examining recently extinct and extant populations. Samples taken from a population at any given time represent a genetic snapshot of that population and we can

compare samples taken at times in the past to current populations and assess changes in genetic parameters, adding a direct temporal component. We can then assess the genetic changes over time in these measurably evolving populations (MEPs–Drummond et al. 2003). The genetic chronology of white-footed mice (*Peromyscus leucopus*) in the Chicago area over the last 150 years was examined and the common genotype over that time was found to have changed (Pergams et al. 2003). Any number of genetic parameters can be measured using aDNA in recently archived specimens to understand the demographic histories in genetically dynamic populations (Figure 1.6). With advancing protocols and the availability of aDNA containing specimens available to biogeographers, these techniques will undoubtedly change the way we approach biogeographic analyses.

Biogeography and Barcoding

The premise of *DNA barcoding* has been gaining momentum since its introduction in 2001 (Hebert et al. 2003), with the goal of sequencing the complete *cytochrome oxidase I* (COI) gene for 10 million species of animals. Similar initiatives have been undertaken that focus on plants and the portions of the *rbcL* and *matK* genes (Lahaye et al. 2008; CBOL Plant Working Group 2009). The purpose of these sequences is to uniquely identify each species with a genetic barcode or sequence of DNA, creating a genetic reference. These reference samples would serve as a resource for species identification and for comparisons with newly generated data. Recent barcoding studies praise the novelty of the barcoding system for uncovering hidden biodiversity and identifying

cryptic species by employing this single locus approach to species discovery (Burns et al. 2008).

While the various barcoding initiatives are having a positive effect on conservation and biodiversity issues (Herre 2006), the ultimate goal should be to attain a systematic discovery of genetic diversity within the proper geographic context of an integrative taxonomy. A recent study of parasitoid flies (Smith et al. 2006) represents the "confluence of genetic taxonomy, classical morphological taxonomy, and 'use it or lose it' concepts of conservation of biodiversity" (Herre 2006). This study makes a very compelling case for a truly integrative taxonomy that uses *a priori* knowledge about a group of organisms to reveal previously undiscovered and morphologically cryptic genetic lineages. Taking into account the geographic and ecological landscapes from which sequences were sampled, coupled with the relationships among lineages, makes it easier to classify the uniqueness of populations and species within this framework. We are not questioning the utility of a genetic reference catalogue or of DNA barcoding, but rather suggest that the use of a proper, biogeographically informed sampling approach will greatly assist efforts to correctly recover the true levels of genetic diversity. The classification and preservation of biodiversity works best within an information rich, well-informed integrative system where genetic characterization of taxa is one part of a much larger information system.

Exploring the Future – Generating, Analyzing, and Visualizing New Data

New uses for new approaches are constantly changing the landscape of biogeography. A recently explored use of modern molecular biogeographic theory is to examine very

recent demographic histories using the fast-evolving viruses as proxies of the genetic structure of their hosts. Very recent changes in population structure are often so new that traditional molecular markers (even the newest ones) do not accurately reflect these changes. While studies of host-parasite interactions and their concomitant biogeographic histories (Hafner and Nadler 1991; Hafner and Page 1995) and the geographic distribution of viruses is not new (Fulhorst et al. 2001; Mantooth et al. 2001), the exploitation of viral genetic diversity to explore biogeographic patterns in host species is a recent strategy. Viruses, intracellular parasites dependent upon a host, exhibit detectable genetic changes very quickly which can serve as evidence of demographic divergences between host populations. This technique has been used to examine otherwise undetectable population structure within mountain lions (*Puma concolor*) using Feline Immunodeficiency Virus as the proxy, (Biek et al. 2006). Such techniques can detect changes that have occurred within only a few generations, helping to detect and predict the probability of more widespread genetic changes. Often, the pathogenicity of viral epidemics forces the need to explore the biogeographic history of the hosts, in light of the epidemiology and pathogenicity of the viruses. This method has been used to track to spread of Avian Flu in natural populations in Africa and the proliferation of other viruses throughout host populations (Ducatez et al. 2006).

An emerging approach in population genetics involves sampling multiple alleles from multi-locus sequence data collected from the nuclear genome (Brito and Edwards 2008; Liu et al. 2008). Data can be collected from multiple, non-linked nuclear loci, with the ultimate number of loci needed based on the complexity of the biogeographic questions. Collectively, these techniques differ from whole gene sequencing because they can be

addressed across levels of divergence and they lend themselves to detailed demographic studies (*genomic phylogeography*) of such variables as recent gene flow, linkage disequilibrium, population size estimates, bottlenecks and patterns of population expansion (Brito and Edwards 2008), parameters that could not be fully explored with previous methodologies (e.g., AFLPs, SNPs, etc.).

The development of next-generation sequencing technologies (e.g. pyrosequencing, sequencing-by-synthesis, and ligation-based sequencing) and the ease with which we can generate massive datasets (100-3000 megabases of DNA in a few hours to a few days) with the smallest quantities of input DNA (only a few micrograms) are making questions and hypotheses that we could not address just a few years ago very plausible (see Mardis 2008, for a review of next generation sequencing techniques). While this technology is still prohibitively expensive for many researchers, the prospect of expanding these technologies in the very near future is a reality. We can overcome the obstacles posed by limited genetic sources (e.g., aDNA) or too little informative data found by screening only a few nuclear exons or even undersampling the genetic variation in populations. These data will lead to more thorough analyses of the demographic properties of populations than were previously unavailable. With the recent identification of microsatellites from extinct moas using this new technology (Allentoft et al. 2009), whole genome analyses and the prospect of population genomics is the next step (Li et al. 2008). With unlimited data, we must determine how to analyze such immense and complex datasets (see Pop and Salzberg 2008 for a review of some of these challenges and potential solutions). To face these challenges head-on, the next-generation

biogeographer will have to become every bit as much a computer scientist as molecular biologist, integrating bioinformatics even more closely with biogeography.

Population level genetic analyses are becoming heavily integrated with ecological niche modeling (ENM). This geographic technique uses occurrence records of species and a set of environmental variables to predict the ecological habitats and distribution of both where species are likely to occur today as well as in the past, such as 18-20,000 years ago during the last glacial maximum (Waltari et al. 2007). These analyses result in models of occurrence that can be mapped across a geographic area (Figure 1.8), allowing researchers to explore hypotheses of population expansion/contraction and gene flow that might have gone untested without the incorporation of ENMs and genetic analyses. Faced with datasets that span broad geographic areas (and vast stretches of evolutionary time) or just contain hundreds or thousands (or more!) terminal taxa, typical phylogenetic trees cannot convey the totality of the information contained in those data. Phylogeographic Information Systems and Geophylogenies (Kidd and Ritchie 2006; Kidd and Liu 2008) have been developed to represent geographically referenced phylogenetic trees (Figure 1.9). These approaches graphically convey the geographic content of evolutionary hypotheses based on georeferenced samples. Geophylogenies can be represented by a two-dimensional (2-D) phylogenetic tree overlaid onto a map, with the tree tips corresponding to the exact points where the samples originated (Phylogeographer–Buckler 1999; Geophylobuilder–Kidd and Ritchie 2006; Mesquite–Maddison and Maddison 2009). Expanding on this concept, researchers are developing 3-D visualizations to explore immense datasets, including navigating phylogenies (Paloverde–Sanderson 2006) and “fly-by movies” of geophylogenies (Kidd and Liu 2008) or in

concert with Google Earth (Buckler 1999; Supramap–Janies et al. 2009); to explore the geographic or spatiotemporal content of the data (Hill et al. 2009).

Molecular biogeography has become the driving force behind the most recent advances in biogeographic analysis (Riddle et al. 2008). Advancing analyses have led to advances in the complexity of the questions that can be addressed within evolutionary biology. Because of these advances, molecular biogeography now encompasses a very broad range of biogeographic approaches, including single taxon biogeography, comparative biogeography and phylogeography, population genetics, phylochronology within measurably evolving populations, and population genomics, with new avenues of research sure to be constantly added to the list. As our ability to examine the complexities of biogeographic histories has advanced, so too has our ability to interpret the results that confound simple explanations.

Glossary

Allopatry – taxa (typically populations or species) occupying distinct and disjunct geographical areas.

Amplified fragment length polymorphisms (AFLP) – molecular markers generated when enzymes are to cut DNA into smaller segments, similar to a genetic fingerprint; useful for identifying population level genetic changes.

Cladistic method – a strict method of classifying organisms based on phylogenetic hypotheses of common evolutionary history.

Coalescent theory – suggests that by sampling present-day populations, you can trace all alleles of a gene present in those populations to a single ancestral copy, referred to as the most recent common ancestor.

Comparative phylogeography **–** the comparison of phylogeographic patterns of multiple co-distributed taxonomic groups, usually species or species-complexes.

Cytochrome b (Cyt b) – mitochondrial gene that codes for a transmembrane mitochondrial protein; used widely in phylogenetic and phylogeographic analyses.

Cytochrome Oxidase I (CO1) – the primary unit of the Cytochrome c oxidase complex, involved in aerobic metabolism; used widely in DNA barcoding analyses of animals.

Dispersal – the movement of individuals.

DNA barcode – a standardized sequence of DNA that is unique to for each species, serving as a method of genetic identification.

Ecological niche models – used to predict the geographic range of a species from occurrence records (presence/absence) and environmental data layers.

Genomic Phylogeography – sampling multiple alleles from multi-locus nuclear sequence data to examine recent gene flow, linkage disequilibrium, population size estimates, bottlenecks and patterns of population expansion.

Geo-dispersal– involves the removal of a geographic barrier followed by coincident dispersal events in multiple species, followed by the formation of a new barrier in the same or similar position as the original barrier, isolating populations that then diverge in allopatry.

Haplotype network– a graphical representation of the relationships of haplotypes (unique alleles) among closely related individuals; useful in population genetic analyses.

Hypothetico-deductive – the scientific method whereby a hypothesis is tested by direct observation of experimental data.

Intersimple Sequence Repeats (ISSR) – population and species-specific microsatellite repeats composed of either 2 or 3 nucleotides; developed for population genetic analyses in plants.

Microsatellites – repeated sequences of DNA that follow Mendelian inheritance; useful in populations genetics.

Molecular Clock – the assumption that there is a direct relationship between the number of mutations between organisms and the time since those organism diverged from each other; taxa within a phylogeny accumulate changes at a standard rate.

Molecular dating – calibrating the nodes on a phylogeny by applying a molecular clock.

Nested Clade Phylogeographic Analysis (NCPA) – uses haplotype networks of molecular data to test the null hypothesis of no geographic correlation with genetic diversity against alternative hypotheses including past range fragmentation or expansion. The

resulting patterns can indicate complex biogeographic histories that include an array of past fragmentation, colonization, or range expansion events.

Phylochronology – the study of populations in space and through time using population genetic and phylogeographic techniques.

Phylogeny – a bifurcating tree representing the relationships between a group of organisms (phylogenetic tree).

Phylogeography – the geographic distribution of genetic diversity within a species or group of closely related species.

Pseudo-congruence – lineage specific processes lead to the false conclusion that congruent patterns result from the same or similar biogeographic histories.

Pseudo-incongruence – when lineage-specific processes result in common yet undetectable patterns.

Single nucleotide polymorphisms (SNP) – sequence variations that occur when a single nucleotide in the genome is altered; a mutation that occurs within at least 1% of the population.

Statistical Phylogeography –incorporates coalescent models of population dynamics into the evolutionary processes that underlie recently diverged or diverging populations.

Ultrametric tree – a phylogenetic tree in which all tips are equally distant from the root; used in molecular clock analyses.

Vicariance – the separation of closely related taxa by some geographical barrier.

Literature Cited

Allentoft, M. E., S. C. Schuster, R. N. Holdaway, M. L. Hale, E. McLay, C. Oskam, M. T. P. Gilbert, P. Spencer, E. Willerslev, and M. Bunce. 2009. Identification of microsatellites from an extinct moa species using high-throughput (454) sequence data. BioTechniques 46:195-200.

Arbogast, B. S., and G. J. Kenagy. 2001. Comparative phylogeography as an integrative approach to historical biogeography. Journal of Biogeography 28:819-825.

Avise, J. 2000. Phylogeography: the History and Formation of Species. Harvard University Press, Cambridge.

Avise, J. 2004. What is the field of biogeography, and where is it going? Taxon 53:893-898.

Avise, J. 2009. Phylogeography: retrospect and prospect. Journal of Biogeography 36:3-15.

Avise, J. C., J. Arnold, R. M. Ball, E. Bermingham, T. Lamb, J. E. Neigel, C. A. Reeb, and N. C. Saunders. 1987. Intraspecific phylogeography – the mitochondrial-DNA bridge between population-genetics and systematics. Annual Review of Ecology and Systematics 18:489-522.

Ballard, J. W. O., and M. C. Whitlock. 2004. The incomplete natural history of mitochondria. Molecular Ecology 13:729-744.

Barker, F. K., A. Cibois, P. Schikler, J. Feinstein, and J. Cracraft. 2004. Phylogeny and diversifican of the largest avian radiation. Proceedings of the National Academy of Sciences of the USA 101:11040-11045.

Barnes, I., P. Matheus, B. Shapiro, D. Jensen, and A. Cooper. 2002. Dynamics of Pleistocene population extinctions in Beringian brown bears. Science 295:2267-2270.

Bazin, E., S. Glemin, and N. Galtier. 2006. Population Size Does Not Influence Mitochondrial Genetic Diversity in Animals. Science 312:570-572.

Beaumont, M. A., and M. Panchal. 2008. On the validity of nested clade phylogeographical analysis. Molecular Ecology 17:2563-2565.

Biek, R., A. J. Drummond, and M. Poss. 2006. A virus reveals population structure and recent demographic history of its carnivore host. Science 311:538-541.

Brito, P. H., and S. V. Edwards. 2008. Multilocus phylogeography and phylogenetics using sequence-based markers. Genetica 135:439-455.

Brown, W. M., M. George, Jr., and A. C. Wilson. 1979. Rapid evolution of animal mitochondrial DNA. Proceedings of the National Academy of Sciences of the USA 76:1967-1971.

Buckler, E. S., IV. 1999. Phylogeographer: software for the analysis of phylogeographic hypotheses.

Burns, J. M., D. H. Janzen, M. Hajibabaei, W. Hallwachs, and P. D. N. Hebert. 2008. DNA barcodes and cryptic species of skipper butterflies in the genus Perichares in Area de Conservacion Guanacaste, Costa Rica. Proceedings of the National Academy of Sciences 105:6350-6355.

Carstens, B. C., S. J. Brunsfeld, J. R. Demboski, J. M. Good, and J. Sullivan. 2005. Investigating the evolutionary history of the Pacific Northwest mesic forest

ecosystem: hypothesis testing within a comparative phylogeographic framework. Evolution 59:1639-1652.

Carstens, B. C., and L. L. Knowles. 2007. Shifting distributions and speciation: species divergence during rapid climate change. Molecular Ecology 16:619-627.

Carstens, B. C., and C. L. Richards. 2007. Integrating coalescent and ecological niche modeling in comparative phylogeography. Evolution 61:1439-1454.

CBOL. 2009. A DNA barcode for land plants. Proceedings of the National Academy of Sciences, USA 106:12794-12797.

Crandall, K. A., and A. R. Templeton. 1996. Applications of intraspecifc phylogenetics. Pp. 81-99 *in* P. H. Harvey, A. J. L. Brown, J. M. Smith, and S. Nee, eds. New Uses for New Phylogenies. Oxford University Press, New York.

Crisci, J. V. 2001. The voice of historical biogeography. Journal of Biogeography 28:157-168.

Cunningham, C. W., and T. M. Collins. 1994. Developing model systems for molecular biogeography: Vicariance and interchange in marine invertebrates. Pp. 405-433 *in* B. Schierwater, B. Streit, G. P. Wagner, and R. DeSalle, eds. Molecular ecology and evolution: Approaches and applications. Birkhauser Verlad, Basel, Switzerland.

DeChaine, E. G., and A. P. Martin. 2006. Using coalescent simulations to test the impact of Quaternary climate cycles on divergence in an alpine plant-insect association. Evolution 60:1004-1013.

Dixon, C. J., P. Schönswetter, P. Vargas, S. Ertl, and G. M. Schneeweiss. 2009. Bayesian hypothesis testing supports long-distance Pleistocene migrations in a European

high mountain plant (*Androsace vitaliana*, Primulaceae). Molecular Phylogenetics and Evolution 53:580-591.

Donoghue, M. J., and B. R. Moore. 2003. Toward an integrative historical biogeography. Integrative and Comparative Biology 43:261-270.

Douady, C. J., F. M. Catzeflis, J. Raman, M. S. Springer, and M. J. Stanhope. 2003. The Sahara as a vicariant agent, and the role of Miocene climatic events in the diversification of the mammalian order Macroscelidea (elephant shrews). Proceedings of the National Academy of Sciences of the USA 100:8325-8330.

Drummond, A., and A. Rambaut. 2007. BEAST: Bayesian evolutionary analysis by sampling trees. BMC Evolutionary Biology 7:214.

Drummond, A. J., S. Y. W. Ho, M. J. Phillips, and A. Rambaut. 2006. Relaxed phylogenetics and dating with confidence. PLOS Biology 4:e88.

Drummond, A. J., O. G. Pybus, A. Rambaut, R. Forsberg, and A. G. Rodrigo. 2003. Measurably evolving populations. Trends in Ecology & Evolution 18:481-488.

Ducatez, M. F., C. M. Olinger, A. A. Owoade, S. De Landtsheer, W. Ammerlaan, H. G. M. Niesters, A. D. M. E. Osterhaus, R. A. M. Fouchier, and C. P. Muller. 2006. Avian Flu: Multiple introductions of H5N1 in Nigeria. Nature 442:37.

Felsenstein, J. 1981. Evolutionary trees and DNA sequences: a maximum likelihood approach. Journal of Molecular Evolution 17:368-376.

Fulhorst, C. F., R. N. Charrel, S. C. Weaver, T. G. Ksiazek, R. D. Bradley, M. L. Milazzo, R. B. Tesh, and M. D. Bowen. 2001. Geographic distribtution and genetic diversity of Whitewater Arroyo Virus in the southwestern United States. Emerging Infectious Diseases 7:403-407.

Funk, D. J., and K. E. Omland. 2003. Species level paraphyly and polyphyly: Frequency, Causes, and Consequences, with Insights from Animal Mitochondrial DNA. Annual Review of Ecology, Evolution, and Systematics 34:397-423.

Gillespie, J. H. 1986. Rates of molecular evolution. Annual Review of Ecology, Evolution, and Systematics 17:637-665.

Good-Avila, S. V., V. Souza, B. S. Gaut, and L. E. Eguiarte. 2006. Timing and rate of speciation in *Agave* (Agavaceae). Proceedings of the National Academy of Sciences of the USA 103:9124-9129.

Graur, D., and W. Martin. 2004. Reading the entrails of chickens: molecular timescales of evolution and the illusion of precision. Trends in Genetics 20:80-86.

Green, R. E., A.-S. Malaspinas, J. Krause, A. W. Briggs, P. L. F. Johnson, C. Uhler, M. Meyer, J. M. Good, T. Maricic, U. Stenzel, K. Prüfer, M. Siebauer, H. A. Burbano, M. Ronan, J. M. Rothberg, M. Egholm, P. Rudan, D. Brajković, Z. Kućan, I. Gušić, M. Wikström, L. Laakkonen, J. Kelso, M. Slatkin, and S. Pääbo. 2008. A complete Neandertal mitochondrial genome sequence determined by high-throughput sequencing. Cell 134:416-426.

Guitierrez, G., D. Sanchez, and A. Marin. 2002. A reanalysis of ancient mitochondrial DNA sequences recovered from Neandertal bones. Molecular Biology and Evolution 19:1359-1366.

Hadly, E. A., U. Ramakrishnan, Y. L. Chan, M. van Tuinen, K. O'Keefe, P. A. Spaeth, and C. J. Conroy. 2004. Genetic responses to climate change: insights from ancient DNA and Phylochronology. PLOS Biology 2:e290.

Hafner, M. S., and S. A. Nadler. 1991. Cospeciation in host-parasite assemblages: analysis of rates of evolution and timing of cospeciation events. Systematic Zoology 39:194-204.

Hafner, M. S., and R. D. M. Page. 1995. Molecular phylogenies and host-parasite cospeciation: gophers and lice as a model system. Philosophical Transactions of the Royal Society of London, Series B 349:77-83.

Harrison, R. G. 1989. Animal mitochondrial DNA as a genetic marker in population and evolutionary biology. Trends in Ecology and Evolution 4:6-11.

Heads, M. 2005. Dating nodes on molecular phylogenies: a critique of molecular biogeography. Cladistics 21:62-78.

Hebert, P. D. N., A. Cywinska, S. L. Ball, and J. R. deWaard. 2003. Biological identifications through DNA barcodes. Proceedings of the Royal Society of London 270:313-321.

Hedges, S. B., and S. Kumar. 2003. Genomic clocks and evolutionary timescales. Trends in Genetics 19:200-206.

Hedges, S. B., and S. Kumar. 2004. Precision of molecular time estimates. Trends in Genetics 20:242-247.

Herre, E. A. 2006. Barcoding helps biodiversity fly. Proceedings of the National Academy of Sciences of the USA 103:3949-3950.

Hey, J., and R. Nielsen. 2004. Multilocus method for estimating population sizes, migration rates and divergence time, with applications to the divergence of Drosophila pseudoobscura and D. persimilis. Genetics 167:747-760.

Higuchi, R., B. Bowman, M. Freiberger, O. A. Ryder, and A. C. Wilson. 1984. DNA sequences from the quagga, an extinct member of the horse family. Nature 312:282-284.

Hill, A. W., R. P. Guralnick, M. J. Wilson, F. Habib, and D. Janies. 2009. Evolution of drug resistance in multiple distinct lineages of H5N1 avian influenza. Infection, Genetics and Evolution 9:169-178.

Janies, D., A. Hill, B. Alexandrov, E. Easley, and T. Treseder. 2009. Supramap 0.20.

Karanth, K. P., T. Delefosse, B. Rakotosamimanana, T. J. Parsons, and A. D. Yoder. 2005. Ancient DNA from giant extinct lemurs confirms single origin of Malagasy primates. Proceedings of the National Academy of Sciences of the USA 102:5090-5095.

Kidd, D. M., and X. Liu. 2008. Geophylobuilder 1.0: an ArcGIS extension for creating 'geophylogenies'. Molecular Ecology Resources 8:88-91.

Kidd, D. M., and M. G. Ritchie. 2006. Phylogeographic information systems: putting the geography into phylogeography. Journal of Biogeography 33:1851-1865.

Knowles, L. L. 2004. The burgeoning field of statistical phylogeography. Journal of Evolutionary Biology 17:1-10.

Knowles, L. L., and D. R. Maddison. 2002. Statistical phylogeography. Molecular Ecology 11:2623-2635.

Kuch, M., N. Rohland, J. L. Betancourt, C. Latorre, S. Steppans, and H. N. Poinar. 2002. Molecular analysis of an 11700-year-old rodent midden from the Atacama Desert, Chile. Molecular Ecology 11:913-924.

Kumar, S. 2005. Molecular clocks: four decades of evolution. Nature Review Genetics 6:654-662.

Kumar, S., A. Filipski, V. Swarna, A. Walker, and S. B. Hedges. 2005. Placing confidence limits on the molecular age of the human-chimpanzee divergence. PNAS 102:18842-18847.

Lahaye, R., M. van der Bank, D. Bogarin, J. Warner, F. Pupulin, G. Gigot, O. Maurin, S. Duthoit, T. G. Barraclough, and V. Savolainen. 2008. DNA barcoding the floras of biodiversity hotspots. Proceedings of the National Academy of Sciences USA 105:2923-2928.

Lalueza-Fox, C., M. L. Sampietro, D. Caramelli, Y. Puder, M. Lari, F. Calafell, C. Martinez-Maza, M. Bastir, J. Fortea, M. d. l. Rasilla, J. Bertranpetit, and A. Rosas. 2005. Neandertal Evolutionary Genetics: Mitochondrial DNA Data from the Iberian Peninsula. Molecular Biology and Evolution 22:1077-1081.

Lambert, D. M., P. A. Ritchie, C. D. Millar, B. Holland, A. J. Drummond, and C. Baroni. 2002. Rates of evolution in ancient DNA from Adelie penguins. Science 295:2270-2273.

Leonard, J. A., R. K. Wayne, J. Wheeler, R. Valadez, S. Guillen, and C. Vila. 2002. Ancient DNA evidence for Old World origin of New World dogs. Science 298:1613-1616.

Lepage, T., D. Bryant, H. Phillippe, and N. Lartillot. 2007. A general comparison of relaxed molecular clock models. Molecular Biology and Evolution 24:2669-2680.

Li, Y. F., J. C. Costello, A. K. Holloway, and M. W. Hahn. 2008. "Reverse ecology" and the power of population genomics. Evolution 62:2984-2994.

Lieberman, B. S. 2003. Paleobiogeography: The Relevance of Fossils to Biogeography. Annual Review of Ecology, Evolution, and Systematics 34:51-69.

Lieberman, B. S. 2004. Range expansion, extinction, and biogeographic congruence: a deep time perspective. Pp. 111-124 *in* M. V. Lomolino, and L. R. Heaney, eds. Frontiers of Biogeography. Sinauer Associates, Inc., Sunderland, MA.

Lieberman, B. S., and N. Eldredge. 1996. Trilobite biogeography in the Middle Devonian: geological processes and analytical methods. Paleobiology 22:66-79.

Liu, L., D. K. Pearl, R. T. Brumfield, and S. V. Edwards. 2008. Estimating Species Trees Using Multiple-Allele DNA Sequence Data. Evolution 62:2080-2091.

Lomolino, M. V., B. R. Riddle, and J. H. Brown. 2006. Biogeography. Sinauer Associates, Inc., Sunderland.

Maddison, W. P., and D. R. Maddison. 2009. Mesquite: a modular system for evolutionary analysis. Version 2.6.

Mantooth, S. J., M. L. Milazzo, R. D. Bradley, C. L. Hice, G. Ceballos, R. B. Tesh, and C. F. Fulhorst. 2001. Geographical distribution of rodent-associated hantaviruses in Texas. Journal of Vector Ecology 26:7-14.

Mardis, E. R. 2008. The impact of next-generation sequencing technology on genetics. Trends in Genetics 24:133-141.

McGlone, M. S. 2005. Goodbye Gondwana. Journal of Biogeography 32:739-740.

Moreau, C. S., C. D. Bell, R. Vila, S. B. Archibald, and N. E. Pierce. 2006. Phylogeny of the ants: diversification in the age of Angiosperms. Science 312:101-104.

Mulligan, C. J., A. Kitchen, and M. M. Miyamoto. 2006. Comment on "Population size does not influence mitochondrial genetic diversity in animals". Science 314:1390a.

NCBI. 1999. NCBI News 7 (Spring 1999). NIH Publication No. 99-3272.

NCBI. 2009. National Center for Biotechnology Information GenBank Taxonomy Browser.

Nei, M. 1987. Molecular Evolutionary Genetics. Columbia University Press, New York.

Noonan, J. P., G. Coop, S. Kudaravalli, D. Smith, J. Krause, J. Alessi, F. Chen, D. Platt, S. Pääbo, J. K. Pritchard, and E. M. Rubin. 2006. Sequencing and Analysis of Neanderthal Genomic DNA. Science 314:1113-1118.

Nystrom, V., A. Angerbjorn, and L. Dalen. 2006. Genetic consequences of a demographic bottleneck in the Scandinavian arctic fox. Oikos 114:84-94.

Pääbo, S. 1985. Molecular cloning of Ancient Egyptian mummy DNA. Nature 314:644-645.

Pääbo, S. 1989. Ancient DNA: extraction, characterization, molecular cloning and enzymatic amplification. Proceedings of the National Academy of Sciences USA 86:1939-1943.

Pääbo, S. 1993. Ancient DNA. Scientific American 269:269.

Pääbo, S., H. N. Poinar, D. Serre, V. Jaenicke-Despres, J. Hebler, N. Rohland, M. Kuch, J. Krause, L. Vigilant, and M. Hofreiter. 2004. Genetic analysis from ancient DNA. Annual Review of Genetics 38:645-679.

Pergams, O. R. W., W. M. Barnes, and D. Nyberg. 2003. Rapid change in mouse mitochondrial DNA. Nature 423:397.

Pop, M., and S. L. Salzberg. 2008. Bioinformatics challenges of new sequencing technology. Trends in Genetics 24:142-149.

Pruvost, M., R. Schwarz, V. B. Correia, S. Champlot, S. Braguier, Y. Fernandez-Jalvo, T. Grange, and E. Geigl. 2007. Freshly excavated fossil bones are best for amplification of ancient DNA. Proceedings of the National Academy of Sciences of the USA 104:739-744.

Ramakrishnan, U., and E. A. Hadly. 2009. Using phylochronology to reveal cryptic population histories: review and synthesis of 29 ancient DNA studies. Molecular Ecology 18:1310-1330.

Riddle, B. R., M. N. Dawson, E. A. Hadly, D. J. Hafner, M. J. Hickerson, S. J. Mantooth, and A. D. Yoder. 2008. The role of molecular genetics in sculpting the future of integrative biogeography. Progress in Physical Geography 32:173-202.

Rokas, A., and S. B. Carroll. 2006. Bushes in the Tree of Life. PLOS Biology 4:e352.

Rubinoff, D., and B. S. Holland. 2005. Between two extremes: mitochondrial DNA is neither the Panacea nor the nemesis of phylogenetic and taxonomic inference. Systematic Biology 54:952-961.

Sanderson, M. J. 1998. Estimating rates and time in molecular phylogenies: beyond the molecular clock? Pp. 242-264 *in* P. S. Soltis, D. E. Soltis, and J. J. Doyle, eds. Molecular Systematics of Plants II: DNA Sequencing. Kluwer Academic Publishers, Norwell, MA.

Sanderson, M. J. 2003. r8s: inferring absolute rates of molecular evolution and divergence times in the absence of a molecular clock. Bioinformatics 19:301-302.

Sanderson, M. J. 2006. Paloverde v1.1: a 3-D tree visualization tool.

Shevchuk, N. A., and M. W. Allard. 2001. Sources of incongruence among mammalian mitochondrial sequences: COII, COIII, ND6 genes are main contributors. Molecular Phylogenetics and Evolution 21:43-54.

Smith, M. A., N. E. Woodley, D. H. Janzen, W. Hallwachs, and P. D. N. Hebert. 2006. DNA barcodes reveal cryptic host-specificity within the presumed polyphagous members of a genus of parasitoid flies (Diptera: Tachinidae). Proceedings of the National Academy of Sciences, USA 103:3657-3662.

Spellman, G. M., and J. Klicka. 2006. Testing hypotheses of Pleistocene population history using coalescent simulations: phylogeography of the pygmy nuthatch (*Sitta pygmaea*). Proceedings of the Royal Society of London, Series B 273:3057-3063.

Spellman, G. M., B. R. Riddle, and J. Klicka. 2007. Phylogeography of the mountain chickadee (*Poecile gambeli*): diversification, introgression, and expansion in response to Quaternary climate change. Molecular Ecology 16:1055-1068.

Stone, A. C., and M. Stoneking. 1999. Analysis of ancient DNA from a prehistoric Amerindian cemetery. Philosophical Transactions of the Royal Society of London, Series B 354:153-159.

Templeton, A. R. 1998a. Nested clade analyses of phylogeographic data: testing hypotheses about gene flow and population history. Molecular Ecology 7:381-397.

Templeton, A. R. 1998b. Using phylogeograpic analyses of gene trees to test species status and processes. Molecular Ecology 10:779-791.

Templeton, A. R. 2004. Statistical phylogeography: methods of evaluating and minimizing inference errors. Molecular Ecology 13:789-809.

Templeton, A. R., E. Routman, and C. A. Phillips. 1995. Separating population structure from population history: a cladistic analysis of the geographical distribution of mitochondrial DNA haplotypes in the tiger salamander, *Ambystoma tigrinum*. Genetics 140:767-782.

Wakeley, J. 2008. Coalescent Theory: An Introduction. Roberts & Company.

Waltari, E., R. J. Hijmans, A. T. Peterson, A. S. Nyari, S. L. Perkins, and R. P. Guralnick. 2007. Locating Pleistocene refugia: comparing phylogeographic and ecological niche model predictions. PLoS ONE 2:e563.

Wang, D. G., J.-B. Fan, C.-J. Siao, A. Berno, P. Young, R. Sapolsky, G. Ghandour, N. Perkins, E. Winchester, J. Spencer, L. Kruglyak, L. Stein, L. Hsie, T. Topaloglou, E. Hubbell, E. Robinson, M. Mittmann, M. S. Morris, N. Shen, D. Kilburn, J. Rioux, C. Nusbaum, S. Rozen, T. J. Hudson, R. Lipshutz, M. Chee, and E. S. Lander. 1998. Large-scale identification, mapping, and genotyping of single-nucleotide polymorphisms in the human genome. Science 280:1077-1082.

Weinstock, J., E. Willerslev, A. Sher, W. Tong, S. Y. W. Ho, D. Rubenstein, J. Storer, J. Burns, L. Martin, C. Bravi, A. Prieto, D. Froese, E. Scott, L. Xulong, and A. Cooper. 2005. Evolution, systematics, and phylogeography of Pleistocene horses in the New World: a molecular perspective. PLOS Biology 3:e241.

Wolfe, A. D., Q. Y. Xiang, and S. R. Kephart. 1998. Assessing hybridization in natural populations of Penstemon (Scrophulariaceae) using hypervariable intersimple sequence repeat (ISSR) bands. Molecular Ecology 7:1107-1125.

Wray, G. A. 2001. Dating branches on the tree of life using DNA. Genome Biology 3:1-7.

Yang, Y., and A. D. Yoder. 2003. Coomparison of likelihood and Bayesian methods for estimating divergence times using multiple gne loci and calibration points, with application to a radiation of cute-looking mouse lemur species. Systematic Biology 52:705-716.

Yang, Z., and B. Rannala. 2005. Bayesian estimation of species divergence times under a molecular clock using multiple fossil calibrations with soft bounds. Molecular Biology and Evolution 23:216-226.

Zhang, D. X., and G. M. Hewitt. 2003. Nuclear DNA analyses in genetic studies of populations: practice, problems and prospects. Molecular Ecology 12:563-584.

Zink, R. M., and G. F. Barrowclough. 2008. Mitochondrial DNA under siege in avian phylogeography. Molecular Ecology 17:2107-2121.

Zuckerkandl, E., and L. Pauling. 1965. Evolutionary divergence and convergence in proteins. Pp. 97-166 *in* V. Bryson, and H. J. Vogel, eds. Evolving Genes and Proteins. Academic Press, New York.

Figure Legends

Figure 1.1: The scope of molecular biogeography: Three-dimensional depiction of lineages across space (*i.e.*, geography) and through time. The gray shapes represent time slices, intersected at different points in space (dashed lines) by various branches in the phylogeny. Molecular biogeography can examine recently diverged populations (lineages close in space & time) and distantly related taxa (distantly related & distributed lineages).

Figure 1.2: Biogeographic forces that can lead to divergence and diversification: A) Dispersal, B) Vicariance, and C) Geo-dispersal.

Figure 1.3: Evolutionary relationships of *Androsace vitaliana* (Primulaceae), a European high mountain plant, based on chloroplast DNA: A) Haplotype network of chloroplast haplotypes; colors match lineages in (B) and length of each line is proportional to the number of mutational differences between haplotypes. A) Time-calibrated phylogeny showing the relationship of populations collected from different mountain ranges; colors refer to separate lineages and correspond with (A). *Redrawn and modified from Dixon et al. (2009).*

Figure 1.4: The impact of topological and temporal congruence on the interpretation of comparative biogeographic patterns. *Congruence* results from a single geologic or climatic event leading to the simultaneous divergence across multiple co-distributed taxa. *Pseudo-congruence* results when the patterns are topologically congruent, but temporally incongruent, leading to the false conclusion that the same geological or climatic

processes caused the patterns. *Pseudo-incongruence* is the result of common temporal patterns that are undetectable based on the topology of the relationships in the trees. *Modified from Donoghue & Moore (2003).*

Figure 1.5: A time-calibrated phylogeny (see text for further explanation of terms). Good fossil calibrations are available for nodes 3, 4, & 7 and the root can have either a good fossil (hard bound) or a bad fossil (soft bounds) calibration. A combination of soft and hard bounds can be used to calibrate a tree when the fossil calibrations conflict with each other and with the molecular data. Relaxed clock models can reduce the time estimates (confidence intervals) surrounding the uncalibrated nodes within the tree (nodes 2, 5, 6, & 8). *Redrawn from Yang & Rannala (2005).*

Figure 1.6: Coalescence of alleles within a hypothetical reciprocally monophyletic gene tree embedded within a population or species tree. The genealogy of alleles within a population is reconstructed to determine when these alleles coalesce to a single ancestral copy, known as the coalescent or most recent common ancestor of all alleles. Two populations are represented as geographically separating at time T_1. Population 1 coalesces after T_1 at C_1; Population 2 coalesces at C_2, prior to T_1. All copies of the allele coalesce at C_3 at time T_2, within the ancestral population, prior to the geographic separation at T_1.

Figure 1.7: Representative ancient DNA (aDNA) studies listed by temporal scope. Most aDNA studies are restricted to samples < ~50,000 years before present (ybp). Reports

>100,000-1 million ybp generally are considered artifactual or a result of contamination (Pääbo et al. 2004). *Inset A*–Representative sample ages of aDNA samples reported since 1984 (deposited in GenBank); *Inset B*–Representative DNA fragment sizes reported since 1984 (arrow indicates the introduction of Next-generation sequencing technology). Example studies include (from left to right): mouse–Pergams *et al*. (2003); Quagga–Higachi *et al*. (1984); arctic fox–Nystrom *et al*. (2006); Amerindians–Stone and Stoneking (1999); brown bears–Barnes *et al*. (2002); dogs–Leonard et al. (2002); penguins–Lambert *et al*. (2002); rodent middens–Kuch *et al*. (2002); complete Neanderthal genome–Pääbo (2009, unpublished data); Neanderthal mtDNA– Green *et al*. (2008); horses–Weinstock *et al*. (2005).

Figure 1.8: Ecological Niche Models (ENM) of the white-tailed antelope squirrel (*Ammospermophilus leucurus*) in western North America, generated using the program Maxent (Phillips and Dudik 2008). The model was generated with 200 records of occurrence (locality data) and 19 environmental variables + elevation. Warmer colors represent areas with better predicted habitat conditions; cooler colors indicate less suitable predicted habitats. Dots correspond to occurrence records used to generate the model (white dots show the locations used to "train" the model and purple dots represent the locations used to "test" the model). Left – ENM for the present-day distribution of this species. Right – ENM for the distribution of this species during the last glacial maximum (18,000 years before present).

Figure 1.9: Geophylogeny depicting the geographic distribution of a hypothetical phylogeny of species in the desert regions of western North America. Each colored clade represents a separate genetic lineage within the phylogeny; dots represent collection localities of individuals. The shaded areas represent the major desert regions (Chihuahuan, Great Basin, Mojave, Peninsular Sonoran) as well as the Apache Highlands in AZ/NM/Mexico, the Colorado Plateau, and the Central Valley in CA.

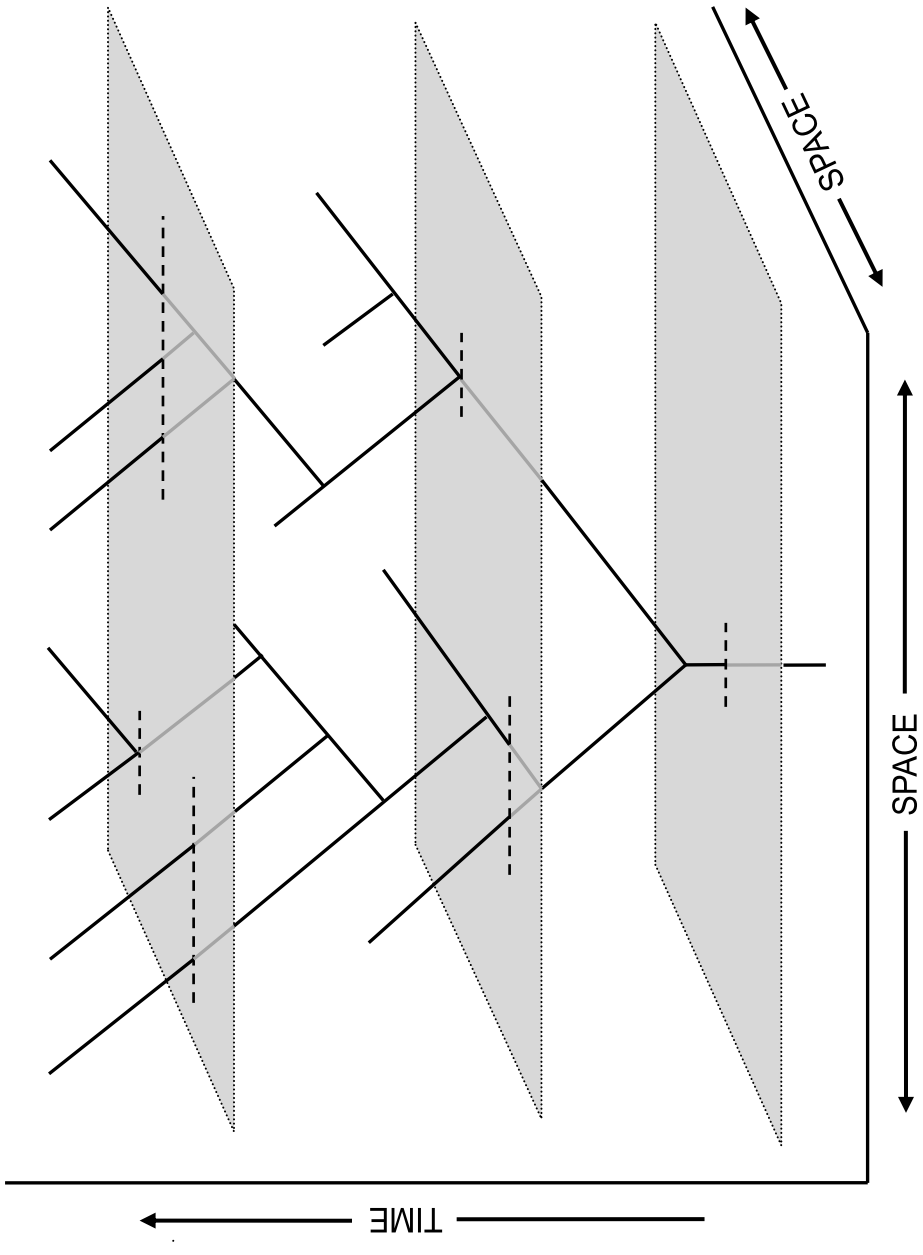

Figure 1.1

Figure 1.2

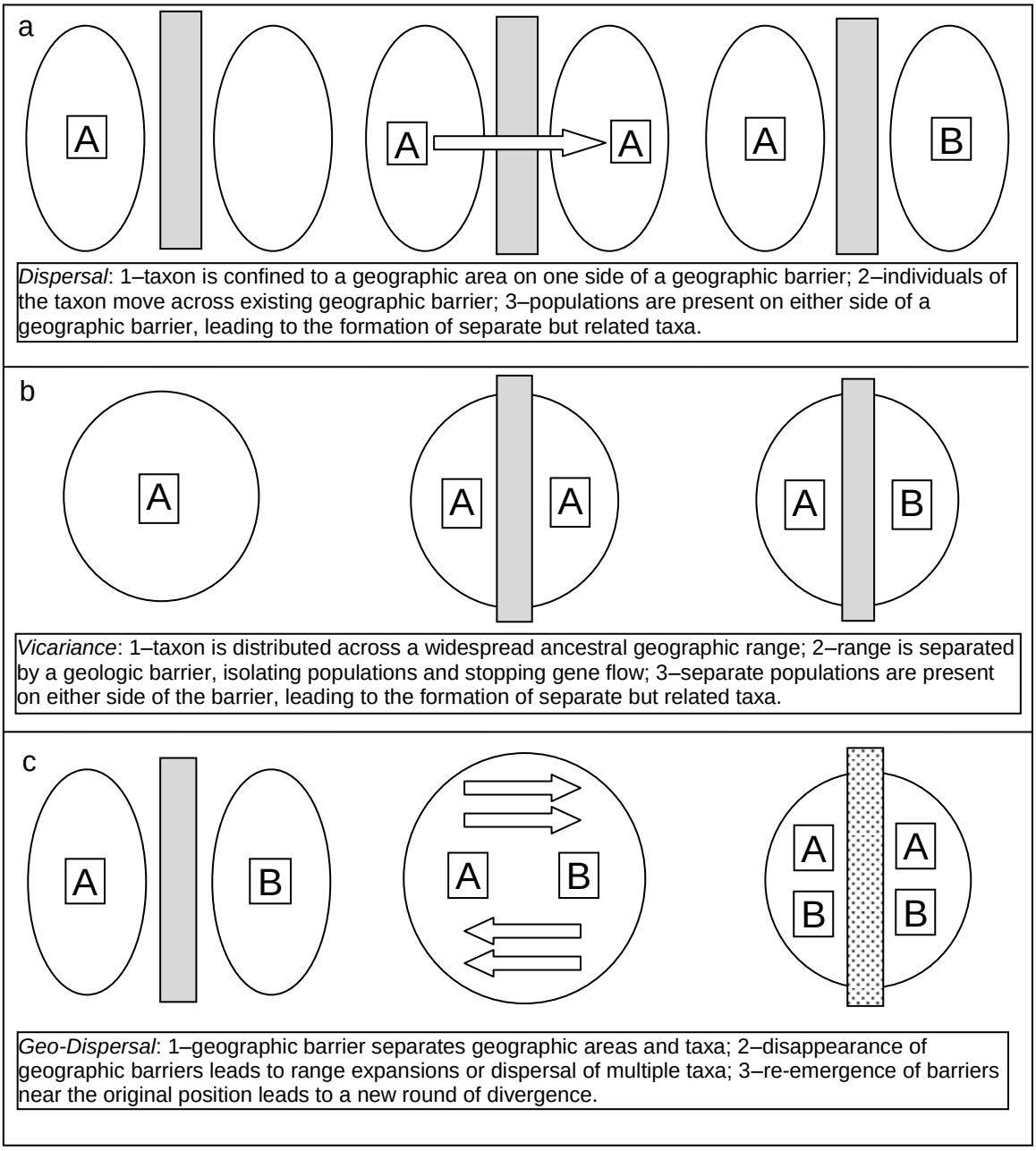
a
A
A
A
A
B
Dispersal: 1–taxon is confined to a geographic area on one side of a geographic barrier; 2–individuals of the taxon move across existing geographic barrier; 3–populations are present on either side of a geographic barrier, leading to the formation of separate but related taxa.
b
A
A
A
A
B
Vicariance: 1–taxon is distributed across a widespread ancestral geographic range; 2–range is separated by a geologic barrier, isolating populations and stopping gene flow; 3–separate populations are present on either side of the barrier, leading to the formation of separate but related taxa.
c
A
B
A
B
A
A
B
B
Geo-Dispersal: 1–geographic barrier separates geographic areas and taxa; 2–disappearance of geographic barriers leads to range expansions or dispersal of multiple taxa; 3–re-emergence of barriers near the original position leads to a new round of divergence.

Figure 1.3

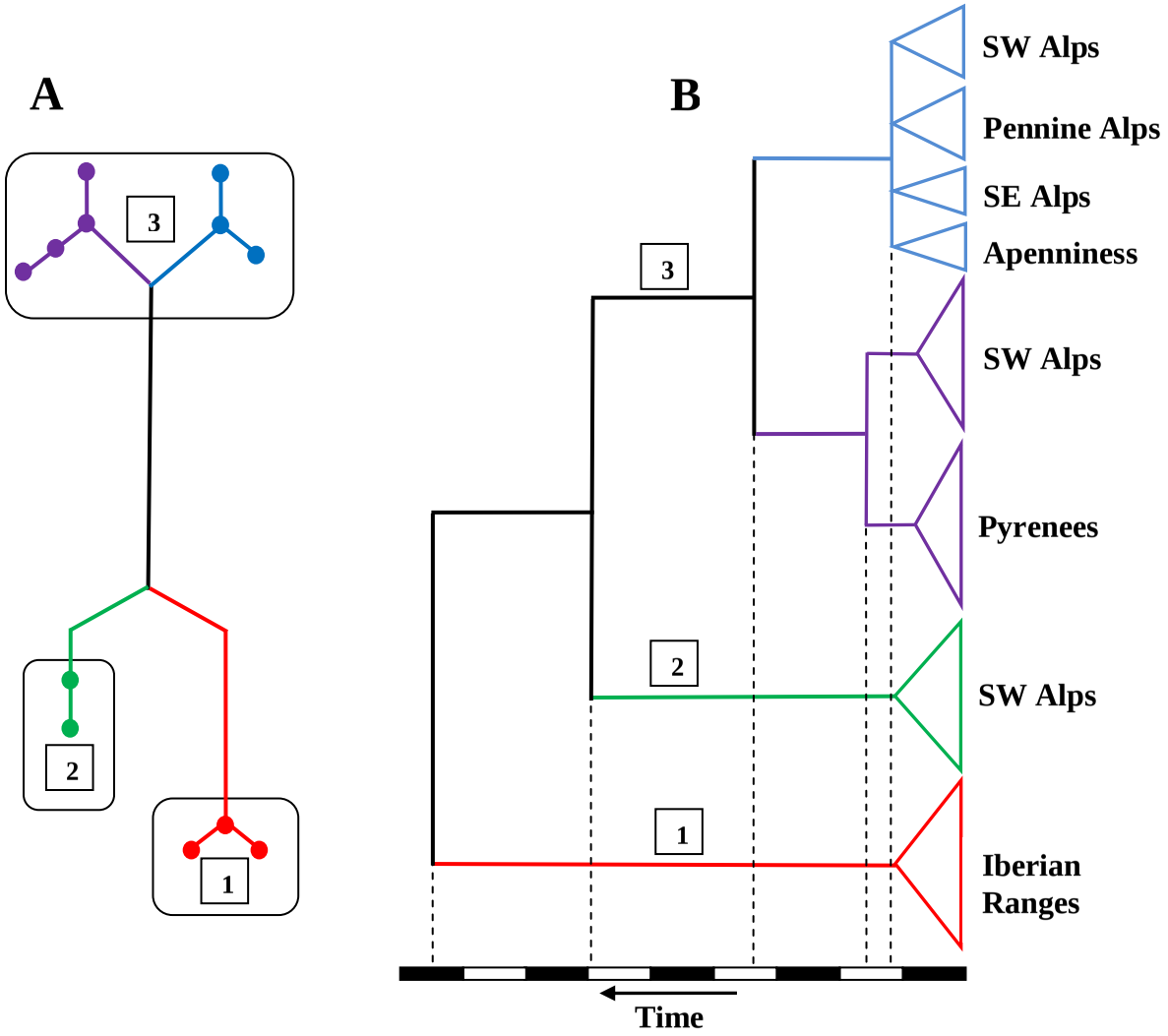
A
3
2
1
B
3
2
1
SW Alps
Pennine Alps
SE Alps
Apenniness
SW Alps
Pyrenees
SW Alps
Iberian
Ranges
Time

Figure 1.4

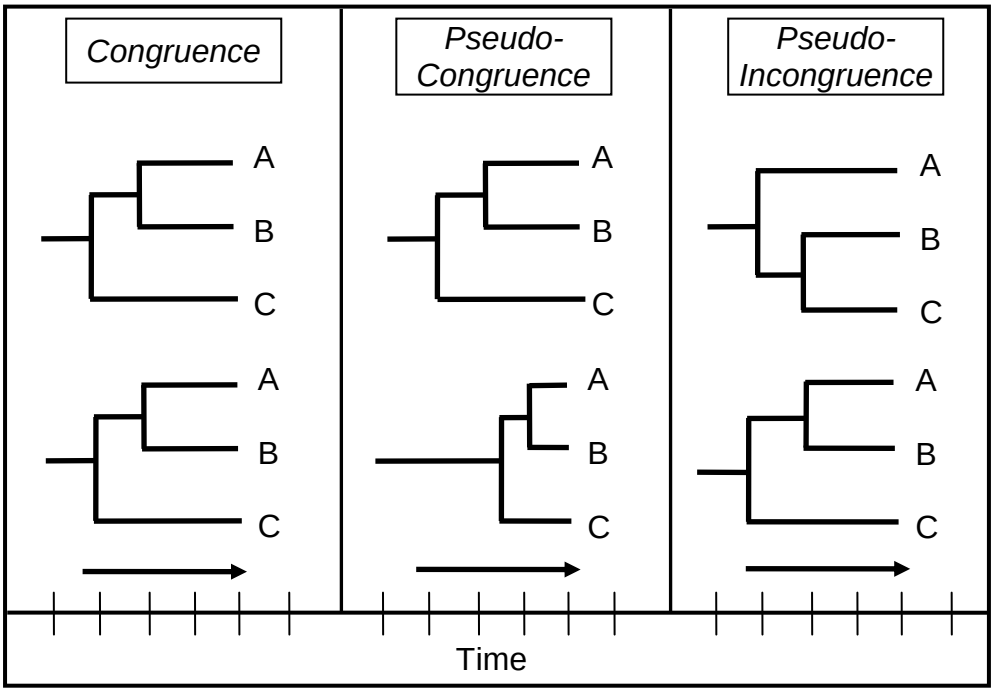
Congruence
Pseudo-Congruence
Pseudo-Incongruence
A
B
C
A
B
C
A
B
C
A
B
C
A
B
C
A
B
C
Time

Figure 1.5

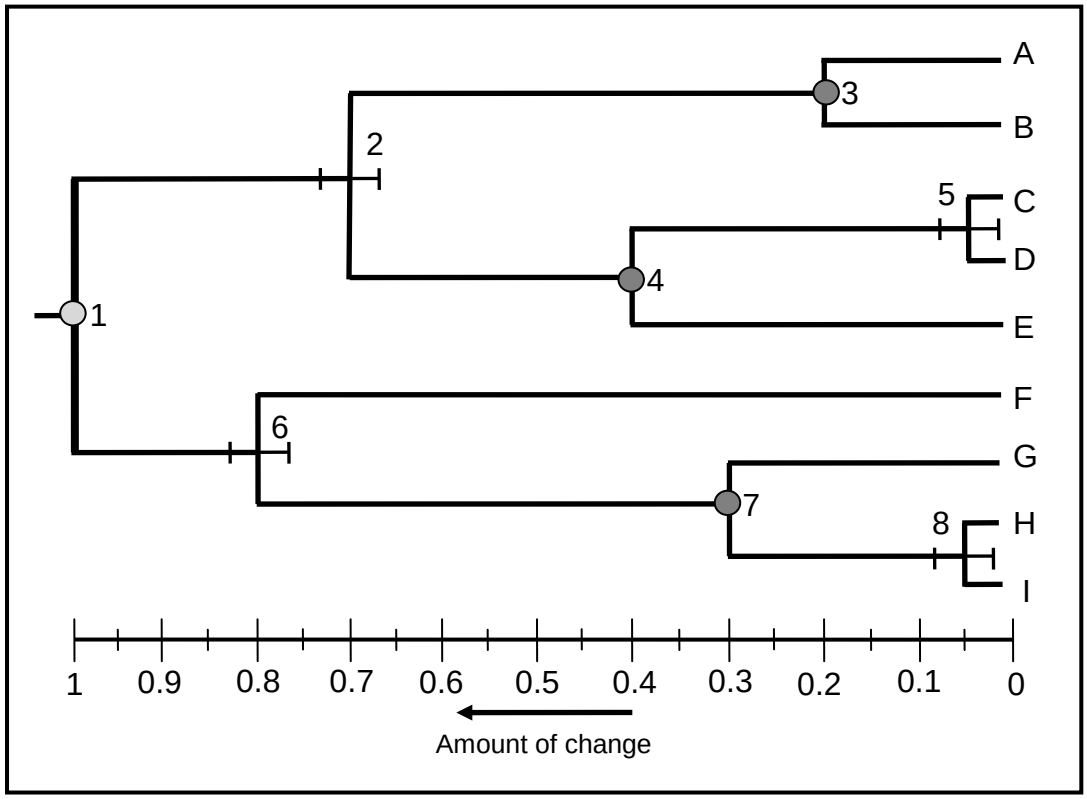
A
3
B
2
5
C
D
4
1
E
F
6
G
7
8
H
I
1
0.9
0.8
0.7
0.6
0.5
0.4
0.3
0.2
0.1
0
Amount of change

Figure 1.6

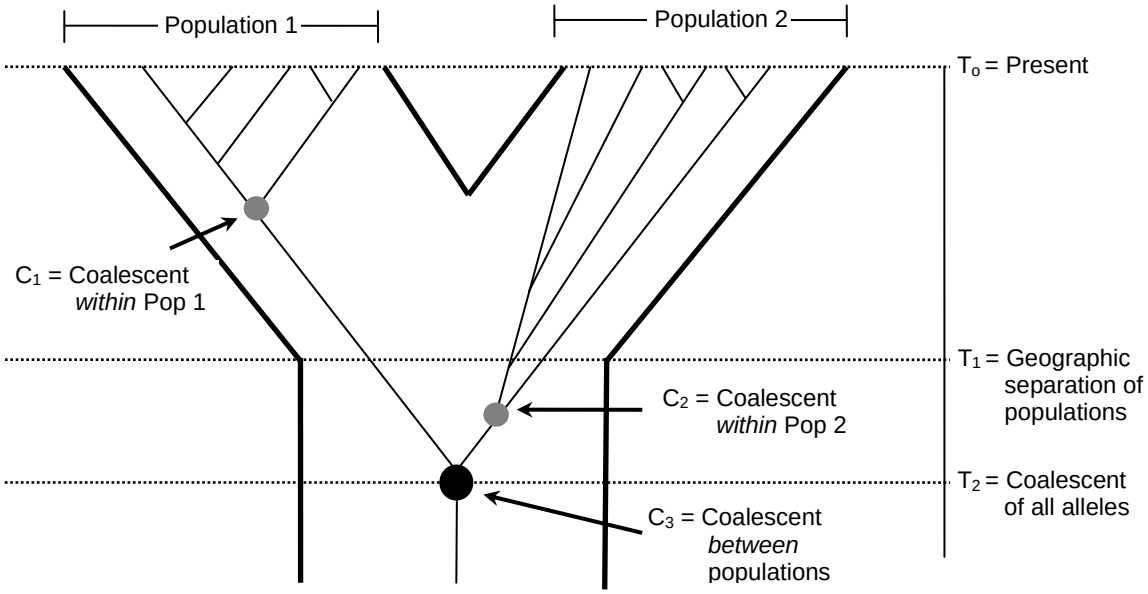
Population 1
Population 2
T_o = Present
C_1 = Coalescent *within* Pop 1
T_1 = Geographic separation of populations
C_2 = Coalescent *within* Pop 2
T_2 = Coalescent of all alleles
C_3 = Coalescent *between* populations

Figure 1.7

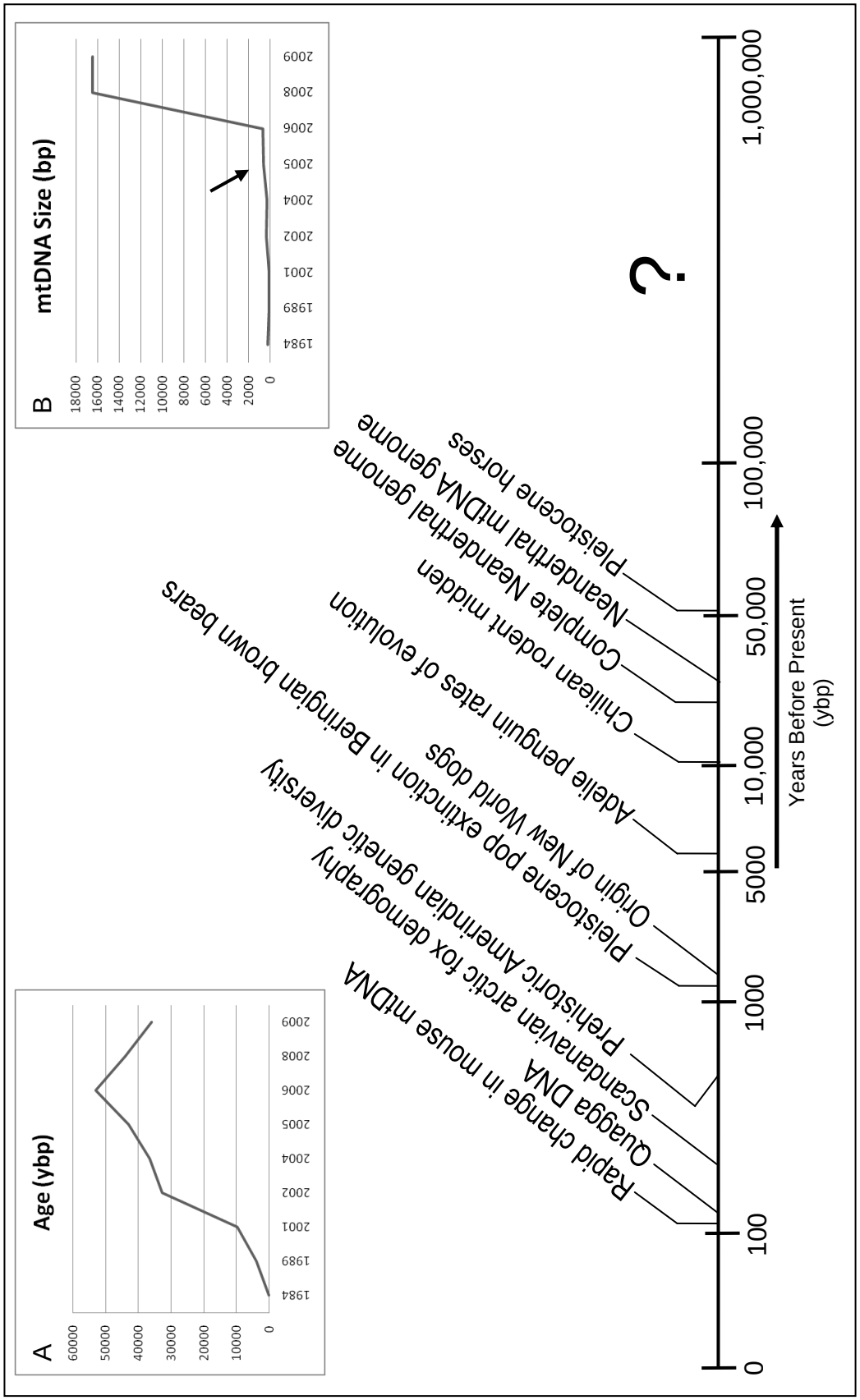
A
Age (ybp)
60000
50000
40000
30000
20000
10000
0
1984
1989
2001
2002
2004
2005
2006
2008
2009
B
mtDNA Size (bp)
18000
16000
14000
12000
10000
8000
6000
4000
2000
0
1984
1989
2001
2002
2004
2005
2006
2008
2009
?
Rapid change in mouse mtDNA
Arctic fox demography
Quagga DNA
Scandanavian Prehistoric Amerindian genetic diversity
Pleistocene pop extinction in Beringian brown bears
Origin of New World dogs
Adelie penguin rates of evolution
Chilliean rodent midden
Complete Neanderthal genome
Neanderthal mtDNA genome
Pleistocene horses
0
100
1000
5000
10,000
50,000
100,000
1,000,000
Years Before Present
(ybp)

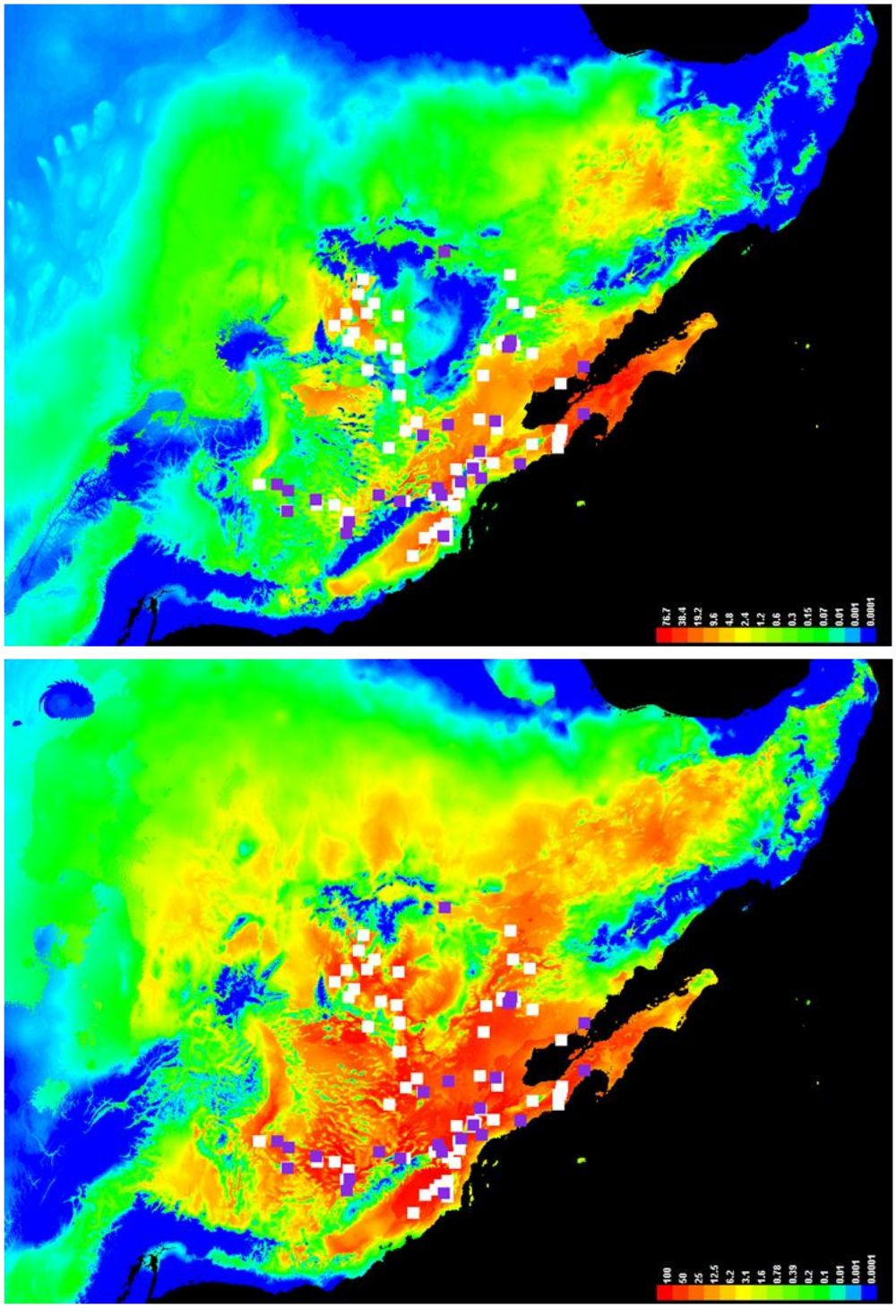
76.7
38.4
19.2
9.6
4.8
2.4
1.2
0.6
0.3
0.15
0.07
0.01
0.001
0.0001
100
50
25
12.5
6.2
3.1
1.6
0.78
0.39
0.2
0.1
0.01
0.001
0.0001

Figure 1.8

Figure 1.9

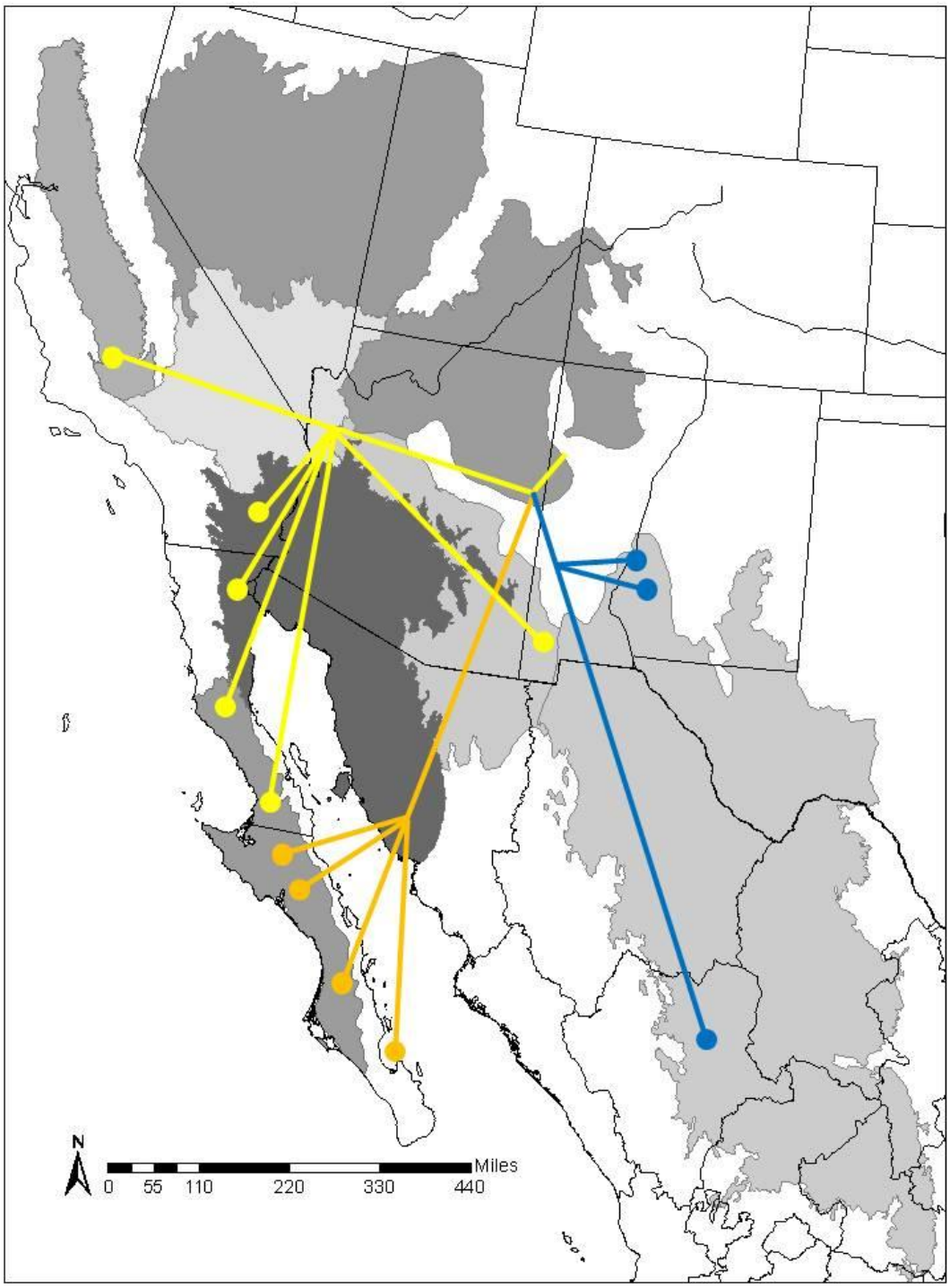

CHAPTER 2

DIVERGENCE AND DIVERSIFICATION OF ANTELOPE SQUIRRELS (GENUS *AMMOSPERMOPHILUS*) IN RESPONSE TO A CHANGING LANDSCAPE IN THE NORTH AMERICAN REGIONAL DESERTS

Introduction

Genetic differentiation within and between species often coincides with significant geological or climatic changes that have shaped species ranges and altered the connectivity between populations over time. As such, we can use a combination of molecular markers with varying evolutionary rates to effectively examine evolutionary and biogeographic histories of populations, species, and regional biotas whose signatures of differentiation are keyed to both older geological events as well as more recent episodes of climatic change.

Within the North American deserts, many endemic taxa experienced high levels of initial divergence associated with geological transformations of the Neogene, with subsequent diversification and geographic structuring of populations associated with climatic changes during the Quaternary (Riddle 1995; Hafner and Riddle 1997). Climatic oscillations throughout the Pleistocene led to repeated cycles of glacial expansion and retreat with the last glacial maximum (LGM) reaching its maximum extent approximately 18,000 years before present (ybp). The distributions of many aridland species show genetic signatures of a history of population isolation and reconnection as well as distribution changes as a result of glacial cycles and the expansion of xeric habitats that occurred subsequent to the LGM. Comparative analyses of similarly distributed species have identified complex patterns of genetic relationships within and between areas of

endemism across the major warm deserts (Riddle and Hafner 2006), but with an underlying signature of congruence across taxa. These complex patterns are the results of both shared and unique responses to various events isolating and reconnecting populations.

The early orogeny of North American western cordilleras initiated the fundamental geologic changes leading to the first signatures of aridification in the early Paleogene and continuing throughout the Neogene (Axelrod 1979; Swanson and McDowell 1984). This series of mountain ranges and plateaus extends along the west coast into central Mexico, blocking the inland movement of precipitation from the Pacific. The Rocky Mountains along with the Sierra Nevada Oriental in eastern Mexico block movement of moisture inland from the Gulf of Mexico (reviewed in Alexander and Riddle 2005). Lack of moisture from both the east and the west led to the formation of the regional deserts: the Chihuahuan, Sonoran, Mojave, and Peninsular warm deserts; and the Great Basin cold deserts and shrublands (Figure 2.1). Semi-arid habitats expanded during a warm interval in the latest Miocene, with a trend toward increasing aridification during a Pliocene cooling and drying trend (Axelrod 1979; Webb 1983). During the late Neogene, the Great Basin and northern extent of the Mojave Desert transformed from woodland savannas into shrub-step. The Mexican Plateau transformed from a semiarid savanna to desert scrub-step woodland, and the Sonoran Desert and southern extent of the Mojave were transformed from semi-desert and thorn-scrub to desert scrub ecosystems (Webb 1977; Levin 1978; Webb 1983; Riddle 1995).

Genetic patterns in a suite of taxa that inhabit the North American deserts have been used to investigate the biogeographic history of this region. Most of these analyses have

focused on taxa distributed primarily in the warm deserts. These include mammals (Riddle et al. 2000a, b; Riddle et al. 2000c; Alvarez-Castañeda and Patton 2004; Bell et al. 2009; Jezkova et al. 2009), birds (Zink et al. 2001; Zink 2002), reptiles (Upton and Murphy 1997; Lindell et al. 2005; Douglas et al. 2006; Leaché et al. 2007; Leaché and Mulcahy 2007), amphibians (Jaeger et al. 2005), spiders (Ayoub and Reichert 2004; Crews and Hedin 2006) and plants (Garrick et al. 2009) as well as fish species bordering warm desert regions (Bernardi and Lape 2005; Reginos 2005). This broad set of exemplar taxa has demonstrated a complex history of vicariance and dispersal, in response to both geologic forces and climatic cycles.

Ammospermophilus (antelope squirrels), represents a distinct genus of five extant species within the rodent family Sciuridae (Tribe Marmotini) that is distributed across the deserts and aridlands of western North America (Hall 1981; Wilson and Reeder 2005). Originally recognized as one of many subgenera within *Spermophilus* (Howell 1938), Bryant (1945) elevated *Ammospermophilus* to the generic level based on diagnostic morphological characters; recent morphological and molecular investigations have upheld this classification (Harrison et al. 2003; Herron et al. 2004; Helgen et al. 2009). Helgen et al. (2009) revised the genus *Spermophilus* and noted that *Ammospermophilus* was not morphologically more distinct from the type *Spermophilus* than any other subgenus originally described by Howell (1938). Subsequent molecular analyses suggested that *Ammospermophilus* is the most divergent genus within the Tribe Marmotini, along with two species of *Notocitellus* (tropical ground squirrels) that are both distributed in Mexico (Harrison et al. 2003; Herron et al. 2004). Under the new taxonomy proposed by Helgen et al. (2009), the genera *Otospermophilus*,

Callospermophilus, *Xerospermophilus*, *Cynomys*, *Poliocitellus*, *Ictidomys*, *Marmota*, *Urocitellus*, and *Spermophilus* (*sensu stricto*) form a sister clade to *Ammospermophilus*/*Notocitellus*. With this most recent generic revision of *Spermophilus*, molecular data were supplemented with morphological analyses and the generic recognitions are warranted (Helgen et al. 2009), but many of the current intergeneric relationships within this tribe remain tenuous at best.

The biogeographic history of species and lineages within *Ammospermophilus* presents an opportunity to add to the growing literature that addresses the development and assembly of the aridlands biota of North America. This genus first appears in the fossil record during the mid-Miocene (approx. 11.5 mya) in southern California (James 1963), prior to expansion of the semi-desert ecosystems during the Pliocene. The depth of this fossil history suggests a causal association between the formation of North American regional deserts and the origin and diversification of *Ammospermophilus*. The current distribution of *Ammospermophilus* spans most of the desert and semi-desert regions in North America (Figure 2.2). The white-tailed antelope squirrel, *A. leucurus*, is the most widespread member of this genus, occurring from the northern Great Basin to the southern tip of Baja California and into central Mexico. This distribution encompasses an ecologically broad area throughout both warm grassland regions in the south and cold shrub-steppe regions in the north.

Recent molecular evidence (Whorley et al. 2004) suggests that populations of *A. leucurus* from the northern Baja California Peninsula expanded northward into the continental deserts, and following an episode of isolation, formed a lineage distinct from a southern peninsular lineage that includes both *A. leucurus* and *A. insularis* (Riddle et al.

2000c; Whorley et al. 2004). These northern populations share a more recent common evolutionary history with *A. harisii*, a morphologically distinct species that is geographically separated by the Colorado River, indicating that *A. leucurus* may represent a paraphyletic assemblage with regard to *A. harisii* and *A. insularis* (Riddle et al. 2000c). Separate analyses of *A. insularis* and populations of *A. leucurus* on islands in the Sea of Cortez suggest that these insular forms are nothing more than isolated populations of *A. leucurus* (Alvarez-Casteñeda 2007). Collectively, these studies suggest that the biogeographic history of *Ammospermophilus* is more complex than what is suggested by the current taxonomy.

While previous studies have examined the phylogeography of select *Ammospermophilus* species (Riddle et al. 2000c; Whorley et al. 2004; Alvarez-Casteñeda 2007), none has sampled individuals from all species and across the broad geographic ranges of the more widespread species. This study represents a more comprehensive examination of the biogeographic and evolutionary history of this genus, with an extensive collection of molecular and distributional data exploring the extent of evolutionary diversification and geographic variation in *Ammospermophilus*. These data are examined in concert with an analysis of habitat evolution throughout the arid regions of western North America, including the impact of the development of regional deserts on faunal evolution and the effects of Pleistocene climatic cycles on recent population histories in the widespread lineages. Early divergence of regional deserts in western North America structured the deeper divergences within *Ammospermophilus*, while the geographic distribution and diversification of genetic lineages within individual species was shaped by Pleistocene climatic oscillations and specifically by range expansions that

followed glacial retreat after the last glacial maximum. Molecular dating methods are used to estimate causal associations between the phylogeny and biogeography of *Ammospermophilus*, and the geological and climatic history North American deserts. The phylogeography of northern and southern clades of *A. leucurus* is examined along with ecological niche modeling to construct habitat models exploring population responses to habitat changes throughout the Pleistocene. Collectively, these analyses allow for a more complete reconstruction of the biogeographic history of *Ammospermophilus* in western North America than has been presented previously.

Materials and Methods

Taxonomic & Genomic Sampling

Tissues were collected from 125 specimens, including representatives of the five nominal species of *Ammospermophilus* (Figure 2.2, Appendix A). A subset of these samples was examined previously (Riddle et al. 2000c) but the current sampling considerably increases the geographic and taxonomic coverage. I included geographically widespread and representative samples for *A. leucurus* (97 individuals, 37 localities), A. *harissii* (9 individuals, 3 localities), and A. *interpres* (9 individuals, 5 localities). Those species with very restricted distributions, *A. nelsoni* and *A. insularis*, are represented by 2 and 3 individuals, respectively. All newly collected individuals were prepared as museum voucher specimens and deposited in the New Mexico Museum of Natural History and Science (NMMNH) and tissue samples were deposited in the NMMNH and the Las Vegas Tissue (LVT) collection at the University of Nevada, Las Vegas (Appendix A). Because of the taxonomic scope and phylogenetic depth of this project, I

examined a suite of mitochondrial genes and non-linked nuclear markers with varying evolutionary rates. Incorporating these different datasets can mitigate stochastic errors resulting from sample size, gene choice, or taxon choice. To explore the extent of geographic variation in *Ammospermophilus*, sequence data was generated from the Cytochrome Oxidase 3 (CO3) gene and the mitochondrial D-loop (within the control region – CR) sequences for 125 individuals of *Ammospermophilus*, including representatives of all five nominal taxa and two outgroup taxa. Based on previous molecular research into the higher level systematic relationships within Sciuridae (Harrison et al. 2003; Mercer and Roth 2003; Herron et al. 2004), representatives of *Cynomys* and *Xeropermophilus* were used as outgroup taxa. In order to examine the systematic relationships of the divergent lineages within the genus, information from the CO3 and CR haplotypes were used to guide a sub-sampling design that included the collection of additional mitochondrial and nuclear sequence data for each major clade within the phylogeny. We generated 5962 base pairs (bp) of DNA sequence data for twenty-two individuals of *Ammospermophilus* and the outgroup taxa, including data from six protein coding genes. This dataset included two nuclear markers, exon 1 of the Interphotoreceptor Retinoid-Binding Protein (IRBP – 1087 base pairs) and the Recombination Activating Gene 2 (RAG2 – 969 bp); three mitochondrial genes, including Cytochrome Oxidase I (CO1, the putative animal DNA barcoding gene – 691 bp), Cytochrome Oxidase 3 (CO3 – 690 bp), and Cytochrome *b* (Cytb – 1140 bp); and two mitochondria-encoded ribosomal genes, the small subunit 12S ribosomal RNA (12S – 832 bp) and the large subunit 16S ribosomal RNA (16S – 550 bp).

Laboratory Protocols

For each specimen, total genomic DNA from liver or kidney tissues was extracted following either a lysis buffer protocol (Longmire et al. 1997) or a Qiagen DNeasy Tissue Extraction Kit (Qiagen, Inc.). We amplified the seven molecular markers using the polymerase chain reaction (PCR) with gene specific primers and temperature profiles (Table 2.1). Double- stranded PCR products were qualitatively examined using a 0.8% agarose gel with a molecular mass ruler for size comparison. The amplified PCR fragments were purified using either GeneClean II Kit (BIO 101, Inc.), Qiaquick PCR Purification Kit (Qiagen, Inc.) or Exo-SAP IT (USB Corp.), following manufacturers' protocols. The purified PCR fragments (including both the light and heavy DNA strands) were sequenced using the ABI PRISM BigDye v.3.1 Cycle Sequencing chemistry (Applied Biosystems, Inc.), using the sequencing primers identified in Table 2.1. Unincorporated dye-teminators were removed using Sephedex spin columns (Centri-Sep, Inc.) and sequence data were generated on either on an ABI 310 or 3130 Genetic Analyzer (Applied Biosystems, Inc). I unambiguously aligned complementary strands of each gene using SEQEUNCHER 4.9 (Gene Codes Corp.), followed by manual proofreading. The protein coding sequences were translated into amino acids using MACCLADE 4 (Maddison and Maddison 2005) and compared to *Rattus* and *Mus* to confirm the correct reading frame and to check for the presence of stop codons.

Phylogenetic Analysis – Multigene Dataset

To examine the species level relationships of all of the nominal species and the major genetic lineages of *Ammospermophilus*, maximum-likelihood (ML) and Bayesian inference (BI) analyses were performed on the combined 5.2 kb dataset. The Akaike

Information Criterion (AIC; Akaike 1973) implemented in JMODELTEST 0.1.1 (Guindon and Gascuel 2003; Posada 2008) with default parameters and ML optimizations, was used to choose the appropriate models of sequence evolution. Recent work has indicated the superiority of the AIC over hLRT, especially when implementing model-averaged inference. TREEFINDER (Jobb et al. 2004) was used to perform the ML analyses using the model chosen in JMODELTEST and calculate bootstrap values after 1000 replicates; typically, boostrap values ≥ 70 signify a well-supported clade (Hillis and Bull 1993) and I follow these recommendations when assessing the realiability of a particular clade reconstructed in the ML analyses.

I used the selected models in MRBAYES 3.1.1 (Huelsenbeck and Ronquist 2001; Ronquist and Huelsenbeck 2003) for BI, incorporating Bayesian posterior probabilities as evidence of nodal support. MCMC Bayesian analyses were run for $4x10^6$ generations using the default parameters of four Markov chains per generation, with random starting trees and subsequent trees sampled every 100 generations. I assessed the stationarity of the analyses by examining the stabilization of cold chain likelihood scores and parameter estimates using Tracer 1.4.1 (Rambaut and Drummond 2007). The convergence of runs was assessed by examining the posterior probabilities of clades for non-overlapping samples of trees using AWTY (Wilgenbusch et al. 2004). After excluding those trees generated during the "burn-in" period prior to stable equilibrium (10000 trees), a 50% majority-rule consensus tree was generated. The frequency of each recovered clade represents the posterior probability (PP) of that clade as evidence of support for a particular node in the analysis. Typically, those nodes with $P \geq 95\%$ indicate significant support for a particular clade (Huelsenbeck and Ronquist 2001). A clade is considered as

well-supported only if both the ML bootstrap value and the posterior probability met or exceeded the values typically indicative of strong support.

Model-based approaches to phylogenetic inference can be problematic if a single model is used across a multi-gene dataset, especially when including unlinked loci. A single model may represent a compromise of the properties of the different loci and inadequately represent each, potentially generating phylogenetic uncertainty (Yang 1996; Brandley et al. 2005). Mixed-model or partitioned analyses can be used to attempt to more accurately describe the evolutionary properties of the data, but these approaches can result in analyses of very reduced datasets with fewer characters available to each partitioned analysis (Yang 1996; Brandley et al. 2005). To examine the impacts of single model versus mixed-model approaches to phylogeny estimation, multiple Bayesian searches were performed: one without data partitions using a single model of nucleotide evolution (P_1) for the entire dataset, a second search with two partitions representing the nuclear and mitochondrial DNA (P_2), and a third search that partitioned each of the six gene regions separately (P_7). The notation follows that of Brandley et al. (2005) and Matocq et al. (2007), where "P" indicates the data partition, followed by a number indicating the number of partitions in that analysis. Following the methods of Matocq et al. (2007), the performance of various models of nucleotide evolution was evaluated with the different data partitions using the AIC (Table 2.2), as implemented in JMODELTEST 1.0 (Posada 2008).

Estimating Divergence Times

The use of molecular clocks and molecular dating techniques has been a contentious issue in recent evolutionary studies (Hedges and Kumar 2003; Graur and Martin 2004;

Hedges and Kumar 2004). Advances in this field, including the increased sophistication of computer algorithms and models with relaxed assumptions about the generality of molecular rates within phylogenies, has strengthened the case for use of molecular dating techniques and their utility in unraveling the evolutionary history of organisms. To obtain divergence time estimates for the 5.2 kb dataset of *Ammospermophilus* (22 individuals, 5 species), a Bayesian approach was used with an uncorrelated lognormal relaxed clock model, implemented in BEAST v.1.4.8 (Drummond et al. 2006; Drummond and Rambaut 2007). Given the difficulty in performing these analyses with unlinked markers, the 7-gene data set was partitioned into three separate alignments: one alignment contained a concatenated dataset with 4 mitochondrial protein-coding genes and the two ribosomal genes (all linked within the mitochondrial genome), a second alignment with only the IRBP data, and a third alignment included the RAG2 sequences. These two nuclear genes were added as separate unlinked partitions. JMODELTEST (Guindon and Gascuel 2003; Posada 2008) was used, with AIC parameters, to choose a model of sequence evolution for each separate alignment as well as to estimate priors for several model parameters (e.g., gamma shape, GTR substitutions, proportion of invariant sites, etc.). Using the selected models of sequence evolution, the Yule process of speciation model was used to set the prior on the tree.

To establish divergence estimates on the nodes in a phylogeny, a method of calibration for the tree must be set. This calibration point typically involves the use of fossil data that have been identified as belonging to a specific branch on a tree. For this phylogeny, *Ammospermophilus fossilis* was used, identified from the Clarendonian North American Land Mammal Age (NALMA – 13.6 mya to 10.3 mya) of the Cuyama Valley

in southern California (James 1963), as the stem node calibration. This fossil was identified as an ancestral form, though the genus had already taken nearly modern form by this time (James 1963). While multiple calibration points, (i.e., multiple fossils) can decrease the errors associated with time estimates on other nodes of the tree, a single calibration point is minimally required. The proper placement of fossil calibrations is an important issue (Hedges and Kumar 2004; Ho et al. 2008; Forest 2009).

Within this phylogeny, the *Ammospermophilus* clade represents the crown group and the node connecting with the outgroup taxa represents the stem node. By rooting at the stem of *Ammospermophilus*, the minimum constraint on the outgroup node is established, and yields a conservative estimate for minimum divergence time within *Ammospermophilus*. If the calibration was placed at the basal node to all *Ammospermophilus*, the results would be divergence time estimates that are much older (Forest 2009). For this analysis, the fossil calibration is placed at the stem node. This placement is further supported by a Mid-Miocene estimate of the divergence of *Ammospermophilus* from the outgroup taxa (*Cynomys* and *Xerospermophilus*), generated from several independent and external fossil calibrations throughout the sciurid phylogeny (Mercer and Roth 2003). The Markov Chain Monte Carlo (MCMC) chains in BEAST were run for 4×10^7 generations, sampling every 1000 generations, discarding the first 4×10^6 (10%) generations as burn-in, before the analysis reaches stationarity. TRACER (Rambaut and Drummond 2007) was used to ensure proper mixing of the chains and to ensure that the analyses reached stationarity. To increase the effective sample size (ESS – the number of independent samples or chain length, excluding the burn-in) values, the analysis was repeated and the data from the two separate runs were combined.

Because of the uncertain placement of *A. fossilis* in relation to the systematic relationships of extant *Ammospermophilus* species, two additional calibration methods were tested to compare divergence estimates within the phylogeny. Using the same MCMC BEAST method (described above), the fossil calibration was applied to the basal node (crown group) of *Ammospermophilus* divergence and divergence dates were estimated for all other nodes. An independent (non-fossil based) estimation of divergence dates was performed in which only the Cytochrome *b* (Cytb) sequence data was used along with a standard mutation rate of 2%/My (0.01subs/site/My) (Arbogast and Slowinski 1998). JMODELTEST 0.1.1 (Guindon and Gascuel 2003; Posada 2008), with default parameters and ML optimizations, was used to choose the appropriate models of sequence evolution for the Cytb dataset using the AIC (Akaike 1973). This calibration method included a relaxed clock (uncorrelated exponential) along with a coalescent model of exponential growth. This MCMC chains in BEAST were run for 4×10^7 generations with a GTR+Γ model of sequence evolution, sampling every 1000 generations, discarding the first 4×10^6 (10%) generations as burn-in. TRACER (Rambaut and Drummond 2007) was used to ensure proper mixing of the chains and to ensure that the analyses reached stationarity and determine the amount of burn-in to exclude from the final analysis.

Phylogeographic & Population Genetic Analyses

The geographic distribution of genetic lineages within *Ammospermophilus* was examined by determining the phylogeographic patterns in the wide ranging *A. leucurus*, as well as individuals for each of the other nominal species. For these analyses, variation within a portion of the protein-coding CO3 (691 bp) and non-coding CR (503 bp) from

the mitochondrial genome was examined. Sequence data was generated for 125 individuals of *Ammospermophilus*, which included 97 *A. leucurus* samples taken from localities throughout the range of this species, as well as 9 *A. harrisii*, 3 *A. insularis*, 9 *A. interpres*, and 2 *A. nelsoni*. The major clades within this species were assessed using a ML phylogenetic analysis with non-parametric bootstrapping (100 replicates; Felsenstein 1985), implemented in TREEFINDER v.2008 (Jobb et al. 2004) Additionally, Bayesian Inference was used, implemented in MrBayes v.3.1.2 (Ronquist and Huelsenbeck 2003) with posterior probabilities as evidence of support for clades. To identify the most appropriate model of nucleotide evolution chosen under AIC, JMODELTEST 0.1.1 (Guindon and Gascuel 2003; Posada 2008) was used and default parameters with ML optimization (Posada and Crandall 1998; Posada and Buckley 2004). These molecular markers were concatenated and from these initial JMODELTEST analyses, the GTR+I+Γ model of nucleotide evolution was chosen for the combined dataset. MRBAYES was run for 10×10^6 generations with an initial burn-in of 2×10^6 generations (25,000 trees) with 4 Monte Carlo Markov chains and a temperature value of 0.05 to promote proper swapping of the chains. As in the multigene phylogenetic analysis, the proper convergence of runs was estimated by examining the posterior probabilities of clades for non-overlapping samples of trees using AWTY (Wilgenbusch et al. 2004).

Additionally, I created a median-joining network, produced by the program NETWORK (Bandelt et al. 1999), to visualize the relationships among haplotypes from all species. This method addresses the problems found with intraspecific datasets with large sample sizes and short genetic distances between samples. Median-joining networks are modified minimum-spanning networks that use a maximum parsimony approach to find

the shortest possible network to explain the relationships between the individuals (Bandelt et al. 1999). Based on the results on the phylogenetic analysis, demographic parameters were estimated for each major geographic cluster of *A. leucurus* haplotypes. These parameters include nucleotide diversity (π), haplotype diversity (*h*), and Tajima's *D* (Tajima 1989). Mismatch distributions, an assessment of the relative frequency of haplotypes, were created using DNASP 5.0 (Rozas et al. 2003). Based on the results of the multi-gene and CO3/CR phylogenetic analyses, three geographically structured clades of *A. leucurus* were analyzed separately. It is important to estimate these demographic parameters separately because these genetic lineages may have experienced separate evolutionary histories ultimately leading to different population genetic patterns.

Ecological Niche Modeling – Current & Paleo-distributions

To explore the generalized distributional changes over time to explore the connection with the demographic properties in populations since the LGM, ecological niche models were constructed for each major lineage of *Ammospermophilus* using occurrence records and climatic conditions both at present (0 kya) and during the LGM (18 kya). This dataset included occurrence records of individuals examined in this study (see Appendix A) as well as a subset of available records listed in MaNIS (http://manisnet.org/). The maximum entropy method implemented in MAXENT 3.2.1 generates these models (Phillips et al. 2006a; Phillips et al. 2006b). MAXENT is designed to find distributions among climatic variables and digital environmental layers to predict logistic non-negative probabilities based on presence-only occurrence data (Stockman and Bond 2007). Niche conservatism is the underlying assumption of this method, indicating that the environmental variables required by the species have remained relatively unchanged over

time. This method has been shown to outperform similar habitat estimators (Phillips and Dudik 2008; Elith and Graham 2009) and has been used in several recent phyloclimatic studies (Carstens and Knowles 2007; Waltari and Guralnick 2009). The predictions for this analysis are based on elevation plus a suite of 19 bioclimatic parameters previously compiled from the WorldClim climate layers (Hijmans et al. 2005; Waltari et al. 2007), with a 5 km^2 pixel resolution.

Model calibrations were performed using 75% of the data as a training group and then the predicted distribution models were tested with the remaining 25% (Evans et al. 2009). Default parameters were used (500 maximum iterations, convergence threshold of 0.00001, regularization multiplier of 1, 10000 background points) with a random seed, the removal of multiple presence records from individual cells resulting from many sampling localities within 5km^2 (i.e., one pixel), and logistic probabilities for the output (Phillips and Dudik 2008). A split-sample approach to separate the geographically closest sample pairs between the training and test groups reduces the effects of spatial autocorrelation (Fielding and Bell 1997; Parolo et al. 2008).

A complete model (including all 20 variables) was initially run to produce "area under the receiver operation characteristic curve" (AUC) values for each bioclimatic parameter. A minimum AUC of 0.75 for the test group is considered the threshold for good model performance (Elith et al. 2006; Suárez-Seoane et al. 2008; Elith and Graham 2009). Consequently, those parameters with AUC values less than 0.75 were removed. Reduced models were run using temporal transfer modeling from the current distribution (0kya) to the LGM (20kya), incorporating information in the Community Climate Model System Model (CCSM – Otto-Bliesner et al. 2006) and the Model for Interdisciplinary

Research on Climate (MIROC – Hasumi and Emori 2004). MaxEnt analyses were performed three separate times using both the CCSM and MIROC climate reconstructions and the habitat models results from both were averaged, accepting only those areas that both methods agreed were suitable (Waltari and Guralnick 2009). Averaging the three independent MaxEnt runs using the Spatial Analyst feature in ArcGIS produced presence/absence binary habitat models using ArcGIS 9.2 (ESRI Corp., Redlands, CA). Because the suitability of the predictive area in the models is based on chosen cut-off values, the models were evaluated across four logistic thresholds: fixed cumulative value of 10.0, equal training sensitivity and specificity, equal test sensitivity and specificity, and equate entropy of thresholded and non-thresholded distributions. These threshold values were used to assess a range of sensitivities and specificities to ensure that our model interpretations are robust. Ultimately, the chosen cutoff of suitable habitat had a fixed cumulative probability of 10, a level that rejects the lowest 10% of predicted logistic values. This value, though conservative, maintained a low omission rate (Pearson et al. 2007) consistent with the expectation that the occurrence records contain georeferencing errors.

Results

Phylogenetic Analyses

The total alignment for phylogenetic analysis contained 5962 nucleotides and contained complete or near complete portions of 7 genetic loci (3903bp mtDNA [2521bp mtDNA, 1382bp rDNA], 2056bp nDNA). Initial analyses indicated variable numbers of informative sites/gene: CO1: 76/557bp; CO3: 115/690bp; Cytb: 173/1143bp; 12S:

54/832bp; 16S: 36/550bp; IRBP: 43/1087bp; Rag2: 17/969bp. Both ML and BI phylogenetic analysis of the concatenated dataset resulted in a phylogenetic tree with several well-supported clades (Figure 2.3). The results were consistent between both ML and BI analyses and the three separate partitioned BI analyses all converged on identical topologies in the final analyses with similarly well supported nodes. Parameter estimates for these partitioned BI analyses are reported in Table 2.2. The phylogenetic tree is separated into three major lineages. One lineage is composed of *A. nelsoni*, *A. leucurus* samples from northern Baja California and continental populations, and *A. harrisii*. Lineages of *A. leucurus* from southern Baja California form a well-resolved clade with *A. insularis*, which is not surprising given results reported previously (Alvarez-Casteñeda 2007). A third, well-supported major clade was composed only of *A. interpres*. All three major clades are connected via an unresolved basal polytomy. While the monophyly of *Ammospermophilus* is clearly supported, the relationship between the three major clades within this genus is unclear. The unresolved nature of these clades may reflect a real attribute of the evolutionary history of these lineages, representing a rapid burst of divergence and diversification in *Ammospermophilus*. Analyzed separately, the mitochondrial phylogeny maintains the same topology as the combined mitochondrial and nuclear phylogeny. Analysis of the nuclear dataset alone confirms the monophyly of *Ammospermophilus*, but does not show support for any structure within the genus (results not shown). Importantly, these data do not conflict with the mitochondrial results.

Divergence Time Estimates

The molecular time estimates within our phylogeny provide plausible divergence time estimates. A potentially complicating factor regarding the certainty surrounding the

divergence time estimates also depends on whether the fossil is of an ancestral (i.e., extinct) or extant lineage. For any given divergence, the minimum time estimate is correlated with the age of the geologic formation containing the fossil and the time of divergence cannot be younger than the age of that calibrated fossil (Hedges and Kumar 2004). Greater accuracy in the molecular time estimates can be obtained with at least one tightly constrained fossil calibration close to the speciation event and we have a well-dated fossil of *Ammospermophilus*. Our divergence estimates represent mean divergence times for each node surrounded by 95% confidence intervals of certainty.

Divergence time estimates based on the most resolved, concatenated phylogeny of *Ammospermophilus* were calculated (Figure 2.4, with 95% confidence intervals). The fossil history of this genus (based on *A. fossilis*) is known to extend at least into the Clarendonian NALMA (13.6 to 10.3 million years ago) of the mid-Miocene (James 1963), so a relaxed clock method was used to conservatively calibrate the stem node of the phylogeny at 11.14 (95% CI: 9.99 – 13.25) million years ago (my) to capture the extent of the Clarendonian. This calibration was applied to the stem node of the phylogeny (Figure 2.4, Node A). A separate model of sequence evolution was applied for each partition. Mean genetic divergence of the three major clades is estimated to have occurred at 4.13 my (2.11 – 6.6). The major time of diversification and divergence within major lineages of *Ammospermophilus* occurred throughout the Neogene (Figure 2.4, Table 2.3). The time to the most recent common ancestor (tmrca) of *A. interpres* is estimated to have occurred in the early Pleistocene at 2.91 my (0.47 – 3.75). The divergence estimate between *A. nelsoni*, with a tmrca of 0.15 my (0.03 – 0.92), and northern *A. leucurus*/*harrisii* is estimated to have occurred at 3.58 my (1.34 – 4.66) and

the divergence between *A. harrisii* and the northern *A. leucurus* is estimated at 2.01 my (0.95 – 3.69). The tmrca of southern *A. leucurus* and *A. insularis* was estimated at 2.52 my (0.99 – 4.25) while the tmrca of *A. insularis* samples was estimated at 0.64 my (0.02 – 1.13), placing this divergence event near mid-Pleistocene, along with the diversification of *A. nelsoni*.

To further examine the robustness of these divergence times, two additional estimation methods were used. The fossil (*A. fossilis*) calibration was placed at the base of the *Ammospermophilus* diversification (Figure 2.4, Node B) and the analysis was repeated to estimate divergence time. By changing the calibration point, divergence of *Ammospermophilus* from the outgroup taxa was estimated to have occured at 25.21 my (95% CI: 11.19 – 41.24 mya). The divergence of several nodes within the phylogeny have been pushed farther back in time (Table 2.3), but many of the dates are close to the estimates generated with the placement of fossil calibration on the stem node. An additional method of molecular dating incorporated a Cytb relaxed clock method (2%/my) without the reliance on a fossil calibration to estimate the coalescence dates of each of the major nodes in the phylogeny. This method indicated a high level agreement with the placement of the fossil calibration at the stem node of the phylogeny (Figure 2.4, Node A), indicating that *Ammospermophilus* diverged from the outgroup taxa at approximately 12.45mya (6.21 – 23.68). This method also indicated a basal divergence among the major *Ammospermophilus* lineages at 5.13 mya (1.19 – 5.18), again consistent with the placement of a fossil calibration at the stem node of the phylogeny (Table 2.3). Pairwise sequence divergence within Cytb was calculated between each of the major lineages (Table 2.4) providing additional evidence for the relatedness among these

lineages. These comparisons indicate 3–4% divergence between the major clades of *Ammospermophilus*, consistent with interspecific genetic distances in a variety of mammalian taxa (Bradley and Baker 2001). The divergence values calculated between *A. harrisii*, *A. nelsoni* and northern *A. leucurus* or between *A. insularis* and southern *A. leucurus* are less than 2%, often indicative of intraspecific variation (Bradley and Baker 2001). While there is some disagreement among the exact divergence time estimates for many nodes across these three calibration methods, there is a high degree of overlap of many of the divergence ages, especially given the confidence intervals. This suggests that the divergence estimates are fairly robust and accurately reflect the evolutionary history of *Ammospermophilus*.

Phylogeographic Patterns

The HKY+*I*+*Γ* model of nucleotide evolution was chosen for the combined CO3 and CR dataset (-lnL = 55965.4746) with a proportion of invariant sites = 0.4770, a gamma shape parameter (α) = 0.4710, kappa = 10.5547 and the following base frequencies: A = 0.3063, C = 0.2611, G = 0.1197, and T = 0.3130. For the molecular markers, the numbers of informative sites/gene were 130/691bp for CO3 and 114/503 for the CR. Analyses of the phylogeographic patterns of the CO3 and CR sequence data indicate a significant amount of phylogeographic structure within *Ammospermophilus*. The phylogenetic relationships within this dataset (Figure 2.5A, Figure 2.6) are consistent with the multigene dataset (Figure 2.3), recovering the same three well-supported major lineages of *A. interpres (interpres* clade), *A. insularis* + *A. leucurus* (southern *leucurus* clade), and *A. harrisii* + *A. nelsoni* + *A. leucurus* (from the continental US) + *A. leucurus* (from northern Baja California). The distribution of sampling localities for the expanded

mtDNA dataset is shown in Figure 2.5B. This phylogeny indicates *A. harrisii* is polyphyletic. Samples of *A. harrisii* collected from Sonora, Mexico and one sample from eastern Arizona are basal to a clade that contains all other *A. harrisii* as well as *A. nelsoni* and the two geographically separate clades of *A. leucurus*. Western samples of *A. harrisii* were not included in the multigene dataset (Figure 2.3). Samples of *A. insularis* were nested within the southern *leucurus* clade (Figure 2.6). Relationships between samples within each of the three major clades lack resolution (based on posterior probabilities and bootstrap values), indicating the relatively recent diversification within each lineage, despite the use of the more rapidly evolving mitochondrial control region. These results are consistent with the three major clades reported in Riddle et al. (2000c) based on only CO3 mtDNA sequences. However, this previous dataset did not include representatives of *A. nelsoni* or northern *A. leucurus* from the Great Basin.

Haplotypes within each major lineage of *Ammospermophilus* reveal a more consistent geographic picture of each of the major lineages. The haplotype network (Figure 2.5C) indicates several conserved and geographically separated haplotypes in southern Baja California, northern Baja California, and the continental US. While fewer samples are represented for each of the other nominal species and the haplotype network indicates multiple haplotypes within each of these species. Each of the major lineages is recovered in the haplotype network and it also indicates a separation within *A. harrisii* (Figure 2.5C). This pattern is consistent with separation of *A. harrisii* samples in the phylogenetic tree (Figure 2.7). The haplotype network supports the close relationship between *A. insularis* and southern Baja California *leucurus*.

Population Genetic Patterns

The population genetic patterns within each of the major geographically restricted lineages of *A. leucurus* were assessed for the combined CO3 and CR dataset. Three distinct lineages within *A. leucurus* are evident in the phylogenetic and haplotype network analyses. These lineages correspond to the continental US (Figure 2.6, Clade A), northern Baja California (Clade B), and southern Baja California (Clade C). Demographic parameters were calculated for each clade separately, but all show similar results. These values indicate (Figure 2.7) each clade has low nucleotide diversity (A: 0.0019, B: 0.00319, C: 0.00315), high haplotype diversity within the Baja California populations (B: 0.889, C: 0.805) and moderately high haplotype diversity within the continental US populations (A: 0.616). Additionally, Tajima's *D* values for each of these clades was significantly negative (A: -2.16215, B: -1.87675, C: -2.16208). The estimate of Tajima's *D* compares the average number of pairwise polymorphisms against a null model of neutral evolution (Tajima 1989). Significantly negative values provide evidence of population expansion. Collectively, the demographic properties of these lineages suggest that the all populations of A. leucurus have undergone recent expansions from smaller ancestral populations leading to an excess of low frequency polymorphisms. Mismatch distributions of haplotypes from each lineage also were used to test the stability of each clade. These distributions analyze the empirical pairwise frequency differences of haplotypes against a Poisson distribution of expected frequencies. These analyses (Figure 2.7) indicate a unimodal distribution of haplotypes for all three clades. This is consistent with the demographic parameters and with a model of recent demographic expansion. These results are somewhat consistent with the data reported by

Whorley et al. (2004), who found evidence of population expansion two clades of *A. leucurus*, though their analyses grouped samples from northern Baja California and the continental US together. While my analyses indicate that all lineages of *A. leucurus* have recently expanded, the geographic separation of northern Baja California samples from continental US samples seems warranted given the results of both the phylogenetic analyses and the haplotype network. These lineages may have collectively experienced population expansion, but from different refugial areas and at different rates over time.

Ecological Habitat Models

The phylogenetic and phylogeographic analyses of our data indicate a divergence of major lineages within *Ammospermophilus* into three well-supported clades (*interpres*, *leucurus* north, and *leucurus* south). Given the allopatry of the lineages and individuals within each of these clades, separate habitat models were generated for each. Occurrence records were partitioned by clade and geographic location and there was no overlap of the samples into these three separate models. In addition to the samples used in the genetic portion of this study, occurrence records from MaNIS were also included. We assigned 44 records to the *interpres* clade, 255 records to the *leucurus* north clade, and 50 records to the *leucurus* south clade.

The results of all models were significantly better than random samples (AUC = 0.5) in receiver operating characteristic analyses (*interpres* clade: training AUC = 0.977, test AUC = 0.962; *leucurus* north clade: training AUC = 0.960, test AUC = 0.950; *leucurus* south clade: training AUC = 0.996, test AUC = 0.995). For the *leucurus* north clade, the present-day habitat model (Figure 2.7A) indicates continuous, high quality habitat from central Baja California north throughout the Mojave and Great Basin, into the Great

Central Valley of California, and onto the Colorado Plateau. Lower quality habitat extends into the Sonoran and even a portion of the Chihuahuan deserts. The present-day model for the *leucurus* south clade (Figure 2.7C) indicates continuous high quality habitat is restricted to the southern half of Baja California and to the coastal continental Sonoran Desert, owing in large part to the floral similarity of these areas. The Peninsular Desert (as recognized by Riddle et al. 2000) was originally considered a component of the Sonoran Desert based on these similarities (Shreve 1942; MacMahon 1988). The present-day model for the *interpres* clade (Figure 2.7E) indicates that appropriate habitat is distributed throughout the Chihuahuan Desert, concentrated in the northern extent of the range. Additional areas of suitable habitat extend onto the Colorado Plateau and along the Mojave/Great Basin boundary. For the most part, the high-quality habitat represented in the present-day models for each of these three clades correctly captures the current distribution of individuals and currently recognized species in each clade.

The reconstructions of paleo-habitat models (paleo-models) for each of the three well-supported clades of *Ammospermophilus* during the last glacial maximum (LGM) predicted an overall loss of suitable habitat for each of these clades. These models suggest that the high-quality habitat for northern *leucurus* (Figure 2.7B) was significantly compressed to central Baja California and the Mojave in southern California, with some residual pockets within the more widespread current day distribution model. The southern *leucurus* clade (Figure 2.7D) was similarly compressed within the southern extent of the Baja California Peninsula, but much less so owing to the restricted land area that is available, regardless of environmental conditions. The paleo-model for the *interpres* clade was the most significantly compressed during the LGM. While the present-day

model for this clade indicated a fairly widespread distribution, the paleo-model indicates a much smaller area of suitable habitat (regardless of quality) in the southern Chihuahuan Desert. Some formerly unsuitable areas in this region become habitable during this period of extreme environmental changes. Each of these major clades is represented by substantial reductions in available habitat and we regard the high-quality areas represented by the paleo-models for the northern and southern *leucurus* and *interpres* clades as putative refugial areas during the LGM. These models are consistent with the results of the population genetic analyses of the *leucurus* clades, indicating a restriction of overall habitat and a concomitant reduction in population sizes. The suitable habitat has since expanded throughout the desert regions of western North America following the retreat of the glaciers, which is consistent with genetic properties of *A. leucurus* that indicate recent rangewide population expansion.

Discussion

Ammospermophilus, widely distributed throughout the aridlands of western North America, presents an assemblage of geographically isolated species and populations appropriate for examining the historical biogeography of this region and the evolution of North American deserts. The age of this genus and its long association with the evolution of the regional deserts makes it especially attractive for examining the patterns of divergence, dispersal, and diversification in this region. The patterns of evolutionary divergence appear consistent with a late Miocene timeframe, with a basal divergence of *Ammospermophilus* into three major lineages (Figure 2.4), prior to the expansion of a semi-desert ecosystem during the Pliocene. There is additional geographic structure

within each of these lineages, though this structure is not well defined with the current phylogenetic analyses. Divergence estimates within each of these lineages suggests a near simultaneous diversification, coincident with dynamic alterations in the landscape of western North America and the formation and of the regional deserts during the late Neogene. The molecular time estimates within the phylogeny provide plausible divergence estimates within *Ammospermophilus* and many of these values are robust across calibration methods (Table 2.3). Given the complex geological history of western North America and the cyclical nature of patterns of dispersal and vicariance, it is likely that the dated phylogeny accurately captures the extent and timing of the major divergences within *Ammospermophilus*.

Ammospermophilus leucurus, as currently recognized, represents a geographically structured polyphyletic species forming at least three distinct lineages. These results indicate that a basal polytomy exists between the three major clades of *Ammospermophilus* that complicates the phylogenetic history and current taxonomic assignments of these lineages. Within A. leucurus, geographically structured lineages correspond to the continental US (north of the Baja California peninsula), northern Baja California, and southern Baja California (Figures 2.5 & 2.6). The Baja California lineages are separated in the mid-peninsular region. This separation, detected previously in *Ammospermophilus* (Riddle et al. 2000c), is similar to patterns of mid-peninsular divergence detected in a suite of other taxa, including mammals (Riddle et al. 2000a, b; Alvarez-Castañeda and Patton 2004; Whorley et al. 2004; Bell et al. 2009), birds (Zink et al. 2001; Zink 2002), reptiles (Upton and Murphy 1997; Lindell et al. 2005; Douglas et al. 2006; Leaché et al. 2007; Leaché and Mulcahy 2007), amphibians (Jaeger et al. 2005),

spiders (Ayoub and Reichert 2004; Crews and Hedin 2006), and plants (Garrick et al. 2009), as well as fish species bordering the peninsula (Bernardi and Lape 2005; Reginos 2005). These taxa consistently support a mid-peninsular vicariance event that may have result of a hypothesized Vizcaíno Seaway during the late Miocene or early Pliocene (Upton and Murphy 1997; Riddle et al. 2000c; Whorley et al. 2004). This hypothesized vicariant event has been a topic of contention because there is no conclusive geological evidence for its existence (Crews and Hedin 2006; Lindell et al. 2006). Even with the absence of geological data, there still exists a strong set environmental factors driving divergence in this area, potentially including geological forces (e.g., periodic submergence of the central peninsula) and abrupt ecological and climatic barriers (Grismer 2000, 2002).

The isolation of *A. interpres* in the Chihuahuan Desert, the easternmost component of the North American deserts, represents a divergent lineage driven by the uplifting Sierra Madre Occidental and the Central Mexican Plateau during a mid-Miocene (ca. 11 mya) timeframe (Coney 1983). This period coincides with the expansion of regional deserts in the latest Miocene (Axelrod 1979; Webb 1983) and with the divergence time estimates for the basal divergence in *Ammospermophilus* (Figure 2.4). Associated with the Chihuahuan Desert and subsequent to the uplift of the Sierra Madre Occidental, a series of filter-barriers drive divergence and maintain genetic separations between taxa that share a Sonoran-Chihuahuan dispersal history. While these two regional deserts are separated by the Sierra Madre Occidental, taxa endemic to these regions meet in a low-elevation northern gap, known as the Cochise filter-barrier (Morafka 1977) in the Deming Plains in southern Arizona/New Mexico. In the southern Chihuahuan Desert, the

Southern Coahuila filter-barrier is formed by the Río Nazas and Río Aguanaval in the west and the Laguna Mayrán and an extension of the Sierra Madre Oriental in the east (Baker 1956; Baker and Greer 1962; Peterson 1976; Schmidly 1977). This barrier has proven to be an important factor is shaping the distributions of mammals in this region (reviewed in Hafner and Riddle 2009). Such barriers are characterized by their dynamic nature in response to climatic conditions and their effectiveness as gateways to dispersal and subsequent vicariant barrier to gene flow. While the Cochise filter-barrier begain its initial formation near the Oligocene-Miocene boundary (23 mya) with the same geological forces that initiated the uplift of the Sierra Madre Occidental, it has experienced periods of environmental change that have repeatedly opened and shut this gateway to dispersal (Hafner and Riddle 2009).

The evolutionary histories of *A. harrisii* and *A. nelsoni* are closely tied to the diversification of northern populations of *A. leucurus* and likely diverged in the early Pliocene into western (*nelsoni*) and eastern (*leucurus/harrisii*) lineages in the vicinity of the Salton Trough around 5 mya (Boehm 1984; Bell et al. 2009). This timeframe is consistent with the divergence time estimates for the divergence of these taxa (Figure 2.4, Node C). This phylogenetic and geographic separation within *A. harrisii* may represent distinct lineages or perhaps an ancient mitochondrial capture or introgression event between populations of *A. harrisii* that contact with populations of *A. leucurus*. The Colorado River in southern Arizona represents the current distributional limit between the eastern extent of *A. leucurus* and the western extent of *A. harrisii*. Detailed sampling throughout the distribution of this species as well as examination of nuclear DNA will enable a more thorough examination and explanation of these patterns, including the

possibility of mitochondrial gene capture. This ancient introgression could then become widespread across northern populations of *A. harrisii* over time, allowing further geographic structuring within this species. A similar pattern of possible polyphyly within *A. harrisii* was suggested (with limited support) by previous molecular analyses (Herron et al. 2004), though additional data are needed to appropriately address the phylogenetic structure in this species and differentiate between the alternative hypotheses.

The San Joaquin Valley, at the southern end of the Central Valley in California, a remnant of a pre-Pliocene marine embayment, was completely separated from the Pacific by the early Pliocene (Dupré et al. 1991). The habitats for *A. nelsoni* have probably expanded and contracted as a result of climate fluctuations, but this lineage has likely remained isolated at or near its current distribution since the initial separation. Rampant agricultural development in this area is reducing the already reduced available habitat for many species in this region, so *A. nelsoni* may be the most threatened and endangered species in the genus.

Quaternary Climate Change and Genetic Consequences

Post-glacial range expansion and dispersal can take place in a number of different ways and the models of these processes take into account the effects of the dispersal processes on genetic diversity. When species expand on a unified front, there is weak genetic differentiation during range expansion without a loss of genetic diversity. This pattern is often characteristic of species with wide ecological tolerances. Alternatively, a stepping-stone model of expansion is characterized by the exchanges of individuals between neighboring populations while a normally-distributed leading edge dispersal model can result in a pattern in which many individuals disperse short distances, fewer

individuals disperse intermediate distances and more disperse long distances (Ibrahim et al. 1996). These last two models of dispersal lead to a loss in genetic diversity (homogeneity) during expansion and they are characteristic of species that colonized areas following glacial retreat (Hewitt 1996, 2004).

The genetic patterns evident in the geographically distinct *leucurus* lineages represent similar responses to the climatic fluctuations associated with the last glacial maximum (LGM) at 18 kya and subsequent glacial retreat beginning at approximately 10 kya. Based on the results of both the ecological niche models as well as the population genetic parameters, we can more fully explore the population responses to these climatic cycles. The southern *leucurus* lineage is confined to the southern half of the Baja California Peninsula and the LGM paleo-distribution exhibits signatures of glacial compression. This clade exhibits genetic signatures of population compression during the LGM, including low levels of nucleotide diversity and high levels of haplotype diversity, hallmarks of rapidly expanding populations (Grant and Bowen 1998)**.** Detailed examination of the phylogenetic relationships of this clade indicates that there is little or no significant genetic structure among samples in the southern peninsula with the available data. The *insularis* haplotypes, while monophyletic, are nested within the southern Baja California *leucurus* lineage (Figures 2.5 & 2.6). An previous analysis of the *Ammospermophilus* from the islands of Espíritu Santo (*A. insularis*) and San Marcos (*A. leucurus extimus*) in the Sea of Cortez did not indicate that these populations were sufficiently distinct, either genetically or morphologically, to warrant specific recognition (Alvarez-Casteñeda 2007).

The northern *leucurus* clades are much more widespread throughout the northern half of the Baja California Peninsula as well as throughout the Mojave, Great Basin and onto the Colorado Plateau in western North America. Each of these lineages experienced separate demographic histories over the last several thousand years in response to climatic oscillations. Currently, *A. leucurus* extends well into the northern extent of the Great Basin in southern Oregon, though its fossil history suggests it reached a northern limit in Washington as recently as the Pliocene (Gustafson 1978). Additional fossil remnants also exist in eastern Oregon (Black 1963), also well outside of the current distributional limits of this species.

While the phylogeographic and demographic history of *A. interpres* was not explicitly analyzed, this species likely experienced a similar patterns of habitat and population contraction and expansion in response to glacial cycles throughout the Pleistocene (Figure 2.8F). Within the Chihuahuan Desert, populations are structured by a set of major river barriers, including the Rio Conchos, running from the Sierra Made Occidental east towards the Rio Grande, which run north-south from northern New Mexico to the Gulf of Mexico. Additionally, the Southern Coahuila filter barrier in the southern Chihuahuan acts as an intermittent barrier as a response to pluvial and interpluvial cycles. The ecological habitat models indicate a severe compression of the distribution of *A. interpres* into the southernmost Chihuahuan in the vicinity of this southern filter-barrier.

The biogeographic history of *Ammospermophilus* represents a dynamic set of events leading to a complex set of phylogenetic and phylogeographic patterns. The deeper divergences within this taxon represent Pliocene divergence of each of the major lineages coincident with the continued aridification and regionalization of the deserts in western

North America. The demographic patterns within these lineages, particularly in *A. leucurus* and likely within all of the widespread species (*harrisii* and *interpres*), represent responses to ongoing climatic oscillations. These climate cycles and the resulting glacial cycles caused contractions of habitats and resident species as they tracked those habitat changes. Demographic parameters reveal patterns of recent population expansion in response to glacial retreat, consistent with a hypothesis of glacial refugia for widespread species.

Literature Cited

Akaike, H. 1973. Information theory as an extension of the maximum likelihood principle. Second International Symposium on Information Theory:267 - 281.

Alexander, L. F., and B. R. Riddle. 2005. Phylogenetics of the New World Rodent family Heteromyidae. Journal of Mammalogy 86:366-379.

Alvarez-Castañeda, S. T., and J. L. Patton. 2004. Geographic genetic architecture of pocket gopher (*Thomomys bottae*) populations in Baja California, Mexico. Molecular Ecology 13:2287-2301.

Alvarez-Casteñeda, S. T. 2007. Systematics of the antelope ground squirrel (Ammospermophilus) from islands adjacent to the Baja California Peninsula. Journal of Mammalogy 88:1160-1169.

Arbogast, B. S., and J. B. Slowinski. 1998. Pleistocene speciation and the mitochondrial clock. Science 282:1955a.

Axelrod, D. I. 1979. Age and origin of Sonoran Desert vegetation. Occassional Papers of the California Academy of Sciences 132:1-74.

Ayoub, N. A., and S. E. Reichert. 2004. Molecular evidence for Pleistocene glacial cycles driving diversification of a North American desert spider, Agelenopsis aperta. Molecular Ecology 13:3453-3465.

Baker, R. H. 1956. Mammals of Coahuila, México. University of Kansas Museum of Natural History Special Publication 9:125-335.

Baker, R. H., and J. K. Greer. 1962. Mammals of the Mexican state of Durango. Publications of the Museum, Michigan State University, Biological Series 2:25-154.

Bandelt, H.-J., P. Forster, and A. Rohl. 1999. Median-joining networks for inferring intraspecific phylogenies. Molecular Biology and Evolution 16:37-48.

Bell, K. C., D. J. Hafner, P. Leitner, and M. D. Matocq. 2009. Phylogeography of the ground squirrel subgenus *Xerospermophilus* and assembly of the Mojave desert biota. Journal of Biogeography 37:363-378.

Bernardi, G., and J. Lape. 2005. Tempo and mode of speciation in the Baja California disjunct fish species *Anisotremus davidsonii*. Molecular Ecology 14:4085-4096.

Boehm, M. C. 1984. An overview of the lithostratigraphhy, biostatigraphy, and paleoenvironments of the Late Neogene San Felipe marine sequence, Baja California, Mexico. Pp. 253-265 *in* J. Frizzell, V.A., ed. Geology of the Baja California Peninsula. Society of Economic Paleontologists and Mineralogists, Pacific Section, Los Angeles, CA.

Bradley, R. D., and R. J. Baker. 2001. A test of the genetic species concept: Cytochrome-*b* sequences and mammals. Journal of Mammalogy 82:960-973.

Brandley, M. C., A. Schmitz, and T. W. Reeder. 2005. Partitioned Bayesian analyses, partition choice, and the phylogenetic relationships of scincid lizards. Systematic Biology 54:373-390.

Bryant, M. D. 1945. Phylogeny of Nearctic Sciuridae. American Midland Naturalist 33:257-390.

Carstens, B. C., and L. L. Knowles. 2007. Shifting distributions and speciation: species divergence during rapid climate change. Molecular Ecology 16:619-627.

Coney, P. J. 1983. The plate tectonic setting of cordilleran deserts. Pp. 81-97 *in* S. G. Wells, and D. R. Haragan, eds. Origin and Evolution of the Deserts. University of New Mexico Press, Albuquerque.

Crews, S. C., and M. Hedin. 2006. Studies of morphological and molecular phylogenetic divergence in spiders (Araneae: *Homalonychus*) from the American southwest, including divergence along the Baja California Peninsula. Molecular Phylogenetics and Evolution 38:470-487.

Douglas, M. E., M. R. Douglas, G. W. Schuett, and L. W. Porras. 2006. Evolution of rattlesnakes (Viperidae; Crotalus) in the warm deserts of western North America shaped by Neogene vicariance and Quaternary climate change. Molecular Ecology 15:3353-3374.

Drummond, A., and A. Rambaut. 2007. BEAST: Bayesian evolutionary analysis by sampling trees. BMC Evolutionary Biology 7:214.

Drummond, A. J., S. Y. W. Ho, M. J. Phillips, and A. Rambaut. 2006. Relaxed phylogenetics and dating with confidence. PLOS Biology 4:e88.

Dupré, W. R., R. B. Morrison, H. E. Clifton, K. R. Lajoie, D. J. Ponti, C. L. Power, S. A. Mathieson, A. M. Sarna-Wojcicki, E. L. Leithold, W. R. Lettis, P. F. McDowell, T. K. Rockwell, J. Unruh, and R. S. Yeats. 1991. Quaternary geology of the Pacific margin. Pp. 141-214 *in* R. B. Morrison, ed. Quaternary Nonglacial Geology; Conterminous US. Geological Society of America, Boulder, CO.

Elith, J., and C. H. Graham. 2009. Do they? How do they? WHY do they differ? On finding reasons for differing performances of species distribution models. Ecography 32:66-77.

Elith, J., C. H. Graham, R. P. Anderson, M. Dudík, S. Ferrier, A. Guisan, R. J. Hijmans, F. Huettmann, J. R. Leathwick, A. Lehmann, J. Li, L. G. Lohmann, B. A. Loiselle, G. Manion, C. Moritz, M. Nakamura, Y. Nakazawa, J. M. C. M. Overton, A. T. Peterson, S. J. Phillips, K. Richardson, R. Scachetti-Pereira, R. E. Schapire, J. Soberón, S. Williams, M. S. Wisz, and N. E. Zimmermann. 2006. Novel methods improve prediction of species' distributions from occurrence data. Ecography 29:129-151.

Evans, M. E. K., S. A. Smith, R. S. Flynn, and M. J. Donoghue. 2009. Climate, niche evolution, and diversification of the "Bird-cage" evening primroses (*Oenothera*, Section *Anogra* and *Kleinia*). The American Naturalist 173:225-240.

Felsenstein, J. 1985. Confidence limits on phylogenies: an approach using the bootstrap. Evolution 39:783-791.

Fielding, A. H., and J. F. Bell. 1997. A review of methods for the assessment of prediction errors in conservation presence/absence models. Environmental Conservation 24:38-49.

Forest, F. 2009. Calibrating the Tree of Life: fossils, molecules and evolutionary timescales. Annals of Botany 104:789-794.

Garrick, R. C., J. D. Nason, C. A. Meadows , and R. J. Dyer. 2009. Not just vicariance: phylogeography of a Sonoran Desert euphorb indicates a major role of range expansion along the Baja peninsula. Molecular Ecology 18:1916-1931.

Grant, W. S., and B. W. Bowen. 1998. Shallow population histories in deep evolutionary lineages of marine fishes: insights from sardines and anchovies and lessons for conservation. Journal of Heredity 89:415-426.

Graur, D., and W. Martin. 2004. Reading the entrails of chickens: molecular timescales of evolution and the illusion of precision. Trends in Genetics 20:80-86.

Grismer, L. L. 2000. Evolutionary biogeography on Mexico's Baja California peninsula: a synthesis of molecules and historical geology. Proceedings of the National Academy of Science of the USA 97:14017-14018.

Grismer, L. L. 2002. A re-evaluation of the evidence for a mid-Pleistocene mid-peninsular seaway in Baja California: a reply to Riddle et al. Herpetological Review 33:15-16.

Guindon, S., and O. Gascuel. 2003. A simple, fast, and accurate algorithm to estimate large phylogenies by maximum likelihood. Systematic Biology 52:696-704.

Gustafson, E. P. 1978. The vertebrate faunas of the Pliocene Ringold formation, south-central Washington. Bulletin of the Museum of Natural History, University of Oregon, Eugene 23:1-62.

Hafner, D. J., and B. R. Riddle. 1997. Biogeography of Baja California peninsular desert mammals. Pp. 39-68 *in* T. L. Yates, W. L. Gannon, and D. E. Wilson, eds. Life Among the Muses: Papers in honor of James S. Findley. The Museum of Southwestern Biology, The University of New Mexico, Albuquerque, NM.

Hafner, D. J., and B. R. Riddle. 2009. Boundaries and barriers of North American warm deserts: an evolutionary perspective. Proceedings from Palaeogeography and Plaeobiogeography: Biodiversity in Space and Time. Cambridge University Press.

Hall, E. R. 1981. The Mammals of North America. John Wiley & Sons, New York.

Harrison, R. G., S. M. Bogdanowicz, R. S. Hoffman, E. Yensen, and P. W. Sherman. 2003. Phylogeny and evolutionary history of the ground squirrels (Rodentia: Marmotinae). Journal of Mammalian Evolution 10:249-276.

Hasumi, H., and S. Emori. 2004. K-1 coupled GCM (MIROC) description. Technical Report No. 1. Center for Climate System Research, University of Tokyo, Tokyo.

Hedges, S. B., and S. Kumar. 2003. Genomic clocks and evolutionary timescales. Trends in Genetics 19:200-206.

Hedges, S. B., and S. Kumar. 2004. Precision of molecular time estimates. Trends in Genetics 20:242-247.

Helgen, K. M., F. R. Cole, L. E. Helgen, and D. E. Wilson. 2009. Generic Revision in the Holarctic Ground Squirrel Genus *Spermophilus*. Journal Of Mammalogy 90:270-305.

Herron, M. D., T. A. Castoe, and C. L. Parkinson. 2004. Sciurid phylogeny and the paraphyly of Holarctic ground squirrels (*Spermophilus*). Molecular Phylogenetics and Evolution 31:1015-1030.

Hewitt, G. M. 1996. Some genetic consequences of ice ages, and their role in divergence and speciation. Biological Journal of the Linnean Society 58:247-276.

Hewitt, G. M. 2004. The structure of biodiversity - insights from molecular phylogeogrpahy. Frontiers in Zoology 1:1-16.

Hijmans, R. J., S. E. Cameron, J. L. Parra, P. G. Jones, and A. Jarvis. 2005. Very high resolution interpolated climate surfaces for global land areas. International Journal of Climatology 25:1965-1978.

Hillis, D. M., and J. J. Bull. 1993. An empirical test of bootstrapping as a method for assessing confidence in phylogenetic analysis. Systematic Biology 42:182-192.

Ho, S. Y. W., U. Saarma, R. Barnett, J. Haile, and B. Shapiro. 2008. The effect of inappropriate calibration: three case studies in molecular ecology. PLoS ONE 3:e1615.

Howell, A. H. 1938. Revision of the North American ground squirrels with a classification of the North American Sciuridae. North American Fauna 56.

Huelsenbeck, J. P., and F. Ronquist. 2001. MrBayes: A program for the Bayesian inference of phylogeny, Rochester, NY.

Ibrahim, K. M., R. A. Nichols, and G. M. Hewitt. 1996. Spatial patterns of genetic variation generated by different forms of dispersal during range expansion. Heredity 77:282-291.

Jaeger, J. R., B. R. Riddle, and D. F. Bradford. 2005. Cryptic neogene vicariance and Quaternary dispersal of the red-spotted toad (Bufo punctatus): insights on the evolution of North American warm deserts biota. Molecular Ecology 14:3033-3048.

James, G. T. 1963. Paleontology and nonmarine stratigraphy of the Cuyama Valley Badlands, California. Part 1. Geology faunal interpretations, and systematic descriptions of Chiroptera. University of California Publications in Geological Sciences 45:1-170.

Jezkova, T., J. R. Jaeger, Z. L. Marshall, and B. R. Riddle. 2009. Pleistocene impacts on the phylogeography of the desert pocket mouse (*Chaetodipus penicillatus*). Journal of Mammalogy 90:306-320.

Jobb, G., A. von Haeseler, and K. Strimmer. 2004. TREEFINDER: a powerful graphical analysis environment for molecular phylogenetics. BMC Evolutionary Biology 4:18.

Leaché, A. D., S. C. Crews, and M. J. Hickerson. 2007. Two waves of diversification in mammals and reptiles of Baja California revealed by hierarchical Bayesian analysis. Biology Letters online:1-5.

Leaché, A. D., and D. G. Mulcahy. 2007. Phylogeny, divergence times and species limits of spiny lizards (Sceloporus magister species group) in western North American deserts and Baja California. Molecular Ecology 16:5216-5233.

Levin, H. L. 1978. The earth through time. W.B. Saunders Company, Philadelphia.

Lindell, J., F. R. Mendez-de la Cruz, and R. W. Murphy. 2005. Deep genealogical history without population differentiation: discordance between mtDNA and allozyme divergence in the zebra-tailed lizard (Callisaurus draconoides). Molecular Phylogenetics and Evolution 36:682-694.

Lindell, J., A. Ngo, and R. W. Murphy. 2006. Deep genealogies and the mid peninsular seaway of Baja California. Journal of Biogeography 33:1327-1331.

Longmire, J. L., M. Maltbie, and R. J. Baker. 1997. Use of "lysis buffer" in DNA isolation and its implication for museum collections. Occasional Papers of the Museum of Texas Tech University 163:1-4.

MacMahon, J. A. 1988. Warm Deserts. Pp. 212-264 *in* M. G. Barbour, and W. D. Billings, eds. North American Terrestrial Vegetation. Cambridge University Press, Cambridge, U.K.

Maddison, D. R., and W. P. Maddison. 2005. MacClade 4: Analysis of phylogeny and character evolution. Version 4.08. Sinauer Associates, Sunderland, MA.

Matocq, M. D., Q. R. Shurtliff, and C. R. Feldman. 2007. Phylogenetics of the woodrat genus Neotoma (Rodentia: Muridae): Implications for the evolution of phenotypic variation in male external genitalia. Molecular Phylogenetics and Evolution 42:637-652.

Mercer, J. M., and V. L. Roth. 2003. The effects of Cenozoic global change on squirrel phylogeny. Science 299:1568-1572.

Morafka, D. J. 1977. A biogeographical analysis of the Chihuahuan Desert through its herpetofauna. Dr. W. Junk B. V. , The Hague, The Netherlands.

Otto-Bliesner, B. L., J. Marshall, G. H. Overpeck, G. H. Miller, A. Hu, and C. L. I. P. members. 2006. Simulating Arctic Climate Warmth and Icefield Retreat in the Last Interglaciation. Science 311:1751-1753.

Parolo, G., G. Rossi, and A. Ferrarini. 2008. Toward improved species niche modelling: Arnica montana in the Alps as a case study. Journal of Applied Ecology 45:1410-1418.

Pearson, R. G., C. J. Raxworthy, M. Nakamura, and A. T. Peterson. 2007. Predicting species distributions from small numbers of occurrence records: a test case using cryptic geckos in Madagascar. Journal of Biogeography 34:102-117.

Peterson, M. K. 1976. The Rio Nazas as a factor in mammalian distribution in Durango, Mexico. The Southewestern Naturalist 20:495-502.

Phillips, M., P. McLenachan, C. Down, G. Gibb, and D. Penny. 2006a. Combined Mitochondrial and Nuclear DNA Sequences Resolve the Interrelations of the Major Australasian Marsupial Radiations. Systematic Biology 55:122-137.

Phillips, S. J., R. P. Anderson, and R. E. Shchapire. 2006b. Maximum entropy modeling of species geographic distributions. Ecological Modelling 190:231-259.

Phillips, S. J., and M. Dudik. 2008. Modeling of species distributions with Maxent: new extensions and a comprehensive evaluation. Ecography 31:161-175.

Posada, D. 2008. jModelTest: Phylogenetic Model Averaging. Molecular Biology and Evolution 25:1253-1256.

Posada, D., and T. Buckley. 2004. Model Selection and Model Averaging in Phylogenetics: Advantages of Akaike Information Criterion and Bayesian Approaches Over Likelihood Ratio Tests. Systematic Biology 53:793-808.

Posada, D., and K. A. Crandall. 1998. MODELTEST: testing the model of DNA substitution. Bioinformatics 14:817 - 818.

Rambaut, A., and A. J. Drummond. 2007. Tracer v.1.4.

Reginos, C. 2005. Cryptic vicariance in Gulf of California fishes parallels vicariant patterns found in Baja California mammals and reptiles. Evolution 59:2678-2690.

Riddle, B. R. 1995. Molecular biogeography in the pocket mice (*Perognathus* and *Chaetodipus*) and grasshopper mice (*Onychomys*): the late Cenozoic development of a North American aridlands rodent guild. Journal of Mammalogy 76:283-301.

Riddle, B. R., and D. J. Hafner. 2006. A step-wise approach to integrating phylogeographic and phylogenetic biogeographic perspectives on the history of a

core North American warm deserts biota. Journal of Arid Environments 66:435-461.

Riddle, B. R., D. J. Hafner, and L. F. Alexander. 2000a. Comparative phylogeography of Baileys' pocket mouse (*Chaetodipus baileyi*) and the *Peromyscus eremicus* species group: historical vicariance of the Baja California Peninsular Desert. Molecular Phylogenetics and Evolution 17:161-172.

Riddle, B. R., D. J. Hafner, and L. F. Alexander. 2000b. Phylogeography and Systematics of the *Peromyscus eremicus* Species Group and the Historical Biogeography of North American Warm Regional Deserts. Molecular Phylogenetics and Evolution 17:145-160.

Riddle, B. R., D. J. Hafner, L. F. Alexander, and J. R. Jaeger. 2000c. Cryptic vicariance in the historical assembly of a Baja California peninsular desert biota. Proceedings of the National Academy of Science of the USA 97:14438-14443.

Ronquist, F., and J. P. Huelsenbeck. 2003. MrBayes 3: Bayesian phylogenetic inference under mixed models. Bioinformatics 19:1572-1574.

Rozas, J., J. C. Sanchez-DelBarrio, X. Messeguer, and R. Rozas. 2003. DnaSP, DNA polymorphism analyses by the coalescent and other methods. Bioinformatics 19:2496 - 2497.

Schmidly, D. J. 1977. Factors governing the distribution of mammals in the Chihuahuan Desert Region. Pp. 163-192 *in* R. H. Wauer, and D. H. Riskind, eds. Transactions of the Symposium on the Biological Resources of the Chihuahuan desert region, United States and Mexico. National Park Service Transactions and Proceedings Series 3.

Shreve, F. 1942. The desert vegetation of North America. Botanical Review 8:195-246.

Stockman, A., and J. Bond. 2007. Delimiting cohesion species: extreme population structuring and the role of ecological interchangeability. Molecular Ecology 16:3374-3392.

Suárez-Seoane, S., E. L. García de la Morena, M. B. Morales Prieto, P. E. Osborne, and E. de Juana. 2008. Maximum entropy niche-based modelling of seasonal changes in little bustard (*Tetrax tetrax*) distribution. Ecological Modelling 219:17-29.

Swanson, E. R., and F. W. McDowell. 1984. Calderas of the Sierra Madre Occidental volcanic field, western Mexico. Journal of Geophysical Research 89:8787-8799.

Tajima, F. 1989. Statistical method for testing the neutral mutation hypothesis by DNA polymorphism. Genetics 123:585-595.

Upton, D. E., and R. W. Murphy. 1997. Phylogeny of the sideblotched lizards (Phrynosomatidae: *Uta*) based on mtDNA sequences: support for a midpeninsular seaway in Baja California. Molecular Phylogenetics and Evolution 8:104-113.

Waltari, E., and R. P. Guralnick. 2009. Ecological niche modelling of montane mammals in the Great Basin, North America: examining past and present connectivity of species across basins and ranges. Journal of Biogeography 36:148-161.

Waltari, E., R. J. Hijmans, A. T. Peterson, A. S. Nyari, S. L. Perkins, and R. P. Guralnick. 2007. Locating Pleistocene refugia: comparing phylogeographic and ecological niche model predictions. PLoS ONE 2:e563.

Webb, S. D. 1977. A history of savanna vertebrates in the New World. Part I. Annual Review of Ecology and Systematics 8:355-380.

Webb, S. D. 1983. The rise and fall of the late Miocene ungulate fauna in North America *in* M. H. Nitecki, ed. Coevolution. University of Chicago Press, Chicago.

Whorley, J. R., S. T. Alvarez-Castaneda, and G. J. Kenagy. 2004. Genetic structure of desert ground sqirrels over the 20-degree-latitude transect from Oregon through the Baja California peninsula. Molecular Ecology 13:2709-2720.

Wilgenbusch, J. C., D. L. Warren, and D. L. Swofford. 2004. AWTY: A system for graphical exploration of MCMC convergence in Bayesian phylogenetic inference.

Wilson, D. E., and D. M. Reeder, eds. 2005. Mammal Species of the World. The Johns Hopkins University Press, Baltimore.

Yang, Z. 1996. Maximum likelihood models for combined analyses of multiple sequence data. Journal of Molecular Evolution 42:587-596.

Zink, R. M. 2002. Methods in comparative phylogeography, and their application to studying evolution in the North American aridlands. Integrative and Comparative Biology 42:953-959.

Zink, R. M., A. E. Kessen, T. V. Line, and R. C. Blackwell-Rago. 2001. Comparative phylogeography of some aridland bird species. The Condor:1-10.

Table 2.1: Oligonucleotide primers used to amplify and sequence mtDNA, rRNA, and nDNA in *Ammospermophilus* and two outgroup taxa (*Cynomys* and *Xerospermophilus*). The Loci are: IRBP – nuclear Interphotoreceptor Retinoid-Binding Protein; Rag2 – nuclear Recombining Activating Gene 2; 12S – small subunit mitochondrially-encoded ribosomal RNA; 16S – large subunit mitochondrially-encoded ribosomal RNA; Cytb – mitochondrial Cytochrome b gene; CO1 – mitochondrial Cytochrome Oxidase 1 gene, CO3 – mitochondrial Cytochrome Oxidase 3 gene; CR – mitochondrial Control Region. The size indicates the expected size of PCR product generated by the combination of primers. Primer names and sequences follow the cited sources, except Ammo LS1, which was generated specifically in this study. (CO1 primers use the standard IUPAC ambiguity code).

Locus	Size (bp)	Primers	Sequence	Source
IRBP	1087	119A	5’ - ATG GCC AAG GTC CTC TTG GAT AAC TAC TGC TT - 3’	Jansa and Voss (2000) &
		1297D	5’ - CAG GTA GCC CAC ATT GCC TGG CAG CAC - 3’	Stanhope et al. (1992)
Rag2	969	283F	5’ - GGA GGG AAA ACA CCA AAC AAT GAG CTT TC - 3’	DeBry and Sagel (2001)
		1415R	5’ - CCT TCT GAC AAG TGG ATG AGT GTG CGT TC - 3’	
12S	832	H900	5’ - TGA CTG CAG AGG GTG ACG GGC GGT GTG T - 3’	Allard and Honeycutt (1992)
		L82	5’ - CAT AGA CAC AGA GGT TTG GTC C - 3’	
16S	550	16AR-F	5’ - CGC CTG TTT ATC AAA AAC AT - 3’	Palumbi et al. (1991)
		16BR-R	5’ - CCG GTC TGA ACT CAG ATC ACG T - 3’	

Cytb	1140	H15915	5' - AAC TGC AGT CAT CTC CGG TTT ACA AGA C - 3'	Irwin et al. (1991)
		L14724	5' - CGA AGC TTG ATA TGA AAA ACC ATC GTT G - 3'	
CO1	691	VF1	5' - TTC TCA ACC AAC CAC AAA GAC ATT GG - 3'	Ivanova et al. (2006)
		VF1d	5' - TTC TCA ACC AAC CAC AAR GAY ATY GG - 3'	
		VF1i	5' - TTC TCA ACC AAC CAI AAI GAI ATI GG - 3'	
		VR1	5' - TAG ACT TCT GGG TGG CCA AAG AAT CA - 3'	
		VR1d	5' - TAG ACT TCT GGG TGG CCR AAR AAY CA - 3'	
		VR1i	5' - TAG ACT TCT GGG TGI CCI AAI AAI CA - 3'	
CO3	690	L8618	5' - CAT GAT AAC ACA TAA TGA CCC ACC AA - 3'	Riddle et al. (1995)
		H9323	5' - ACT ACG TCT ACG AAA TGT CAG TAT CA - 3'	
CR	503	L15926	5' - TCA AAG CTT ACA CCA GTC TTG TAA ACC - 3'	Kocher et al. (1989)
		H00651	5' - TAA CTG CAG AAG GCT AGG ACC AAA CCT - 3'	
		AmmoLS1	5' - AGA GCA ATT AAT TTC AGG GAA G - 3'	This Study

Table 2.2: Table 2.2. Summary statistics and parameter estimates for Bayesian Inference data partitions for seven molecular markers used in the multi-gene *Ammospermophilus* dataset. To assess the influence of data partitioning, parameters have been estimated based on three different data partitions: P1 = all data combined, P2 = mtDNA + nucDNA, P3 = each gene analyzed separately. The Models of DNA substitution represent the best fit models using AIC criteria in JModeltest 0.0.1.

Partition type	Model of DNA substitution	- lnL	Mean α	Mean P_{inv}	Mean ti/tv	Mean πA	Mean πC	Mean πG	Mean πT
P_1									
all DNA	GTR + I + Γ	14323.8242	0.6530	0.5770	—	0.2653	0.2429	0.1946	0.2972
P_2									
mtDNA	GTR + Γ	9777.2400	0.1740	—	—	0.2747	0.2377	0.1691	0.3186
nucDNA	K80 + I + Γ	4100.2347	0.7660	0.8280	2.0986	0.2436	0.2566	0.2462	0.2537
P_7									
IRBP	HKY + I + Γ	2367.4248	0.6410	0.7120	1.2283	0.2063	0.2855	0.2928	0.2155
Rag2	HKY + I	1591.8348	—	0.8900	8.9683	0.2864	0.2208	0.1918	0.3010
12S	GTR + I	1670.1056	—	0.7650	—	0.2581	0.1761	0.2177	0.3481
16S	GTR + I	1087.5568	—	0.6069	—	0.3215	0.2053	0.1989	0.2743
Cytb	GTR + Γ	3101.5892	0.2100	—	—	0.2776	0.2814	0.1285	0.3125
CO1	GTR + Γ	1729.3489	0.1910	—	—	0.2562	0.2499	0.1699	0.3241
CO3	GTR + Γ	1972.7049	0.4350	—	—	0.2723	0.2643	0.1515	0.3119

Table 2.3: Estimated divergence dates for each node depicted in Figure 2.4 based on three calibration methods: fossil calibration placement at node A, fossil calibration placement at node B, and calibration using only Cytochrome *b* data with a mutation rate of 2% per million years.

	Divergence Time (mya) 95% CI		
Calibration	A fossil	B fossil	Cyt b 2%/My
Node			
A	11.14* (9.99 – 13.25)	25.21 (11.19 – 41.24)	12.45 (6.21 – 23.68)
B	4.13 (2.11 – 6.6)	11.77* (10.1 – 13.37)	5.05 (1.19 – 5.18)
C	3.58 (1.34 – 4.66)	5.08 (2.22 – 8.21)	1.05 (0.48 – 1.95)
D	2.91 (0.47 – 3.75)	2.37 (0.5 – 5.02)	0.53 (0.03 – 0.76)
E	2.52 (0.99 – 4.25)	4.17 (1.6 – 7.34)	0.63 (0.13 – 1.16)
F	2.01 (0.95 – 3.69)	3.42 (1.33 – 5.83)	1.05 (0.48 – 1.95)
G	0.64 (0.02 – 1.13)	0.85 (0.05 – 2.31)	0.27 (0.0 – 0.38)
H	0.15 (0.03 – 0.92)	1.05 (0.09 – 2.78)	0.54 (0.0 – 0.51)
I	0.17 (0.01 – 0.98)	0.64 (0.04 – 1.68)	0.06 (0.0 – 0.19)

Table 2.4: Table 2.4. Pairwise uncorrected sequence divergence values for each major lineage depicted in Figure 2.4, based on Cytochrome *b* sequence data.

Pairise Cytb Sequence Divergence uncorrected *p*-distance					
	harrisii	*insularis*	*interpres*	*nelsoni*	*leucurus* north
harrisii	–				
insularis	0.034	–			
interpres	0.041	0.043	–		
nelsoni	0.017	0.030	0.041	–	
leucurus north	0.012	0.032	0.040	0.015	–
leucurus south	0.035	0.019	0.045	0.031	0.034

Figure Legends

Figure 2.1: Map depicting the distribution of North American Deserts (Chihuahuan, Great Basin, Mojave, Peninsular, and Sonoran) and some associated aridlands (Apache Highlands and Central Valley) in western North America (based on Shreve 1942, Hafner and Riddle 1997, and Riddle et al. 2000).

Figure 2.2: Map depicting the distribution of each species of *Ammospermophilus* (colored areas) superimposed on the North American deserts (grayscale). Asterisks represent pre-Holocene fossil deposits within the current distribution of the genus: white asterisk indicates the oldest known fossil, *A. fossilis*, in Cuyama Valley, CA; black asterisk indicates a separate fossil locality Baja California Sur, Mexico (*A. jeffreisi*).

Figure 2.3: ML and BI Phylogenetic tree depicting the relationships of all the major lineages of *Ammospermophilus*, based on seven genes (3 mtDNA, 2 rRNA, 2 nDNA: 5962 total base pairs). Asterisks represent nodes with a BI posterior probability >0.95 and a ML bootstrap value >70%. Horizontal dashed lines separate the 3 major clades.

Figure 2.4: ML/BI phylogenetic tree depicting the divergence dates of each major lineage of *Ammospermophilus*. Arrows at nodes A and B represents alternative placements of the fossil (*A. fossilis*) calibration. Numbers below each node represent divergence time estimates (mya) based on the fossil calibration placed at node A (grey bars represent the 95% confidence intervals surrounding each estimate). Numbers above each node represent divergence time estimates based on the fossil calibration placed at

node B (no confidence intervals are indicated for these values. Geologic time scale and branch lengths correspond to fossil calibration at node A. Node letters correspond to divergence time estimates listed in Table 2.3.

Figure 2.5: Results of the phylogeographic analysis of *Ammospermophilus* samples based on mitochondrial CO3 and Control Region data (all haplotypes represented). A – Bayesian Inference tree depicting relationships between all haplotypes sampled across the range of all species. Asterisks represent nodes with posterior probabilities ≥ 0.95. B – collection localities for all samples. C – median-joining network depicting the relationship between haplotypes of all samples. Branch lengths are proportional to number of differences (except where indicated by hash marks). Circle size is proportional to the number of each haplotypes. Colors in each figure represent each species: orange - *leucurus*, light blue - *interpres*, red - *insularis*, green - *nelsoni*, dark/light blue - *harrisii*).

Figure 2.6: ML phylogenetic trees showing the relationships of mtDNA haplotypes (mitochondrial CO3 + Control Region) in the mainland US (A) and northern Baja California (B) and southern Baja California (C) *leucurus* clades. Horizontal dashed lines indicate location of each major lineage. Though resolved trees are shown, nodes are well supported (≥0.95 Bayesian posterior probability, ≥70% ML bootstrap) only if denoted by an asterisk.

Figure 2.7: Mismatch distributions (expected – red; observed – blue) representing the haplotype frequency distribution of the three major lineages of *Ammospermophilus leucurus:* mainland US (A), Baja California north (B) and Baja California south (C) clades. X-axis = pairwise haplotype differences; Y-axis = frequency of each haplotype. Each mismatch distribution corresponds to the populations depicted in Figure 2.6 (clades A, B, and C). Insets include nucleotide diversity (π), haplotype diversity (h), and Tajima's *D* statistics. Unimodal mismatch distributions, high haplotype diversity, low nucleotide diversity, and significantly negative values of Tajima's *D*, consistent across all three geographically distinct population sets, are characteristic of recently expanding populations.

Figure 2.8: Ecological niche models of predicted distributions based on current climatic conditions (present-day) for A – northern *leucurus* clade, C – southern *leucurus* clade, and E – *interpres* clade. Ecological niche models of predicted distribution at the last glacial maximum (18k ybp) for B – northern *leucurus* clade, D – *southern* leucurus clade, and F – *interpres* clade. The grayscale shading represents the probability of occurrence, with the darkest color (black) indicating most suitable predicted habitat and the lightest shading (light gray) indicating least suitable predicted habitat. A probability of occurrence less than 5% is indicated by the white areas and represents unsuitable habitat.

Figure 2.1


Great Basin
Central Valley
Colorado Plateau
Mojave
Sonoran
Apache Highlands
Chihuahuan
Peninsular
N
0
110
220
440
Miles

Figure 2.2

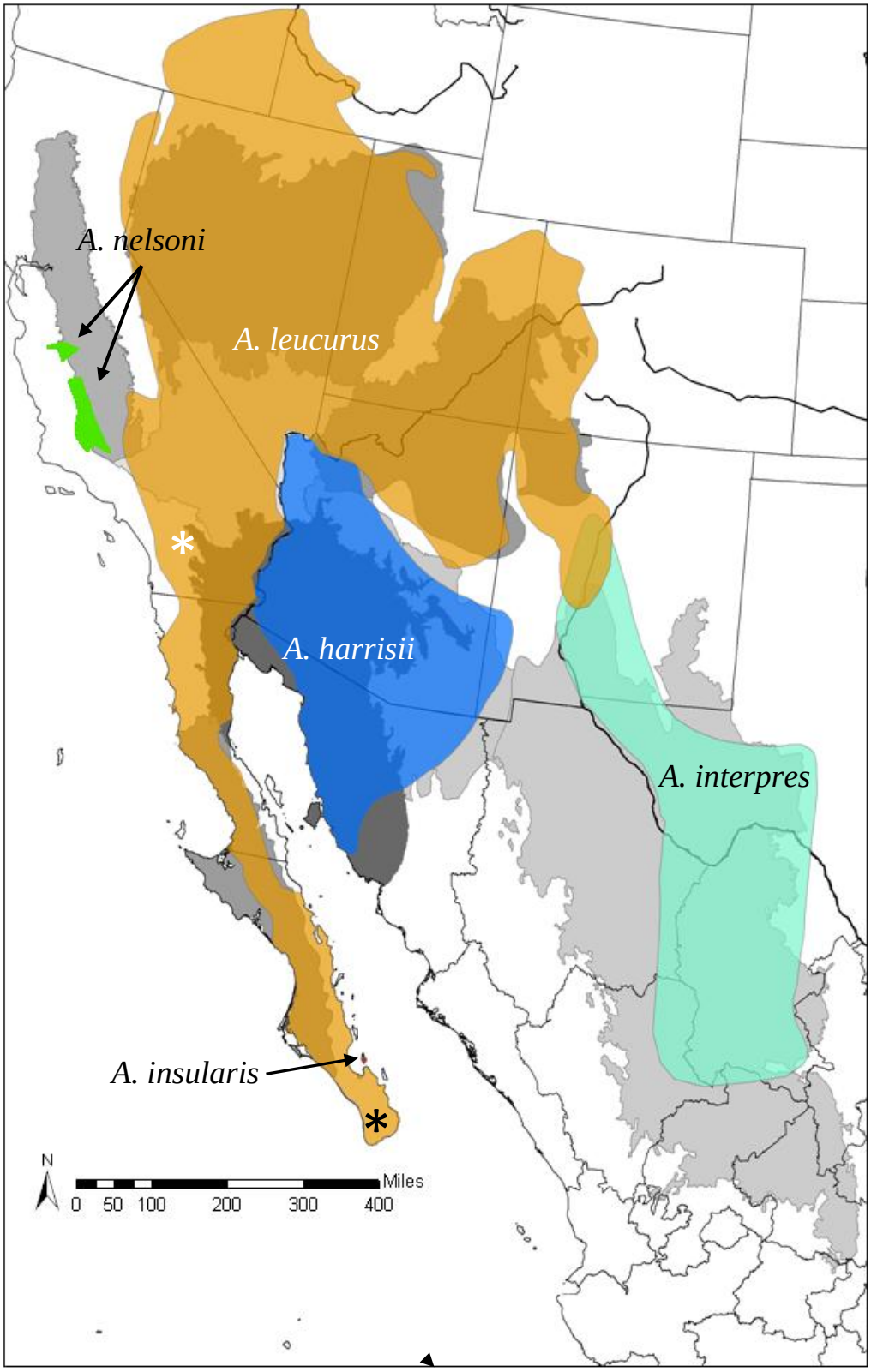
A. nelsoni
A. leucurus
A. harrisii
A. interpres
A. insularis
N
Miles
0 50 100 200 300 400

Figure 2.3

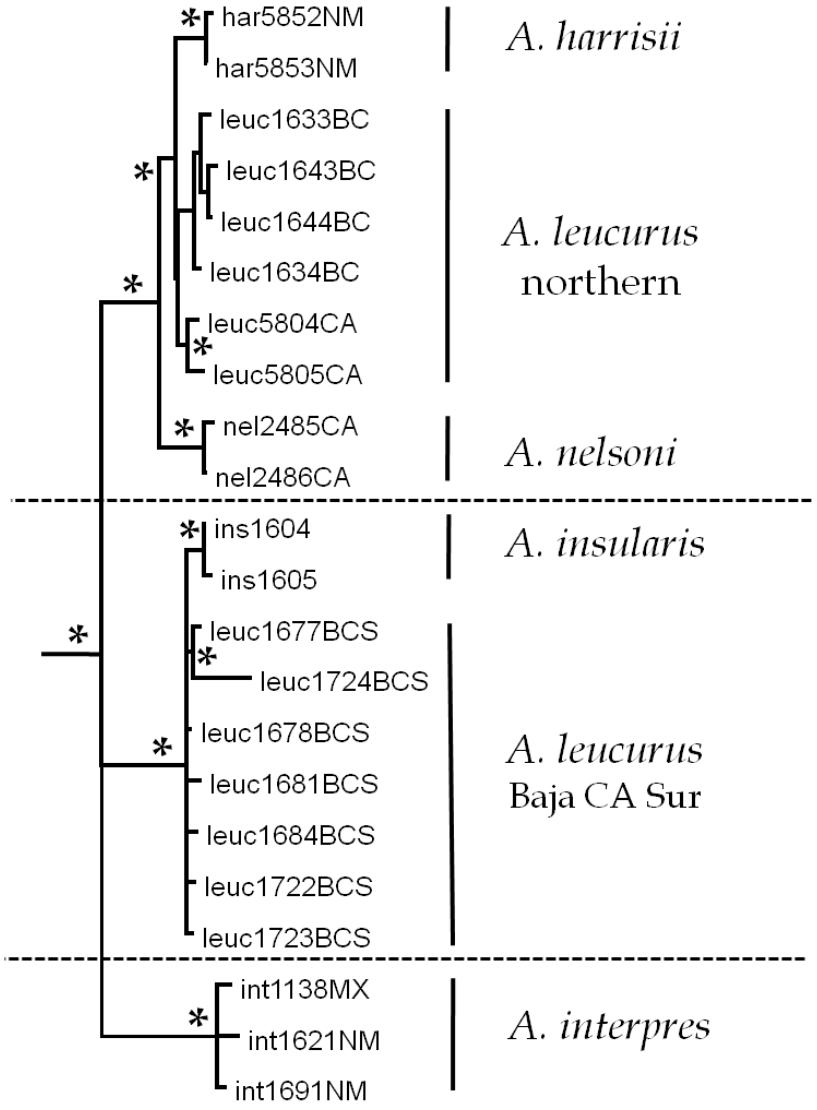
har5852NM
har5853NM
A. harrisii
leuc1633BC
leuc1643BC
leuc1644BC
leuc1634BC
leuc5804CA
leuc5805CA
A. leucurus
northern
nel2485CA
nel2486CA
A. nelsoni
ins1604
ins1605
A. insularis
leuc1677BCS
leuc1724BCS
leuc1678BCS
leuc1681BCS
leuc1684BCS
leuc1722BCS
leuc1723BCS
A. leucurus
Baja CA Sur
int1138MX
int1621NM
int1691NM
A. interpres

Figure 2.4

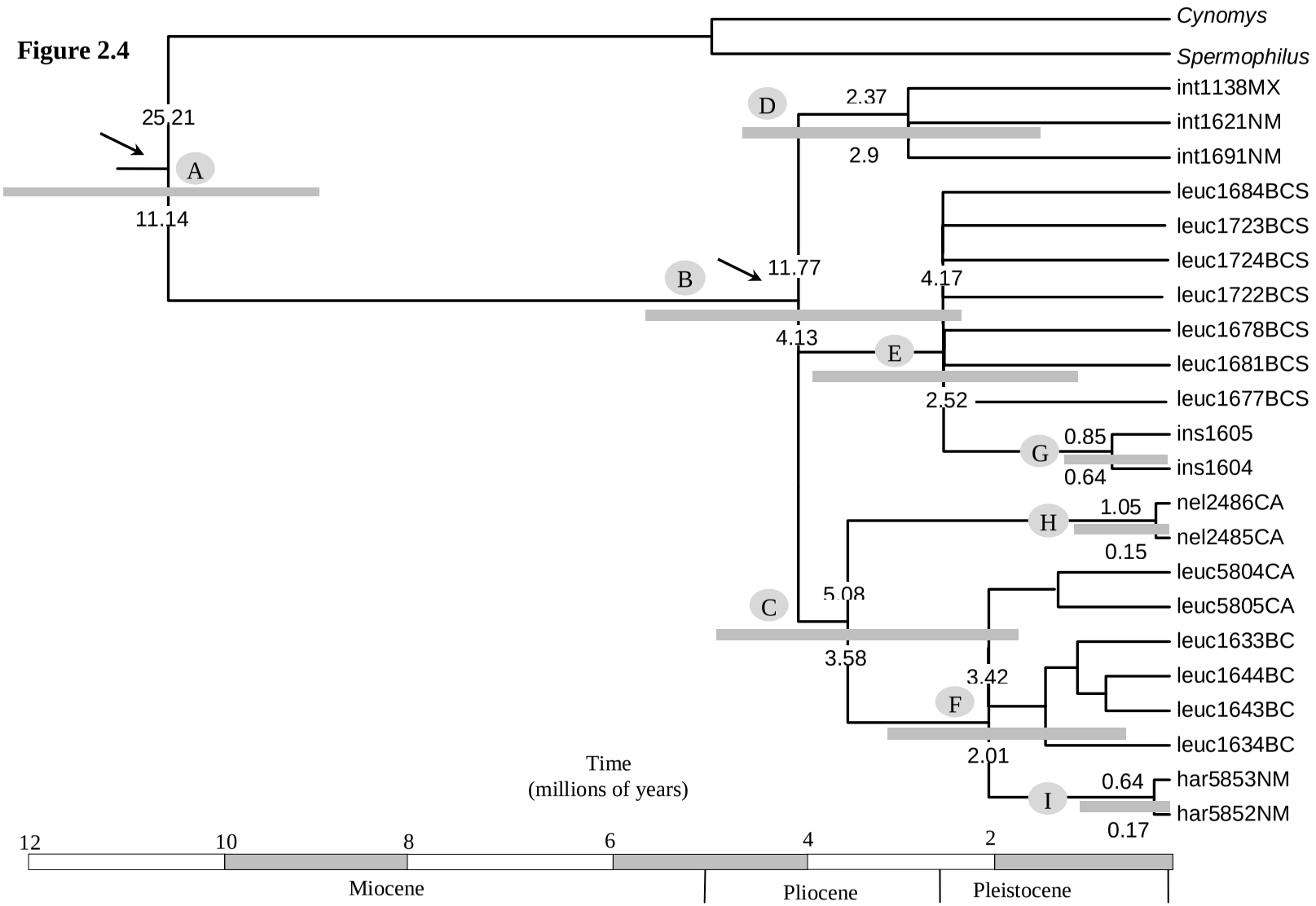
Cynomys
Spermophilus
int1138MX
int1621NM
int1691NM
leuc1684BCS
leuc1723BCS
leuc1724BCS
leuc1722BCS
leuc1678BCS
leuc1681BCS
leuc1677BCS
ins1605
ins1604
nel2486CA
nel2485CA
leuc5804CA
leuc5805CA
leuc1633BC
leuc1644BC
leuc1643BC
leuc1634BC
har5853NM
har5852NM
25.21
A
11.14
B
11.77
4.13
C
5.08
3.58
D
2.37
2.9
E
4.17
2.52
G
0.85
0.64
H
1.05
0.15
F
3.42
2.01
I
0.64
0.17
Time
(millions of years)
12
10
8
6
4
2
Miocene
Pliocene
Pleistocene

Figure 2.5

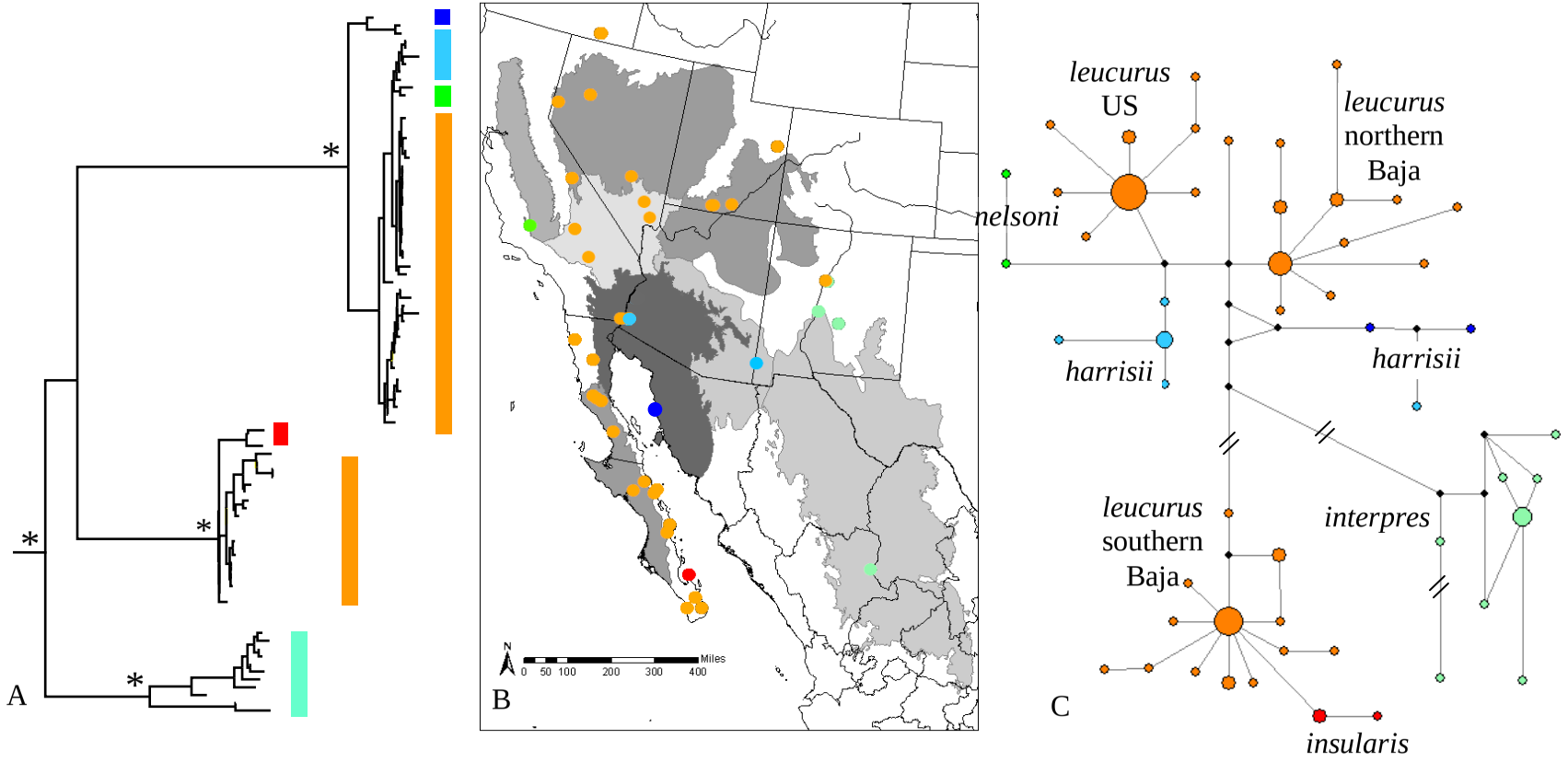
A
B
C
N
0 50 100 200 300 400
Miles
leucurus
US
leucurus
northern
Baja
nelsoni
harrisii
harrisii
leucurus
southern
Baja
interpres
insularis

Figure 2.6

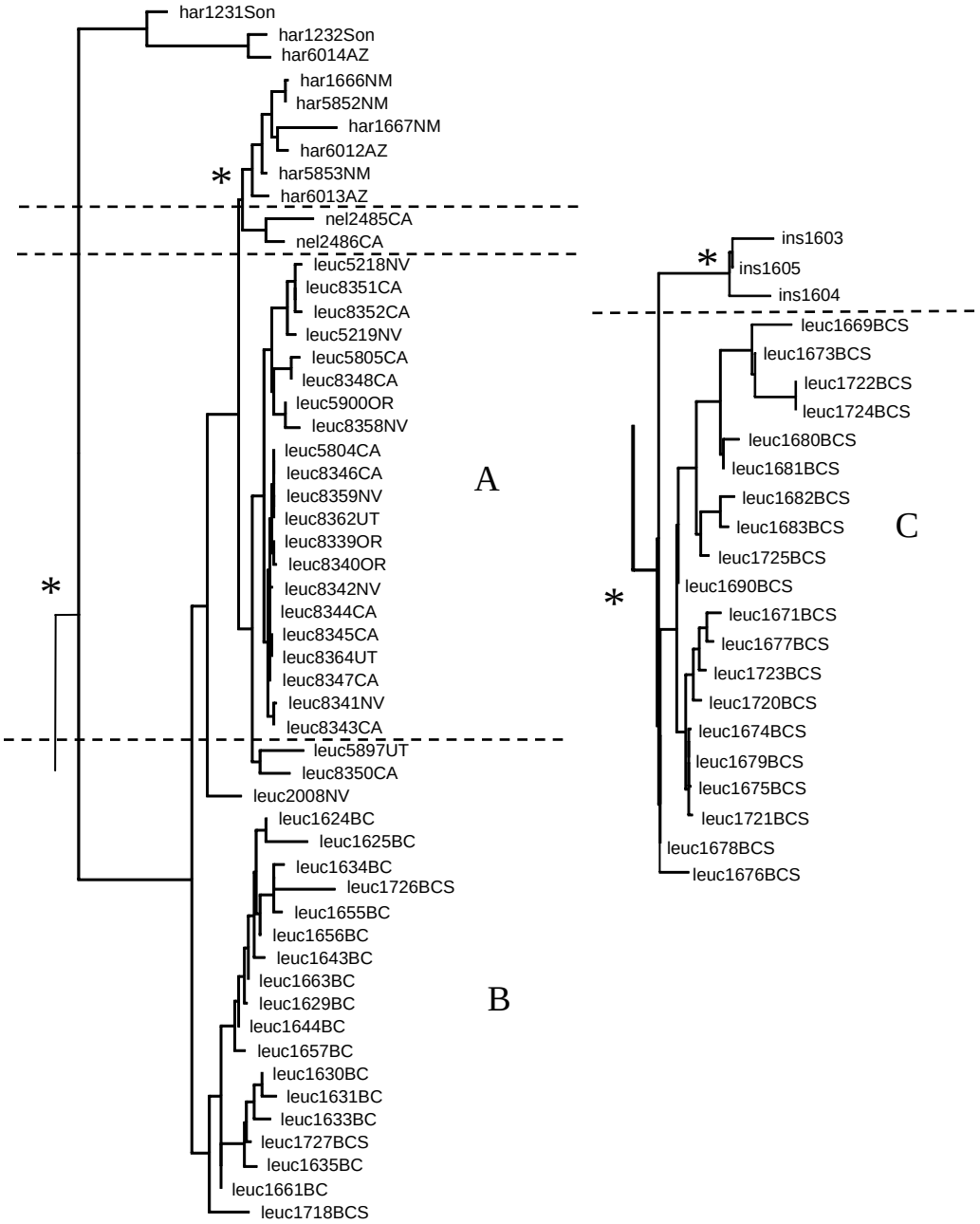
har1231Son
har1232Son
har6014AZ
har1666NM
har5852NM
har1667NM
har6012AZ
har5853NM
har6013AZ
nel2485CA
nel2486CA
leuc5218NV
leuc8351CA
leuc8352CA
leuc5219NV
leuc5805CA
leuc8348CA
leuc5900OR
leuc8358NV
leuc5804CA
leuc8346CA
leuc8359NV
leuc8362UT
leuc8339OR
leuc8340OR
leuc8342NV
leuc8344CA
leuc8345CA
leuc8364UT
leuc8347CA
leuc8341NV
leuc8343CA
leuc5897UT
leuc8350CA
leuc2008NV
leuc1624BC
leuc1625BC
leuc1634BC
leuc1726BCS
leuc1655BC
leuc1656BC
leuc1643BC
leuc1663BC
leuc1629BC
leuc1644BC
leuc1657BC
leuc1630BC
leuc1631BC
leuc1633BC
leuc1727BCS
leuc1635BC
leuc1661BC
leuc1718BCS
A
B
ins1603
ins1605
ins1604
leuc1669BCS
leuc1673BCS
leuc1722BCS
leuc1724BCS
leuc1680BCS
leuc1681BCS
leuc1682BCS
leuc1683BCS
leuc1725BCS
leuc1690BCS
leuc1671BCS
leuc1677BCS
leuc1723BCS
leuc1720BCS
leuc1674BCS
leuc1679BCS
leuc1675BCS
leuc1721BCS
leuc1678BCS
leuc1676BCS
C

Figure 2.7

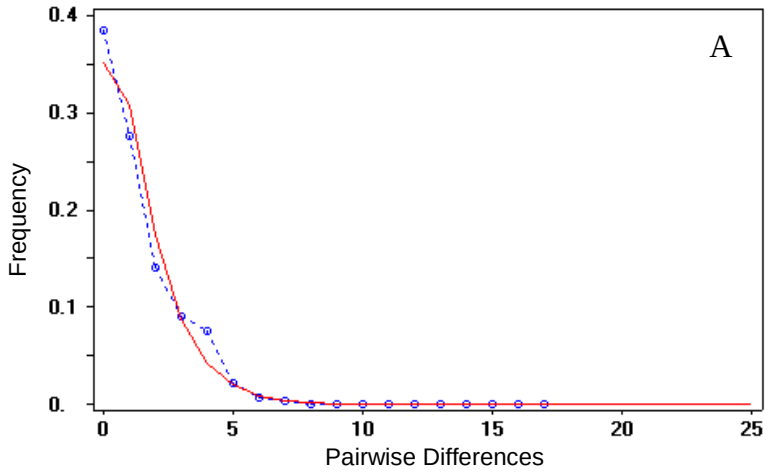

leucurus – US

π = 0.0019 (nucleotide diversity)
H = 0.616 (haplotype diversity)

Tajima's *D* = -2.16215 (P < 0.01)

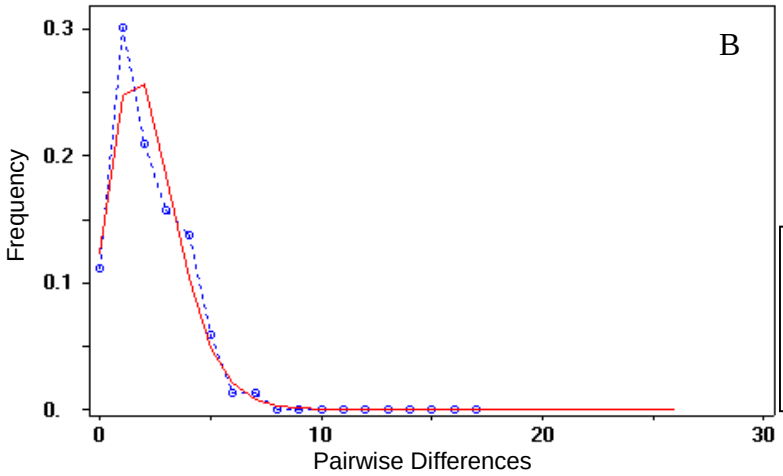

leucurus – Baja California North

π = 0.00319 (nucleotide diversity)
H = 0.982 (haplotype diversity)

Tajima's *D* = -1.87675 (P < 0.05)

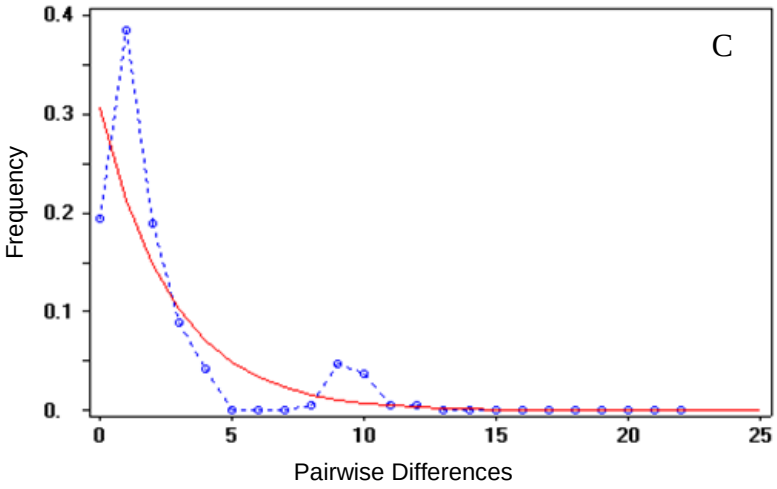

leucurus – Baja California South

π = 0.00315 (nucleotide diversity)
H = 0.805 (haplotype diversity)

Tajima's *D* = -2.16208 (P < 0.01)

Figure 2.8

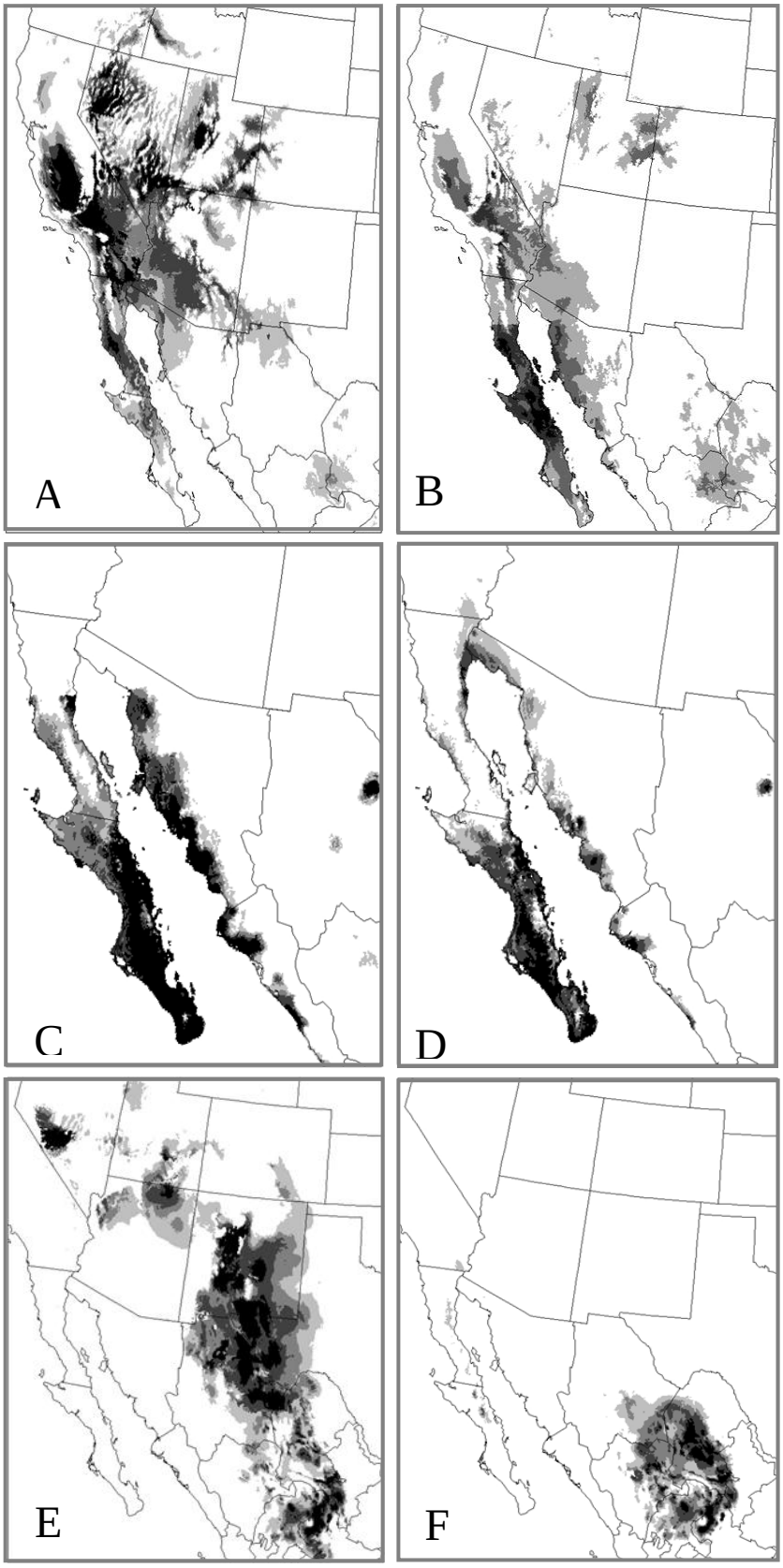

CHAPTER 3

INTEGRATING PHYLOGEOGRAPHY AND POPULATION GENETICS WITH ECOLOGICAL NICHE MODELING ACROSS A CONTINUOUS LANDSCAPE IN A DESERT BAT (*PIPISTRELLUS HESPERUS*)

Introduction

The geographic distributions of organisms are shaped by their abilities to adjust to dynamic and often unpredictable biotic and abiotic environments, including a history of geologic and climatic changes. In western North America, where deserts currently occupy close to two million square kilometers, the glacial cycles that occurred throughout the late Pleistocene directly affected population connectivity and gene flow, and thus the evolutionary trajectories of the resident taxa. Within the North American deserts, many taxa experienced high levels of initial divergence prior to the Pleistocene (Miocene and Pliocene) and subsequent population diversification during the Pleistocene (Riddle 1995; Hafner and Riddle 1997). The Pleistocene is characterized by repeated isolation and reconnection of populations as well as distributional changes as a result of climatic changes associated with the expansion of xeric habitats that occurred following the last glacial maximum (LGM) at approximately 18,000 years ago (Pielou 1991).

We now have powerful genetic methods for inferring the evolutionary history and dynamics of gene flow among populations and metapopulations across the distribution of species. Phylogeography is an approach in historical biogeography that seeks to reconstruct the evolutionary and ecological histories of taxa and biotas, often at relatively recent temporal (e.g., thousands to several millions of years) and relatively small (e.g., intra-continental) spatial scales. By comparing the geographic distribution of genetic

lineages within co-distributed species, we can develop and test plausible hypotheses as to the overall importance of biogeographic factors that have shaped current species distributions and patterns of diversification (Riddle et al. 2000c; Arbogast and Kenagy 2001; Riddle and Hafner 2006).

Most recently, molecular sequencing techniques have allowed even more thorough investigations of the phylogeography of desert taxa in western North America (reviewed in Riddle and Hafner 2006c). This region presents particularly interesting abiotic challenges to widespread species because there are both warm (Chihuahuan, Mojave, Sonoran, Peninsular) and cold (Great Basin) deserts, as well as associated semi-arid regions that contain an array of varied desert environments with an equally broad array of environmental and physiological challenges (Bradley and O'Farrell 1969; Walsberg 2000; Tracy and Walsberg 2002). Most of these analyses have focused on taxa distributed primarily in the warm deserts. These include mammals (Riddle et al. 2000a, b; Riddle et al. 2000c; Alvarez-Castañeda and Patton 2004; Bell et al. 2009; Jezkova et al. 2009), birds (Zink et al. 2001; Zink 2002), reptiles (Upton and Murphy 1997; Lindell et al. 2005; Douglas et al. 2006; Leaché et al. 2007; Leaché and Mulcahy 2007), amphibians (Jaeger et al. 2005), spiders (Ayoub and Reichert 2004; Crews and Hedin 2006) and plants (Nason et al. 2002; Garrick et al. 2009) as well as fish species bordering warm desert regions (Bernardi and Lape 2005; Reginos 2005).

Comparative analyses of multiple taxa in the deserts of western North America have identified a mosaic of differing genetic relationships within and between major geographic areas (Figure 3.1), including both shared and differential responses to a suite of postulated isolating events. The complexity is probably a consequence of the differing

abilities of different species to disperse across putative isolating barriers. Absence of genetic differentiation across the range of a species could result if a species was not influenced by a particular barrier. This pattern has been reported, for example, for species of desert birds (*Polioptila melanura* – Zink et al. 2001) and bats (*Myotis californicus* – Rodriguez and Ammerman 2004). One of the most pervasive patterns of divergence occurs between southern and northern populations on the Baja California Peninsula (PS vs. PN; Figure 3.1), even when there is little or no structure between additional populations in the continental regions (e.g., *Ammospermophilus* – see Chapter 2; *Campylorhynchus brunneicapillus*, *Auriparus flaviceps* – Zink 2001; *Dipodomys merriami* –L.F. Alexander, pers. comm.,). This division is often attributed to one or more mid-peninsular Vizcaíno seaways hypothesized to have existed sometime between ca. 4 – 1 mya (Upton and Murphy 1997; Riddle et al. 2000c; Lindell et al. 2006).

In certain species, western continental desert populations have been separated from eastern continental desert populations as a result of the uplift of the secondary Sierra Madre Occidental and the Mexican Plateau, ca. 10-5 mya, creating a significant genetic separation across these regions (Coney 1983; Riddle and Hafner 2006). Many widespread taxa exhibit significant genetic structure across all of these major isolating barriers, and those that occur into the cold deserts of the Great Basin and Colorado Plateau may show additional splits as well. There are also co-distributed taxa that appear to not fit these general patterns or have responded to varying degrees to some or all of these and other isolating events, creating unique patterns (e.g., lizards in the genus *Xantusia* – Sinclair et al. 2004; spiders in the genus *Agelenopsis* – Ayoub and Reichert 2004).

The western pipistrelle (*Pipistrellus hesperus*), a bat in the family Vespertilionidae, represents an additional species to add to the growing comparative framework for examining the embedded phylogeographic structure of biotas within the North American deserts. The western pipistrelle is restricted to the aridlands of western North America, distributed broadly across both the warm and cold deserts (Fig. 3.2). This species extends into the semi-arid habitats west of the Sierra Nevada Mountains in California, south into the subtropical deciduous thorn scrub forests in western Mexico, east onto the Colorado Plateau in Utah, Colorado and New Mexico, and southward into the states of Guerrero and Hidalgo in south-central Mexico (Hall 1981). This insectivorous species is the smallest bat in North America and is generally confined to desert mountain ranges and canyon-lands where roost sites are abundant (Findley and Traut 1970; Kuenzi et al. 1999). Recent work (Hoofer and Van Den Bussche 2003, 2006) suggested that the two New World species of *Pipistrellus* (*P. hesperus* in western North America and *P. subflavus* in the east) do not share a most recent common ancestor with a diverse assemblage of *Pipistrellus* species in other biogeographic regions or with each other. The authors recommended a taxonomic revision of the genus that included placing *P. hesperus* in the genus *Parastrellus* and *P. subflavus* in the genus *Perimyotis* (Hoofer and Van Den Bussche 2006). However, for simplicity and because the higher level relationships and taxonomy of vespertilionid bats and *Pipistrellus* (*sensu lato*) are not well resolved, *Pipistrellus hesperus* is used herein.

The western pipistrelle has been traditionally considered a single species but exhibits identifiable patterns of coloration and size variation across its range. Based on a morphological analysis of individuals collected across the entire range (Findley and Traut

1970), there is a separation into eastern (*P. h. hesperus*) and western (*P. h. maximus*) subspecies at the continental divide (roughly at 110° W, between New Mexico and Arizona and south into Mexico). Population substructure has been correlated with morphological differentiation in bats (Miller-Butterworth et al. 2003), and so the morphological patterns in *P. hesperus* may indicate underlying genetic differentiation between populations.

Populations of *P. hesperus* in the southwest deserts were postulated by Findley (1969) to have been divided into an eastern Chihuahuan and a western Sonoran refugium during the LGM, coupled with population expansions following glacial retreat. While such LGM isolation may represent the deepest divergence within *P. hesperus* (Findley and Traut 1970), divergences in several co-distributed vertebrates have been estimated to have occurred much earlier in the Miocene or Pliocene (reviewed in Riddle and Hafner 2006b). These deeper divergences could have been driven by the formation of the regional deserts during these earlier times. Ultimately, by examining the phylogeographic patterns within *P. hesperus*, this study will add another component to the comparative phylogeography of western North American desert vertebrates.

Objectives

Geographic differentiation within *P. hesperus* was evaluated using a combination of phylogeographic and population genetic analyses along with ecological modeling of shifting habitats. This approach was be applied to examine populations collected across much of the range of this species to better understand the relative roles of dispersal, vicariance, and range-shifting in shaping geographic patterns of genetic structure and differentiation. This approach integrates ecological niche modeling with phylogeographic

analyses to: 1) examine the overall phylogeographic patterns of genetic diversity; and 2) assess the distributional shifts of this species, including signatures of post-Pleistocene range expansion, to late Pleistocene and Holocene changes in habitats. This research adds to growing body of research that focuses on the regional phylogeography of North American desert bats: *Myotis* (Rodriguez and Ammerman 2004); *Antrozous* (Weyandt and Van Den Bussche 2007), and a cadre of other members of an aridlands biota (reviewed in Riddle and Hafner 2006).

Hypothesis Testing

A series of nested hypotheses have been developed that span the potential temporal breadth of biogeographic and evolutionary history of *P. hesperus* across a late Neogene (e.g., Plio-Pleistocene) timeframe. These hypotheses recognize that the distributions and diversification of taxa within western North America have been generated through a complex set of multiple vicariance and dispersal events, influenced by the climatic cycles during this period. Across the distribution, a widespread *P. hesperus* lineage may never have been completely separated by a barrier, maintaining widespread gene flow. Alternatively, a widespread lineage could have responded to deeper divisions (≥1–5 mya) across the deserts, with extant population and phylogeographic structure retaining signatures of these Neogene divergences (i.e., vicariance of widespread taxa), in accord with the generalized history postulated in Figure 3.3. The null fragmentation hypothesis (Figure 3.3a) depicts the fragmentation of a single widespread ancestral population, and is consistent with a pattern of no correlation between geographic and genetic distances, and constant population size through time. Nested within this long-term history of possible vicariance, *P. hesperus* lineages may also retain signatures of Pleistocene range

expansion out of multiple refugia (Figure 3.3b). If *P. hesperus* has responded to various biogeographic events, we can expect this species to show phylogeographic structure and genetic divergence between populations, in contrast to the expectation of a correlation of flight ability with lack of genetic divergence (Lloyd 2003). Following a hypothesis of "leading edge expansion," (Hewitt 2001) southern populations will show evidence of relatively high haplotype diversity, consistent with refugial areas, while northern populations will show patterns of decreased haplotype diversity, indicating recent range expansions. To the extent that late Pleistocene range shifting dynamics are embedded within any earlier, large-scale episodes of biogeographic isolation and divergence within multiple refugia (Figure 3.3), lineages within *P. hesperus* will be partitioned into major geographic areas – e.g., Peninsular/Mojave/Great Basin Deserts (western), Sonoran Desert (central), and Chihuahuan Desert (eastern) – with gene flow occurring within these major areas to a much greater degree than among them (Figure 3.3).

Materials and Methods

Sampling & Laboratory Protocols

A collection of tissues from 96 individuals was assembled, including representatives of *P. hesperus* from 35 localities across western North America (Figure 3.2; Appendix B). All newly collected individuals were prepared as voucher specimens and deposited in the New Mexico Museum of Natural History (NMMNH) and tissue samples were deposited in the Las Vegas Tissue Collection (LVT) at the University of Nevada, Las Vegas (Appendix B). DNA sequence data was generated from a portion of the mitochondrial Cytochrome *b* (Cytb) gene and a portion of the D-loop from the mitochondrial Control Region (CR) for at least one individual from each collecting

locality (n = 36) to establish the basic phylogenetic structure among populations. To further explore the extent of geographic variation in *P. hesperus,* sequence data was generated for the same portion of Cytb for all 96 individuals.

For each specimen, total genomic DNA was extracted from liver or kidney tissues using the Qiagen DNeasy Tissue Extraction Kit (Qiagen, Inc.). The polymerase chain reaction (PCR) was used to amplify the specific molecular markers, incorporating *Ex-Taq* (Takara-Bio USA) DNA polymerase and gene specific primers. The CR was amplified with primers "C" and **"**E" (Kocher et al. 1989; Wilkinson and Chapman 1991) and a temperature profile of 95ºC for 5 minutes, 55ºC for 1 min., 72ºC for 1 min., and a final extension of 72ºC for 10 minutes. The Cytb was amplified using primers H15915 and L14724 (Kocher et al. 1989) with a temperature profile of 95ºC for 5 minutes, 50ºC for 1 min., 72ºC for 1 min., and a final extension of 72ºC for 10 minutes. Double-stranded PCR products were qualitatively examined using a 0.8% agarose gel with a molecular mass ruler for size comparison. The amplified PCR fragments were purified using either the Qiaquick PCR Purification Kit (Qiagen, Inc.) or Exo-SAP IT (USB Corp.), following manufacturers' protocols. Sequencing reactions were performed using the purified PCR products (including both the light and heavy DNA strands) and ABI PRISM BigDye v.3.1 Cycle Sequencing chemistry (Applied Biosystems, Inc.). For the CR, the sequencing reactions were performed with primers "P" and "F" (Wilkinson and Chapman 1991) and the Cytb sequencing reactions used the same primers as the PCR (see above). Unincorporated dye-teminators were removed using Sephedex spin columns (Centri-Sep, Inc.) and sequence data were generated on an ABI 3130 Genetic Analyzer (Applied Biosystems, Inc). Complementary DNA strands were aligned for each molecular marker

using SEQEUNCHER 4.9 (Gene Codes Corp.), followed by manual proofreading. The Cytb protein coding sequences were translated into amino acids using MACCLADE 4. (Maddison and Maddison 2005) and compared to *Pipistrellus abramus* and *Artibeus jamaicensus* to confirm the correct reading frame and to check for the presence of stop codons.

Phylogenetic Analyses

Recent work on the systematics of vespertilionid bats indicates that not only is *P. hesperus* not closely aligned with other members of the genus *Pipistrellus* (*sensu stricto*), but it may be distantly related to other vespertilionid species as well. The placement of *P. hesperus* within the Vespertilionidae and the intergeneric relationships of most vespertilionid genera remains unresolved and so there is not a readily apparent sister taxon to use as an outgroup for rooting purposes (Hoofer and Van Den Bussche 2003, 2006). For these analyses, *Antrozous pallidus* (pallid bat) was used for rooting purposes as. *Antrozous* was identified as belonging to a potential sister clade to *P. hesperus* (Hoofer and Van Den Bussche 2003).

The basic phylogenetic structure among samples of *P. hesperus* was determined with the combined Cytb and CR dataset. These molecular markers were concatenated and JMODELTEST 0.1.1 (Guindon and Gascuel 2003; Posada 2008) was used with default parameters and ML optimization to determine the appropriate model of nucleotide substitution under the Akaike Information Criterion (AIC – Posada and Crandall 1998; Posada and Buckley 2004). Using this model, a maximum likelihood (ML) phylogenetic analysis was performed with non-parametric bootstrapping (1000 replicates; Felsenstein 1985), implemented in TREEFINDER v.2008 (Jobb et al. 2004). Bayesian Inference (BI),

implemented in MRBAYES v.3.1.2 (Ronquist and Huelsenbeck 2003), was also used with posterior probabilities as evidence of support for relationships within the phylogeny. MrBayes was run for 2 x 10^6 generations (sampling every 100 generation) with an initial burn-in of 2 x 10^3 generations (2,000 trees), four Monte Carlo Markov Chains, and a temperature value of 0.05 to promote proper swapping of the chains. The program AWTY (Wilgenbusch et al. 2004) was used to assess the proper convergence of runs by examining the posterior probabilities of clades for non-overlapping samples of trees.

Estimating Demographic Parameters

A median-joining network was generated by the program Network v.4.516 (Bandelt et al. 1999) to visualize the relationships among haplotypes of all samples in the Cytb dataset. This network method addresses the problems found with intraspecific datasets with large sample sizes and short genetic distances between samples. Median-joining networks are modified minimum-spanning networks that use a maximum parsimony approach to find the shortest possible network to explain the relationships between the individuals (Bandelt et al. 1999). An Analysis of Molecular Variance (AMOVA) was performed using ARLEQUIN 2.0 (Schneider et al. 2000) to assess levels of within versus among population variation across the major clades identified in the phylogenetic analyses. Based on the results of the AMOVA (within vs. among clade variation), a suite of demographic parameters were calculated for the major geographically defined sets of populations (clades). Tajima's *D* (Tajima 1989b, a) and Fu's *Fs* (Fu 1997) neutrality statistics were calculated using ARLEQUIN 2.0 (Sokal and Rohlf 1995), and mismatch distributions of pairwise differences versus haplotype frequency and pairwise uncorrected

sequence divergence values were calculated for each clade using DNASP 5 (Rozas et al. 2003).

Coalescence Analyses – Estimating Divergence Times

To estimate the coalescence times (divergence dates) for the genetic lineages within each major clade and for all lineages represented in the Cytb dataset, an MCMC Bayesian approach was implemented in the program BEAST 1.5.1 (Drummond and Rambaut 2007) with a strict molecular clock. This method allows us to estimate the coalescent time to most recent common ancestor (Tmrca) for all alleles in a sample, scaled by the mutation rate (μ) of the gene. For the Cytb gene, an evolutionary rate of 2%/My (0.01 substitutions/site/My) was used, which is standard rate estimated across several mammalian divergences (Arbogast and Slowinski 1998; Pesole et al. 1999). The coalescence analyses were conducted with the appropriate model chosen by jModeltest for this dataset. Several short chains were run to optimize the scaling factors for the model parameters and then chains of 4×10^7 generations were run, with parameters sampled every 1000 generations (40,000 trees). The first 4×10^6 generations (10% – 4000 trees) were discarded as burn-in before the analysis reached stationarity, determined using the program Tracer 1.4.1 (Rambaut and Drummond 2007).

Ecological Niche Modeling – Current & Paleo-distributions

Ecological niche models (ENMs) were constructed for *P. hesperus* using occurrence records and climatic conditions both at present-day (0 kya) and during the last glacial maximum (18kya). Occurrence records of individuals examined in this study (Appendix B) as well as a subset of available records (n = 525) listed in MaNIS (http://manisnet.org) were used to construct these models. Following the methods of Waltari and Guralnick

(2008), duplicate locality records were removed and the final models included only samples with a radius of geographical uncertainty that was less than 5km (Wieczorek et al. 2004). This method reduces the bias inherent in imprecise occurrence data (Waltari and Guralnick 2009). The maximum entropy method, implemented in MAXENT 3.2.1 (Phillips et al. 2006; Phillips and Dudik 2008) is designed to find distributions among climatic variables and digital environmental layers to predict logistic non-negative probabilities based on presence-only occurrence data (Stockman and Bond 2007). This method has been shown to outperform similar habitat estimators (Phillips and Dudik 2008; Elith and Graham 2009) and has been used in several recent phyloclimatic studies (Carstens and Knowles 2007; Waltari and Guralnick 2009). The predictions for this analysis are based on elevation plus a suite of 19 bioclimatic parameters previously compiled from the WorldClim climate layers (Hijmans et al. 2005; Waltari et al. 2007), with a 5 km^2 pixel resolution.

Model calibrations were performed using 75% of the data as a training group and then the predicted distribution models were tested with the remaining 25% (Evans et al. 2009). Default parameters (500 maximum iterations, convergence threshold of 0.00001, regularization multiplier of 1, 10000 background points) were used with a random seed, the removal of multiple presence records from individual cells resulting from many sampling localities within $5km^2$ (i.e., one pixel), and logistic probabilities for the output (Phillips and Dudik 2008). To reduce the effects of spatial autocorrelation, split-sample approach was used that separates the geographically closest sample pairs between the training and test groups (Fielding and Bell 1997; Parolo et al. 2008).

A complete model (including all 20 variables) was run initially to produce "area under the receiver operation characteristic curve" (AUC) values for each bioclimatic parameter. A minimum AUC of 0.75 for the test group is considered the threshold for good model performance (Elith et al. 2006; Suárez-Seoane et al. 2008; Elith and Graham 2009). Consequently, those parameters with AUC values less than 0.75 were removed. The reduced models were run using temporal transfer modeling from the present-day distribution (0 kya) to the LGM (18 kya), incorporating information in the Community Climate Model System Model (CCSM–Otto-Bliesner et al. 2006) and the Model for Interdisciplinary Research on Climate (MIROC – Hasumi and Emori 2004). MaxEnt was run three separate times using both the CCSM and MIROC climate reconstructions and the habitat models were averaged, accepting only those areas that both methods agreed were suitable (Waltari and Guralnick 2009). Binary maps were created of the habitat models using ARCGIS 9.2 (ESRI Corp., Redlands, CA) by averaging the three independent MaxEnt runs using the Spatial Analyst feature (Raster Calculator) in ARCGIS. Because the suitability of the predictive area in the models is based on chosen threshold values, the models were evaluated across four logistic thresholds: fixed cumulative value of 10.0, equal training sensitivity and specificity, equal test sensitivity and specificity, and equate entropy of thresholded and non-thresholded distributions. These threshold values were used to assess a range of sensitivities and specificities to ensure that our model interpretations are robust. Ultimately, the cutoff of suitable habitat was set at a fixed cumulative probability of 10, a level that rejects the lowest 10% of predicted logistic values. This value, though conservative, maintains a low emission rate

(Pearson et al. 2007) consistent with the expectation that the occurrence records contain georeferencing errors.

Results

Phylogenetic Analyses

To establish the basic phylogenetic structure of the populations, a portion of the mitochondrial CR was sequenced (482 bp) along with a portion of the Cytb gene (402 bp) for at least one individual from each collecting locality. This dataset yielded 36 total samples with 94 informative characters for CR and 32 informative characters for Cytb. Using JModeltest, the GTR+*I*+*Γ* model was chosen as the best fit for the data (-ln = 3059.1776, K=82) with a gamma shape parameter (α) = 0.6540 and a proportion of invariant sites = 0.6230 (base frequencies: A=0.3508, C=0.2294, G=0.1214, and T=0.2985). The resulting phylogeny of the combined dataset, using both ML and BI, produced a phylogenetic tree with three well-supported, monophyletic clades (Figure 3.4). Strong nodal support includes bootstrap values above 70% and posterior probabilities above 0.95 (Hillis and Bull 1993; Huelsenbeck and Ronquist 2001). The clades correspond to three non-overlapping geographic areas (Figure 3.3). Clade 1 includes samples collected throughout the Chihuahuan Desert in Coahuila, New Mexico, and Texas; Clade 2 includes individuals collected in California; and Clade 3 includes individuals collected in the Great Basin and Mojave, Peninsular, and Sonoran Deserts (Arizona, Baja California, Baja California Sur, Chihuahua, Durango, Nevada, Sonora, and Utah). For simplicity, this clade will be referred to as the "Sonoran" clade. The phylogeny indicates that Clade 2 is most closely related to Clade 3, indicating that the

samples from California share and close evolutionary relationship with populations currently distributed throughout the Baja California Peninsula, Colorado Plateau, Great Basin, Mojave, and Sonoran Deserts (Figure 3.4). Within Clade 3, samples from Baja California Sur appear to be the most basal lineage with strong nodal support of this placement. Northernmost samples from Nevada and Utah also show a strong relationship, supported by nodal support values. While these relationships are well-supported, many of the internal branches within each major clade are unresolved (Figure 3.4).

Estimating Demographic Parameters

A median-joining haplotype network was created (Figure 3.5) that included Cytb from all samples in the dataset (n = 96). This haplotype network included 31 distinct haplotypes (37 informative characters) and indicated that these were separated into three geographically defined clusters matching the pattern detected in the phylogenetic analysis (Figure 3.4). A large number of mutation steps separated each of these regions with only a few mutational steps separating haplotypes within each region (Figure 3.4). Generally, haplotypes were confined to a single sampling locality, however haplotypes from Arizona, Durango, and Sonora were found in multiple locations (see Figure 3.5). Based on the results of the phylogenetic analysis of the combined dataset (Cytb and CR) and the Cytb haplotype network, samples from the larger Cytb dataset were partitioned into three geographic areas corresponding to the three clades. An AMOVA (Excoffier et al. 1992) on the Cytb dataset (Table 3.1), using HYK85 adjusted genetic distances, indicated that a almost all of the genetic variation is found within each of the major clades (99.85%) compared with almost no variation found among those clades (0.15%), which is consistent with monophyly among the major clades. Based on the AMOVA and the

phylogenetic analyses, populations corresponding to the three major clades were pooled and classified as three separate "populations" for estimating demographic parameters. Demographic and neutrality statistics were calculated based on these three pooled populations. Neutrality statistics (Tajima's *D* and Fu's F_s) were not significant for any single population and pooling all populations also did not produce significant values. Mismatch distributions for both the California (Clade 2, Figure 3.6A) and Chihuahuan clades (Clade 1, Figure 3.6C) generated unimodal curves, which is consistent with recent population expansions. The mismatch distribution for all pooled samples in Clade 3 (Colorado Plateau, Great Basin, Mojave, Peninsular, and Sonoran Deserts) appears bimodal (Figure 3.6B) when all samples from these regions are included. However, samples from the southern Baja California peninsula are separated from the remaining samples in this region by several mutation steps in the haplotype network (Figure 3.5) and are the most basal lineages within this clade (Figure 3.4), suggesting a possible geographic separation and distinct population processes within these populations. Removal of the Baja California samples resulted in a unimodal mismatch distribution for Clade 3 (results not shown), consistent the patterns generated for each of the other clades. For each clade, haplotype diversity (h) is high while nucleotide diversity (π) is low (Table 3.2). Pairwise uncorrected Cytb sequence divergence values for each clade (Table 3.3) indicate that the Sonoran clade is separated from the California clade by 4.7% and from the Chihuahuan clade by 4.5%. The Chihuahuan clade is separated from the California clade by 4.2%. These values are consistent with Cytb sequence divergence values for conspecific populations across many species of mammals (Bradley and Baker 2001).

Coalescence Analyses – Estimating Divergence Times

Coalescence times were generated for the Cytb dataset (n = 96) using the program BEAST 1.5.1 (Drummond and Rambaut 2007) and the HKY + Γ model of nucleotide evolution, chosen in JMODELTEST 0.1.1 with.the following model parameters: -ln = 937.1311, nucleotide frequencies (A = 0.3171, C = 0.2357, G = 0.1388, T = 0.3084), and gamma (α) = 0.030. The coalescence estimate of Tmrca for all alleles sampled in *P. hesperus* was 3.2 million years ago (95% CI: 2.0– 4.5 mya) using a substitution rate of 2%/My (0.01 subs/site/My) for Cytb. The coalescence estimate for lineages within the California clade is 0.67 mya (0.21 – 1.2 mya), the coalescence estimate for the Sonoran clade is 1.02 mya (0.55 – 1.5 mya) and lineages within the California and Sonoran clades coalesce at 2.7 mya (1.7 – 3.9 mya). The coalescent estimate for the Chihuahuan clade is 0.33 mya (0.13 – 0.57 mya), the most recent divergence among the three major lineages of *P. hesperus*. The broad confidence intervals are consistent with analyses performed on a single genetic locus and a short sequence of DNA. These analyses indicate that the initial divergence between the major lineages occurred in the mid-Pliocene and the California and Sonoran clades diverged shortly thereafter near the Plio-Pleistocene boundary and each of the clades experienced divergences within the Pleistocene.

Ecological Niche Modeling

Habitat models were generated for *P. hesperus* using both CCSM and MIROC models, which were not qualitatively different in their predictions. The ecological niche models indicate predicted habitats for *P. hesperus* both at the present-day (0 kya) and during the last glacial maximum (18 kya), assuming a high degree of niche conservatism within this species over time. The results of all models were significantly better than

random samples (AUC = 0.5) in receiver operating characteristic analyses (training AUC = 0.912, test AUC = 0.893). For *P. hesperus*, the present-day ecological niche models indicate relatively continuous habitat extending across all of the major desert regions in North America (Figure 3.7A). These models predict an abundance of high quality habitat throughout the Central Valley in California and south into northern Baja California. The predicted habitat extends northward into the Mojave and Great Basin with disjunct areas of habitat predicted along the Snake River in southwestern Idaho, onto the Columbia Plateau along the Oregon/Washington border, and into the Wasatch Mountains in Utah. Habitat also extends south along the Baja California peninsula and eastward throughout the Sonoran Desert, onto the Colorado Plateau and into the Chihuahuan Desert, with a mosaic of suitability among these areas. This habitat extends south into Mexico on either side of the Sierra Madre Occidental. Overall, the areas of predicted habitat in the present-day models for *P. hesperus* very closely approximate the current distribution of this species (see Figure 3.3 for current distribution).

The paleo-habitat models for *P. hesperus* during the LGM (18 kya) predict an overall loss of habitat across the range of this species (Figure 3.7B), especially across the Mojave, Great Basin, and Colorado Plateau and throughout the Peninsular Desert in Baja California. High concentrations of highly suitable habitat remained throughout Central Valley in California with moderate levels of separation between predicted habitat in the Mojave Desert of southern California, south to northern Baja California and east into the westernmost extent of the Sonoran Desert in Arizona and northern Sonora. There is a disjunct, but concentrated area of predicted habitat in the southern Chihuahuan Desert (east of the Sierra Madre Occidental) and along the western coast (west of the Sierra

Madre Occidental) in Mexico. The genetic analyses indicate a separation of *P. hesperus* populations into three major geographically defined lineages that may be roughly coincident with the predicted areas of habitat during the LGM. With a high level of niche conservatism and the accuracy of the included bioclimatic variables, the distribution of *P. hesperus* may have been severely contracted southward during the LGM, into multiple refugial areas corresponding to the habitat predicted in the paleo-habitat model (Figure 3.7B).

Discussion

A combination of phylogenetic, population genetic, and coalescence approaches in concert with ecological niche modeling has been used to explore the evolutionary history of *Pipistrellus hesperus* in western North America. Three well-supported clades were identified across the distribution of *P. hesperus*, separated into three distinct geographic areas (Figures 3.3 and 3.4). These results are consistent with the results of a genetic analysis of pallid bats (*Antrozous pallidus*) that has a very similar distribution in western North America (Weyandt and Van Den Bussche 2007) and similar ecological preferences (Hall 1981). The major eastern versus western separation between the Sonoran and Chihuahuan Deserts is consistent with geographic variation in morphology reported for *P. hesperus* (Findley and Traut 1970). While some bat species do exhibit population level phylogeographic patterns (Russell et al. 2008), many species experience high levels of gene flow between populations with few or no phylogeographic breaks when they are distributed across broad geographic areas (Lloyd 2003; Russell et al. 2005). The major clades within *P. hesperus* correspond to populations in California (western); the Colorado

Plateau, Mojave, Peninsular, Sonoran, and Great Basin Deserts (west-central); and the Chihuahuan Desert (eastern). The California and Sonoran clades share an evolutionary affinity with each other more recently than either does with the Chihuahuan clade (Figure 3.4). The Chihuahuan lineages diverged from populations in the remaining regions earlier in the evolutionary history of this species. However, the genetic lineages within the Chihuahuan Desert have the most recent coalescence time of the three major clades. This suggests that while these lineages diverged from Sonoran and California clades earlier, the Chihuahuan populations may have experienced an extreme bottleneck causing a severe decline in genetic diversity and a recent coalescence among these lineages. Again, this reduced variability in the Chihuahuan populations matches decreased morphological variability (compared to other regions) reported for populations in the Chihuahuan Desert (Findley and Traut 1970).

The genetic patterns within *P. hesperus* clearly indicate a divergence into western and eastern continental lineages consistent with many of the geographic barriers that have influenced the genetic separations of many of the other taxa in this region. The uplift of the Sierra Nevada Occidental and the Central Mexican Plateau in the Pliocene effectively separated many lineages across Sonoran and Chihuahuan Deserts (see Figure 3.2). A suite of ecological filter barriers have also been effective drivers of divergence throughout this region, some consistent with the boundaries of regional deserts and others acting as drivers of sub-regional diversity within each of the major deserts.

By examining the coalescence of lineages of *P. hesperus* both within each clade and the overall coalescence, we can estimate that the initial divergence began in the late Pliocene and divergence of each of the regional clades occurred within the Pleistocene.

The coalescence estimates can be affected by inherent genetic structure within the ancestral populations, before the divergence of the regional clades, as well as separation of populations without an immediate impact on genetic divergences between lineages. This general timeframe for the initial divergences within *P. hesperus* corresponds to the continued formation of regional deserts in North America (Coney 1983; Riddle 1995), including ongoing uplift of mountain ranges that act as biogeographic barriers between desert regions. The Pleistocene divergence dates correspond to the climatic oscillations and the glacial cycles in the Pleistocene (Pielou 1991; Gates 1993). These repeated glaciations throughout the Pleistocene influenced the phylogeographic patterns in species globally (Hewitt 1999; Hewitt 2000, 2004), including causing the repeated contraction and expansion of species distributions south of the glaciated areas in North America (Pielou 1991; Gates 1993).

Another influential factor affecting phylogeographic and population genetic patterns in North American aridlands biota is the contraction of widespread species into glacial refugia during glacial maxima. Using ecological niche modeling and the distribution of present-day species, we can predict the distribution of species during the last glacial maximum (18 kya), assuming a high degree of niche conservatism within the species and the accuracy of the bioclimatic variables used to inform the models. These predicted LGM distributions represent potential refugial areas and contracted habitats during the LGM. The ecological niche models predict at least three potential refugial areas for *P. hesperus*, including the Central Valley in California, a possibly separate area at the intersection of the northern Peninsular, southern Mojave, and western Sonoran Desert, and a disjunct refugial area in the southern Chihuahuan Desert in central Mexico. While

the coalescence time of lineages within *P. hesperus* pre-date the LGM, it may be reasonable to hypothesize that similar disjunct refugial areas existed during each of the repeated glacial maxima throughout the Pleistocene. Ongoing cycles of population contraction into geographically separate refugial areas could have repeatedly reinforced the ongoing divergence of the three separate groups of populations (Jaeger et al. 2005) which correspond to the three distinct lineages in *P. hesperus*.

The population genetic analyses further suggest that each clade may have experienced a recent history of expansion from refugial populations during the LGM. While mismatch distributions coupled with high haplotype diversity and low nucleotide diversity correspond to a pattern of recent population expansions, the neutrality tests (Fu's *Fs* and Tajima's *D*) do not significantly differ from a neutral expectation of stable populations. An expansion model in which the time since population expansion was long enough to produce haplotype variation through mutation but insufficient to produce significant nucleotide differences in the haplotypes is consistent with the haplotype and nucleotide diversity values for populations of *P. hesperus* (Grant and Bowen 1998; Avise 2000). However, the neutrality statistics do not support these patterns and so the two sets of demographic parameters are equivocal. A more localized approach to examine the demographic properties of individual populations may help address the inconsistencies between these demographic analyses and could indicate that populations or groups of populations exhibit more pronounced patterns of recent populations expansions.

Are the climatic isolations alone sufficient to produce the deep phylogeographic breaks seen within *P. hesperus*? While the retreat of populations into separate refugia may have reinforced phylogeographic differentiation, the timing of coalescence of all

lineages suggests that geologic events in the Pliocene may have been the driver forces that initiated divergence within *P. hesperus*. This hypothesis is consistent with the genetic patterns reported from pallid bats (Weyandt and Van Den Bussche 2007) as well as for aridland rodents with similar levels and patterns of genetic divergence in the late Neogene (Riddle 1995).

Additional samples and additional sequence data from *P. hesperus* are needed to further address the sub-regional genetic diversity within this species. Ultimately, differing dispersal abilities in concert with ecological and physiological traits and the degree of niche conservatism can influence the biogeographic patterns among species within a biota, including their responses to potential isolating barriers and patterns of population expansion or shifting following the erosion of barriers or glaciations (Zink et al. 2001; Zink 2002; Riddle and Hafner 2006). The evolutionary history and phylogeography of *Pipistrellus hesperus* contributes to the comparative biogeographic history and the evolution of deserts in western North America and the biotic history of this region (Riddle and Hafner 2006, and references therein), including analyses that focus on widespread bats in this region (Rodriguez and Ammerman 2004; Weyandt and Van Den Bussche 2007).

Conservation Implications

Often, widespread taxa do not easily lend themselves to particular conservation concerns. However, these species are tightly linked to a specific set of often patchily distributed resources (e.g., spring-fed surface waters in desert ecosystems) and they become integral components for signaling the overall health of these ecosystems. As key resources are destroyed or co-opted for other uses (e.g., diverting or draining water

sources to support urban development), the populations that depend upon them are directly and often adversely affected. It is increasingly important to understand resource and population connectivity in order to understand both regional and sub-regional diversity and population structure within the desert environments so that we can more clearly understand to what extent alterations to the resources will perturb or eliminate natural populations, biotic assemblages, and entire ecosystems.

As human populations expand rapidly within desert ecosystems, the available resources are increasingly strained to cope with this sudden demand. Accelerating losses of habitat and connectivity among habitats are jeopardizing ecological connectivity among regional populations in many species. As a result, the integrity of populations of desert organisms such as bats, which depend upon scarce and unevenly distributed resources, are particularly susceptible to anthropogenic effects. Urbanization and landscape changes specifically threaten organisms that depend on habitat elements, such as foraging and watering sites that are often separated by long distances from other such resources across the natural landscape. In accord with bat populations globally, populations of *P. hesperus* are directly affected by increasing human populations that result in gross habitat destruction and modification, agricultural changes and pesticide use that can influence the availability of prey species, as well as various roost site disturbances, both incidental and deliberate, that result from the increased proximity to humans (Hutson et al. 2001), and even emerging pathogens without an identified source, such as white-nose syndrome (Blehert et al. 2009). While we typically focus our conservation efforts on species and populations with restricted distributions, it is also important to consider the impacts on a seemingly ubiquitous species because by inferring

the evolutionary history of population gene flow across regional landscapes, we will have a means of predicting the severity of impacts of landscape modifications that would destroy or severely alter current ecological connections that have been shaped by strong, persistent evolutionary forces. As evident in this study, the evolutionary history of resident biota have been shaped over hundreds of thousands and millions of years and the resulting genetic patterns may not be adequately predicted by present-day ecology and vagility. The ultimate goal is to prevent further artificial erosion of genetic diversity and population connectivity. This research serves to increase our understanding of the historical biogeography, evolutionary ecology, and conservation biology of a desert-adapted biota across the North American regional deserts.

Literature Cited

Alvarez-Castañeda, S. T., and J. L. Patton. 2004. Geographic genetic architecture of pocket gopher (*Thomomys bottae*) populations in Baja California, Mexico. Molecular Ecology 13:2287-2301.

Arbogast, B. S., and G. J. Kenagy. 2001. Comparative phylogeography as an integrative approach to historical biogeography. Journal of Biogeography 28:819-825.

Arbogast, B. S., and J. B. Slowinski. 1998. Pleistocene speciation and the mitochondrial clock. Science 282:1955a.

Avise, J. 2000. Phylogeography: the History and Formation of Species. Harvard University Press, Cambridge.

Ayoub, N. A., and S. E. Reichert. 2004. Molecular evidence for Pleistocene glacial cycles driving diversification of a North American desert spider, Agelenopsis aperta. Molecular Ecology 13:3453-3465.

Bandelt, H.-J., P. Forster, and A. Rohl. 1999. Median-joining networks for inferring intraspecific phylogenies. Molecular Biology and Evolution 16:37-48.

Bell, K. C., D. J. Hafner, P. Leitner, and M. D. Matocq. 2009. Phylogeography of the ground squirrel subgenus *Xerospermophilus* and assembly of the Mojave desert biota. Journal of Biogeography 37:363-378.

Bernardi, G., and J. Lape. 2005. Tempo and mode of speciation in the Baja California disjunct fish species *Anisotremus davidsonii*. Molecular Ecology 14:4085-4096.

Blehert, D. S., A. C. Hicks, M. Behr, C. U. Meteyer, B. M. Berlowski-Zier, E. L. Buckles, J. T. H. Coleman, S. R. Darling, A. Gargas, R. Niver, J. C. Okoniewski,

R. J. Rudd, and W. B. Stone. 2009. Bat white-nose syndrome: an emerging fungal pathogen? Science 323:227.

Bradley, R. D., and R. J. Baker. 2001. A test of the genetic species concept: Cytochrome-*b* sequences and mammals. Journal of Mammalogy 82:960-973.

Bradley, W. G., and M. J. O'Farrell. 1969. Temperature relationships of the western pipistrelle (*Pipistrellus hesperus*). Pp. 95-96 *in* C. C. Hoff, and M. L. Riedesel, eds. Physiological Systems in Semiarid Environments. University of New Mexico Press, Albuquerque, New Mexico.

Carstens, B. C., and L. L. Knowles. 2007. Shifting distributions and speciation: species divergence during rapid climate change. Molecular Ecology 16:619-627.

Coney, P. J. 1983. The plate tectonic setting of cordilleran deserts. Pp. 81-97 *in* S. G. Wells, and D. R. Haragan, eds. Origin and Evolution of the Deserts. University of New Mexico Press, Albuquerque.

Crews, S. C., and M. Hedin. 2006. Studies of morphological and molecular phylogenetic divergence in spiders (Araneae: *Homalonychus*) from the American southwest, including divergence along the Baja California Peninsula. Molecular Phylogenetics and Evolution 38:470-487.

Douglas, M. E., M. R. Douglas, G. W. Schuett, and L. W. Porras. 2006. Evolution of rattlesnakes (Viperidae; Crotalus) in the warm deserts of western North America shaped by Neogene vicariance and Quaternary climate change. Molecular Ecology 15:3353-3374.

Drummond, A., and A. Rambaut. 2007. BEAST: Bayesian evolutionary analysis by sampling trees. BMC Evolutionary Biology 7:214.

Elith, J., and C. H. Graham. 2009. Do they? How do they? WHY do they differ? On finding reasons for differing performances of species distribution models. Ecography 32:66-77.

Elith, J., C. H. Graham, R. P. Anderson, M. Dudík, S. Ferrier, A. Guisan, R. J. Hijmans, F. Huettmann, J. R. Leathwick, A. Lehmann, J. Li, L. G. Lohmann, B. A. Loiselle, G. Manion, C. Moritz, M. Nakamura, Y. Nakazawa, J. M. C. M. Overton, A. T. Peterson, S. J. Phillips, K. Richardson, R. Scachetti-Pereira, R. E. Schapire, J. Soberón, S. Williams, M. S. Wisz, and N. E. Zimmermann. 2006. Novel methods improve prediction of species' distributions from occurrence data. Ecography 29:129-151.

Evans, M. E. K., S. A. Smith, R. S. Flynn, and M. J. Donoghue. 2009. Climate, niche evolution, and diversification of the "Bird-cage" evening primroses (*Oenothera*, Section *Anogra* and *Kleinia*). The American Naturalist 173:225-240.

Excoffier, L., P. E. Smouse, and J. M. Quattro. 1992. Analysis of Molecular Variance Inferred from Metric Distances among DNA Haplotypes - Application to Human Mitochondrial-DNA Restriction Data. Genetics 131:479 - 491.

Felsenstein, J. 1985. Confidence limits on phylogenies: an approach using the bootstrap. Evolution 39:783-791.

Fielding, A. H., and J. F. Bell. 1997. A review of methods for the assessment of prediction errors in conservation presence/absence models. Environmental Conservation 24:38-49.

Findley, J. S., and G. L. Traut. 1970. Geographic variation in *Pipistrellus hesperus*. Journal of Mammalogy 51:741-765.

Fu, Y.-X. 1997. Statistical tests of neutrality of mutations against population growth, hitchhiking and background selection. Genetics 147:915-925.

Garrick, R. C., J. D. Nason, C. A. Meadows , and R. J. Dyer. 2009. Not just vicariance: phylogeography of a Sonoran Desert euphorb indicates a major role of range expansion along the Baja peninsula. Molecular Ecology 18:1916-1931.

Gates, D. M. 1993. Climate Change and Its Biological Consequences. Sinauer Associates, Sunderland, MA.

Grant, W. S., and B. W. Bowen. 1998. Shallow population histories in deep evolutionary lineages of marine fishes: insights from sardines and anchovies and lessons for conservation. Journal of Heredity 89:415-426.

Guindon, S., and O. Gascuel. 2003. A simple, fast, and accurate algorithm to estimate large phylogenies by maximum likelihood. Systematic Biology 52:696-704.

Hafner, D. J., and B. R. Riddle. 1997. Biogeography of Baja California peninsular desert mammals. Pp. 39-68 *in* T. L. Yates, W. L. Gannon, and D. E. Wilson, eds. Life Among the Muses: Papers in honor of James S. Findley. The Museum of Southwestern Biology, The University of New Mexico, Albuquerque, NM.

Hall, E. R. 1981. The Mammals of North America. John Wiley & Sons, New York.

Hasumi, H., and S. Emori. 2004. K-1 coupled GCM (MIROC) description. Technical Report No. 1. Center for Climate System Research, University of Tokyo, Tokyo.

Hewitt, G. M. 1999. Post-glacial re-colonization of European biota. Biological Journal of the Linnean Society 68:87 - 112.

Hewitt, G. M. 2000. The genetic legacy of the Quaternary ice ages. Nature 405:907-913.

Hewitt, G. M. 2001. Speciation, hybrid zones and phylogeography - or seeing genes in space and time. Molecular Ecology 10:537-549.

Hewitt, G. M. 2004. Genetic consequences of climatic oscillations in the Quaternary. Philisophical Transactions of the Royal Society of London B 359:183-195.

Hijmans, R. J., S. E. Cameron, J. L. Parra, P. G. Jones, and A. Jarvis. 2005. Very high resolution interpolated climate surfaces for global land areas. International Journal of Climatology 25:1965-1978.

Hillis, D. M., and J. J. Bull. 1993. An empirical test of bootstrapping as a method for assessing confidence in phylogenetic analysis. Systematic Biology 42:182-192.

Hoofer, S. R., and R. A. Van Den Bussche. 2003. Molecular phylogenetics of the chiropteran family Vespertilionidae. Acta Chiropterologica 5:1-63.

Hoofer, S. R., and R. A. Van Den Bussche. 2006. Generic status of the American pipistrelles (Vespertilionidae) with description of a new genus. Journal of Mammalogy 87:981-992.

Huelsenbeck, J. P., and F. Ronquist. 2001. MrBayes: A program for the Bayesian inference of phylogeny, Rochester, NY.

Jaeger, J. R., B. R. Riddle, and D. F. Bradford. 2005. Cryptic neogene vicariance and Quaternary dispersal of the red-spotted toad (*Bufo punctatus*): insights on the evolution of North American warm deserts biota. Molecular Ecology 14:3033-3048.

Jezkova, T., J. R. Jaeger, Z. L. Marshall, and B. R. Riddle. 2009. Pleistocene impacts on the phylogeography of the desert pocket mouse (*Chaetodipus penicillatus*). Journal of Mammalogy 90:306-320.

Jobb, G., A. von Haeseler, and K. Strimmer. 2004. TREEFINDER: a powerful graphical analysis environment for molecular phylogenetics. BMC Evolutionary Biology 4:18.

Knowles, L. L., and D. R. Maddison. 2002. Statistical phylogeography. Molecular Ecology 11:2623-2635.

Kocher, T. D., W. K. Thomas, A. Meyer, S. V. Edwards, S. Paabo, F. X. Villablanca, and A. C. C. Wilson. 1989. Dynamics of mitochondrial DNA evolution in animals: amplification and sequencing with conserved primers. Proceedings of the National Academy of Sciences of the USA 86:6196-6200.

Kuenzi, A. J., G. T. Downward, and M. L. Morrison. 1999. Bat distribution and hibernacula use in west central Nevada. Great Basin Naturalist 59:213-220.

Leaché, A. D., S. C. Crews, and M. J. Hickerson. 2007. Two waves of diversification in mammals and reptiles of Baja California revealed by hierarchical Bayesian analysis. Biology Letters online:1-5.

Leaché, A. D., and D. G. Mulcahy. 2007. Phylogeny, divergence times and species limits of spiny lizards (Sceloporus magister species group) in western North American deserts and Baja California. Molecular Ecology 16:5216-5233.

Lindell, J., F. R. Mendez-de la Cruz, and R. W. Murphy. 2005. Deep genealogical history without population differentiation: discordance between mtDNA and allozyme divergence in the zebra-tailed lizard (Callisaurus draconoides). Molecular Phylogenetics and Evolution 36:682-694.

Lindell, J., A. Ngo, and R. W. Murphy. 2006. Deep genealogies and the mid peninsular seaway of Baja California. Journal of Biogeography 33:1327-1331.

Lloyd, B. 2003. Intraspecific phylogeny of New Zealand short-tailed bat Mystacina tuberculata inferred from multiple mitochondrial gene sequences. Systematic Biology 52:460-476.

Maddison, D. R., and W. P. Maddison. 2005. MacClade 4: Analysis of phylogeny and character evolution. Version 4.08. Sinauer Associates, Sunderland, MA.

Miller-Butterworth, C. M., D. S. Jacobs, and E. H. Harley. 2003. Strong population substructure is correlated with morphology and ecology in a migratory bat. Nature 424:187-191.

Nason, J. D., J. L. Hamrick, and T. H. Fleming. 2002. Historical vicariance and the postglacial colonization effects on the evolution of genetic structure in *Lophocereus*, a Sonoran Desert columnar cactus. Evolution 56:2214-2226.

Otto-Bliesner, B. L., J. Marshall, G. H. Overpeck, G. H. Miller, A. Hu, and C. L. I. P. members. 2006. Simulating Arctic Climate Warmth and Icefield Retreat in the Last Interglaciation. Science 311:1751-1753.

Parolo, G., G. Rossi, and A. Ferrarini. 2008. Toward improved species niche modelling: Arnica montana in the Alps as a case study. Journal of Applied Ecology 45:1410-1418.

Pearson, R. G., C. J. Raxworthy, M. Nakamura, and A. T. Peterson. 2007. Predicting species distributions from small numbers of occurrence records: a test case using cryptic geckos in Madagascar. Journal of Biogeography 34:102-117.

Pesole, G., C. Gissi, A. De Chirico, and C. Saccone. 1999. Nucleotide substitution rate of mammalian mitochondrial genomes. Journal of Molecular Evolution 48:427-434.

Phillips, S. J., R. P. Anderson, and R. E. Shchapire. 2006. Maximum entropy modeling of species geographic distributions. Ecological Modelling 190:231-259.

Phillips, S. J., and M. Dudik. 2008. Modeling of species distributions with Maxent: new extensions and a comprehensive evaluation. Ecography 31:161-175.

Pielou, E. C. 1991. After the Ice Age: the Return of Life to Glaciated North America. University of Chicago Press, Chicago.

Posada, D. 2008. jModelTest: Phylogenetic Model Averaging. Molecular Biology and Evolution 25:1253-1256.

Posada, D., and T. Buckley. 2004. Model Selection and Model Averaging in Phylogenetics: Advantages of Akaike Information Criterion and Bayesian Approaches Over Likelihood Ratio Tests. Systematic Biology 53:793-808.

Posada, D., and K. A. Crandall. 1998. MODELTEST: testing the model of DNA substitution. Bioinformatics 14:817 - 818.

Rambaut, A., and A. J. Drummond. 2007. Tracer v.1.4.

Reginos, C. 2005. Cryptic vicariance in Gulf of California fishes parallels vicariant patterns found in Baja California mammals and reptiles. Evolution 59:2678-2690.

Riddle, B. R. 1995. Molecular biogeography in the pocket mice (*Perognathus* and *Chaetodipus*) and grasshopper mice (*Onychomys*): the late Cenozoic development of a North American aridlands rodent guild. Journal of Mammalogy 76:283-301.

Riddle, B. R., and D. J. Hafner. 2006. A step-wise approach to integrating phylogeographic and phylogenetic biogeographic perspectives on the history of a core North American warm deserts biota. Journal of Arid Environments 66:435-461.

Riddle, B. R., D. J. Hafner, and L. F. Alexander. 2000a. Comparative phylogeography of Baileys' pocket mouse (*Chaetodipus baileyi*) and the *Peromyscus eremicus* species group: historical vicariance of the Baja California Peninsular Desert. Molecular Phylogenetics and Evolution 17:161-172.

Riddle, B. R., D. J. Hafner, and L. F. Alexander. 2000b. Phylogeography and Systematics of the *Peromyscus eremicus* Species Group and the Historical Biogeography of North American Warm Regional Deserts. Molecular Phylogenetics and Evolution 17:145-160.

Riddle, B. R., D. J. Hafner, L. F. Alexander, and J. R. Jaeger. 2000c. Cryptic vicariance in the historical assembly of a Baja California peninsular desert biota. Proceedings of the National Academy of Science of the USA 97:14438-14443.

Rodriguez, R. M., and L. K. Ammerman. 2004. Mitochondrial DNA divergence does not reflect morphological differences between *Myotis californicus* and *Myotis ciliolabrum*. Journal of Mammalogy 85:842-851.

Ronquist, F., and J. P. Huelsenbeck. 2003. MrBayes 3: Bayesian phylogenetic inference under mixed models. Bioinformatics 19:1572-1574.

Rozas, J., J. C. Sanchez-DelBarrio, X. Messeguer, and R. Rozas. 2003. DnaSP, DNA polymorphism analyses by the coalescent and other methods. Bioinformatics 19:2496 - 2497.

Russell, A. L., S. M. Goodman, I. Fiorentino, and A. D. Yoder. 2008. Population genetic analysis of Myzopoda (Chiroptera: Myzopodidae) in Madagascar. Journal of Mammalogy 89:209-221.

Russell, A. L., R. A. Medellín, and G. F. McCracken. 2005. Genetic variation and migration in the Mexican free-tailed bat (*Tadarida brasiliensis mexicana*). Molecular Ecology 14:2207-2222.

Schneider, S., D. Roessli, and L. Excoffier. 2000. Arlequin: a Software Package for Population Genetics.

Sokal, R. R., and F. J. Rohlf. 1995. Biometry: the Principles and Practice of Statistics in Biological Research. W.H. Freeman & Company, New York.

Stockman, A., and J. Bond. 2007. Delimiting cohesion species: extreme population structuring and the role of ecological interchangeability. Molecular Ecology 16:3374-3392.

Suárez-Seoane, S., E. L. García de la Morena, M. B. Morales Prieto, P. E. Osborne, and E. de Juana. 2008. Maximum entropy niche-based modelling of seasonal changes in little bustard (*Tetrax tetrax*) distribution. Ecological Modelling 219:17-29.

Tajima, F. 1989a. The effect of change in population size on DNA polymorphism. Genetics 123:597-601.

Tajima, F. 1989b. Statistical method for testing the neutral mutation hypothesis by DNA polymorphism. Genetics 123:585-595.

Tracy, R. L., and G. E. Walsberg. 2002. Kangaroo rats revisited: re-evaluating a classic case of desert survivial. Oecologia 133:449-457.

Upton, D. E., and R. W. Murphy. 1997. Phylogeny of the sideblotched lizards (Phrynosomatidae: *Uta*) based on mtDNA sequences: support for a midpeninsular seaway in Baja California. Molecular Phylogenetics and Evolution 8:104-113.

Walsberg, G. E. 2000. Small mammals in hot deserts: some generalizations revisited. BioScience 50:109-122.

Waltari, E., and R. P. Guralnick. 2009. Ecological niche modelling of montane mammals in the Great Basin, North America: examining past and present connectivity of species across basins and ranges. Journal of Biogeography 36:148-161.

Waltari, E., R. J. Hijmans, A. T. Peterson, A. S. Nyari, S. L. Perkins, and R. P. Guralnick. 2007. Locating Pleistocene refugia: comparing phylogeographic and ecological niche model predictions. PLoS ONE 2:e563.

Weyandt, S. E., and R. A. Van Den Bussche. 2007. Phylogeographic structuring and volant mammals: the case of the Pallid Bat (A*ntrozous pallidus*). Journal of Biogeography:1-13.

Wieczorek, J., Q. Guo, and R. J. Hijmans. 2004. The point-radius method for georeferencing locality descriptions and calculating associated uncertainty. International Journal of Geographical Information Sciences 18:745-767.

Wilgenbusch, J. C., D. L. Warren, and D. L. Swofford. 2004. AWTY: A system for graphical exploration of MCMC convergence in Bayesian phylogenetic inference.

Wilkinson, G. S., and A. M. Chapman. 1991. Length and Sequence Variation in Evening Bat D-Loop mtDNA. Genetics 128:607-617.

Zink, R. M. 2002. Methods in comparative phylogeography, and their application to studying evolution in the North American aridlands. Integrative and Comparative Biology 42:953-959.

Zink, R. M., A. E. Kessen, T. V. Line, and R. C. Blackwell-Rago. 2001. Comparative phylogeography of some aridland bird species. The Condor:1-10.

Table 3.1. Analysis of Molecular Variance (AMOVA) with a comparison of among population variation versus within population variation in *P. hesperus*. Populations correspond to geographically defined clades (Figure 3.4).

Source of Variation	Sum of squares	Variance components	Percentage of Variation
Among Populations	1.027	0.00073 Va	0.15
Within Populations	34.432	0.49901 Vb	99.85
Total	35.458	0.49974	100.00

Table 3.2. Demographic parameters of populations corresponding to the major geographically defined clades of *P. hesperus*. N = number of individuals, h = haplotype diversity, π = nucleotide diversity, *D* = Tajima's D, *Fs* = Fu's Fs, r = raggedness index. Locality abbreviations: AZ – Arizona, , BC – Baja California, BCS – Baja California Sur, CA – California, CHI – Chihuahua, COA – Coahuila, DUR – Durango, NM – New Mexico, NV – Nevada, TX – Texas, SON – Sonora, UT – Utah.

Clade	Localities	N	Haplotypes	*h*	π	*D*	*Fs*	r
1	CA	13	5	0.756 ± 0.097	0.00472 ± 0.00151	-1.3621	-0.191	0.0531
2	AZ, BC, BCS, CHI, DUR, NV, SON, UT	56	11	0.870 ± 0.023	0.0.00960 ± 0.00069	-0.04583	0.296	0.0713
3	COA, NM, TX	27	15	0.900 ± 0.045	0.00523 ± 0.00058	-1.58288	-10.513	0.0747
	All	96	31	0.944 ± 0.010	0.02925 ± 0.00116	-0.82231	-1.697	0.0285

Table 3.3: Average pairwise uncorrected Cytochrome *b* sequence divergence **v**alues (percentages) for each major clade of *P. hesperus*.

	California	Sonoran	Chihuahuan
California	—		
Sonoran	4.7	—	
Chihuahuan	4.2	4.5	—

Figure 3.1: Summary of area relationships among the core warm desert areas of endemism in western North America (Riddle and Hafner 2006) based on a primary/secondary Brooks Parsimony Analysis (BPA). Black areas and branches depict postulated vicariance (primary BPA); gray areas and branches depict exceptions to vicariance (secondary BPA). Major Biogeographic Events correspond to lettered nodes. Numbers on branches indicate number of terminal taxa (species and phylogroups) that support a given branch. PS, Peninsular South; PN, Peninsular North; CW, Continental West; CE, Continental East..

Figure 3.2: Distribution of *P. hesperus* in western North America (shaded area) and **s**ampling localities of *P. hesperus*. Colors correspond to individual clades shown in Figure 3.4 and circles are proportional in size to the number of individuals collected at each locality (See Appendix B for details).

Figure 3.3: Alternative models of phylogeographic history within defined geographic areas in western North America (using the visual approach of Knowles and Maddison 2002). A) Fragmentation of a widespread population, with no correlation between areas and genetic lineages. B) Refugial model with genetic lineages separated into major geographic regions; widespread gene flow occurs within each region. PN, Peninsular North; PS, Peninsular South; GB, Great Basin; Moj, Mojave; Son, Sonoran; Chi, Chihuahuan.

Figure 3.4: Phylogenetic tree of combined data (mitochondrial Cytochrome *b* and Control Region) depicting the phylogeographic relationships among populations of *P. hesperus*, with *Antrozous* as an outgroup. The populations form three well-supported clades corresponding to different geographic regions. Clade colors correspond to sampling localities shown in Figure 3.3 and clade numbers correspond to text (Clade 1 = Chihuahuan, Clade 2 = California, Clade 3 = Sonoran). Asterisks denote nodes with ≥ 70% bootstrap support values (maximum likelihood) and ≥ 0.95 posterior probabilities (Bayesian inference). Numbers at nodes represent divergence time estimates (in millions of years). Locality abbreviations: AZ – Arizona, BC – Baja California, BCS – Baja California Sur, CA – California, CHI – Chihuahua, COA – Coahuila, DUR – Durango, NV – Nevada, NM – New Mexico, SON – Sonora, TX – Texas, UT – Utah.

Figure 3.5: Median-joining network of unique Cytochrome *b* haplotypes in *P. hesperus*. Colors correspond to sampling localities shown in Figure 3.3 and phylogeographic relationships depicted in Figure 3.2. Black circles represent missing haplotypes, branch lengths are proportional to the number of mutational differences between haplotypes and circle size is proportional to the number of samples with that haplotype. Hash marks represent a single mutation, except where indicated by paired hash marks (where numbers correspond to the number of mutations). Abbreviations: AZ – Arizona, BC – Baja California, BCS – Baja California Sur, CHI – Chihuahua, COA – Coahuila, DUR – Durango, NM, NM – New Mexico, NV – Nevada, TX – Texas, SON – Sonora, UT – Utah.

Figure 3.6: Mismatch distributions for Cytochrome *b* haplotypes for each of the three major clades of *P. hesperus*. X-axis represents the pairwise differences among haplotypes and Y-axis represents the frequency of each haplotype. A) individuals collected in California; B) individuals collected in Arizona, Baja California, Baja California Sur, Chihuahua, Durango, Nevada, Sonora, and Utah; C) individuals collected in New Mexico, Coahuila, and Texas.

Figure 3.7: Ecological niche models for *P. hesperus* predicting A) present-day distributions (0 kya) and B) during the last glacial maximum (18 kya). Darker areas represent predicted areas of highly suitable habitat with decreasing suitability corresponding to lighter colors. White areas represent predicted areas of unsuitable habitat.

Figure 3.1

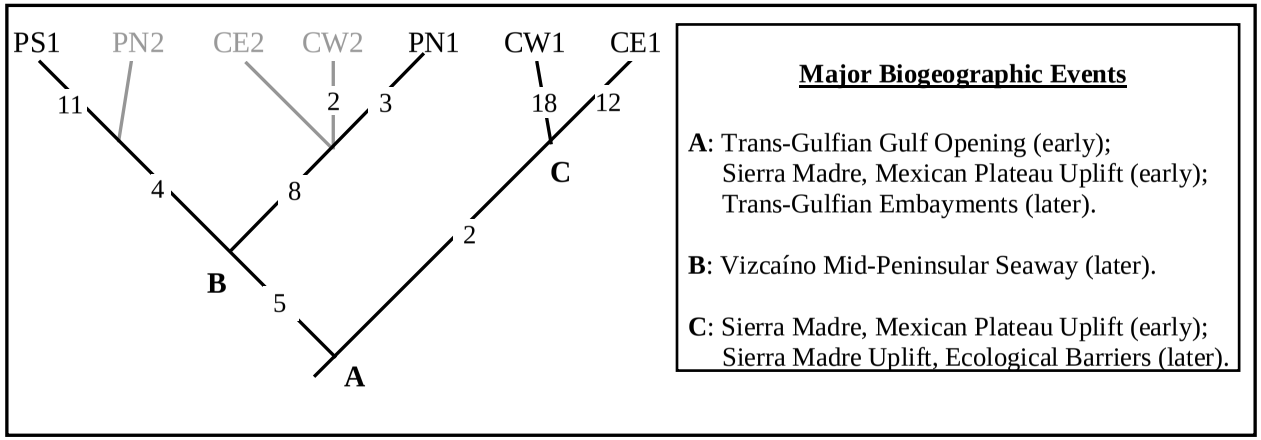
PS1
PN2
CE2
CW2
PN1
CW1
CE1
11
2
3
18
12
4
8
C
2
B
5
A
Major Biogeographic Events
A: Trans-Gulfian Gulf Opening (early);
Sierra Madre, Mexican Plateau Uplift (early);
Trans-Gulfian Embayments (later).
B: Vizcaíno Mid-Peninsular Seaway (later).
C: Sierra Madre, Mexican Plateau Uplift (early);
Sierra Madre Uplift, Ecological Barriers (later).

Figure 3.2

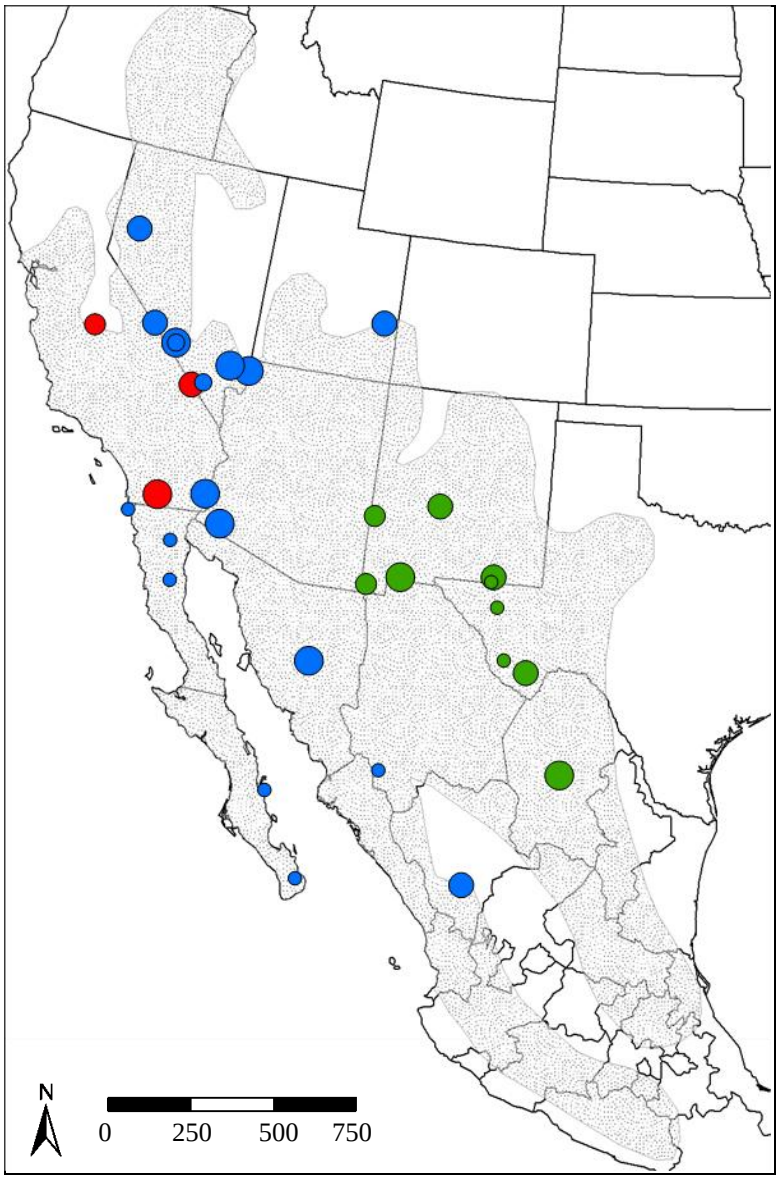

Figure 3.3

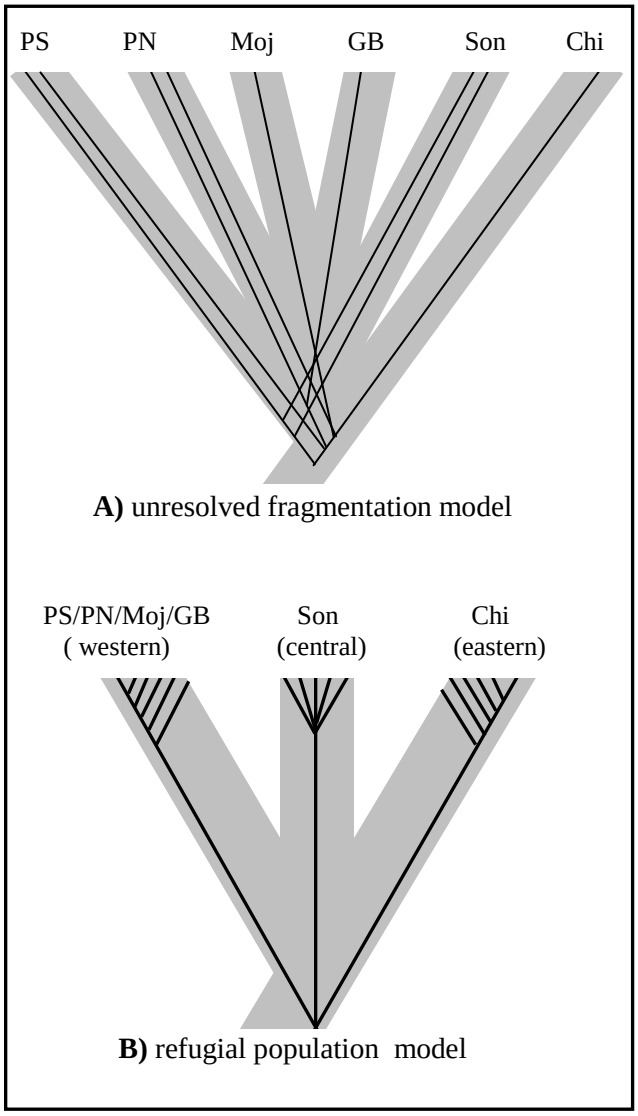
PS
PN
Moj
GB
Son
Chi
A) unresolved fragmentation model
PS/PN/Moj/GB
(western)
Son
(central)
Chi
(eastern)
B) refugial population model

Figure 3.4

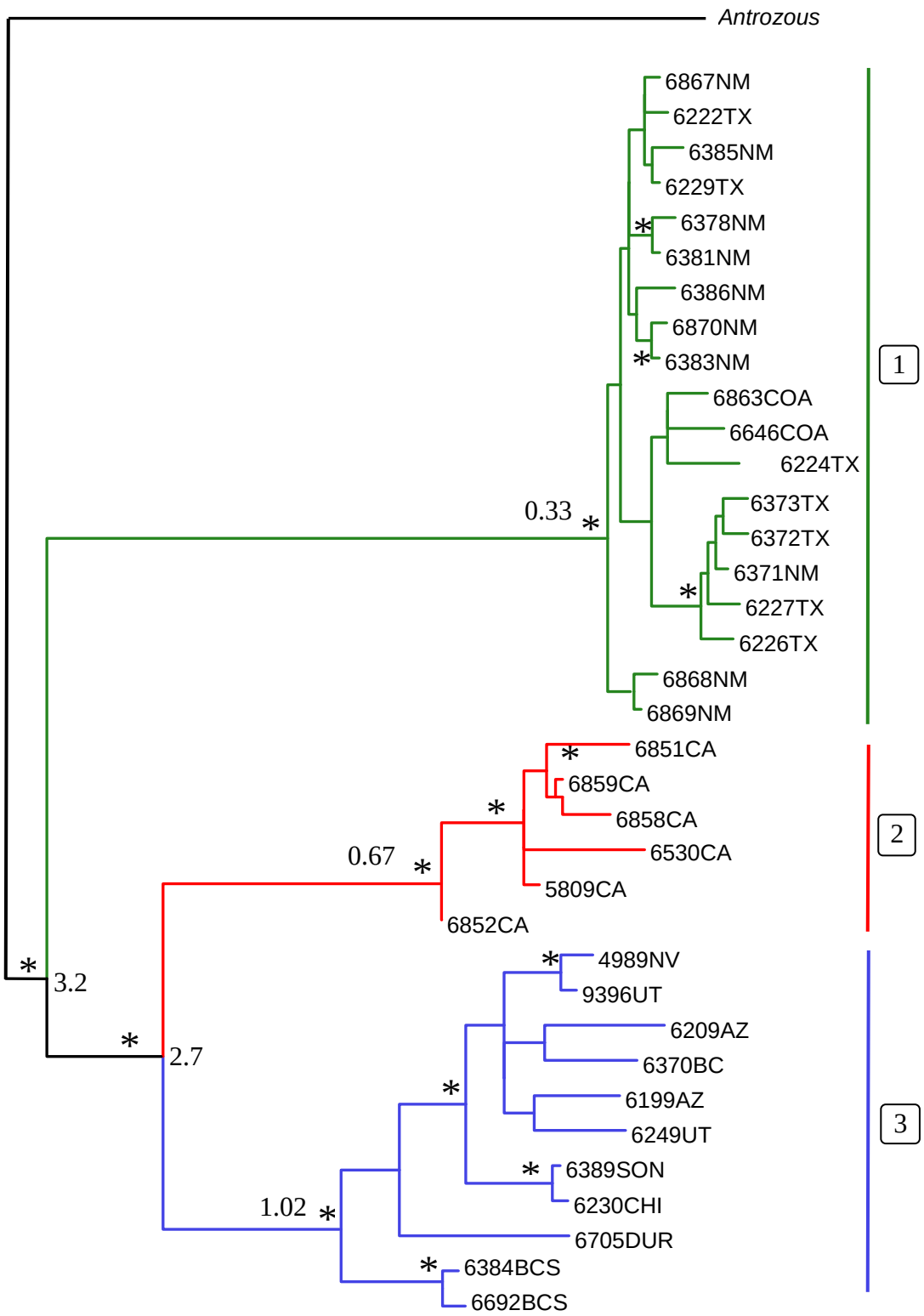
Antrozous
6867NM
6222TX
6385NM
6229TX
6378NM
6381NM
6386NM
6870NM
6383NM
6863COA
6646COA
6224TX
6373TX
6372TX
6371NM
6227TX
6226TX
6868NM
6869NM
0.33
1
6851CA
6859CA
6858CA
6530CA
5809CA
6852CA
0.67
2
4989NV
9396UT
6209AZ
6370BC
6199AZ
6249UT
6389SON
6230CHI
6705DUR
6384BCS
6692BCS
1.02
3
3.2
2.7

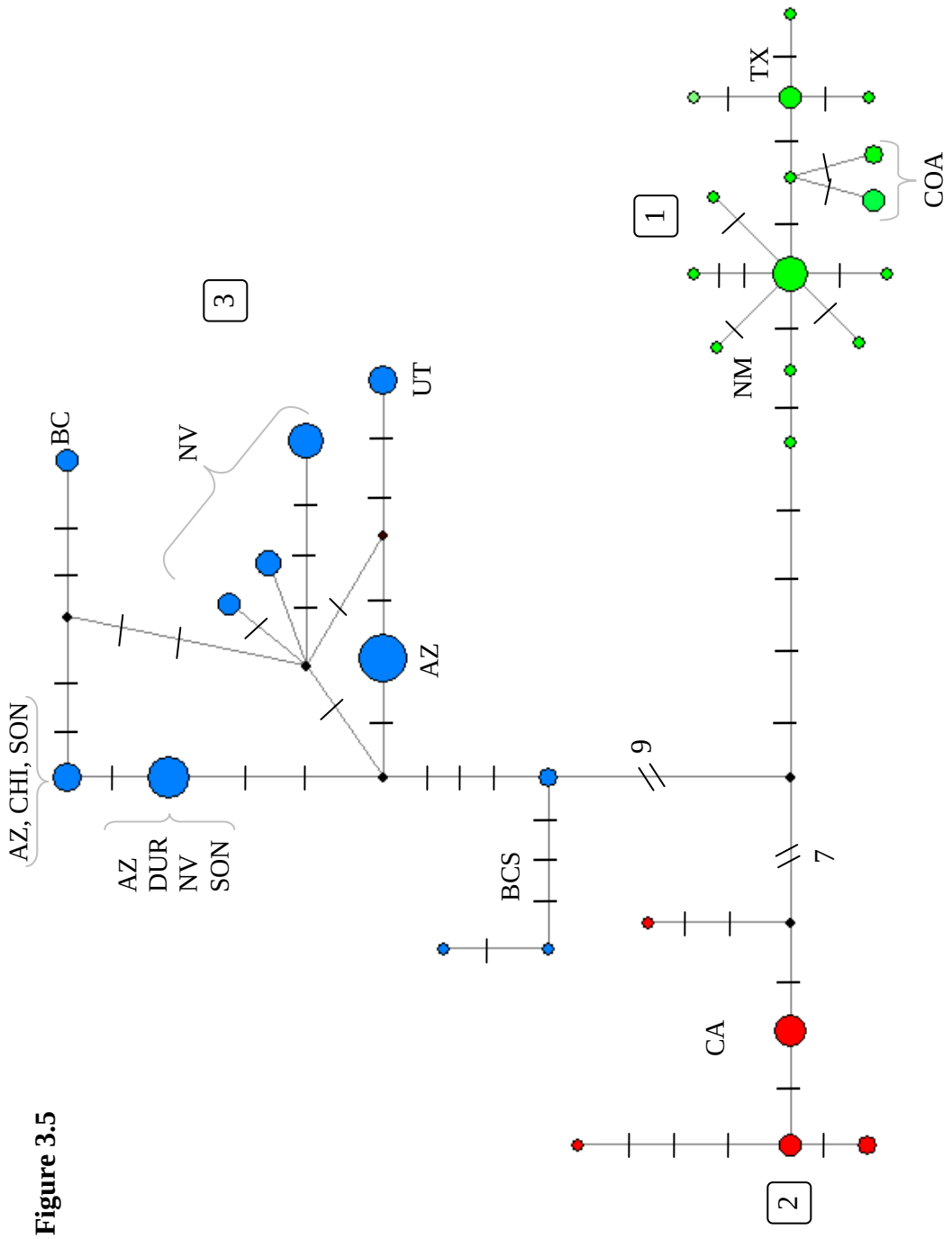

Figure 3.5

Figure 3.6

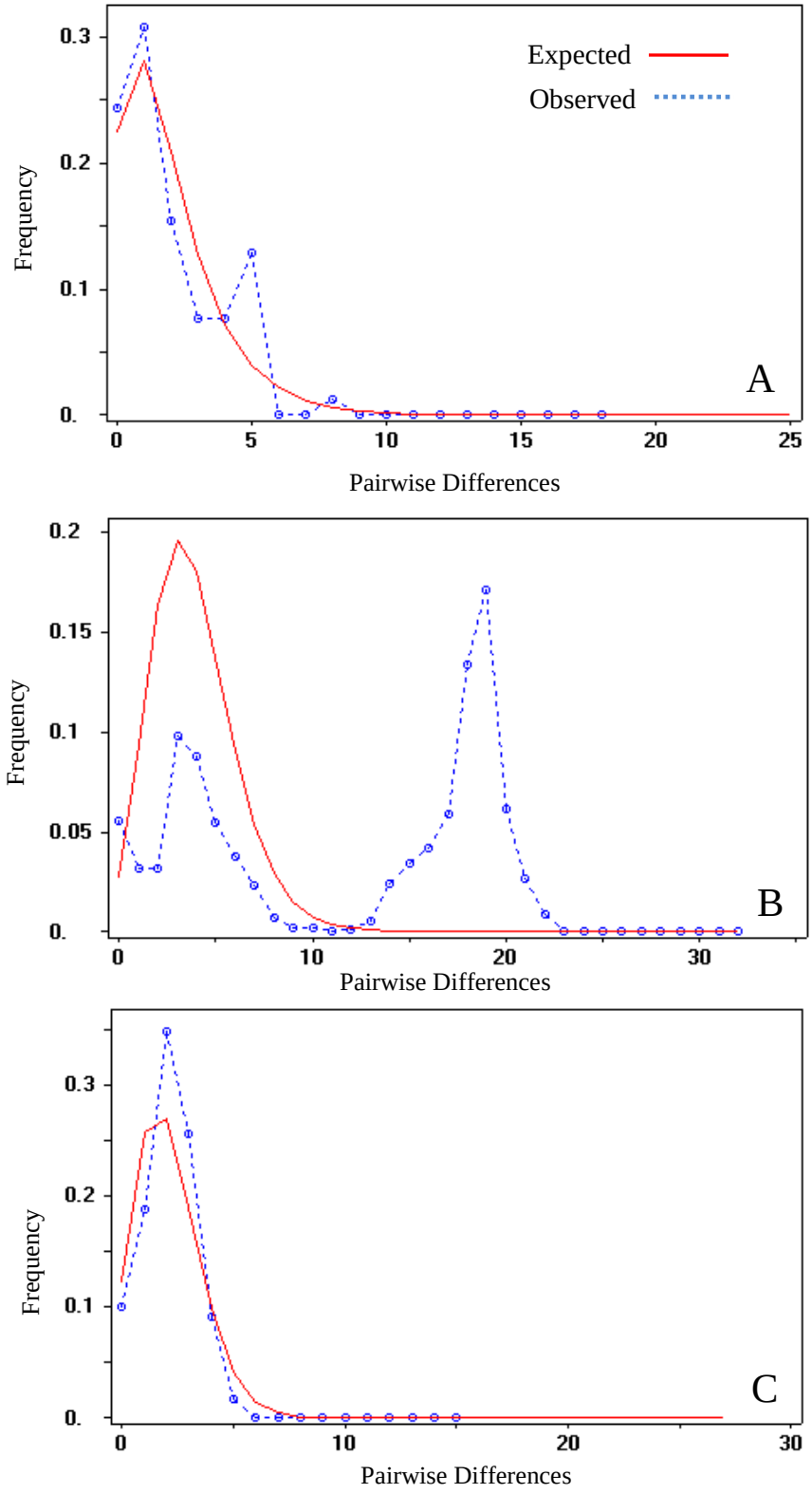
Expected
Observed
Frequency
Pairwise Differences
A
B
C
0.3
0.2
0.1
0.
0.15
0.05
0
5
10
15
20
25
30

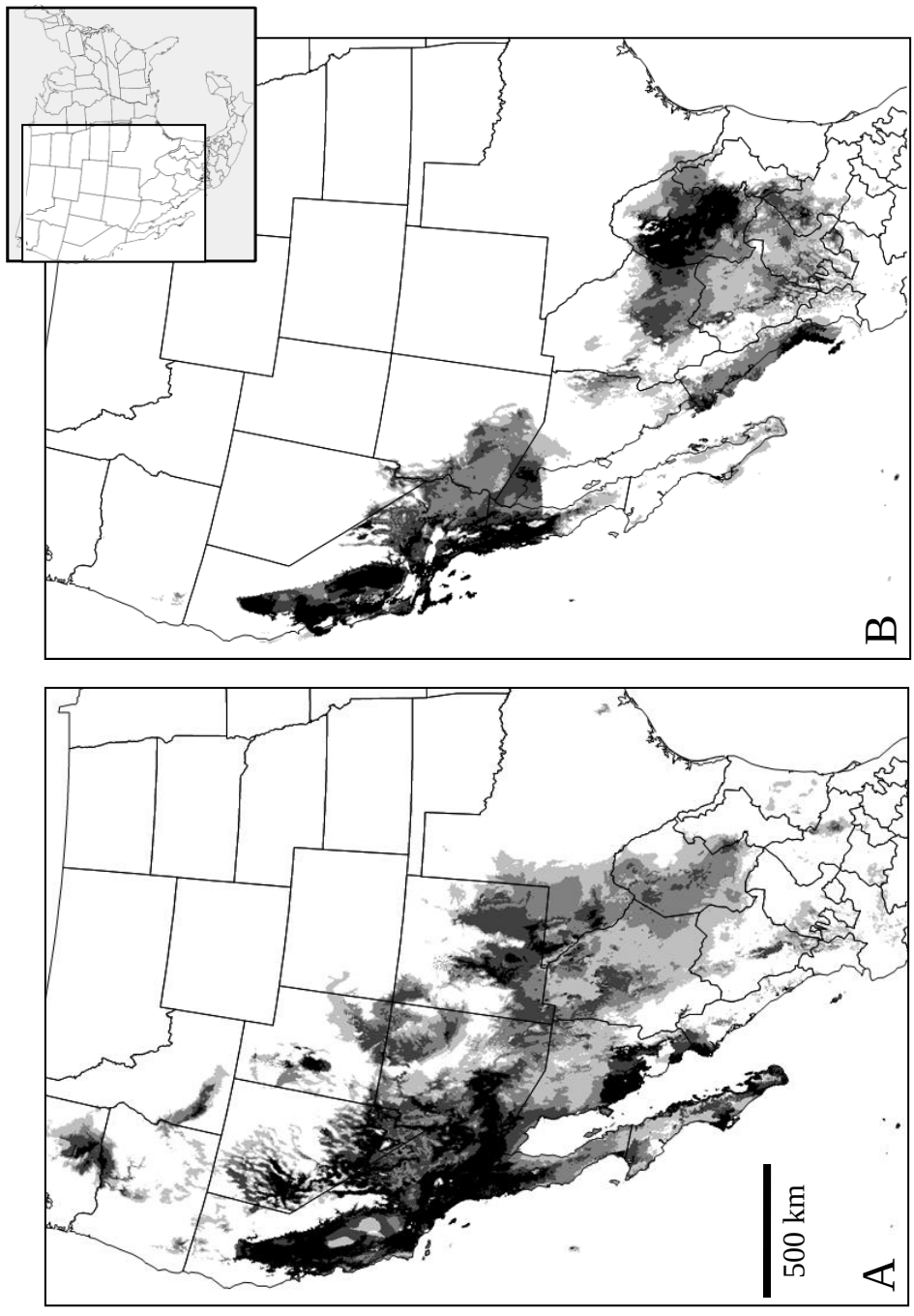

Figure 3.7

CHAPTER 4

INTEGRATING ECOLOGICAL NICHE MODELING AND PHYLOGEOGRAPHY TO INFER THE PLEISTOCENE HISTORY OF THE UINTA CHIPMUNK (*NEOTAMIAS UMBRINUS*) IN THE GREAT BASIN OF WESTERN NORTH AMERICA

Introduction

Within the last several years, phylogeography and landscape genetics have been strengthened by emerging techniques for analyzing genetic data, examining historical patterns of population expansion/contraction and gene flow, and thus interpretation of the processes that lead to present-day phylogeographic patterns. Previously, researchers were challenged by an overall lack of analytical power to address the full range of plausible historical and ongoing processes that lead to geographic population structure. However, the development of enhanced phylogeographic techniques and capacity to dynamically test *a priori* hypotheses (Knowles and Maddison 2002; Jezkova et al. 2009) has overcome many of these challenges, by giving researchers an array of methods to address the role of past biological processes on demographic parameters (e.g., gene flow, population expansion/contraction, etc.), yielding estimates of population and species histories, complete with estimates of errors associated with alternative hypotheses.

Ecological niche models (ENM), also called bioclimatic envelope or species distribution models, have become another emerging tool that can be used to inform *a priori* hypotheses of population histories (Waltari et al. 2007; Waltari and Guralnick 2009). While predictive habitat models based on presence/absence data of species under present-day conditions is not new (Guisan and Zimmermann 2000; Pulliam 2000; Austin

2002), we can now create paleo-distributional models projecting ENMs of extant distributions onto models of past environmental conditions (Carstens and Richards 2007; Phillips and Dudik 2008). The power of ENMs to infer paleo-distributions is currently limited by: 1) recent advances in climatic simulations (Collins et al. 2004; Hasumi and Emori 2004) that allow us to recreate the environmental conditions of the last glacial maximum (18,000 years before present [18kya]), a period that has directly influenced the extant genetic and distributional patterns of floras and faunas (Hewitt 1996, 2004); 2) the estimation of past climatic conditions during specific timeframes, and typically the inclusion of a suite of only 19 bioclimatic variables as estimators of niche parameters; and 3) an assumption of a high degree of niche conservatism – the tendency of species to retain ancestral ecological characteristics (Wiens and Graham 2005) – within species. Even with these limitations, ENMs can provide an independent means of exploring the role of long-term climate changes in shaping phylogeographic structures within extant species.

The Great Basin of western North America (Figure 4.1) represents an ideal region to test the synergistic value of phylogeography and ecological niche modeling to reconstruct the recent biogeographic history of resident taxa. The Great Basin, part of the Basin and Range Biotic Province, is a dynamic landscape composed of terrain that has been shaped by geologic forces beginning with the uplift of the Coast and Cascade ranges during the Miocene. These mountains formed a rain shadow that created drier climates to the east, expanding the grasslands on the inland sides of the ranges in the northern Great Basin (Swanson and McDowell 1984). During the early to mid-Miocene, an expansion of the continental crust east of the Sierra Nevada created a series of north-south trending valleys

and mountain ranges in the heart of the Great Basin (Baldridge 2004). Most recently, habitat shifts driven by cycles of glaciation throughout the Pleistocene caused repeated changes in the distribution and connectivity of populations in this region (Grayson and Madsen 2000; Floyd et al. 2005; Grayson 2006; Galbreath et al. 2009a; Waltari and Guralnick 2009). The intermountain west, and particularly the Great Basin (Figure 4.1), represents a unique system in which the mountainous habitats represent isolated islands surrounded by a "vast sea of sagebrush desert" (Brown 1971).

Brown (1971) used records of mammalian occurrences in this region to test the equilibrium theory of island biogeography (MacArthur and Wilson 1963, 1967). The basic hypothesis was that montane mammalian species assemblages on the 'sky islands' in the Great Basin represent insular faunas derived from source populations in the adjacent Sierra Nevada to the west and the Rocky Mountains to the east, that now exist in a colonization-extinction equilibrium with species richness on each mountain island predicted according to size and isolation from source populations. He rejected this hypothesis, however, by concluding that a common set of species distributed throughout the Great Basin colonized the insular mountain ranges during the Pleistocene and there have been no subsequent colonizations during the Holocene. Thus, species extinctions have created the species assemblages and distributions seen today – a non-equilibrium island system (extinction without colonization) that has been relaxing to a new set of species-area relationships throughout the Holocene.

Ongoing evaluation of the distributional and genetic patterns of montane mammals indicates that the arid lowlands of the Great Basin may not be impenetrable barriers to post-Pleistocene gene flow (Lawlor 1998; Floyd et al. 2005). Several species of mammals

that Brown (Brown 1971) reported as absent on various mountain ranges were discovered to have existed on those ranges well into the early Holocene and some species still exist there today (Grayson and Madsen 2000; Rickart 2001). Some mammals, including pikas (Ochotona princeps – Beever et al. 2008) and woodrats (Neotoma – Grayson and Madsen 2000), thought to be restricted to higher elevations have been discovered in lower elevation populations. These new data could support Brown's model of ongoing extinction without colonization (early Holocene occurrences of a species on montane islands where it no longer occurs might simply capture an earlier snapshot of this process) or alternatively, extinction with subsequent colonization. Regardless of which of these alternatives eventually proves to be more accurate, re-analyses including updated distributional data indicate that Brown's original list of montane species assemblages is not accurate, weakening the relationship between mountaintop island size and species richness, requiring a revision of his original conclusions (Lawlor 1998).

Climatic oscillations throughout the Pleistocene played a role in altering the elevational distributions of the montane habitats found throughout the Great Basin (Grayson and Madsen 2000; Floyd et al. 2005; Grayson 2006; Galbreath et al. 2009a; Waltari and Guralnick 2009). The most recent glaciation reached its maximum advance (last glacial maximum – LGM) in the late Pleistocene, approximately 18 kya. Glaciations and accompanying temperature changes altered the distribution of species in western North America, either compressing them southward into refugial areas or allowing for a likely expansion of many boreal and montane species into lower elevations. In either case, species altered their distributions to track habitats that shifted with the changing climates (Thompson 1990; Grayson 1993; Hewitt 2000; Grayson 2002; Hewitt 2004). In

an analysis of ecological niche models for 13 montane mammals in the Great Basin, Waltari and Guralnick (2009) found that suitable habitat extended to lower elevations in the LGM than we find in this region today. They concluded that this expanded habitat could have provided plausible dispersal routes between previously isolated mountain ranges.

Based on vegetation macrofossils collected from ancient packrat middens found in the Great Basin, the lower elevations in this area that are today characterized by desert or semi-desert shrub vegetation, were inhabited by coniferous woodlands during periods of cooler temperatures and glacial advance (Wells and Berger 1967; Van Devender and Spaulding 1983; Wells 1983; Thompson 1990), supporting Brown's (1971) assumption that current habitat islands were more continuously connected during the LGM. The late Pleistocene Great Basin was characterized by montane habitats that were up to 100m lower than their current elevational limits (Thompson 1990). These patterns indicate that the boreal habitats, inhabited by species such as the Uinta chipmunk (*Neotamias umbriunus*), may have experienced some degree of connectivity at various times throughout the Pleistocene. While these corridors or isolated patches of habitat may not have been continuous at any time, the lowering of montane habitats effectively enlarged the habitat islands, decreasing the distance between these islands and increasing the potential for dispersal (Thompson 1990).

Recent genetic analyses of marmots (*Marmota flaviventris*), a widespread montane species with populations on several Great Basin mountains, supports a strong pattern of isolation-by-distance. Depending on historical populations sizes and the degree of isolation, this may suggest that colonization either occurs now or has occurred

sufficiently recently to override a pattern of lineage sorting that would have been predicted by a model of instantaneous post-Pleistocene isolation among Great Basin mountain ranges (Floyd et al. 2005). Similarly, genetic studies of pikas (*Ochotona princeps*) in the Great Basin have similarly found that populations isolated on mountain rages have experienced ongoing periods of range fluctuations with climatic oscillations (Galbreath et al. 2009a; Galbreath et al. 2009b). Pikas consist of several geographically restricted lineages representing mountain systems, not individual ranges, and each of these lineages has experienced independent demographic histories. While there may not be ongoing contemporary gene flow between populations, introgression has occurred since their initial isolation (Galbreath et al. 2009a; Galbreath et al. 2009b). These results contradict Brown's hypothesis that posits a lack of dispersal between insular montane habitats. Additionally, Holocene cave deposits have indicated low-elevation colonization by woodrats in the genus *Neotoma* (Grayson and Madsen 2000). These results suggest that, if recent or ongoing colonization characterizes montane mammal species assemblages on Great Basin sky islands, each species within the Great Basin may have had its own independent history of colonization and extinction, rather than being part of a single ecologically-defined species assemblage with a shared Late Quaternary biogeographic history (Floyd et al. 2005; Grayson 2006). Individual responses of montane mammal species to climate change would be in line with the differential dispersal histories reported for species of plants in the Great Basin as well (Thompson 1990).

Chipmunks (genus *Neotamias*) are ubiquitous in the montane habitats across western North America. The Uinta chipmunk (*N. umbrinus*), common in coniferous forests above

1800m throughout the intermountain west, occupies a number of the montane sky islands in the Great Basin, as well as mountains farther east throughout Utah and Colorado, and west into the White and Sierra Nevada Mountains in California (Figure 4.1 inset) (Durrant 1952; Hall 1995). Herein, the Spring Mountains and Sheep Range in the Mojave region of southern Nevada are included within a hydrographically-defined Great Basin and a separate Mojave distribution is not referred to again. Because of the inclusion of Spring Mountains within this distribution, the endemic *N. palmeri*, suggested as a possible sister species to *N. umbrinus* (Piaggio and Spicer 2000, 2001), from this range is included within a more broadly-defined *N. umbrinus* species group. While *N. palmeri* is morphologically distinct from *N. umbrinus* (Hall 1981; Stanley 1991; Hall 1995), both species have a similar karyotype (Sutton and Nadler 1969). Because of the very limited distribution of *N. palmeri*, it is listed as "endangered" on the IUCN Red List of Threatened Species (IUCN 2009) and its evolutionary history and genetic diversity is a particular concern for conservation efforts.

The present-day restriction of the *N. umbrinus* species-group to montane forests throughout the intermountain west suggests that the biogeographic history this species may be tightly linked to the availability and shifting elevational distribution of montane forest habitats. Here, I use phylogeographic analyses to test the hypothesis that colonization of the Great Basin mountain ranges by *N. umbrinus* occurred during the Pleistocene with no subsequent or ongoing gene flow between populations isolated on the mountains. Under this hypothesis, genetic lineages may coalesce either during or at some time prior the LGM, although if the latter, dispersal and gene flow at or near the LGM would then reinforce patterns of incomplete lineage sorting. Ecological niche modeling of

current and LGM distributions of *N. umbrinus* are used to assess the likelihood of habitat connectivity across mountain ranges, and possible sources of subsequent colonization. An alternative to this hypothesis would be ongoing, periodic gene flow since the LGM that would serve to prevent the sorting of lineages between populations, thus maintaining patterns of widespread lineages among many different populations.

Materials and Methods

Taxonomic & Genomic Sampling

A collection of tissues from 286 individuals was assembled, including representatives of *N. umbrinus* (130 samples) from 31 localities in Arizona, California, Nevada, and Utah and *N. palmeri* (138 samples) from the Spring Mountains in southern Nevada (Figure 4.1, Appendix C). While populations of this species are found farther east into the Rocky Mountains, we are focusing on a recent Pleistocene history and the possibility of dispersal within the Great Basin, following the studies of Brown (1971) and Lawlor (1998). Samples of *N. umbrinus nevadensis*, a subspecies that is suspected to have been extirpated from the Sheep Range in southern Nevada (Lawlor 1998) are also included. The systematic relationships among species of *Neotamias* have yet to be conclusively determined (Piaggio and Spicer 2000, 2001) and some studies have detected introgressive hybridization and ancient hybridization between sympatric pairs of *Neotamias* (Good et al. 2003; Good et al. 2008) which could confound estimates of population history for any one species. Possible introgression has been detected between *N. umbrinus* and *N. dorsalis*, although the extent and impact on demographic parameters in these two species is unknown (J. Demboski, pers. comm.). The large numbers of *N. palmeri* were collected previously during an investigation of population structure within the Spring Mountains

(C. Lowrey, pers. comm.). For all newly captured individuals, ear-clips were collected or animals were sacrificed and voucher specimens were prepared. Vouchers were deposited in the New Mexico Museum of Natural History. All tissue samples were deposited in the Las Vegas Tissue (LVT) collection at the University of Nevada, Las Vegas (Appendix C). To explore the extent of geographic variation in *Neotamias*, we generated DNA sequence data from the non-protein coding mitochondrial Control Region (CR) and from protein-coding Cytochrome *b* (Cytb) gene for all 286 individuals in this dataset.

Laboratory Protocols

For each specimen, total genomic DNA was extracted from liver or kidney tissues following either a lysis buffer protocol (Longmire et al. 1997) or using the Qiagen DNeasy Tissue Extraction Kit (Qiagen, Inc.). A portion of the hypervariable left domain of the mitochondrial Control Region (CR) was amplified for this study. This molecular marker has been used effectively to address questions of recent population dynamics and conservation genetics (Taberlet 1996; Weyandt and Van Den Bussche 2007). A polymerase chain reaction (PCR) using *Ex-Taq* (Takara-Bio USA) was used with CR specific primers. The primers used were H00651 and L15926 (Kocher et al. 1989) with a PCR temperature profile of 95ºC for 1 minute, 55ºC for 1 min., and 72ºC for 1 min (30 cycles) and a final extension step of 72ºC for 10 minutes. For Cytb, samples were amplified using the primers H15915 and L14724 (Kocher et al. 1989) and a temperature profile of 95ºC for 1 minute, 50ºC for 1 min., and 72ºC for 1 min (30 cycles) and a final extension step of 72ºC for 10 minutes. Double-stranded PCR products were qualitatively examined using a 0.8% agarose gel with a molecular mass ruler for size comparison. The amplified PCR fragments were purified using either a GeneClean II Kit (BIO 101, Inc.),

Qiaquick PCR Purification Kit (Qiagen, Inc.) or Exo-SAP IT (USB Corp.), following manufacturers' protocols. Purified PCR products (including both the light and heavy DNA strands) were cycle sequenced using the ABI PRISM BigDye v.3.1 Cycle Sequencing chemistry (Applied Biosystems, Inc.). Cycle sequencing reactions were performed with the primers H00651 (Kocher et al. 1989) and TumbproL (5'-GCT GAT ATT CTA TTT TAA ACT ATT-3', designed specifically for this study) for CR and Cytb sequencing reactions were performed with the same primers used during PCR amplification (see above). Unincorporated dye-terminators were removed using Sephedex spin columns (Centri-Sep, Inc.) and sequence data were generated on either an ABI 310 or 3130 Genetic Analyzer (Applied Biosystems, Inc). Complementary strands of each gene were unambiguously aligned using SEQEUNCHER 4.9 (Gene Codes Corp.), followed by manual proofreading and alignment.

Phylogenetic and Population Genetic Analyses

The phylogenetic structure within this species complex was assessed using a maximum likelihood (ML) analysis with non-parametric bootstrapping (100 replicates, Felsenstein 1985), implemented in Treefinder v.2008 (Jobb et al. 2004), as well as an analysis of Bayesian Inference (BI) implemented in MRBAYES v.3.1.2 (Ronquist and Huelsenbeck 2003), with posterior probabilities as evidence of support for clades. We used JMODELTEST 0.1.1 (Guindon and Gascuel 2003; Posada 2008) and default parameters with ML optimization to identify the most appropriate model of nucleotide evolution chosen under Akaike Information Criteria (AIC – Posada and Crandall 1998; Posada and Buckley 2004) to perform ML and BI analyses on the combined dataset as well as a partitioned (by molecular marker) BI analysis using different substitution

models for each genetic partition. MRBAYES was run for 4 x 10^6 generations with an initial burn-in of 1 x 10^5 generations (10,000 trees) with four Monte Carlo Markov chains and a temperature value of 0.05 to promote proper swapping of the chains. The proper convergence of runs was assessed by examining the posterior probabilities of clades for non-overlapping samples of trees using AWTY (Wilgenbusch et al. 2004), which determines the proper mixing of chains and helps to determine if the analysis has reached stationarity.

Estimating Demographic Parameters

A median-joining network of the combined CR and Cytb data, generated by the program NETWORK (Bandelt et al. 1999), was estimated to visualize the relationships among haplotypes of all samples. This method addresses the problems found with intraspecific datasets with large sample sizes and short genetic distances between samples. Median-joining networks are modified minimum-spanning networks that use a maximum parsimony approach to find the shortest possible network to explain the relationships between the individuals (Bandelt et al. 1999). Population genetic parameters were estimated, including Tajima's *D* (Tajima 1989b, a) and Fu's *Fs* (Fu 1997) for all populations using DNASP 5 (Rozas et al. 2003). An Analysis of Molecular Variance (AMOVA) was performed using ARLEQUIN 2.0 (Schneider et al. 2000) to assess levels of within versus among population variation. Pairwise F_{ST} values (Charlesworth 1998) were calculated for all populations using ARLEQUIN 2.0 with a Bonferonni correction of the level of statistical significance (Sokal and Rohlf 1995).

To estimate the coalescence time for all lineages represented in the dataset, a Markov Chain Monte Carlo (MCMC) approach was implemented in the program BEAST 1.4.8

(Drummond and Rambaut 2007) to estimate the time to most recent common ancestor (tmrca) for all alleles (scaled by a mutation rate μ). The HKY+*I*+*Γ* model of sequence evolution was used with a coalescent model of constant population size over time, assuming a relatively recent coalescence among lineages (and alleles). A number of short chains were run to optimize scaling factors for model parameters and then chains of 2 x 10^7 generations were run with parameters sampled every 1000 generations after an initial burn-in of 2 x 10^6 generations. The rate of evolution of the CR is known to vary among mammalian lineages (Pesole et al. 1999) and it is problematic to estimate a standard substitution rate because the rate can be higher for recently diverged or diverging taxa with genomes that have not yet experienced high levels of saturation typical of mitochondrial protein-coding genes (Ruokonen and Kvist 2002). Therefore, the coalescence analyses were conducted using two different mutation rates for the CR: a substitution rate of 30% (0.15 substitutions/site/million years), based on early estimated rates for human CR (Ward et al. 1991; Schneider and Excoffier 1999) and applied to *Glaucomys* (Petersen and Stewart 2006), a genus within the same family (Sciuridae) as *Neotamias*. Additionally, a more conservative 15% (0.75 subs/site/My) total divergence rate was used for the CR. For the Cytb partition, a rate of 2% (0.01 subs/site/My) was used (Arbogast and Slowinski 1998).

To evaluate the history of gene flow between populations in the Great Basin, coalescent analyses were performed using the isolation with migration model implemented in the program IM (Hey and Nielsen 2004). This model is qualitatively different than models that assume populations have been exchanging genes for infinitely long periods of time. The isolation with migration assumes that populations separated at

some point in the past with the possibility of ongoing gene flow (dispersal in the form of immigration or emigration). Generally, samples collected from each mountain range do not represent well-supported monophyletic lineages of haplotypes. This pattern can result either from incomplete lineage sorting since the populations were isolated or ongoing gene flow between populations. Based on the results of the ecological niche models (see Results), pairwise patterns of gene flow were estimated between the White Mountain on the Nevada/California border and the Spring Mountains in southern Nevada as well as between the White Mountains and and the closest five central Nevada ranges (Desatoya, Monitor, Toiyabe, Toquima, and Shoshone Mountains – Figure 4.1). To evaluate the initial performance of the demographic estimators, the program was run with default values supplied by the authors (Hey and Nielsen 2004; Hey 2007b, a) and each value was adjusted based on the preliminary results. To analyze demographic properties of the White and Spring Mountains, the following prior parameter values were used in IM: upper bounds on priors for theta of the White Mountains (Θ_1) and Spring Mountains (Θ_2) were set at 10 and 80, respectively; upper bounds for priors for migration from the White Mountains (m_1) and from the Spring Mountains (m_1) were each set at 10; the upper bound for the divergence time (t) was set at 30. Analyses were run for 50×10^7 generations and discarded the first 5×10^6 (10%) generations as the burn-in and used 10 separate chains. The analysis was run three separate times to assess the repeatability of the demographic estimates.

The isolation with migration model includes the assumptions that when performing pairwise comparisons between populations, there cannot be other populations that are more closely related to the sampled populations than the two populations under analysis

are to each other and there cannot be un-sampled populations exchanging genes with the populations of interest (Hey 2007b, a). To analyze demographic properties of the White Mountains and the closest five central Nevada ranges (Desatoya, Monitor, Toiyabe, Toquima, and Shoshone Mountains), samples from these mountain ranges were analyzed both individually and collectively. Given the geographic proximity of these ranges to each other and the approximately equal distance between each of these ranges and the White Mountains, it cannot be determined *a priori* if any one range could be exchanging genes with the White Mountains. For these analysis, the following prior parameter values in were used in IM: upper bounds on priors for theta of the White Mountains (Θ_1) and each of the closest central Nevada ranges (Θ_2) were set at 10 and 20, respectively; upper bounds for priors for migration from the White Mountains (m_1) and from each of the central Nevada ranges (m_1) were each set at 10; the upper bound for the divergence time (t) was set at 50. The analyses were run using 10 chains for 50 x 10^6 generations and the first 5 x 10^5 (10%) generations were discarded as burn-in values. The analyses were each performed three separate times, with a random starting seed for each analysis.

Ecological Niche Modeling – Current & Paleo-distributions

Ecological niche models (ENM) were constructed for *Neotamias umbrinus* and *N. palmeri* using occurrence records and climatic conditions both at present (0 kya) and during the LGM (18 kya). We used occurrence records of individuals examined in this study (see Appendix A) as well as a subset of available records listed in MaNIS (http://manisnet.org/). Following the methods of Waltari and Guralnick (2009) and Rowe (2005), we removed duplicate records collected at the same locality and only included samples with a radius of geographical uncertainty that was less than 0.8 km, thereby

reducing bias inherent in imprecise occurrence data. Also, to offset the possibly of confounding effects of elevation in montane habitats, we used only those records with an elevational uncertainty of less than or equal to 100m, following the methods of Rowe (2005). To construct the habitat models, we used the maximum entropy method implemented in MAXENT 3.3.1 (Phillips et al. 2006; Phillips and Dudik 2008). Because of the uncertainty regarding the relationship of *N. umbrinus* and *N. palmeri* and the high degree of overlap in suitable habitat, ENMs of these species were estimated jointly (160 total occurrence records). MAXENT is designed to find distributions among climatic variables and digital environmental layers to predict logistic non-negative probabilities based on presence-only occurrence data (Stockman and Bond 2007). This method has been shown to outperform similar habitat estimators (Phillips and Dudik 2008; Elith and Graham 2009) and has been used in recent phyloclimatic studies (Carstens and Knowles 2007; Waltari and Guralnick 2009). The predictions for this analysis are based on elevation plus a suite of 19 bioclimatic parameters previously compiled from the WorldClim climate layers (Hijmans et al. 2005; Waltari et al. 2007).

Model calibrations were performed using 75% of the data as a training group and then the predicted distribution models were tested with the remaining 25% (Evans et al. 2009). We used default parameters (500 maximum iterations, convergence threshold of 0.00001, regularization multiplier of 1, 10000 background points) with a random seed, the removal of multiple presence records from individual cells resulting from many sampling localities within $5km^2$ (i.e., one pixel), and we used logistic probabilities for the output (Phillips and Dudik 2008). To reduce the effects of spatial autocorrelation, we used a

split-sample approach to separate the geographically closest sample pairs between the training and test groups (Fielding and Bell 1997; Parolo et al. 2008).

A complete model (including all 20 variables) was run initially to produce "area under the receiver operation characteristic curve" (AUC) values for each bioclimatic parameter. A minimum AUC of 0.75 for the test group is considered the threshold for good model performance (Elith et al. 2006; Suárez-Seoane et al. 2008; Elith and Graham 2009). Consequently, we removed those parameters with AUC values less than 0.75. The reduced models were run using temporal transfer modeling from the current distribution (0 kya) to the LGM (20 kya), incorporating information in the Community Climate Model System Model (CCSM – Otto-Bliesner et al. 2006) and the Model for Interdisciplinary Research on Climate (MIROC – Hasumi and Emori 2004). MaxEnt was run three separate times using both the CCSM and MIROC climate reconstructions and habitat models results from both were averaged, accepting only those areas that both methods agreed were suitable (Waltari and Guralnick 2009). Binary maps of the predicted habitat models were created using ARCGIS 9.2 (ESRI Corp., Redlands, CA) by averaging three independent MaxEnt runs using the Spatial Analyst feature (Raster Calculator) in ARCGIS. Because the suitability of the predictive area in the models is based on chosen threshold values, the models were evaluated across four logistic thresholds: fixed cumulative value of 10.0, equal training sensitivity and specificity, equal test sensitivity and specificity, and equate entropy of thresholded and non-thresholded distributions. These threshold values were used to assess a range of sensitivities and specificities to ensure that the model interpretations are robust. Ultimately, the analyses used a cutoff of suitable habitat at a fixed cumulative probability

of 10, a level that rejects the lowest 10% of predicted logistic values. This value, though conservative, maintained a low omission rate (Pearson 2007; Pearson et al. 2007) consistent with the expectation that the occurrence records contain georeferencing errors.

Results

Phylogenetic Analyses

The dataset consisted of 500 base pairs (bp) of sequence data from the CR with 78 informative characters (15.6%) and 500bp from Cytb with 34 informative characters (6.8%). This dataset yielded 78 unique total haplotypes (Figure 4.2), including 67 unique haplotypes from *N. umbrinus*. The dataset included a large number of *N. palmeri* from the Spring Mountains in southern Nevada and eliminating redundant haplotypes reduced this sample size to only 11 unique haplotypes. Using jModeltest with AIC selection values, the HKY+I+Γ model was chosen as the best fit for the data (-lnL = 1492.25, K = 160) for the combined dataset. The resulting phylogeny, using both maximum likelihood and Bayesian inference, produced a mostly unresolved phylogeny with very few internal nodes with support values above 0.95 for Bayesian posterior probabilities and 70% ML bootstrap support (phylogeny not shown). No basal nodes within the phylogenetic tree were well-supported and those nodes with higher levels of support were near the tips of the phylogeny, often taken from the same populations.

While little divergence across mountain ranges was evident from the phylogenetic analysis, geographic structuring of the haplotypes is more apparent in the median-joining network (Figure 4.2). Samples from the White Mountains, near the Sierra Nevada in the west, were most similar to the individuals from the Spring Mountains in southern Nevada

and this set of haplotypes forms a discrete geographic unit, separate from the remaining populations. Haplotypes taken from the eastern extent of the sampling distribution, including populations from the Wasatch Mountains and the Markagunt Plateau in Utah, formed a geographically clustered set of haplotypes, along with individuals from the Snake Range in Nevada, the geographically closest locality from which samples are included. Populations from the Grant and Monitor Ranges are closely related to a unique set of haplotypes from the White and Wasatch Mountains. The central Great Basin contains a set of populations with more haplotypes shared between populations, consistent with an assemblage of populations in very close proximity to each other. Overall, the haplotype network yields several discernable geographic patterns, with private haplotypes in the most isolated populations and shared haplotypes common among geographically closer sets of mountain ranges (Figure 4.2).

The distribution of haplotype diversity (h) within populations and across the Great Basin indicates that those mountain ranges in the eastern Great Basin have the highest levels of genetic diversity (Table 4.1). The genetic diversity shows a general trend of decreasing from east to west across the sampled populations in the Great Basin. The Markagunt Plateau (Pop 7: n = 6 haps; h = 1.0) and Wasatch Mountains (Pop 19: n = 7 haps; h = 0.917) in Utah and the White Pine Range (Pop 21: n = 6 haps; h = 0.917) in Nevada represent the highest levels of haplotype diversity. The westernmost population represented by the White Mountains (Pop 21) has among the lowest haplotype diversity (n = 2 haps, h = 0.556), along with the Diamond Mountains (Pop 4: n = 3 haps; h = 0.524) in the central Great Basin. Nucleotide diversity (π) shows a similar pattern of decrease from east to west across the Great Basin (Table 4.1). The Wasatch Mountains (π

= 0.01734) and Spruce Mountains (π = 0.2311), along with most central Great basin ranges, show levels of nucleotide diversity that is almost 10-fold higher than the White Mountains (π = 0.00418) and Spring Mountains (π = 0.00504) in the western and southern extents of the distribution.

Demographic Parameters

An AMOVA (Excoffier et al. 1992) using HYK85 adjusted genetic distances (Table 4.1) indicated that most of the genetic variation in the dataset was found among populations (69.03%) compared with much less variation within populations (30.97%). Neutrality statistics (Tajima's D and Fu's Fs) were not significantly negative for any single population. Pooling all populations also did not produce significantly negative values (Table 4.2). These values suggest low levels of polymorphism within populations indicative of stable populations over time. Raggedness indices (r) of haplotypes within populations were insignificant for most populations, except the Ruby/Humboldt and the White Mountains (Table 4.2). An insignificant raggedness index indicates the possibility of an expanding population. Failure to reject the null hypothesis of expansion does not absolutely mean that these populations have undergone expansion, but they do not support an alternative hypothesis of stability (Slatkin and Hudson 1991; Rogers and Harpending 1992; Harpending 1994). Individual populations could have experienced localized demographic expansions, consistent with continued isolation on separate mountain ranges. The F_{ST} values estimated for pairs of populations were significant at a level of P = 0.0028 (Table 4.3), which is a more conservative level of significance (using a Bonferroni correction) and is consistent with the high among-population variation explained by the AMOVA. The estimates of tmrca for all CR alleles sampled in *N.*

umbrinus was 310,700 years ago (95% CI: 213,500 – 429,100) using a substitution rate of 30% (0.15 subs/site/My) for CR and 2% for Cytb. The coalescence estimate using a more conservative substitution rate of 15% (0.075 subs/site/My) for CR and 2% for Cytb was 1,039,700 years ago (95% CI: 721, 900 – 1,383,700 years).

The results of IM analyses were limited in their ability to estimate all of the available demographic parameters. With a small number of individuals per population and a limited amount of sequence data per population, the analysis may be limited in its ability to adequately explore the model space since the likelihood surface of the parameters can be very flat over the parameter ranges. The data simply do not contain enough information to properly identify the model (Hey 2007b). These data were unable to reliably estimate the time since splitting (*t*) of the populations because the estimates of *t* peaked sharply at a low value followed by a plateau that extended indefinitely, regardless of the length of the analyses. Even with limited population sizes, the data were able to adequately estimate values of migration for each of the pairwise analyses between selected mountain ranges. For the comparison of the White Mountains (Pop_1) and the Spring Mountains (Pop_2), the estimate for the migration rate (m_1) into the White Mountains was 0.015 (95% CI: 0.005 – 9.575) individuals per generation and the estimation of the migration rate (m_2) into the Spring Mountains was 0.005 (95% CI: 0.005 – 8.015). Because the generation time in chipmunks is one year (Hirshfeld 1975), the migration rate can be calculated independent of mutation rate. For the comparison of the White Mountains (Pop_1) and set of closest central Great Basin mountain ranges (Pop_2), the estimate of migration rate (m_1) into the White Mountains was 0.025 (0.015, 9.075) individuals per generation and the estimation of the migration rate (m_2) into the

central Great Basin ranges was 0.005 (0.005, 1.755) individuals per generation, effectively indicating no ongoing migration between populations. While the confidence intervals seem high, they are 95% confidence intervals on the mean of each run, which increases with increasing number of generations. The high confidence values surrounding the estimates of migration (m_1 and m_2) in both analyses are likely a result of the small sample size and the use of a single genetic locus.

Ecological Niche Models

The habitat models for *N. umbrinus* and *N. palmeri* were estimated together, given the small distribution of *N. palmeri* in the Spring Mountains in southern Nevada, the highly similar habitats occupied by both species, and lack of mtDNA reciprocal monophyly between species. The results of all models were significantly better than random samples (AUC = 0.5) in receiver operating characteristic analyses (training AUC = 0.989, test AUC = 0.982). For *N. umbrinus*, the present-day habitat model (Figure 4.3A) indicates high-elevation montane habitat from the Sierra Nevada in the west throughout the Great Basin and east into Utah and the eastern slopes of the Rocky Mountains in Colorado and Wyoming. Lower quality habitat extends north into Idaho and southeast into New Mexico, well outside the known distribution of this species. For the most part, the higher-quality habitat represented in the current models for each of these three clades correctly captures the current distribution of individuals and currently recognized species. The reconstructions of paleo-habitat models (paleo-models) for *N. umbrinus* and *N. palmeri* during the last glacial maximum (18 kya) predicted a shift in available habitat, both in total coverage and in elevation. This shift was most apparent in the western extent of the distribution. Previously unoccupied valleys between ranges show the presence of

moderately suitable habitat with a large continuous area of predicted habitat along the eastern extent of the Sierra Nevada and western Nevada (Figure 4.3B). There was an overall loss of habitat in the eastern portion of the range, in the vicinity of the Rocky Mountains, though pockets of higher quality habitat remained in the Uinta Mountains and the eastern extent of the Wasatch Mountains in Utah. The LGM model is consistent with previous ENMs generated for *N. umbrinus* that predict an overall increase of total habitat and shift to lower elevations throughout the Great Basin (Waltari and Guralnick 2009).

Discussion

The results of this study support the conclusion that populations of *N. umbrinus* in the western (White Mountains) and southern (Spring Mountains) Great Basin are effectively isolated on montane habitat islands, with no ongoing gene flow between them. These conclusions are further supported by the relatively lower amount of genetic diversity within these regions compared to other areas in the Great Basin. Coalescence estimates indicate that current lineages originated in the Pleistocene, before the last glaciation but well within the prolonged period of late Pleistocene glaciation cycles (Pielou 1991; Gates 1993). The ecological niche models indicate that the Sierra Nevada and other isolated ranges (e.g., Spring Mountains) in the west and the Uinta Mountains in northeastern Utah maintained the largest areas of high quality habitat during the LGM, suggesting that these areas may represent refugial sources for the post-glacial expansion of current populations. While some measures of the stability of populations (both individually and collectively) indicate that they may be somewhat stable, the demographic parameters (high haplotype

diversity coupled with low nucleotide diversity) suggest that many of the populations have experienced recent expansions, possibly from the postulated glacial refugia.

The mitochondrial control region has a much higher rate of evolution than protein-coding genes (Pesole et al. 1999) and there may be a negative correlation between the effective population size and the mutation rate per generation within animal mtDNA (Piganeau and Eyre-Walker 2009). This relationship could be amplified by the evolutionary rate of the control region, which can vary widely among species and among regions within the control Region (Pesole et al. 1999). To the extent that coalescent times of sampled mitochondrial alleles approximately reflect coalescent times of lineages within a population, the estimated coalescent date of the lineages almost certainly predates the actual divergence of populations (Wakeley 2008). While the coalescence dates for *N. umbrinus* lineages do not correspond to the most recent glacial period (110,000 to 9,600 ybp, with a maximum extent at 18,000 ybp), the LGM may represent a period of reinforcement for previously existing genetic patterns caused by repeated glaciations throughout the Pleistocene. Periodic gene flow can prevent genetic isolation, repeatedly reinforcing incomplete lineage sorting across seemingly isolated populations. Alternatively, the use of a single genetic locus (mtDNA) and inconsistencies in the analyses could overestimate the coalescence times of the lineages, resulting in the lineages coalescing within a more recent Pleistocene timeframe and indicating that the recent climatic cycles are actually the drivers of lineage divergence and not just providing reinforcement of previously existing patterns.

The ENMs indicate an asymmetrical growth of LGM habitat in the western Great Basin and a widespread reduction in quality habitat in the east, with a large pocket of

habitat remaining in the Uinta Mountains in northeastern Utah. If this model accurately reflects the changing distribution of habitats during the LGM, the only way to generate higher overall genetic diversity in the east is to have broad habitat connectivity and range expansion from the west without the loss of diversity typical of rapidly expanding populations. This would be coupled with a subsequent loss of diversity in the west within the more isolated populations. This is reasonable if the White and Spring Mountains, geographically more isolated from other populations, are driving a pattern of eastward expansion. The genetic data do not support the recent connectivity of these western ranges with the central and eastern Great Basin ranges suggested by the habitat models (Figure 4.3) or the likelihood of an eastward pattern of dispersal.

The demographic data further reveal that those populations in the easternmost Great Basin have levels of nucleotide diversity almost a full order of magnitude higher than western (White Mountains) and southern populations (Spring Mountains). Haplotype diversity shows a similar trend of higher levels in the east and decreasing in western populations. Under the assumption that higher genetic diversity is indicative of ancestral populations, the genetic data suggest that this species colonized from an eastern origin. Within the Great Basin, the eastern mountain ranges show the highest levels of genetic diversity with shared haplotypes across several isolated mountain ranges. The Rocky Mountains were suggested as a possible source population in Brown's (1971) non-equilibrium theory of island colonization in this system. The ecological niche models suggest that the Uinta Mountains in eastern Utah maintained a large area of high quality habitat during the LGM, suggesting that this area could serve as either the proximate (during the LGM) or ultimate (original colonization of this area) source of present-day

populations. An east to west colonization pattern is consistent with the higher levels of genetic diversity in the eastern Great Basin, supporting the hypothesis that the either the Uinta or the Rocky Mountains represent the source populations for the colonization of this species westward throughout the Great Basin.

The distribution of *N. umbrinus* extends eastward into Utah and farther east into the Rocky Mountains in western Wyoming and Colorado (Figure 4.1). Coupled with this eastern extension of distribution beyond the Great Basin, the genetic data suggest that *N. umbrinus* most likely originated in the east followed by westward dispersal, ultimately reaching its current distribution. Therefore, the prediction from the ecological niche models that the greatest areas of habitat diversity are in the western portion of the distribution may be misleading for genetic analyses targeted at uncovering patterns of ongoing migration. Given the extreme three-dimensionality of this complex terrain throughout western North America, the ENMs may be over-predicting habitat availability and indicating a much higher probability of habitat connectivity in the western Great Basin than actually existed during the LGM.

Haplotypes in the more isolated western mountain ranges are geographically restricted (e.g., the White and Spring Mountains) while specific haplotypes are widespread throughout localized regions (e.g, central Great Basin). The most widespread haplotypes originated in or spread into the Wasatch mountains in Utah, providing further evidence for an eastern origin for this species. Widespread haplotypes shared among many isolated mountain ranges suggest that the current distribution of genetic lineages may be the result of either incomplete lineage sorting or ongoing dispersal between these mountain ranges. While gene flow between the western ranges (White and Spring

Mountains) is non-existent, dispersal between the central Great Basin ranges may be a very likely given both their proximity to each other and their shared haplotypes in this region.

Periods of even patchy habitat connectivity, suggested for coniferous forests in the Great Basin (Wells and Berger 1967), would facilitate some level of gene flow which would maintain genetic mixing among otherwise isolated populations. The reconstructions of habitats during the LGM suggest that the overall availability of habitats do shift over time in response to changing climatic conditions, but the true extent of these shifts remains unknown. These shifting habitats may lead to some level of connectivity between seemingly disconnected mountain ranges or at least decreasing the dispersal distance and the potential for dispersal between isolated habitats. With warming temperatures and glacial retreat, the coniferous forests that may have shifted downslope would have retreated back to higher elevations, decreasing the likelihood for dispersal between mountain ranges. If populations were forced into glacial refugia (e.g., within the Uinta Mountains), then population genetic analyses would show evidence of widespread recent population expansions, consistent with these demographic data.

Moreover, the current patterns of genetic connectivity suggest the possibility of multiple colonization events from the eastern populations in the Wasatch Mountains. The populations within the heart of the Great Basin are closely related to each other, suggesting the likelihood that at least one episode of dispersal gave rise to these populations. The haplotype network further reveals that samples from the Snake Range in southeastern Nevada are more closely allied with the Wasatch Mountain samples from Utah rather than to other central Great Basin ranges (Figure 4.2). This pattern presents the

possibility that there may have been multiple pulses or colonization events from the eastern source populations in Utah. Additional analyses are needed to address the timing and the extent of the relationships between these lineages.

To further investigate the origin of this species, the direction of colonization, and the connectivity between all populations (mountain ranges) in shaping the complete biogeographic history of *N. umbrinus*, additional data and analyses are needed. Samples from populations outside of the Great Basin, especially from the eastern populations in the Wasatch, Uinta, and Rocky Mountains, would enable a more thorough test of the alternative hypotheses of eastern versus western origin of the current populations. To assess whether ongoing gene flow or incomplete lineage sorting is driving the widespread distribution of genetic lineages throughout the central Great Basin, pairwise comparisons of migration between each of these populations is necessary. These data would also allow for a more complete assessment of Brown's hypothesis of a single colonization event into the Great Basin with no subsequent dispersal in the Great Basin. Additionally, nuclear sequence data could provide another line of evidence to detect patterns and directionality of migration since mtDNA is restricted to tracing only maternal lineages and thus only female mediated gene flow. A more complete and robust phylogeny of *Neotamias* is ultimately necessary to address demographic issues that may complicate the genetic patterns within *N. umbrinus* (e.g., ancient or introgressive hybridization) and the genetic relationships to sympatric and syntopic species.

The genetic signatures of several widespread species of mammals (e.g., marmots and pikas) in the Great Basin indicate strong signatures of isolation-by-distance with populations restricted to disjunct mountain ranges (Floyd et al. 2005; Galbreath et al.

2009a; Galbreath et al. 2009b). In many cases, genetic lineages are restricted to mountain systems rather than individual mountain ranges. These patterns are consistent with the geographic distribution of haplotypes in *N. umbrinus* across the Great Basin. While more isolated mountain rages contain geographically isolated lineages (e.g. Spring and White Mountains), there appears to be an overall lack of reciprocal monophyly within individual ranges in the central Great Basin, evident by geographically widespread haplotypes. We now have a more complete picture of the shifting distribution of montane species (Wells 1983; Thompson 1990) throughout the Great Basin during the Quaternary (Lawlor 1998; Grayson and Madsen 2000; Grayson 2002; Grayson 2005). Species and populations of mammals within the Great Basin can be characterized by a unique history of colonization and differential response to climatic changes leading to their current distributions and genetic signatures. Detailed analyses of widespread plants in this region suggest a similar pattern of species specific colonization and dispersal histories. (Thompson 1990). Given the growing body of evidence from species with different life history traits, Brown's (1971) hypothesis of a common colonization history across a suite of Great Basin mammals seems unlikely. With the accumulation of genetic evidence (this study; Floyd et al. 2005; Galbreath et al. 2009a; Galbreath et al. 2009b), we now understand that the montane mammals within the Great Basin form a dynamic assemblage of species that has responded to a common set of abiotic factors (climatic oscillations) and unique abiotic influences (shifting habitats in response to the climate changes). The synergy of these forces has served to create a unique biogeographic history for each species of montane mammal in the Great Basin, creating a much more complex system than originally envisioned by Brown (1971).

Conservation Implications

Climate change is increasingly impacting complex ecosystems (Belant et al. 2010) and montane species are among the first to experience extinction events resulting from climatic disturbances (Parmesan 2006). Montane mammals are particularly susceptible to the effects of habitat loss because they are effectively isolated on islands of limited suitable habitat. The distribution of coniferous forests are highly reactive to temperature changes (Beever et al. 2003), which explains the shifting availability of habitats along elevational gradients with expanding and contracting glacial cycles. Ongoing climate change caused by increases in atmospheric CO_2 and other greenhouse gases can increase the rate at which montane habitats contract upslope into higher elevations. However, habitats do not necessarily need to change drastically to negatively impact species distributions (Beever et al. 2003). Montane populations of pikas (*Ochotona princeps*) have been extirpated recently, owing to a variety of factors including climate change (Beever et al. 2003; Beever et al. 2010). There is evidence for climate-mediated extinction in the Sheep Mountains in southern Nevada where the subspecies *N. umbrinus nevadensis* is restricted to high elevation habitats. This endemic subspecies has not been recorded since the 1960s (Lawlor 1998), despite extensive efforts to document its existence. Sampling efforts at historical collection sites and additional suitable habitats have detected only *N. dorsalis* (cliff chipmunk), a related but typically lower-elevation species (C. Klinger and C. Tomlinson, pers. comm.). This suggests that *N. dorsalis* may have either expanded or shifted its distribution to higher elevations, displacing and perhaps ultimately causing the extinction of *N. umbrinus nevadensis*, a unique genetic lineage.

Neotamias palmeri is endemic to the Spring Mountains in southern Nevada and is officially listed as "Endangered" on the IUCN Red List of Threatened Species because of this restricted distribution (IUCN 2009). Analyses indicate that lineages of *N. palmeri* are genetically distinct from *N. umbrinus*, though these two species do share a close evolutionary history (Piaggio and Spicer 2000, 2001). Additional genetic data are needed to fully address the evolutionary history of *N. palmeri* within the broader context of *Neotamias* systematics and taxonomy. Given that samples of *N. palmeri* form a very geographically isolated yet cohesive genetic lineage confined to a high-elevation habitat within a single mountain range in southern Nevada, conservation efforts that support the continued management and protection of this species are justified.

Literature Cited

Arbogast, B. S., and J. B. Slowinski. 1998. Pleistocene speciation and the mitochondrial clock. Science 282:1955a.

Austin, M. P. 2002. Spatial prediction of species distribution: an interface between ecological theory and statistical modeling. Ecological Modelling 157:101-118.

Baldridge, W. S. 2004. Geology of the American Southwest. Cambridge University Press, New York.

Bandelt, H.-J., P. Forster, and A. Rohl. 1999. Median-joining networks for inferring intraspecific phylogenies. Molecular Biology and Evolution 16:37-48.

Beever, E. A., P. F. Brussard, and J. Berger. 2003. Patterns of apparent extirpation among isolated populations of pikas (*Ochotona princeps*) in the Great Basin. Journal of Mammalogy 84:37-56.

Beever, E. A., C. Ray, P. W. Mote, and J. L. Wilkening. 2010. Testing alternative models of climate-mediated extirpations. Ecological Applications 20:164-178.

Beever, E. A., J. L. Wilkening, D. E. McIvor, S. S. Weber, and P. E. Brussard. 2008. American pikas (*Ochotona princeps*) in northwestern Nevada: a newly discovered population at a low-elevation site. Western North American Naturalist 68:8-14.

Belant, J. L., E. A. Beever, J. E. Gross, and J. J. Laler. 2010. Ecological response to contemporary climate change within species, communities, and ecosystems. Conservation Biology 24:7-9.

Brown, J. H. 1971. Mammals on mountaintops: nonequilibrium insular biogeography. The American Naturalist 105:467-478.

Carstens, B. C., and L. L. Knowles. 2007. Shifting distributions and speciation: species divergence during rapid climate change. Molecular Ecology 16:619-627.

Carstens, B. C., and C. L. Richards. 2007. Integrating coalescent and ecological niche modeling in comparative phylogeography. Evolution 61:1439-1454.

Charlesworth, B. 1998. Measures of divergence between populations and the effect of forces that reduce variability. Molecular Biology and Evolution 15:538-543.

Collins, W. D., C. M. Bitz, M. L. Blackmon, G. B. Bonan, C. S. Bretherton, J. A. Carton, P. Chang, S. C. Doney, J. J. Hack, T. B. Henderson, J. T. Kiehl, W. G. Large, D. S. McKenna, B. D. Santer, and R. D. Smith. 2004. The Community Climate System Model Version 3 (CCSM3). Journal of Climate 19:2122-2143.

Drummond, A., and A. Rambaut. 2007. BEAST: Bayesian evolutionary analysis by sampling trees. BMC Evolutionary Biology 7:214.

Durrant, S. D. 1952. Mammals of Utah, taxonomy and distribution. University of Kansas Publications of the Museum of Natural History 6:1-549.

Elith, J., and C. H. Graham. 2009. Do they? How do they? WHY do they differ? On finding reasons for differing performances of species distribution models. Ecography 32:66-77.

Elith, J., C. H. Graham, R. P. Anderson, M. Dudík, S. Ferrier, A. Guisan, R. J. Hijmans, F. Huettmann, J. R. Leathwick, A. Lehmann, J. Li, L. G. Lohmann, B. A. Loiselle, G. Manion, C. Moritz, M. Nakamura, Y. Nakazawa, J. M. C. M. Overton, A. T. Peterson, S. J. Phillips, K. Richardson, R. Scachetti-Pereira, R. E. Schapire, J. Soberón, S. Williams, M. S. Wisz, and N. E. Zimmermann. 2006.

Novel methods improve prediction of species' distributions from occurrence data. Ecography 29:129-151.

Evans, M. E. K., S. A. Smith, R. S. Flynn, and M. J. Donoghue. 2009. Climate, niche evolution, and diversification of the "Bird-cage" evening primroses (*Oenothera*, Section *Anogra* and *Kleinia*). The American Naturalist 173:225-240.

Excoffier, L., P. E. Smouse, and J. M. Quattro. 1992. Analysis of molecular variance inferred from metric distances among DNA haplotypes: application to human mitochondrial DNA restriction data. Genetics 131:479-491.

Felsenstein, J. 1985. Confidence limits on phylogenies: an approach using the bootstrap. Evolution 39:783-791.

Fielding, A. H., and J. F. Bell. 1997. A review of methods for the assessment of prediction errors in conservation presence/absence models. Environmental Conservation 24:38-49.

Floyd, C. H., D. H. Van Vuren, and B. May. 2005. Marmots on Great Basin mountaintops: using genetics to test a biogeographic paradigm. Ecology 86:2141-2153.

Fu, Y.-X. 1997. Statistical tests of neutrality of mutations against population growth, hitchhiking and background selection. Genetics 147:915-925.

Galbreath, K. E., D. J. Hafner, K. Zamudio, and K. Agnew. 2009a. Isolation and introgression in the Intermountain West: contrasting gene genealogies reveal the complex biogeographic history of the American pika (*Ochotona princeps*). Journal of Biogeography in press.

Galbreath, K. E., D. J. Hafner, and K. R. Zamudio. 2009b. When cold is better: climate-driven elevation shifts yield complex patterns of diversification and demography in an alpine specialis (American pika, *Ochotona princeps*). Evolution 63:2848-2863.

Gates, D. M. 1993. Climate Change and Its Biological Consequences. Sinauer Associates, Sunderland, MA.

Good, J. M., J. R. Demboski, D. W. Nagorsen, and J. Sullivan. 2003. Phylogeography and introgressive hybridization: Chipmunks (genus *Tamias*) in the northern Rocky Mountains. Evolution 57:1900-1916.

Good, J. M., S. Hird, N. Reid, J. R. Demboski, S. J. Steppan, T. R. Martin-Nims, and J. Sullivan. 2008. Ancient hybridization and mitochondrial capture between two species of chipmunks. Molecular Ecology 17:1313-1327.

Grayson, D. K. 1993. The Desert's Past: A Natural Prehistory of the Great Basin. Smithsonian Institution Press, Washington, D.C.

Grayson, D. K. 2002. Great Basin mammals and late Quaternary climate history. Pp. 369-385 *in* R. Hershler, D. B. Madsen, and D. R. Currey, eds. Great Basin Aquatic Systems History. Smithsonian Institution Press, Washington, D.C.

Grayson, D. K. 2005. A brief history of Great Basin pikas. Journal of Biogeography 32:2103-2111.

Grayson, D. K. 2006. The Late Quaternary biogeographic histories of some Great Basin mammals (western USA). Quaternary Science Reviews 25:2964-2991.

Grayson, D. K., and D. B. Madsen. 2000. Biogeographic implications of recent low-elevation recolonization by *Neotoma cinerea* in the Great Basin. Journal of Mammalogy 81:1100-1105.

Guindon, S., and O. Gascuel. 2003. A simple, fast, and accurate algorithm to estimate large phylogenies by maximum likelihood. Systematic Biology 52:696-704.

Guisan, A., and N. E. Zimmermann. 2000. Predictive habitat distribution models in ecology. Ecological Modelling 135:147-186.

Hall, E. R. 1981. The Mammals of North America. John Wiley & Sons, New York.

Hall, E. R. 1995. Mammals of Nevada; forward by T.E. Lawlor. University of Nevada Press, Reno.

Harpending, H. C. 1994. Signature of ancient population growth in a low-resolution mitochondrial mismatch distribution. Human Biology 66:591-600.

Hasumi, H., and S. Emori. 2004. K-1 coupled GCM (MIROC) description. Technical Report No. 1. Center for Climate System Research, University of Tokyo, Tokyo.

Hewitt, G. M. 1996. Some genetic consequences of ice ages, and their role in divergence and speciation. Biological Journal of the Linnean Society 58:247-276.

Hewitt, G. M. 2000. The genetic legacy of the Quaternary ice ages. Nature 405:907-913.

Hewitt, G. M. 2004. The structure of biodiversity - insights from molecular phylogeogrpahy. Frontiers in Zoology 1:1-16.

Hey, J. 2007a. IM Documentation: Using the IM Program. Pp. 27.

Hey, J. 2007b. IM User Documentation: Introduction to the IM and IMa computer programs. Pp. 16.

Hey, J., and R. Nielsen. 2004. Multilocus method for estimating population sizes, migration rates and divergence time, with applications to the divergence of Drosophila pseudoobscura and D. persimilis. Genetics 167:747-760.

Hijmans, R. J., S. E. Cameron, J. L. Parra, P. G. Jones, and A. Jarvis. 2005. Very high resolution interpolated climate surfaces for global land areas. International Journal of Climatology 25:1965-1978.

Hirshfeld, J. R. 1975. Reproduction, growth, and development of two species of chipmunks: *Eutamias panamintinus* and *Eutamias palmeri*. Pp. 84. University of Nevada, Las Vegas, Las Vegas.

IUCN. 2009. IUCN Red List of Threatened Species.

Jezkova, T., J. R. Jaeger, Z. L. Marshall, and B. R. Riddle. 2009. Pleistocene impacts on the phylogeography of the desert pocket mouse (*Chaetodipus penicillatus*). Journal of Mammalogy 90:306-320.

Jobb, G., A. von Haeseler, and K. Strimmer. 2004. TREEFINDER: a powerful graphical analysis environment for molecular phylogenetics. BMC Evolutionary Biology 4:18.

Knowles, L. L., and D. R. Maddison. 2002. Statistical phylogeography. Molecular Ecology 11:2623-2635.

Kocher, T. D., W. K. Thomas, A. Meyer, S. V. Edwards, S. Paabo, F. X. Villablanca, and A. C. C. Wilson. 1989. Dynamics of mitochondrial DNA evolution in animals: amplification and sequencing with conserved primers. Proceedings of the National Academy of Sciences of the USA 86:6196-6200.

Lawlor, T. E. 1998. Biogeography of Great Basin mammals: paradigm lost? Journal of Mammalogy 79:1111-1130.

Longmire, J. L., M. Maltbie, and R. J. Baker. 1997. Use of "lysis buffer" in DNA isolation and its implication for museum collections. Occasional Papers of the Museum of Texas Tech University 163:1-4.

MacArthur, R. H., and E. O. Wilson. 1963. An equilibrium theory of insular zoogeography. Evolution 17:373-387.

MacArthur, R. H., and E. O. Wilson. 1967. The Theory of Island Biogeography. Princeton University Press, Princeton, NJ.

Otto-Bliesner, B. L., J. Marshall, G. H. Overpeck, G. H. Miller, A. Hu, and C. L. I. P. members. 2006. Simulating Arctic Climate Warmth and Icefield Retreat in the Last Interglaciation. Science 311:1751-1753.

Parmesan, C. 2006. Ecological and evolutionary responses to recetn climate change. Annual Review of Ecology and Systematics 37:637-669.

Parolo, G., G. Rossi, and A. Ferrarini. 2008. Toward improved species niche modelling: Arnica montana in the Alps as a case study. Journal of Applied Ecology 45:1410-1418.

Pearson, R. G. 2007. Species' Distribution Modeling for Conservation Educators and Practitioners. Pp. 1-50. Synthesis. American Museum of Natural History New York.

Pearson, R. G., C. J. Raxworthy, M. Nakamura, and A. T. Peterson. 2007. Predicting species distributions from small numbers of occurrence records: a test case using cryptic geckos in Madagascar. Journal of Biogeography 34:102-117.

Pesole, G., C. Gissi, A. De Chirico, and C. Saccone. 1999. Nucleotide substitution rate of mammalian mitochondrial genomes. Journal of Molecular Evolution 48:427-434.

Petersen, S. D., and D. T. Stewart. 2006. Phylogeography and conservation genetics of southern flying squirrels (*Glaucomys volans*) from Nova Scotia. Journal of Mammalogy 87:153-160.

Phillips, S. J., R. P. Anderson, and R. E. Shchapire. 2006. Maximum entropy modeling of species geographic distributions. Ecological Modelling 190:231-259.

Phillips, S. J., and M. Dudik. 2008. Modeling of species distributions with Maxent: new extensions and a comprehensive evaluation. Ecography 31:161-175.

Piaggio, A. J., and G. S. Spicer. 2000. Molecular phylogeny of the chipmunk genus Tamias based on the mitochondrial cytochrome oxidase subunit II gene. Journal of Mammalian Evolution 7:147-166.

Piaggio, A. J., and G. S. Spicer. 2001. Molecular phylogeny of the Chipmunks inferred from mitochondrial cytochrome b and cytochrome oxidase II gene sequences. Molecular Phylogenetics and Evolution 20:335-350.

Pielou, E. C. 1991. After the Ice Age: the Return of Life to Glaciated North America. University of Chicago Press, Chicago.

Piganeau, G., and A. Eyre-Walker. 2009. Evidence for variation in the effective population size of animal mitochondrial DNA. PLoS ONE 4:e4396.

Posada, D. 2008. jModelTest: Phylogenetic Model Averaging. Molecular Biology and Evolution 25:1253-1256.

Posada, D., and T. Buckley. 2004. Model Selection and Model Averaging in Phylogenetics: Advantages of Akaike Information Criterion and Bayesian Approaches Over Likelihood Ratio Tests. Systematic Biology 53:793-808.

Posada, D., and K. A. Crandall. 1998. MODELTEST: testing the model of DNA substitution. Bioinformatics 14:817 - 818.

Pulliam, H. R. 2000. On the relationship between niche and distribution. Ecology Letters 3:349-361.

Rickart, E. A. 2001. Elevational diversity gradients, biogeography and the structure of montane mammal communities in the intermountain region of North America. Global Ecology and Biogeography 10:77-100.

Rogers, A. R., and H. C. Harpending. 1992. Population growth makes waves in the distribution of pairwise genetic differences. Molecular Biology and Evolution 9:552-569.

Ronquist, F., and J. P. Huelsenbeck. 2003. MrBayes 3: Bayesian phylogenetic inference under mixed models. Bioinformatics 19:1572-1574.

Rowe, R. J. 2005. Elevational gradient analyses and the use of historical museum specimens: a cautionary tale. Journal of Biogeography 32:1883-1897.

Rozas, J., J. C. Sanchez-DelBarrio, X. Messeguer, and R. Rozas. 2003. DnaSP, DNA polymorphism analyses by the coalescent and other methods. Bioinformatics 19:2496 - 2497.

Ruokonen, M., and L. Kvist. 2002. Structure and evolution of the avian mitochondrial control region. Molecular Phylogenetics and Evolution 23:422-432.

Schneider, S., and L. Excoffier. 1999. Estimation of past demographic parameters from the distribution of pairwise differences when the mutation rates vary among sites: application to human mitochondrial DNA. Genetics 153:1079-1089.

Schneider, S., D. Roessli, and L. Excoffier. 2000. Arlequin: a Software Package for Population Genetics.

Slatkin, M., and R. R. Hudson. 1991. Pairwise comparisons of mitochondrial DNA sequences in stable and exponentially growing populations. Genetics 129:555-562.

Sokal, R. R., and F. J. Rohlf. 1995. Biometry: the Principles and Practice of Statistics in Biological Research. W.H. Freeman & Company, New York.

Stanley, W. T. 1991. An analysis of the biogeographic relationships of four populations of the Uinta chipmunk (*Eutamias umbrinus*) using phallic morphology. Pp. 41. Humboldt State University, Arcata, California.

Stockman, A., and J. Bond. 2007. Delimiting cohesion species: extreme population structuring and the role of ecological interchangeability. Molecular Ecology 16:3374-3392.

Suárez-Seoane, S., E. L. García de la Morena, M. B. Morales Prieto, P. E. Osborne, and E. de Juana. 2008. Maximum entropy niche-based modelling of seasonal changes in little bustard (*Tetrax tetrax*) distribution. Ecological Modelling 219:17-29.

Sutton, D. A., and C. F. Nadler. 1969. Chromosomes of the North American chipmunk genus Eutamias. Journal of Mammalogy 50:527-535.

Swanson, E. R., and F. W. McDowell. 1984. Calderas of the Sierra Madre Occidental volcanic field, western Mexico. Journal of Geophysical Research 89:8787-8799.

Taberlet, P. 1996. The use of mitochondrial DNA control region sequencing in conservation genetics. Pp. 125-142 *in* T. B. Smith, and R. K. Wayne, eds. Molecular Genetic Approaches in Conservation. Oxford University Press, New York.

Tajima, F. 1989a. The effect of change in population size on DNA polymorphism. Genetics 123:597-601.

Tajima, F. 1989b. Statistical method for testing the neutral mutation hypothesis by DNA polymorphism. Genetics 123:585-595.

Thompson, R. S. 1990. Late Quaternary vegetation and climate in the Great Basin. Pp. 200-239 *in* J. L. Betancourt, T. R. Van Devender, and P. S. Martin, eds. Packrat middens: the last 40,000 years of biotic change. The University of Arizona Press, Tucson.

Van Devender, T. R., and W. G. Spaulding. 1983. Development of vegetation and climate in the southwestern United States. Pp. 131-156 *in* S. G. Wells, and D. R. Haragan, eds. Origin and Evolution of Deserts. University of New Mexico Press, Albuquerque.

Wakeley, J. 2008. Coalescent Theory: An Introduction. Roberts & Company.

Waltari, E., and R. P. Guralnick. 2009. Ecological niche modelling of montane mammals in the Great Basin, North America: examining past and present connectivity of species across basins and ranges. Journal of Biogeography 36:148-161.

Waltari, E., R. J. Hijmans, A. T. Peterson, A. S. Nyari, S. L. Perkins, and R. P. Guralnick. 2007. Locating Pleistocene refugia: comparing phylogeographic and ecological niche model predictions. PLoS ONE 2:e563.

Ward, R. H., B. L. Frazier, K. Dew-Jager, and S. Pääbo. 1991. Extensive mitochondrial diversity within a single Amerindian tribe. Proceedings of the National Academy of Science of the USA 88:8720-8724.

Wells, P. V. 1983. Paleobiogeography of montane islands in the Great Basin since the last glaciopluvial. Ecological Monographs 53:341-382.

Wells, P. V., and R. Berger. 1967. Late Pleistocene history of coniferous woodland in the Mojave Desert. Science 155:1640-1647.

Weyandt, S. E., and R. A. Van Den Bussche. 2007. Phylogeographic structuring and volant mammals: the case of the Pallid Bat (A*ntrozous pallidus*). Journal of Biogeography:1-13.

Wiens, J. J., and C. H. Graham. 2005. Niche conservatism: integrating evolution, ecology, and conservation biology. Annual Review of Ecology, Evolution, and Systematics 36:519-539.

Wilgenbusch, J. C., D. L. Warren, and D. L. Swofford. 2004. AWTY: A system for graphical exploration of MCMC convergence in Bayesian phylogenetic inference.

Table 4.1: Population demographic parameter for *N. umbrinus* and *N. palmeri*. N = number of individuals, h = haplotypes diversity (± SD), π = nucleotide diversity (± SD), *D* = Tajima's *D*, F_s = Fu's F_s, r = raggedness index of mismatch distribution (bold numbers indicate significant values). [1]Sheep Mountains subspecies (*N. u. nevadensis*) possibly extinct; [2]Spring Mountains population is represented by *N. palmeri*; [3]dashes indicate no values calculated for populations where n < 5.

	Population	**State**	**County**	**N**[3]	**Haps**	**h**	***π***	***D***	***Fs***	***r***
CO	Coconino	AZ	Coconino	3	3	–	0.02339 ± 0.01027	–	–	–
DC	Deep Creek	UT	Juab	10	5	0.667 ± 0.163	0.01481 ± 0.00493	0.56168	2.02	0.2178
DS	Desatoya	NV	Lander	2	2	–	0.00758 ± 0.00379	–	–	–
DM	Diamond	NV	Eureka	7	3	0.524 ± 0.209	0.01170 ± 0.00694	1.31438	3.329	0.4580
GR	Grant	NV	Nye	10	7	0.911 ± 0.077	0.01866 ± 0.00371	0.50803	0.192	0.1373
MP	Markagunt Plateau	UT	Kane	6	6	1.0	0.01320 ± 0.00199	-0.45829	-2.059	0.1689
MN/TQ	Monitor + Toquima	NV	Nye	5	5	1.0	0.01253 ± 0.00384	-0.95426	-1.345	0.1800
RC	Robert's Creek	NV	Eureka	10	4	0.711 ± 0.117	0.01676 ± 0.00403	1.20452	3.975	0.2286
RU/EH	Ruby + East Humboldt	NV	Elko	12	4	0.818 ± 0.084	0.02092 ± 0.00427	0.03767	2.529	**0.2011**
SH	Sheep[1]	NV	Clark	3	2	–	0.00501 ± 0.00236	–	–	–
SS	Shoshone	NV	Lander	5	3	0.800 ± 0.164	0.00251 ± 0.00069	0.24314	-0.475	0.3600
SN	Snake	NV	White Pine	10	6	0.836 ± 0.089	0.01080 ± 0.00375	-1.51576	0.352	0.0863
SP	Spring[2]	NV	Clark	138	11	0.756 ± 0.021	0.00504 ± 0.00062	-1.32903	-0.968	0.0531
SR	Spruce	NV	Elko	10	6	0.889 ± 0.075	0.02311 ± 0.00381	1.43126	1.914	0.0746
TY	Toiyabe	NV	Lander	4	1	–	–	–	–	–
UN	Uinta	UT	Emery	3	2	–	0.00835 ± 0.00394	–	–	–

WA	Wasatch	UT		9	7	0.917 ± 0.092	0.01734 ± 0.00404	0.71943	-0.498	0.0563
WH	White	CA	Mono	9	2	0.556 ± 0.090	0.00418 ± 0.00068	1.94806	3.276	**0.8148**
WP	White Pine	NV	White Pine	9	6	0.917 ± 0.073	0.00780 ± 0.00129	0.25846	-1.076	0.0486
	Total			262	76	0.929 ± 0.009	0.02318 ± 0.00119	-1.10081	-37.41	0.0105

Table 4.2 AMOVA indicating the amount of genetic variation within and between populations of N. *umbrinus*/*N. palmeri* in the Great Basin.

Source of Variation	d.f.	Sum of squares	Variance components	Percentage of Variation
Among Populations (mountain ranges)	18	780.471	3.95945 Va	69.03
Within Populations	246	436.933	1.77615 Vb	30.97

Table 4.3 Pairwise Fst values for each population of *Neotamias*. Population abbreviations follow Figure 4.1. Values are significant at a value of P = 0.017 (with a Bonferonni correction), indicating population differentiation; *Note*: values in brackets [ ] are non-significant.

		SP	CO	DC	DM	DS	GR	MO-TQ	MP	RC	RB-EH
		1	2	3	4	5	6	7	8	9	10
SP	1	–									
CO	2	0.40293	–								
DC	3	0.72129	0.31564	–							
DM	4	0.80682	0.48745	0.44578	–						
DS	5	0.95451	[0.8353]	[0.86498]	[0.90073]	–					
GR	6	0.73907	0.27257	0.30367	0.33831	0.84199	–				
MO-TQ	7	0.79562	0.36496	0.46405	0.58743	[0.89136]	[0.18768]	–			
MP	8	0.84674	[0.41643]	0.58439	0.68288	0.89131	0.51923	0.636	–		
RC	9	0.78881	0.39894	0.41341	[0.16667]	0.86037	0.30309	0.43473	0.59914	–	
RB-EH	10	0.69551	0.20209	0.30276	[0.11058]	0.82479	0.26323	0.37989	0.53992	0.19716	–
SH	11	0.66782	[0.23982]	0.51478	0.71429	0.96629	0.43412	0.6	0.6683	0.57914	0.43706
SN	12	0.82293	0.46678	0.54087	0.66955	0.89829	0.5242	0.60092	0.45062	0.60771	0.52873
SR	13	0.69321	[0.17568]	0.27313	[0.07102]	0.81024	0.20936	0.34761	0.52256	0.15366	[-0.00031]
SS	14	0.84015	0.68499	0.63272	0.7886	[0.96302]	0.59219	0.6888	0.81021	0.68318	0.59498
TY	15	0.84778	0.69399	0.621	0.78959	0.97985	0.57561	0.69651	0.81095	0.67273	0.58719
UN	16	0.81577	[0.38043]	0.51803	0.64591	[0.92301]	0.4083	0.54407	0.54167	0.52782	0.45138
WA	17	0.7586	[0.2849]	0.38538	0.57227	0.84793	0.36699	0.42137	0.44444	0.51399	0.4117
WH	18	0.77625	0.64474	0.66739	0.79907	0.95543	0.63935	0.73641	0.78667	0.7141	0.59538
WP	19	0.82305	0.58318	0.49824	0.22894	0.93005	0.46669	0.66193	0.74274	0.3097	[0.09285]

		SH	SN	SR	SS	TY	UN	WA	WH	WP
		11	12	13	14	15	16	17	18	
SH	11	–								
SN	12	0.64333	–							
SR	13	[0.34953]	0.51827	–						
SS	14	0.93174	0.71814	0.58012	–					
TY	15	[1.0]	0.71448	0.56102	0.11111	–				
UN	16	[0.76654]	0.48268	0.39428	0.84839	0.8806	–			
WA	17	0.41606	0.4268	0.38606	0.64029	0.62718	[0.1554]	–		
WH	18	0.84602	0.74305	0.592	0.84321	0.87355	0.78049	0.55203	–	
WP	19	0.79902	0.71746	[0.11847]	0.84028	0.84601	0.76653	0.63803	0.83712	–

Figure Legends

Figure 4.1: Elevational relief map of the Great Basin in western North America (outlined in yellow) indicating collecting localities for samples of *Neotamias umbrinus* and *N. palmeri*. The colors (with corresponding numbers and abbreviations) correspond to individual mountain ranges and haplotypes shown in Figure 4.2; size of each circle is proportional to the number of samples from that locality (from 1 to 11 individuals); the Spring Mountains are represented by the number of haplotypes (n = 11). Shaded blue areas represent the distribution of *N. umbrinus* within the Great Basin and the yellow line represents the boundary of the hydrographic Great Basin. Inset – complete distribution of *N. umbrinus* in western North America.

Figure 4.2: Median-joining network of all haplotypes of the *Neotamias umbrinus* species group (*N. umbrinus* + *N. palmeri*). The size of each circle is proportional to the haplotype frequency and the colors correspond to localities indicated in Figure 4.1. General geographic locality within the Great Basin for each haplotype assemblage is indicated.

Figure 4.3: Ecological niche models representing the suitable habitat for A) the present-day distribution of *Neotamias umbrinus* and *N. palmeri* in western North America, and B) the extent of predicted habitat during the last glacial maximum (18k years before present). Darker areas represent highly suitable habitat with decreasing suitability corresponding to lighter colors. The white areas represent unsuitable habitats.

Figure 4.1

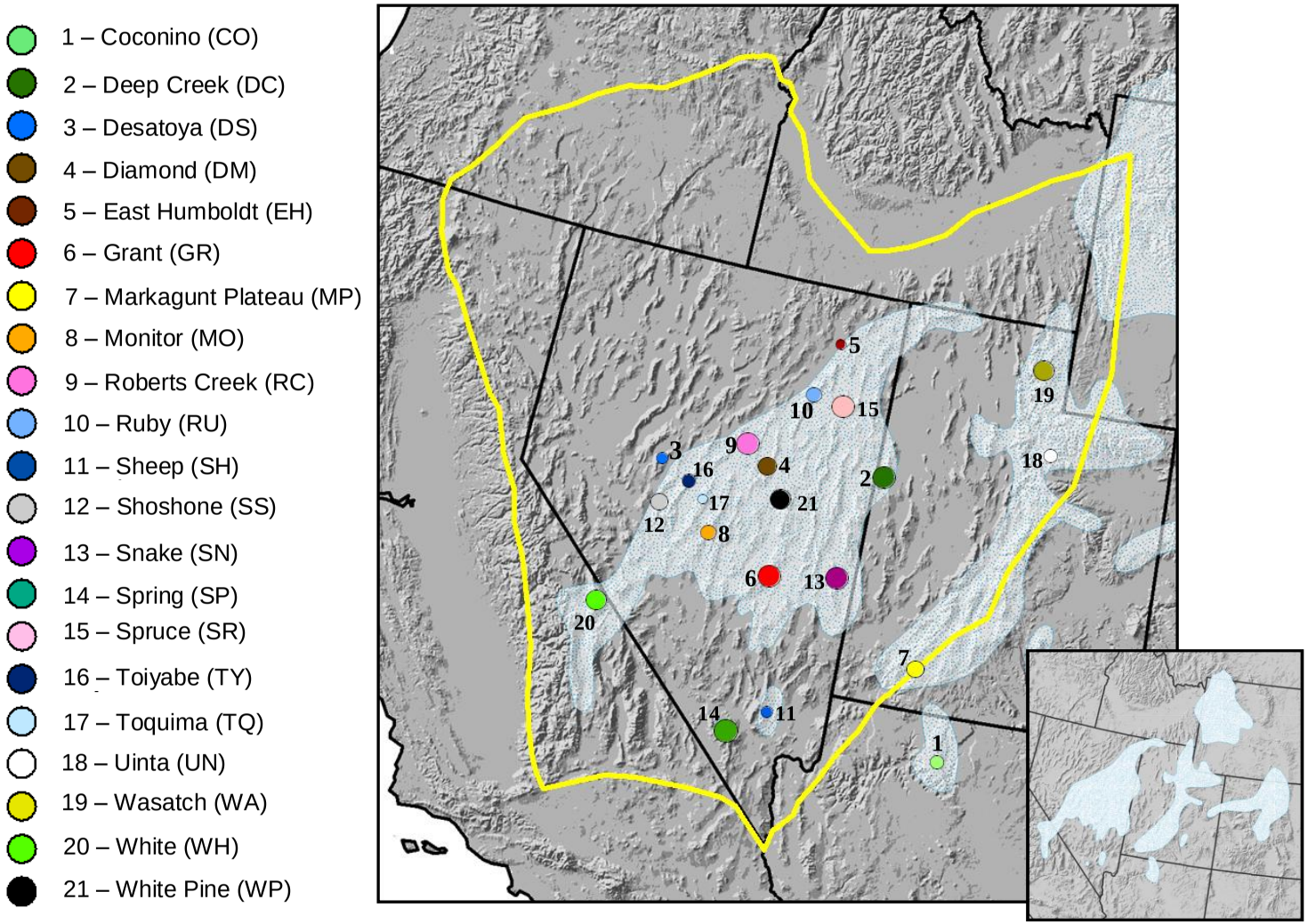
1 – Coconino (CO)
2 – Deep Creek (DC)
3 – Desatoya (DS)
4 – Diamond (DM)
5 – East Humboldt (EH)
6 – Grant (GR)
7 – Markagunt Plateau (MP)
8 – Monitor (MO)
9 – Roberts Creek (RC)
10 – Ruby (RU)
11 – Sheep (SH)
12 – Shoshone (SS)
13 – Snake (SN)
14 – Spring (SP)
15 – Spruce (SR)
16 – Toiyabe (TY)
17 – Toquima (TQ)
18 – Uinta (UN)
19 – Wasatch (WA)
20 – White (WH)
21 – White Pine (WP)

Figure 4.2

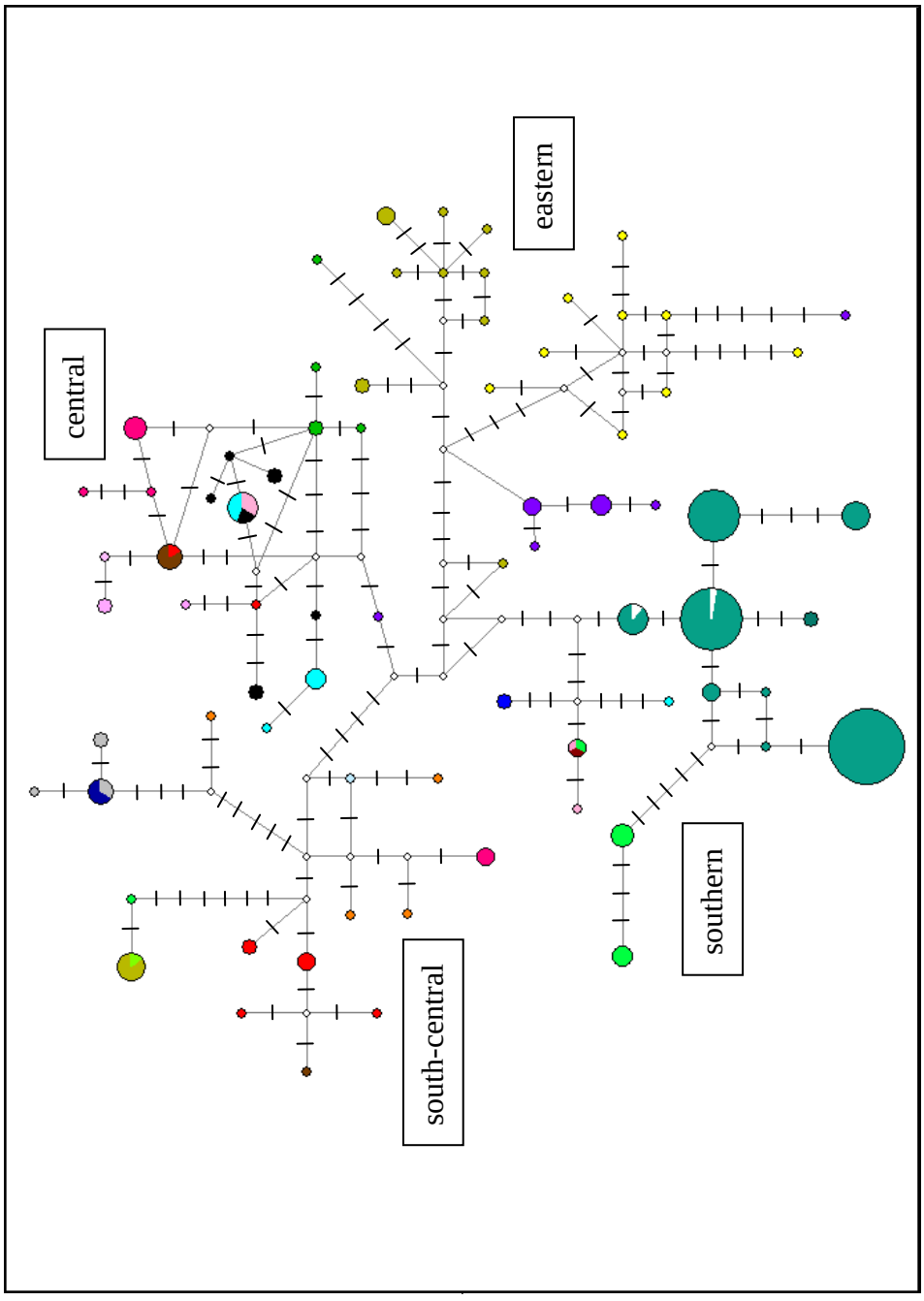

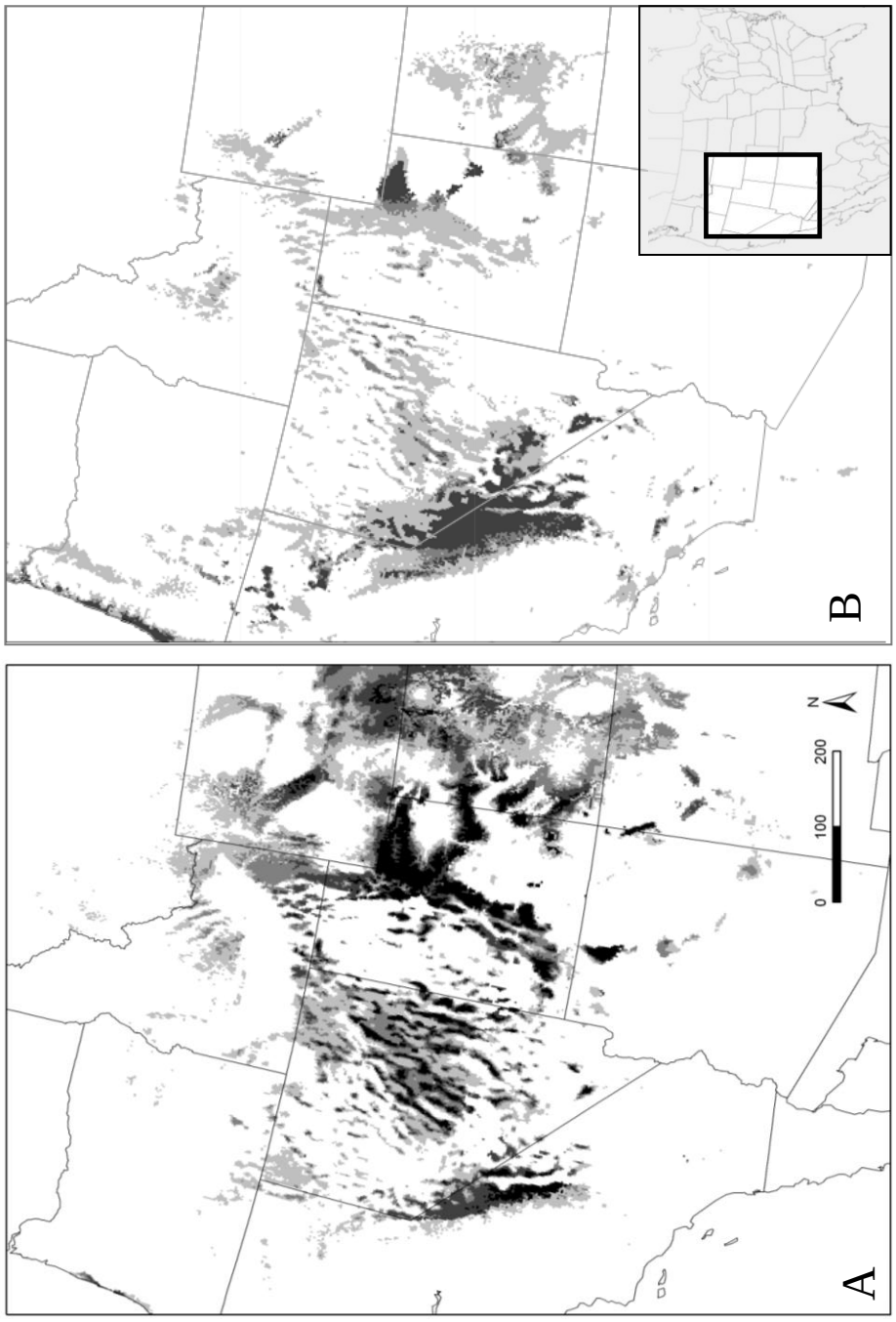

Figure 4.3

Appendix A: Specimen localities of all individuals of *Ammospermophilus* and outgroups analyzed in Chapter 2. The LVT # represents the Las Vegas Tissue Collection reference number.

Species	LVT #	Country	State	County	Locality
Cynomys gunnisoni	6926	USA	New Mexico	Colfax	35.394245; -107.322954
Spermophilus tereticaudus	7571	Mexico	Sonora		30.691389; -112.134167
A. insularis	1603	Mexico	Baja California Sur		24.477234; -110.305226
A. insularis	1604	Mexico	Baja California Sur		24.477234; -110.305226
A. insularis	1605	Mexico	Baja California Sur		
A. nelsoni	2485	USA	California	Kern	35.240434, -119.501676
A. nelsoni	2486	USA	California	Kern	35.240434, -119.501676
A. harrisii	1231	Mexico	Sonora		29.933333; -112716667
A. harrisii	1232	Mexico	Sonora		29.933333; -112716667
A. harrisii	1233	Mexico	Sonora		29.933333; -112716667
A. harrisii	1666	USA	New Mexico	Hidalgo	32.083712; -108.971633
A. harrisii	1667	USA	New Mexico	Hidalgo	32.083712; -108.971634
A. harrisii	5852	USA	New Mexico	Hidalgo	32.083712; -108.971633
A. harrisii	5853	USA	New Mexico	Hidalgo	32.083712; -108.971634
A. harrisii	6012	USA	Arizona	Yuma	33.584514; -114.381678
A. harrisii	6013	USA	Arizona	Yuma	32.813333; -114.486889
A. harrisii	6014	USA	Arizona	Yuma	32.813333; -114.486889
A. interpres	1138	Mexico	Durango		25.383408; -103.588917
A. interpres	1621	USA	New Mexico	Lincoln	33.764729; -105.813814
A. interpres	1691	USA	New Mexico	Socorro	34.118474; -106.697790
A. interpres	1693	USA	New Mexico	Bernalillo	35.175454; -106.490814

A. interpres	8353	USA	New Mexico	Socorro	34.118580; -106.696185
A. interpres	8354	USA	New Mexico	Socorro	34.118580; -106.696185
A. interpres	8355	USA	New Mexico	Socorro	34.118580; -106.696185
A. interpres	8356	USA	New Mexico	Socorro	34.118580; -106.696185
A. interpres	8357	USA	New Mexico	Socorro	34.118580; -106.696185
A. leucurus	1624	Mexico	Baja California		31.224939; -115.574344
A. leucurus	1625	Mexico	Baja California		31.224939; -115.574344
A. leucurus	1629	Mexico	Baja California		29.992339; -115.266396
A. leucurus	1630	Mexico	Baja California		29.925394; -115.083398
A. leucurus	1631	Mexico	Baja California		29.925394; -115.083398
A. leucurus	1633	Mexico	Baja California		29.888824; -114.883898
A. leucurus	1634	Mexico	Baja California		29.888824; -114.883898
A. leucurus	1635	Mexico	Baja California		29.888824; -114.883898
A. leucurus	1643	Mexico	Baja California		28.913930; -114.160292
A. leucurus	1644	Mexico	Baja California		28.913930; -114.160292
A. leucurus	1655	Mexico	Baja California		31.775215; -116.488866
A. leucurus	1656	Mexico	Baja California		31.775215; -116.488866
A. leucurus	1657	Mexico	Baja California		31.775215; -116.488866
A. leucurus	1661	Mexico	Baja California		29.992339; -115.266396
A. leucurus	1663	Mexico	Baja California		29.992339; -115.266396
A. leucurus	1669	Mexico	Baja California Sur		27.056639; -112.964853
A. leucurus	1671	Mexico	Baja California Sur		27.211608; -112.057606
A. leucurus	1673	Mexico	Baja California Sur		23.743293; -109.942845
A. leucurus	1674	Mexico	Baja California Sur		23.743293; -109.942845
A. leucurus	1675	Mexico	Baja California Sur		23.743293; -109.942845
A. leucurus	1676	Mexico	Baja California Sur		23.428174; -109.631198
A. leucurus	1677	Mexico	Baja California Sur		23.329943; -110.173551
A. leucurus	1678	Mexico	Baja California Sur		23.329943; -110.173551

A. leucurus	1679	Mexico	Baja California Sur		23.329943; -110.173551
A. leucurus	1680	Mexico	Baja California Sur		23.329943; -110.173551
A. leucurus	1681	Mexico	Baja California Sur		23.329943; -110.173551
A. leucurus	1682	Mexico	Baja California Sur		25.808189; -111.361702
A. leucurus	1683	Mexico	Baja California Sur		25.808189; -111.361702
A. leucurus	1690	Mexico	Baja California Sur		27.093100; -112.125615
A. leucurus	1718	Mexico	Baja California Sur		27.416478; -112.605203
A. leucurus	1720	Mexico	Baja California Sur		23.743293; -109.942845
A. leucurus	1721	Mexico	Baja California Sur		23.743293; -109.942845
A. leucurus	1722	Mexico	Baja California Sur		23.329943; -110.173551
A. leucurus	1723	Mexico	Baja California Sur		23.329943; -110.173551
A. leucurus	1724	Mexico	Baja California Sur		23.329943; -110.173551
A. leucurus	1725	Mexico	Baja California Sur		26.097500; -111.326187
A. leucurus	1726	Mexico	Baja California Sur		27.093100; -112.125615
A. leucurus	1727	Mexico	Baja California Sur		27.093100; -112.125615
A. leucurus	2008	USA	Nevada	Clark	36.425236; -114.533552
A. leucurus	5218	USA	Nevada	Lincoln	36.921258; -114.932868
A. leucurus	5219	USA	Nevada	Lincoln	36.921258; -114.932868
A. leucurus	5804	USA	California	Kern	32.878167; -114.497917
A. leucurus	5805	USA	California	Kern	32.878167; -114.497917
A. leucurus	5897	USA	Utah	Kane	37.237959; -111.960452
A. leucurus	5900	USA	Oregon	Harney	42.283333; -118.650000
A. leucurus	8339	USA	Oregon	Harney	42.250000; -118.666667
A. leucurus	8340	USA	Oregon	Harney	42.283333; -118.650000
A. leucurus	8341	USA	Nevada	Pershing	40.133056; -118.399722
A. leucurus	8342	USA	Nevada	Pershing	40.133056; -118.399722
A. leucurus	8343	USA	California	Inyo	37.181389; -118.233056
A. leucurus	8344	USA	California	Inyo	37.181389; -118.233056

A. leucurus	8345	USA	California	San Bernardino	34.666389; -116.716389
A. leucurus	8346	USA	California	San Bernardino	34.666389; -116.716389
A. leucurus	8347	USA	California	Imperial	32.799722; -114.839722
A. leucurus	8348	USA	California	Imperial	32.817500; -114.818333
A. leucurus	8350	USA	California	San Bernardino	35.498066; -117.587269
A. leucurus	8351	USA	California	San Bernardino	35.498066; -117.587269
A. leucurus	8352	USA	California	San Bernardino	35.498066; -117.587269
A. leucurus	8358	USA	Nevada	Washoe	39.622501; -119.733769
A. leucurus	8359	USA	Nevada	Washoe	39.622501; -119.733769
A. leucurus	8360	USA	Nevada	Lincoln	37.682922; -115.713323
A. leucurus	8361	USA	New Mexico	Bernalillo	35.197574; -106.555592
A. leucurus	8362	USA	Utah	Kane	37.246974; -111.878181
A. leucurus	8364	USA	Utah	Kane	37.357220; -111.099440

Appendix B: Specimen localities of all individuals of *Pipistrellus hesperus* analyzed in Chapter 3. The LVT # represents the Las Vegas Tissue Collection reference number.

Species	LVT#	Country	State	County	Locality
Pipistrellus hesperus	1565	USA	Nevada	Clark	36.1203 -115.5109
Pipistrellus hesperus	1567	USA	Nevada	Clark	36.1203 -115.5109
Pipistrellus hesperus	4989	USA	Nevada	Clark	36.7111 -114.7161
Pipistrellus hesperus	4990	USA	Nevada	Clark	36.7111 -114.7161
Pipistrellus hesperus	5807	USA	California	San Diego	32.9194 -116.2188
Pipistrellus hesperus	5808	USA	California	San Diego	32.9194 -116.2188
Pipistrellus hesperus	5809	USA	California	San Diego	32.9194 -116.2188
Pipistrellus hesperus	5810	USA	California	San Diego	32.9194 -116.2188
Pipistrellus hesperus	5811	USA	California	San Diego	32.9194 -116.2188
Pipistrellus hesperus	5812	USA	California	San Diego	32.9194 -116.2188
Pipistrellus hesperus	6015	USA	Nevada	Esmeralda	37.3872 -117.6525
Pipistrellus hesperus	6016	USA	Nevada	Esmeralda	37.3872 -117.6525
Pipistrellus hesperus	6017	USA	Nevada	Esmeralda	37.3872 -117.6525
Pipistrellus hesperus	6018	USA	Nevada	Esmeralda	37.3872 -117.6525
Pipistrellus hesperus	6019	USA	Arizona	Mojave	36.6677 -114.0252
Pipistrellus hesperus	6020	USA	Arizona	Mojave	36.6677 -114.0252
Pipistrellus hesperus	6021	USA	Arizona	Mojave	36.6677 -114.0252
Pipistrellus hesperus	6022	USA	Arizona	Mojave	36.6677 -114.0252
Pipistrellus hesperus	6023	USA	Arizona	Mojave	36.6677 -114.0252
Pipistrellus hesperus	6024	USA	Arizona	Mojave	36.6677 -114.0252
Pipistrellus hesperus	6025	USA	Nevada	Clark	36.7108 -114.7126
Pipistrellus hesperus	6026	USA	Nevada	Clark	36.7108 -114.7126
Pipistrellus hesperus	6027	USA	Nevada	Clark	36.7108 -114.7126

Pipistrellus hesperus	6028	USA	Nevada	Clark	36.7108 -114.7126
Pipistrellus hesperus	6197	USA	Arizona	Yuma	33.2093 -114.6556
Pipistrellus hesperus	6198	USA	Arizona	Yuma	33.2093 -114.6556
Pipistrellus hesperus	6199	USA	Arizona	Yuma	33.2093 -114.6556
Pipistrellus hesperus	6200	USA	Arizona	Yuma	33.2093 -114.6556
Pipistrellus hesperus	6201	USA	Arizona	Yuma	33.2093 -114.6556
Pipistrellus hesperus	6207	USA	Arizona	Yuma	32.4993 -113.9769
Pipistrellus hesperus	6208	USA	Arizona	Yuma	32.4993 -113.9769
Pipistrellus hesperus	6209	USA	Arizona	Yuma	32.4993 -113.9769
Pipistrellus hesperus	6210	USA	Arizona	Yuma	32.4993 -113.9769
Pipistrellus hesperus	6211	USA	Arizona	Yuma	32.4993 -113.9769
Pipistrellus hesperus	6216	Mexico	Sonora		29.3005 -110.3233
Pipistrellus hesperus	6222	USA	Texas	Culberson	31.3477 -104.4742
Pipistrellus hesperus	6224	USA	Texas	Presidio	29.9481 -104.1001
Pipistrellus hesperus	6226	USA	Texas	Brewster	29.6638 -103.3625
Pipistrellus hesperus	6227	USA	Texas	Brewster	29.6638 -103.3625
Pipistrellus hesperus	6228	USA	Texas	Brewster	29.6638 -103.3625
Pipistrellus hesperus	6229	USA	Texas	Brewster	29.6638 -103.3625
Pipistrellus hesperus	6230	Mexico	Chihuahua		26.6519 -107.6667
Pipistrellus hesperus	6245	USA	Nevada	Clark	36.7108 -114.7126
Pipistrellus hesperus	6247	USA	Utah	Grand	38.6164 -109.5342
Pipistrellus hesperus	6248	USA	Utah	Grand	38.55 -109.5167
Pipistrellus hesperus	6249	USA	Utah	Grand	38.55 -109.5167
Pipistrellus hesperus	6250	USA	Utah	Grand	38.55 -109.5167
Pipistrellus hesperus	6251	USA	Utah	Grand	38.55 -109.5167
Pipistrellus hesperus	6370	Mexico	Baja California		31.7986 -115.4797
Pipistrellus hesperus	6371	USA	New Mexico	Hidalgo	31.5656 -107.7592
Pipistrellus hesperus	6372	USA	New Mexico	Hidalgo	31.5656 -107.7592

Pipistrellus hesperus	6373	USA	New Mexico	Hidalgo	31.5656 -107.7592
Pipistrellus hesperus	6374	Mexico	Baja California		30.7504 -115.2176
Pipistrellus hesperus	6375	Mexico	Baja California		32.3539 -117.0605
Pipistrellus hesperus	6377	USA	New Mexico	Socorro	33.8848 -106.7242
Pipistrellus hesperus	6378	USA	New Mexico	Eddy	32.15 -104.6833
Pipistrellus hesperus	6379	USA	New Mexico	Eddy	32.15 -104.6833
Pipistrellus hesperus	6380	USA	New Mexico	Eddy	32.15 -104.6833
Pipistrellus hesperus	6381	USA	New Mexico	Eddy	32.15 -104.6833
Pipistrellus hesperus	6382	USA	New Mexico	Eddy	32.0167 -104.75
Pipistrellus hesperus	6383	USA	New Mexico	Socorro	33.8848 -106.7242
Pipistrellus hesperus	6384	Mexico	Baja California Sur		23.0524 -116.7592
Pipistrellus hesperus	6385	USA	New Mexico	Socorro	33.8848 -106.7242
Pipistrellus hesperus	6386	USA	New Mexico	Socorro	33.8848 -106.7242
Pipistrellus hesperus	6387	Mexico	Sonora		29.3005 -110.3233
Pipistrellus hesperus	6388	Mexico	Sonora		29.3005 -110.3233
Pipistrellus hesperus	6389	Mexico	Sonora		29.3005 -110.3233
Pipistrellus hesperus	6390	Mexico	Sonora		29.3005 -110.3233
Pipistrellus hesperus	6391	Mexico	Sonora		29.3005 -110.3233
Pipistrellus hesperus	6646	Mexico	Coahuila		26.9888 -102.0665
Pipistrellus hesperus	6691	Mexico	Baja California Sur		23.0524 -116.7592
Pipistrellus hesperus	6692	Mexico	Baja California Sur		23.4673 -109.7171
Pipistrellus hesperus	6701	Mexico	Baja California Sur		25.6838 -111.0464
Pipistrellus hesperus	6702	Mexico	Durango		23.8323 -104.7705
Pipistrellus hesperus	6704	Mexico	Durango		23.8323 -104.7705
Pipistrellus hesperus	6705	Mexico	Durango		23.8323 -104.7705
Pipistrellus hesperus	6706	Mexico	Durango		23.8323 -104.7705
Pipistrellus hesperus	6851	USA	California	San Bernardino	35.9952 -115.9057
Pipistrellus hesperus	6852	USA	California	San Bernardino	35.9952 -115.9057

Pipistrellus hesperus	6853	USA	California	San Bernardino	35.9952 -115.9057
Pipistrellus hesperus	6854	USA	California	San Bernardino	35.9952 -115.9057
Pipistrellus hesperus	6856	USA	California	San Bernardino	36.9447 -119.7141
Pipistrellus hesperus	6858	USA	California	San Bernardino	36.9447 -119.7141
Pipistrellus hesperus	6859	USA	California	San Bernardino	36.9447 -119.7141
Pipistrellus hesperus	6863	Mexico	Coahuila		26.9888 -102.0665
Pipistrellus hesperus	6864	Mexico	Coahuila		26.9888 -102.0665
Pipistrellus hesperus	6865	Mexico	Coahuila		26.9888 -102.0665
Pipistrellus hesperus	6866	Mexico	Coahuila		26.9888 -102.0665
Pipistrellus hesperus	6867	USA	New Mexico	Catron	33.4038 -108.8834
Pipistrellus hesperus	6868	USA	New Mexico	Catron	33.4038 -108.8834
Pipistrellus hesperus	6869	USA	New Mexico	Catron	33.4038 -108.8834
Pipistrellus hesperus	6870	USA	New Mexico	Luna	31.8753 -107.7592
Pipistrellus hesperus	6871	USA	New Mexico	Luna	31.8753 -107.7592
Pipistrellus hesperus	6872	USA	New Mexico	Luna	31.8753 -107.7592
Pipistrellus hesperus	6873	USA	New Mexico	Luna	31.8753 -107.7592
Pipistrellus hesperus	6874	USA	New Mexico	Luna	31.8753 -107.7592
Pipistrellus hesperus	6875	USA	Nevada	Nye	36.9993 -116.7592
Pipistrellus hesperus	6876	USA	Nevada	Nye	36.9993 -116.7592
Pipistrellus hesperus	6877	USA	Nevada	Nye	36.9993 -116.7592
Pipistrellus hesperus	6878	USA	Nevada	Nye	36.9993 -116.7592
Pipistrellus hesperus	6879	USA	Nevada	Nye	36.9993 -116.7592
Pipistrellus hesperus	9395	USA	Nevada	Churchill	39.73356 -119.0235
Pipistrellus hesperus	9396	USA	Nevada	Churchill	39.73356 -119.0235
Pipistrellus hesperus	9397	USA	Nevada	Churchill	39.73356 -119.0235
Pipistrellus hesperus	9398	USA	Nevada	Churchill	39.73356 -119.0235

Appendix C: Specimen localities of all individuals analyzed in Chapter 4. The LVT # represents the Las Vegas Tissue Collection reference number.

Species	LVT #	State	County	Range	Specific Locality (if available)
Neotamias palmeri	5031	Nevada	Clark	Spring	
Neotamias palmeri	5032	Nevada	Clark	Spring	
Neotamias palmeri	5033	Nevada	Clark	Spring	
Neotamias palmeri	5034	Nevada	Clark	Spring	
Neotamias palmeri	5035	Nevada	Clark	Spring	
Neotamias palmeri	5036	Nevada	Clark	Spring	
Neotamias palmeri	5037	Nevada	Clark	Spring	
Neotamias palmeri	5038	Nevada	Clark	Spring	
Neotamias palmeri	5039	Nevada	Clark	Spring	
Neotamias palmeri	5040	Nevada	Clark	Spring	
Neotamias palmeri	5041	Nevada	Clark	Spring	
Neotamias palmeri	5042	Nevada	Clark	Spring	
Neotamias palmeri	5043	Nevada	Clark	Spring	
Neotamias palmeri	5044	Nevada	Clark	Spring	
Neotamias palmeri	5045	Nevada	Clark	Spring	
Neotamias palmeri	5046	Nevada	Clark	Spring	
Neotamias palmeri	5047	Nevada	Clark	Spring	
Neotamias palmeri	5048	Nevada	Clark	Spring	
Neotamias palmeri	5049	Nevada	Clark	Spring	
Neotamias palmeri	5050	Nevada	Clark	Spring	
Neotamias palmeri	5051	Nevada	Clark	Spring	
Neotamias palmeri	5052	Nevada	Clark	Spring	
Neotamias palmeri	5053	Nevada	Clark	Spring	

Neotamias palmeri	5054	Nevada	Clark	Spring
Neotamias palmeri	5055	Nevada	Clark	Spring
Neotamias palmeri	5056	Nevada	Clark	Spring
Neotamias palmeri	5057	Nevada	Clark	Spring
Neotamias palmeri	5058	Nevada	Clark	Spring
Neotamias palmeri	5059	Nevada	Clark	Spring
Neotamias palmeri	5060	Nevada	Clark	Spring
Neotamias palmeri	5061	Nevada	Clark	Spring
Neotamias palmeri	5062	Nevada	Clark	Spring
Neotamias palmeri	5063	Nevada	Clark	Spring
Neotamias palmeri	5064	Nevada	Clark	Spring
Neotamias palmeri	5065	Nevada	Clark	Spring
Neotamias palmeri	5066	Nevada	Clark	Spring
Neotamias palmeri	5067	Nevada	Clark	Spring
Neotamias palmeri	5068	Nevada	Clark	Spring
Neotamias palmeri	5069	Nevada	Clark	Spring
Neotamias palmeri	5204	Nevada	Clark	Spring
Neotamias palmeri	5205	Nevada	Clark	Spring
Neotamias palmeri	5206	Nevada	Clark	Spring
Neotamias palmeri	5207	Nevada	Clark	Spring
Neotamias palmeri	5208	Nevada	Clark	Spring
Neotamias palmeri	5209	Nevada	Clark	Spring
Neotamias palmeri	5210	Nevada	Clark	Spring
Neotamias palmeri	5211	Nevada	Clark	Spring
Neotamias palmeri	5212	Nevada	Clark	Spring
Neotamias palmeri	5213	Nevada	Clark	Spring
Neotamias palmeri	5214	Nevada	Clark	Spring
Neotamias palmeri	5215	Nevada	Clark	Spring

Neotamias palmeri	5281	Nevada	Clark	Spring
Neotamias palmeri	5282	Nevada	Clark	Spring
Neotamias palmeri	5283	Nevada	Clark	Spring
Neotamias palmeri	5284	Nevada	Clark	Spring
Neotamias palmeri	5285	Nevada	Clark	Spring
Neotamias palmeri	5286	Nevada	Clark	Spring
Neotamias palmeri	5287	Nevada	Clark	Spring
Neotamias palmeri	5288	Nevada	Clark	Spring
Neotamias palmeri	5289	Nevada	Clark	Spring
Neotamias palmeri	5290	Nevada	Clark	Spring
Neotamias palmeri	5291	Nevada	Clark	Spring
Neotamias palmeri	5292	Nevada	Clark	Spring
Neotamias palmeri	5293	Nevada	Clark	Spring
Neotamias palmeri	5294	Nevada	Clark	Spring
Neotamias palmeri	5295	Nevada	Clark	Spring
Neotamias palmeri	5296	Nevada	Clark	Spring
Neotamias palmeri	5297	Nevada	Clark	Spring
Neotamias palmeri	5298	Nevada	Clark	Spring
Neotamias palmeri	5299	Nevada	Clark	Spring
Neotamias palmeri	5300	Nevada	Clark	Spring
Neotamias palmeri	5301	Nevada	Clark	Spring
Neotamias palmeri	5302	Nevada	Clark	Spring
Neotamias palmeri	5303	Nevada	Clark	Spring
Neotamias palmeri	5304	Nevada	Clark	Spring
Neotamias palmeri	5305	Nevada	Clark	Spring
Neotamias palmeri	5306	Nevada	Clark	Spring
Neotamias palmeri	5308	Nevada	Clark	Spring
Neotamias palmeri	5310	Nevada	Clark	Spring

Neotamias palmeri	5311	Nevada	Clark	Spring
Neotamias palmeri	5313	Nevada	Clark	Spring
Neotamias palmeri	5314	Nevada	Clark	Spring
Neotamias palmeri	5315	Nevada	Clark	Spring
Neotamias palmeri	5317	Nevada	Clark	Spring
Neotamias palmeri	5318	Nevada	Clark	Spring
Neotamias palmeri	5319	Nevada	Clark	Spring
Neotamias palmeri	5320	Nevada	Clark	Spring
Neotamias palmeri	5322	Nevada	Clark	Spring
Neotamias palmeri	5323	Nevada	Clark	Spring
Neotamias palmeri	5324	Nevada	Clark	Spring
Neotamias palmeri	5325	Nevada	Clark	Spring
Neotamias palmeri	5326	Nevada	Clark	Spring
Neotamias palmeri	5327	Nevada	Clark	Spring
Neotamias palmeri	5328	Nevada	Clark	Spring
Neotamias palmeri	5329	Nevada	Clark	Spring
Neotamias palmeri	5330	Nevada	Clark	Spring
Neotamias palmeri	5331	Nevada	Clark	Spring
Neotamias palmeri	5332	Nevada	Clark	Spring
Neotamias palmeri	5333	Nevada	Clark	Spring
Neotamias palmeri	5334	Nevada	Clark	Spring
Neotamias palmeri	5337	Nevada	Clark	Spring
Neotamias palmeri	5338	Nevada	Clark	Spring
Neotamias palmeri	5339	Nevada	Clark	Spring
Neotamias palmeri	5340	Nevada	Clark	Spring
Neotamias palmeri	5343	Nevada	Clark	Spring
Neotamias palmeri	5344	Nevada	Clark	Spring
Neotamias palmeri	5345	Nevada	Clark	Spring

Neotamias palmeri	5346	Nevada	Clark	Spring
Neotamias palmeri	5347	Nevada	Clark	Spring
Neotamias palmeri	5348	Nevada	Clark	Spring
Neotamias palmeri	5349	Nevada	Clark	Spring
Neotamias palmeri	5350	Nevada	Clark	Spring
Neotamias palmeri	5352	Nevada	Clark	Spring
Neotamias palmeri	5353	Nevada	Clark	Spring
Neotamias palmeri	5355	Nevada	Clark	Spring
Neotamias palmeri	5356	Nevada	Clark	Spring
Neotamias palmeri	5357	Nevada	Clark	Spring
Neotamias palmeri	5358	Nevada	Clark	Spring
Neotamias palmeri	5359	Nevada	Clark	Spring
Neotamias palmeri	5361	Nevada	Clark	Spring
Neotamias palmeri	5362	Nevada	Clark	Spring
Neotamias palmeri	5363	Nevada	Clark	Spring
Neotamias palmeri	5364	Nevada	Clark	Spring
Neotamias palmeri	5365	Nevada	Clark	Spring
Neotamias palmeri	5366	Nevada	Clark	Spring
Neotamias palmeri	5367	Nevada	Clark	Spring
Neotamias palmeri	5368	Nevada	Clark	Spring
Neotamias palmeri	5371	Nevada	Clark	Spring
Neotamias palmeri	5373	Nevada	Clark	Spring
Neotamias palmeri	5374	Nevada	Clark	Spring
Neotamias palmeri	5375	Nevada	Clark	Spring
Neotamias palmeri	5376	Nevada	Clark	Spring
Neotamias palmeri	5377	Nevada	Clark	Spring
Neotamias palmeri	5378	Nevada	Clark	Spring
Neotamias palmeri	5379	Nevada	Clark	Spring

Neotamias palmeri	5381	Nevada	Clark	Spring		
Neotamias palmeri	5382	Nevada	Clark	Spring		
Neotamias palmeri	5383	Nevada	Clark	Spring		
Neotamias palmeri	5384	Nevada	Clark	Spring		
Neotamias palmeri	5385	Nevada	Clark	Spring		
Neotamias palmeri	5386	Nevada	Clark	Spring		
Neotamias palmeri	5387	Nevada	Clark	Spring		
Neotamias palmeri	5388	Nevada	Clark	Spring		
Neotamias palmeri	5389	Nevada	Clark	Spring	36.30362;	-115.62669
Neotamias palmeri	5390	Nevada	Clark	Spring	36.29647;	-115.63239
Neotamias palmeri	5391	Nevada	Clark	Spring		
Neotamias palmeri	5392	Nevada	Clark	Spring		
Neotamias palmeri	5393	Nevada	Clark	Spring	36.30362;	-115.62669
Neotamias palmeri	5394	Nevada	Clark	Spring	36.30362;	-115.62669
Neotamias palmeri	5395	Nevada	Clark	Spring	36.30362;	-115.62669
Neotamias palmeri	5396	Nevada	Clark	Spring	36.30362;	-115.62669
Neotamias palmeri	5397	Nevada	Clark	Spring	36.30362;	-115.62669
Neotamias palmeri	5398	Nevada	Clark	Spring	36.30362;	-115.62669
Neotamias palmeri	5399	Nevada	Clark	Spring	36.30362;	-115.62669
Neotamias palmeri	5400	Nevada	Clark	Spring	36.30362;	-115.62669
Neotamias palmeri	5421	Nevada	Clark	Spring		
Neotamias palmeri	5422	Nevada	Clark	Spring		
Neotamias palmeri	5423	Nevada	Clark	Spring		
Neotamias palmeri	5424	Nevada	Clark	Spring		
Neotamias palmeri	5425	Nevada	Clark	Spring		
Neotamias palmeri	5426	Nevada	Clark	Spring		
Neotamias palmeri	5427	Nevada	Clark	Spring		
Neotamias palmeri	5428	Nevada	Clark	Spring		

Neotamias palmeri	5429	Nevada	Clark	Spring
Neotamias palmeri	5430	Nevada	Clark	Spring
Neotamias palmeri	5431	Nevada	Clark	Spring
Neotamias palmeri	5432	Nevada	Clark	Spring
Neotamias palmeri	5433	Nevada	Clark	Spring
Neotamias palmeri	5434	Nevada	Clark	Spring
Neotamias palmeri	5435	Nevada	Clark	Spring
Neotamias palmeri	5436	Nevada	Clark	Spring
Neotamias palmeri	5437	Nevada	Clark	Spring
Neotamias palmeri	5438	Nevada	Clark	Spring
Neotamias palmeri	5439	Nevada	Clark	Spring
Neotamias palmeri	5440	Nevada	Clark	Spring
Neotamias palmeri	5441	Nevada	Clark	Spring
Neotamias palmeri	5442	Nevada	Clark	Spring
Neotamias palmeri	5443	Nevada	Clark	Spring
Neotamias palmeri	5445	Nevada	Clark	Spring
Neotamias palmeri	5446	Nevada	Clark	Spring
Neotamias palmeri	5447	Nevada	Clark	Spring
Neotamias palmeri	5448	Nevada	Clark	Spring
Neotamias palmeri	5449	Nevada	Clark	Spring
Neotamias palmeri	5450	Nevada	Clark	Spring
Neotamias palmeri	5451	Nevada	Clark	Spring
Neotamias palmeri	5452	Nevada	Clark	Spring
Neotamias palmeri	5453	Nevada	Clark	Spring
Neotamias palmeri	5455	Nevada	Clark	Spring
Neotamias palmeri	5456	Nevada	Clark	Spring
Neotamias palmeri	5458	Nevada	Clark	Spring
Neotamias palmeri	5459	Nevada	Clark	Spring

Neotamias palmeri	5460	Nevada	Clark	Spring		
Neotamias palmeri	5461	Nevada	Clark	Spring		
Neotamias palmeri	5464	Nevada	Clark	Spring		
Neotamias palmeri	5465	Nevada	Clark	Spring		
Neotamias palmeri	5466	Nevada	Clark	Spring		
Neotamias palmeri	5467	Nevada	Clark	Spring		
Neotamias palmeri	5468	Nevada	Clark	Spring	36.29647;	-11563239
Neotamias palmeri	5469	Nevada	Clark	Spring	36.29647;	-11563239
Neotamias palmeri	5470	Nevada	Clark	Spring	36.29647;	-11563239
Neotamias palmeri	6023	Nevada	Clark	Spring	36.266323;	-115.655655
Neotamias palmeri	6024	Nevada	Clark	Spring	36.298298;	-115.66931
Neotamias palmeri	6025	Nevada	Clark	Spring	36.317413;	-115.682945
Neotamias umbrinus	5163	Nevada	Nye	Toquima	39.05833;	-116.83833
Neotamias umbrinus	5165	Nevada	Nye	Monitor	38.655;	-116.6183
Neotamias umbrinus	5170	Nevada	Nye	Monitor	38.655;	-116.6183
Neotamias umbrinus	5171	Nevada	Nye	Monitor	38.655;	-116.6183
Neotamias umbrinus	5172	Nevada	Nye	Monitor	38.655;	-116.6183
Neotamias umbrinus	5187	Nevada	Elko	East Humboldt	41.302539;	-115.084045
Neotamias umbrinus	5189	Nevada	Elko	East Humboldt	41.302539;	-115.084045
Neotamias umbrinus	5194	Arizona	Coconino	Coconino	36.412194;	-112.135806
Neotamias umbrinus	5195	Arizona	Coconino	Coconino	36.412194;	-112.135806
Neotamias umbrinus	5196	Arizona	Coconino	Coconino	36.412194;	-112.135806
Neotamias umbrinus	5197	Utah	Kane	Markagunt Plateau	37.5185;	-112.738472
Neotamias umbrinus	5198	Utah	Kane	Markagunt Plateau	37.5185;	-112.738472
Neotamias umbrinus	5199	Utah	Kane	Markagunt Plateau	37.5185;	-112.738472
Neotamias umbrinus	5200	Utah	Kane	Markagunt Plateau	37.5185;	-112.738472
Neotamias umbrinus	5201	Utah	Kane	Markagunt Plateau	37.5185;	-112.738472
Neotamias umbrinus	5202	Utah	Kane	Markagunt Plateau	37.5185;	-112.738472

Neotamias umbrinus	5351	Utah	Emery	Uinta	39.424;	-111.131
Neotamias umbrinus	5354	Utah	Emery	Uinta	39.424;	-111.131
Neotamias umbrinus	5471	Nevada	Elko	Ruby	40.617314;	-115.367525
Neotamias umbrinus	5473	Utah	Rich	Wasatch	41.459597;	-111.495578
Neotamias umbrinus	5474	Utah	Cache	Wasatch	41.890081;	-111.632692
Neotamias umbrinus	5901	Nevada	Lander	Desatoya	39.4243679;	-117.6676064
Neotamias umbrinus	5902	Nevada	Lander	Toiyabe	45.0587196;	-123.9028893
Neotamias umbrinus	5903	Nevada	Lander	Toiyabe	45.0587196;	-123.9028893
Neotamias umbrinus	5904	Nevada	Lander	Toiyabe	45.0587196;	-123.9028893
Neotamias umbrinus	5905	Nevada	Lander	Toiyabe	45.0587196;	-123.9028893
Neotamias umbrinus	5906	Nevada	Lander	Toiyabe	45.0587196;	-123.9028893
Neotamias umbrinus	5908	Nevada	Lander	Shoshone	38.8990974;	-117.5426025
Neotamias umbrinus	5909	Nevada	Lander	Shoshone	38.8990974;	-117.5426025
Neotamias umbrinus	5910	Nevada	Lander	Shoshone	38.8990974;	-117.5426025
Neotamias umbrinus	5911	Nevada	Lander	Shoshone	38.8990974;	-117.5426025
Neotamias umbrinus	5912	Nevada	Lander	Shoshone	38.8990974;	-117.5426025
Neotamias umbrinus	5913	Nevada	Lander	Desatoya	39.4243679;	-117.6676064
Neotamias umbrinus	5914	Nevada	Nye	Monitor	38.7315998;	-116.47118
Neotamias umbrinus	5916	Nevada	Elko	Ruby	40.5649261;	-115.5545006
Neotamias umbrinus	5917	Nevada	Elko	Ruby	40.5649261;	-115.5545006
Neotamias umbrinus	5918	Nevada	Elko	Ruby	40.5649261;	-115.5545006
Neotamias umbrinus	5919	Nevada	Elko	Ruby	40.5649261;	-115.5545006
Neotamias umbrinus	5920	Nevada	Elko	Ruby	40.5649261;	-115.5545006
Neotamias umbrinus	5921	Nevada	Elko	Ruby	40.5649261;	-115.5545006
Neotamias umbrinus	5922	Nevada	Elko	Ruby	40.5649261;	-115.5545006
Neotamias umbrinus	5923	Nevada	Elko	Ruby	40.5649261;	-115.5545006
Neotamias umbrinus	5924	Nevada	Elko	Ruby	40.5649261;	-115.5545006
Neotamias umbrinus	5925	California	Mono	White	37.511425;	-118.179633

Neotamias umbrinus	5926	California	Mono	White	37.511425;	-118.179633
Neotamias umbrinus	5927	California	Mono	White	37.511425;	-118.179633
Neotamias umbrinus	5928	California	Mono	White	37.531727;	-118168558
Neotamias umbrinus	5929	California	Mono	White	37.531727;	-118168558
Neotamias umbrinus	5930	Utah	Utah	Wasatch	40.294636;	-111.3922
Neotamias umbrinus	5931	Utah	Utah	Wasatch	40.294636;	-111.3922
Neotamias umbrinus	5932	Utah	Utah	Wasatch	40.294636;	-111.3922
Neotamias umbrinus	5933	Utah	Beaver	Wasatch	38.288333;	-112.408333
Neotamias umbrinus	5934	Utah	Beaver	Wasatch	38.288333;	-112.41
Neotamias umbrinus	5935	Utah	Beaver	Wasatch	38.288333;	-112.411667
Neotamias umbrinus	5936	Nevada	White Pine	Snake	36.441667;	-114.325
Neotamias umbrinus	5937	Nevada	White Pine	Snake	36.441667;	-114.325
Neotamias umbrinus	5938	Utah	Juab	Deep Creek	39.793333;	-113.876667
Neotamias umbrinus	5939	Utah	Juab	Deep Creek	39.793333;	-113.876667
Neotamias umbrinus	5940	Utah	Juab	Deep Creek	39.793333;	-113.876667
Neotamias umbrinus	5941	Utah	Juab	Deep Creek	39.793333;	-113.876667
Neotamias umbrinus	5942	Utah	Juab	Deep Creek	39.793333;	-113.876667
Neotamias umbrinus	5943	Utah	Juab	Deep Creek	39.793333;	-113.876667
Neotamias umbrinus	5944	Utah	Juab	Deep Creek	39.793333;	-113.876667
Neotamias umbrinus	5945	Utah	Juab	Deep Creek	39.793333;	-113.876667
Neotamias umbrinus	5946	Utah	Juab	Deep Creek	39.793333;	-113.876667
Neotamias umbrinus	5947	Utah	Juab	Deep Creek	39.793333;	-113.876667
Neotamias umbrinus	5948	Nevada	Nye	Grant	39.793333;	-113.876667
Neotamias umbrinus	5949	Nevada	Nye	Grant	39.793333;	-113.876667
Neotamias umbrinus	5950	Nevada	Nye	Grant	39.793333;	-113.876667
Neotamias umbrinus	5951	Nevada	Nye	Grant	39.793333;	-113.876667
Neotamias umbrinus	5952	Nevada	Nye	Grant	39.793333;	-113.876667
Neotamias umbrinus	5953	Nevada	Nye	Grant	39.793333;	-113.876667

Neotamias umbrinus	5955	Nevada	Nye	Grant	39.793333;	-113.876667
Neotamias umbrinus	5956	Nevada	White Pine	White Pine	39.266667;	-115.543333
Neotamias umbrinus	5957	Nevada	White Pine	White Pine	39.266667;	-115.543333
Neotamias umbrinus	5958	Nevada	White Pine	White Pine	39.266667;	-115.543333
Neotamias umbrinus	5959	Nevada	White Pine	White Pine	39.266667;	-115.543333
Neotamias umbrinus	5960	Nevada	White Pine	White Pine	39.266667;	-115.543333
Neotamias umbrinus	5961	Nevada	White Pine	White Pine	39.266667;	-115.543333
Neotamias umbrinus	5962	Nevada	White Pine	White Pine	39.266667;	-115.543333
Neotamias umbrinus	5963	Nevada	White Pine	White Pine	39.266667;	-115.543333
Neotamias umbrinus	5964	Nevada	White Pine	White Pine	39.266667;	-115.543333
Neotamias umbrinus	5965	Nevada	Eureka	Roberts Creek	39.845;	-116.298333
Neotamias umbrinus	5966	Nevada	Eureka	Roberts Creek	39.845;	-116.298333
Neotamias umbrinus	5967	Nevada	Eureka	Roberts Creek	39.845;	-116.298333
Neotamias umbrinus	5968	Nevada	Eureka	Roberts Creek	39.845;	-116.298333
Neotamias umbrinus	5969	Nevada	Eureka	Roberts Creek	39.845;	-116.298333
Neotamias umbrinus	5970	Nevada	Elko	Spruce	40.553333;	-114.828333
Neotamias umbrinus	5971	Nevada	Elko	Spruce	40.553333;	-114.828333
Neotamias umbrinus	5972	Nevada	Elko	Spruce	40.553333;	-114.828333
Neotamias umbrinus	5973	Nevada	Elko	Spruce	40.553333;	-114.828333
Neotamias umbrinus	5974	Nevada	Elko	Spruce	40.553333;	-114.828333
Neotamias umbrinus	5975	Nevada	Eureka	Diamond	39.621667;	-115.88
Neotamias umbrinus	5976	Nevada	Eureka	Diamond	39.621667;	-115.88
Neotamias umbrinus	5977	Nevada	Eureka	Diamond	39.621667;	-115.88
Neotamias umbrinus	5978	Nevada	Eureka	Diamond	39.621667;	-115.88
Neotamias umbrinus	5979	Nevada	Nye	Grant	38.293333;	-115.481667
Neotamias umbrinus	5980	Nevada	Nye	Grant	38.293333;	-115.481667
Neotamias umbrinus	5981	Nevada	Nye	Grant	38.293333;	-115.481667
Neotamias umbrinus	5982	Nevada	White Pine	White Pine	38.293333;	-115.481667

Neotamias umbrinus	5983	Nevada	Eureka	Roberts Creek	39.845;	-116.298333
Neotamias umbrinus	5984	Nevada	Eureka	Roberts Creek	39.845;	-116.298333
Neotamias umbrinus	5985	Nevada	Eureka	Roberts Creek	39.845;	-116.298333
Neotamias umbrinus	5986	Nevada	Eureka	Roberts Creek	39.845;	-116.298333
Neotamias umbrinus	5987	Nevada	Eureka	Roberts Creek	39.845;	-116.298333
Neotamias umbrinus	5988	Nevada	Elko	Spruce	40.553333;	-114.828333
Neotamias umbrinus	5989	Nevada	Elko	Spruce	40.553333;	-114.828333
Neotamias umbrinus	5990	Nevada	Elko	Spruce	40.553333;	-114.828333
Neotamias umbrinus	5991	Nevada	Elko	Spruce	40.553333;	-114.828333
Neotamias umbrinus	5992	Nevada	Elko	Spruce	40.553333;	-114.828333
Neotamias umbrinus	5993	Nevada	Eureka	Diamond	47.506667;	-104.82
Neotamias umbrinus	5994	Nevada	Eureka	Diamond	47.506667;	-104.82
Neotamias umbrinus	5995	Nevada	Eureka	Diamond	47.506667;	-104.82
Neotamias umbrinus	5996	California	Mono	White	37.511425;	-118.179633
Neotamias umbrinus	5997	California	Mono	White	37.511425;	-118.179633
Neotamias umbrinus	5998	California	Mono	White	37.511425;	-118.179633
Neotamias umbrinus	5999	California	Mono	White	37.511425;	-118.179633
Neotamias umbrinus	6000	California	Mono	White	37.511425;	-118.179633
Neotamias umbrinus	5312	Nevada	White Pine	Snake	39.0038357;	-114.3022194
Neotamias umbrinus	5316	Nevada	White Pine	Snake	39.0038357;	-114.3022194
Neotamias umbrinus	5321	Nevada	White Pine	Snake	39.0038357;	-114.3022194
Neotamias umbrinus	5335	Nevada	White Pine	Snake	39.0038357;	-114.3022194
Neotamias umbrinus	5336	Nevada	White Pine	Snake	39.0038357;	-114.3022194
Neotamias umbrinus	5369	Nevada	White Pine	Snake	38.9860554;	-114.3133278
Neotamias umbrinus	5370	Nevada	White Pine	Snake	38.9860554;	-114.3133278
Neotamias umbrinus	5372	Nevada	White Pine	Snake	39.0038357;	-114.3022194
Neotamias umbrinus	5380	Nevada	White Pine	Snake	39.0038357;	-114.3022194
Neotamias umbrinus	5341	Utah	Summit	Wasatch	40.6575017;	-110.9382746

Neotamias umbrinus	5342	Utah	Summit	Wasatch	40.6575017;	-110.9382746
Neotamias umbrinus	5351	Utah	Emery	Uinta	39.424;	-111.131
Neotamias umbrinus	5354	Utah	Emery	Uinta	39.424;	-111.131
Neotamias umbrinus	5360	Utah	Emery	Uinta	39.424;	-111.131
Neotamias umbrinus	668	Nevada	Clark	Sheep	36.629025;	-11520753
Neotamias umbrinus	669	Nevada	Clark	Sheep	36.629025;	-11520753

VITA

Graduate College
University of Nevada, Las Vegas

Stacy James Mantooth

Degrees:

Bachelor of Science, Biology, 1997
Angelo State University

Master of Science, Zoology, 1999
Texas Tech University

Publications:

Mantooth, S.J., and B.R. Riddle. Molecular biogeography: the intersection between geographic and molecular variation. Geography Compass - in press.

Riddle, B.R., M.N. Dawson, E.A. Hadly, D.J. Hafner, M.J. Hickerson, S.J. Mantooth, and A.D. Yoder. 2008. The role of molecular genetics in sculpting the future of integrative biogeography. Progress in Physical Geography 32:173-202.

Mantooth, S.J., and B.R. Riddle. 2005. Annotated Checklist of the Recent Mammals of Nevada. Occasional Papers, The Museum of Texas Tech University 245:1-19.

Mantooth, S.J., and T.L. Best. 2005. *Chaetodipus penicillatus*. Mammalian Species Account 767:1-7. American Society of Mammalogists.

Mantooth, S.J., and T.L. Best. 2005. *Chaetodipus eremicus*. Mammalian Species Account 768:1-3. American Society of Mammalogists.

Mantooth, S.J., M.L. Milazzo, R.D. Bradley, C.L. Hice, G. Ceballos, R.B. Tesh, and C.F. Fulhorst. 2001. Geographic distribution of rodent-associated hantaviruses in Texas. Journal of Vector Ecology 26:7-14.

Mantooth, S.J., C. Jones, and R.D. Bradley. 2000. Molecular systematics of *Dipodomys elator* (Rodentia: Heteromyidae) and its phylogeographic implications. Journal of Mammalogy 81:885-894.

Clary, M.L., D.M. Bell, C.W. Edwards, D.J. Howell, T.W. Jolley, N. Lewis-Oritt, S.J. Mantooth, L.L. Peppers, I. Tiemann-Boege, B. Locke, R.J. Baker, and R.D. Bradley. 1999. Checklist of Mammals from Twelve Habitat Types at Fort Bliss Military Base; 1997-1998. Occasional Papers, The Museum of Texas Tech University 192:1-16.

Dissertation Title: From the Valleys to the Mountains: the Biogeographic History of Antelope Squirrels, Bats, and Chipmunks in Western North America

Dissertation Examination Committee:

Chairperson, Brett R. Riddle, Ph. D.
Committee Member, John Klicka, Ph. D.
Committee Member, Javier A. Rodríguez, Ph. D.
Committee Member, Gary Voelker, Ph. D.
Graduate Faculty Representative, Andrew Kirk, Ph. D.